THE DEVELOPMENT OF ANODISED SILVER - SILVER CHLORIDE ELECTRODES

PhD THESIS

Submitted by: Alan David Roberts B.Sc. M.Sc.

October 1979

Supervisor: Dr. D.J. Arrowsmith

The University of Aston in Birmingham

Department of Metallurgy.

CHAPTER I

ABSTRACT

THE DEVELOPMENT OF ANODISED SILVER-SILVER CHLORIDE ELECTRODES

ALAN DAVID ROBERTS B.Sc. M.Sc.

PhD THESIS 1979

The silver chloride anodic film is found to be a very complex structure with intricate morphology.

The film comprises, depending upon the anodising conditions, of a multilayer structure with up to three different layers. Each of these layers is porous and are composed of nodular and plate-like individual particles. Pores occur between these particles, and also in an extended form of large pores, several particle diameters in width, which act as the main transport arteries for material from the pore bases.

The material from the silver base is in the form of silver ions, or complexes of theso, which are transported up the pores to the growth sites. Primary layer growth is preceded by deposition of very small nuclei over the surface, followed by particle growth at irregularities, assisted by dissolution and deposition at areas of stress on the metal surface.

Second layer nucleation and growth occurs when complex ions cannot satisfy growth conditions further due to the primary layer thickness, the thicker second layer with larger particles is then formed. When this attains limiting thickness, pore blockage occurs which causes the growth of needle like particles on the film surface.

When the pores are unblocked, or new large pores nucleated by material dissolution, these needle particles act as nuclei for the growth of the very thick third layer. The initial morphologies of this third layer are crystalline platelets or joined nodular "cactus" particles, but the final morphology is of a massive columnar or plate-like structure.

KEY WORDS

ANODIC, POROUS, MULTILAYER, SILVER CHLORIDE

THE UNIVERSITY
OF ASTON
IN BIRMINGHAM

MEMORANDUM

Ref MET/DJA/CMK

To Academic Registrar

9 March 1979

From Dr. D.J. Arrowsmith
Metallurgy & Materials.

CERTIFICATE

I certify that ALAN DAVID ROBERTS was occupied on full-time research as a Research Student from 1st October 1976 to 30th September 1978

THE UNIVERSITY
OF ASTON
IN BIRMINGHAM

MEMORANDUM

Ref MET/ADR/CMK

To Academic Registrar

9 March 1979

From Mr. A.D. Roberts
Metallurgy & Materials

I hereby certify that no part of the work described in this thesis was done in collaboration, unless specifically so described, and that the work has not been submitted for any other award.

A.D.Roberts

CONTENTS

ACKNOWLEDGEMENTS

I would like to thank my supervisor Dr. D.J. Arrowsmith and Dr. J. Aston for the time and help in the preparation and planning of this Thesis, and the computer work undertaken, and my wife Carys for her patience and art work.

I would also like to thank the personnel and management of Foseco (F.S.) Limited for their help in typing and preparation, and also for leave granted to help finish in the writing of it.

Alan Roberts
July 1979

To see a World in a Grain of Sand
And a Heaven in a Wild Flower,
Hold Infinity in the palm of your hand
And Eternity in an hour.

William Blake

CHAPTER 2

INTRODUCTION

INTRODUCTION

SECTION (I)

GENERAL VIEW OF ELECTRODE

The growth of chloride films on silver is not a subject that has attracted great attention in past work by a variety of researchers.

Until the recent advent of the scanning electron microscope, most work done on the system has mainly concentrated on the electrochemical properties of the films and not on its structure. The structure, though, defines its physical chemical and electrochemical properties and must therefore be well understood to enable the best use of the system in its many applications.

One author put the state of the art of anodic film electrode production quite succinctly (36).

"The reproducibility of the electrolytic electrode depends upon many factors either accidental or imperceptible. This remark is readily appreciated by those who have to recapture the magic recipe for anodising conditions from the scanty and frequently contradictory information found in the original publications."

There has been speculation as to the actual physical structure of the anodic film and its mode of growth, but no real physical information on this could be put forward until the S.E.M. became available.

Vermilyea (22) looked at anodic films and stated that nucleation and growth of an anodic film requires an appreciable overvoltage in the range 10 - 1000 mV and that nucleation may be confined to certain catalytic regions on the surface, i.e. impurities.

The continued growth, after nucleation, of the film requires an overvoltage which would result from energy to

1. Create and move atomic steps on the corroding electrode surface.
2. Deposit the anodic material.
3. Transport charged particles.

Nucleation can be followed by growth by the spreading of platelets, and thickening by transport of ions through the film and by precipitation from solution.

Vermilyea states that non-continuous anodic films contain pores which are formed by the cation of the film entering solution as an ion. They also have very low resistance and can grow very thick, not usually less than 10^{-8}m thick, and can be 10^{-3}m thick.

The structure tends to be crystalline with crystallites or very large crystals formed and bounded by well formed crystal faces. The surface has differently orientated atoms at its surface, and some will dissolve easier than others (diffusion sites), due to the different binding energies. This happens especially at irregularities on the surface, like dislocations.

With a discontinuous film, the metal base is faceted and roughened as the dissolution reaction is confined to certain regions on the surface.

Loose fluffy matter of very fine dendrites can be precipitated also at the top and sides of the pores under conditions of porous anodic film and high current density. Recrystallisation can also occur causing multilayers of anodic films, or an amorphous film transforming to a stable crystalline film.

In the case of Ta_2O_5, the original amorphous film is replaced by a crystalline film growing under the amorphous film and pushing it away. Fleischmann (23) looked at passivating layers on metals. He suggests that discrete centres nucleate and grow and passivation occurs when these centres coalesce. The centres growth is controlled by two potential dependents

1. Nucleation rate constant, nucleations cm^{-2} sec^{-1}.
2. The crystal growth constant, moles cm^{-2} sec^{-1}.

SECTION (2)

FILMS ON OTHER METALS AND GENERAL PRINCIPLES

There is quite some similarity in the mode of growth of some other types of film to the mode of chloride film growth on silver. One instance of this is the growth of (1) ZnO on Zn.

The colours achieved in the film, which vary from yellow to brown to violet or black depending upon the concentration of NaOH in the anodising solution, are suggested to arise from excess Zn in the film. The detached ZnO film also optically appears porous, or fibrous, with layers containing crystalline platelets of dimensions 5.0×10^{-9}m - 15.0×10^{-9}m.

Another similarity is, as in high current density silver chloride films, that in certain solutions a yellow layer is overlain by a white layer. The yellow layer is blue black at higher voltages.

It is also reported that (1) lead sulphate films form needles of micron size with increasing current density. Also as the lead sulphate film thickens it breaks away from the metal surface by mechanical stress. Tetragonal or orthorhombic large crystals can be deposited on the lead sulphate surface also.

In aluminium (1) a porous film can be achieved with concentration of pores of 4.0×10^{8} cm $^{-2}$and a pore diameter of 10^{-7} m. The size of the pores seems to increase proportionally to the formation potential in the form

$C = aV+b$

C is the size of pores

aV is twice the wall thickness round the pore

b is the diameter of the pores.

The hexagonal cells seem to first appear round sub grain boundries and then to fill the area, the higher the formation voltage the lower the number of cells per area. It is reported that crystalline solids can appear on the surface of anodic films which are held under voltage at temperatures even well below 100°C. This may not be recrystallisation, but a formation de novo, mechanically replacing a formally amorphous film.

Also the change in potential with time increased with increasing anodising voltage during film formation under galvanestatic conditions when the surface of the metal was in the "as rolled", abraded or scratched state. In zinc (3) and copper (4) it was shown that the corrosion rate declined with increase in temperature over a certain range, this probably being due to the pores being blocked by the increased amount of oxide produced by the rise in temperature. Stifling could be by physical self blocking or compressional stresses from neighbouring pores causing mutual blocking.

It must be noted that there is a difference between processes with applied potential and those like magnetite formation where there is no applied potential, but a growth process involving the formation of a porous structure, with precipitation from solution, and absence of pore blocking.

Field and Holmes (13) looked at the nucleation and growth of magnetite on iron in water at 250°C. In the early stages of nucleation, nuclei are formed at $10^{10} cm^{-2}$ density, and these seem to have dependence on the iron grain orientation. After the crystallites have impinged and are at a diameter of $3.0 \times 10^{-8} m - 1.0 \times 10^{-7} m$, then pores are left between them.

The outer layer then forms, this being made up of aggregations of crystallites in the form of triangular platelets at up to 10^{-4}m across or 5×10^{-6}m across tetrahedral crystallites on abraded surfaces. These crystals seem relatively non-porous. The inner compact layer is about the same volume as the metal it replaces, and ions seem to diffuse out through pores in the inner layer.

The outer layer forms probably through a solution reprecipitation process, giving rise to the well formed crystals. Nucleation sites do not seem to be associated with metal dislocations. There is about 10 - 15% porosity in the inner layer and the pores are about 3×10^{-7}m diameter, the growth of the layer being by a log law relation, so there is a tendency for mutual pore blocking.

In the outer layer the pores are about $2 \times 10^{-6} - 2 \times 10^{-5}$ m diameter. Nucleation may be due to impurities or growth steps in the surface.

Turner & Brook (14) looked at the $CuCl_2$ film on Cu. They suggested that as they have growth centres of various sizes, then progressive nucleation dominates as opposed to instantaneous nucleation which would produce centres of all the same size. They also found nodules growing on individual nodules.

Bignold, Garnsey and Mann (15) also looked at magnetite formation, and the development of a porous oxide. They suggest that two layers of oxide exist, with oxide growth involving a solution transport process, iron dissolving at the pore bases in the inner oxide, diffusing through the pores and depositing to form the outer macro crystalline layer.

The porous inner layer grows at the inner surface of the metal/oxide to fill in the metal removed and keep a contact with the surface.

They suggest that there is an oxide or hydroxide thin layer next to the surface of the metal, and that the driving force for the diffusion is caused by the difference in solubility between this oxide and the magnetite.

If the oxide is less porous than the magnetite then this explains why there is no pore blocking, and the nucleation of another layer on top. The growth is controlled by a parabolic growth law relationship which is dependent on concentration.

Grauer and Feitknecht (17) looked at the oxidation of iron at 200°C; they report that as the oxidation proceeds, small crystals of Fe_3O_4 nuclei form giving a relatively coherent porous layer. An oxide layer of Fe_2O_3 then forms covering the Fe_3O_4, this forms by whiskers of about 10^{-6}m long growing out of the oxide and then developing into plates.

Vermilyea (22) reports that whiskers and platelets have been found also in the halide films of lead and mercury.

SECTION (3)

NUCLEATION OF CHLORIDE FILM

The film can nucleate (43) at certain points over the surface and grows laterally until a layer of uniform thickness covers the surface. Then growth in depth starts.

Attack at the anode may occur where the atomic structure is in disarray, i.e. points, holes etc., so the rest of the surface is more perfect, and the activation energy of the solid to solution change at these points is higher. Attack will proceed in silver anodes at very close to that current efficiency predicted by Faradays Laws even when the current density is high. Where discrete nuclei occur a growth curve of thickness to time in the form of a sigmoid curve would be expected.

Anodic dissolution (2) starts at abrasion lines or on rolled specimens at certain points situated parallel to the original rolling lines, i.e. where internal stress is likely to be situated. The effect of stress on the dissolution of the metal is described in section (8), and the reasons why deposition occurs, and the formation of porosity, along the rolling or scratched lines. On freshly polished (18) silver, a large number of nucleation centres exist at the beginning of anodisation and as the anodising progresses, a porous film is produced which thickens with a slow decrease in porosity.

Where (18) the KCl anodising solution concentration is higher, then the time for surface coverage is shorter, this indicating that higher chloride ion concentration gives earlier silver chloride coverage, this may be due to an increase in nucleation sites.

Gu and Bennion indicate that the initially higher overpotential at the beginning of anodisation may be due to slow nucleation leading to a nucleation overpotential. Katan (19) found holes or pits in the base silver appearing during anodic treatment to a density of 1×10^{8} pits cm^{-2}. This surface density appears to be constant and is not affected by change of anodic treatment except at the grain boundaries and the narrow bands surrounding the silver chloride layers.

This band was found to be wider at the front of the bed of silver spheres that Katan used as an anode, and varied from 4×10^{-7}m to 4×10^{-6}m wide. The pits seemed angular or triangular and were about 3×10^{-7}m in diameter but varied between 1×10^{-7}m and 6×10^{-7}m diameter.

At the nucleation stage of anodising, small rounded pits appeared of about 2×10^{-7}m diameter and density 1×10^{8} cm^{-2} with silver chloride deposits round the pit mouths and nearby, these being 1×10^{-7}m to 8×10^{-7}m diameter and density 1.1×10^{8} cm^{-2}.

They found that the density of these initial deposits were largely independent of depth into the silver sphere bed anode. It is suggested that the pits are the sites of dislocations, having a surface density 1×10^{-8} cm^{-2} in Ag, which seems reasonable, the pits having a surface density of the same value. At high current densities there are roughly the same number of nucleation sites, and bulbed mounds, as at lower current densities before the discrete Ag Cl particles can grow together. Numbers of particles at lower current densities are $9 \times 10^{7} \pm 2 \times 10^{7}$ centres cm^{-2} and $1.3 \times 10^{8} \pm 3 \times 10^{7}$ centres cm^{-2} at higher current densities, showing that as with the pits, the number of nucleation centres remains roughly constant even though widely different conditions prevail.

Vermilyea (22) states that the formation of Ag Cl nuclei occurs only in a relatively short period of time after application of potential. He suggests that this is due to depletion of chloride ions near the electrode once this growth starts, so the driving force for continued nucleation is reduced, so the nucleation stops with a certain number of nuclei formed, which are of the order of $10^9 cm^{-2}$ (on an Ag single crystal), and which are of uniform size.

On polycrystalline silver surfaces, non-uniformity of particle sizes are formed and he suggests that silver is not an excellent catalyst for the formation of silver chloride as a monolayer is not formed over the entire surface, which could be due to impurity effects. Spherical crystallites are also reported. Vermilyea (22) also report that Jaenicke (29) showed resistance of the film increases and becomes independent of electrolyte concentration after the film had thickened to a few microns, and that Huber (30) found no detectable diffusion through a stripped silver halide film. Also the current may decrease due to increased pore length.

Lal et al (24,25) report that at the start of anodising, there is a trough in the chronopotentiometric graph before a linear relationship develops between the potential and time. Sometimes this slope increases later, i.e. Graph I below:

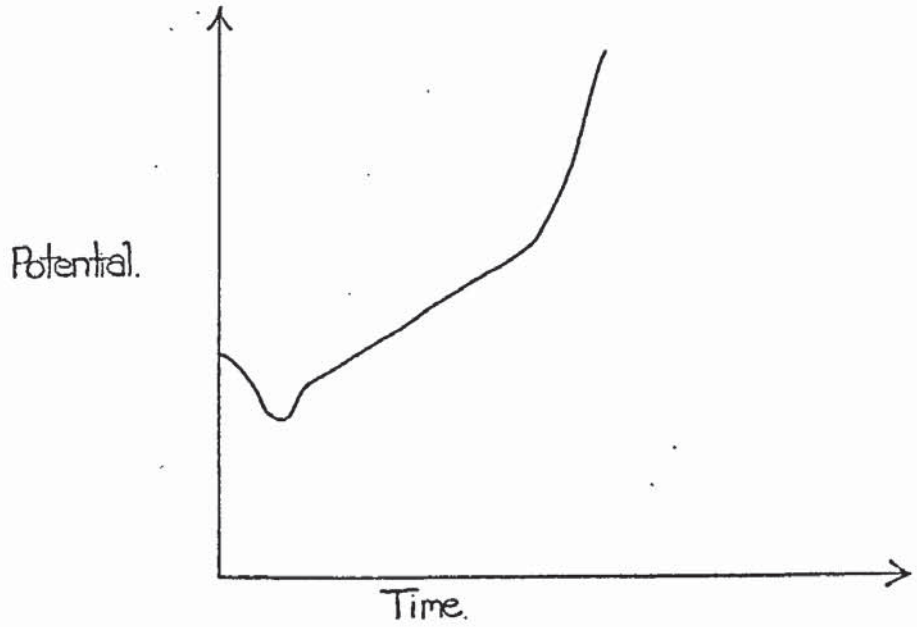

GRAPH I

Lal reports that the linear part of the graph shows that under constant current density additions, the resistance of the electrode increases linearly with time over a long period. Kabanov's work suggests this is an effect of supersaturation.

Biggs and Thirsk (26) found that electrolytic cleaning leads to uneven anodic attack in chloride solutions. In experiments carried out in this work also, this was found to be the case.

The cleaning leads to a roughening of the surface, in nitrate solutions, which leads when anodising to enhanced attack at irregularities on the surface for the reasons discussed later in this work. A perfectly smooth surface leads to even nucleation and growth over the whole surface.

SECTION (4)

GROWTH OF FILM

It is reported (1) that in chloride film growth on silver a porous film is produced which has two modes of growth.

1. Above 18 ma cm^{-2} uniform film growth showing interference colours before reaching a thickness where a white layer formed. The growth is analogous to growth on valve metals.
2. Below 18 ma cm^{-2} uniform film growth with no formation of white layer.

It is possible (2) to have a situation, when the solid crystallises, where there is a decrease in the absolute current, but this means that the true current density of the uncovered areas rises and where this occurs there is a greater formation of film and oxygen can also be evolved.

There are various laws governing the growth of a film (2) in relation to the porosity. If film thickness versus time is plotted and a log relationship is gained, then it can be surmised that movement through the pores is causing mutual stifling, that is, neighbouring pores are blocking each other in some way.

If an asymptotic curve is gained, then the pores are self stifling. A sigmoid curve occurs where discrete nuclei occur which spread over the surface; when the film becomes thick enough, the curve will become parabolic. Outward movement of the metal ions will cause cavities to form at the base.

It is reported (5) that outgrowths from some metal oxide films can be seen in the form of needles springing from the pores in the film, rising at right angles to the film surface. At low current densities (7) the potential quickly attains a steady value, but above 10 ma cm^{-2}, it rises sharply and keeps on rising, this showing a different growth mechanism at different current densities.

Katan (19) found silver chloride deposits without crystal planes and with rounded smooth surfaces, although the occasional cubic crystal was found in the film. He used a bed of silver spheres as the anode, and looked at growth morphology with reference to distance into the anode bed. At the front of the anode, growth was in the form of small discrete bulbed mounds (similar to the particle type M19 and M6a as defined in this work) of about 7×10^{-7}m diameter with mound density of 1.1×10^{8} mounds cm^{-2}. This type gradually changes as progress is made into the electrode bed, with a branch-like or continuous form, with interconnecting branches, towards the bed base. The Ag Cl film was found to be 5×10^{-7}m thick or less, with an overhang at the edge of 1×10^{-7}m or less, as seen in Fig 1.

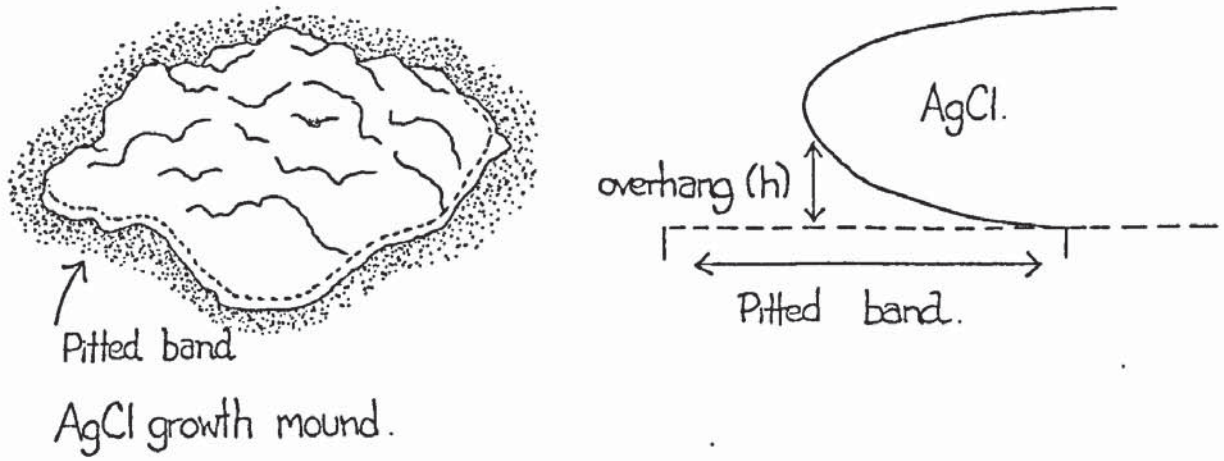

Fig 1

When the film has grown to substantial proportions, cubic crystals of Ag Cl were seen on the surface, coinciding with the pits becoming angular in shape.

Szpak, Nedolulla and Katan (21) looked at the different morphology obtained in the deposits from the surface of the silver sphere anode down into the bulk of the electrode. At the surface a coating, looking like dried clay, is obtained and the deposits change to a pyramidal and cubic crystal form, then to rounded cubed particles, then spherical particles the further into the electrode examined.

Crystal Morphology	Diameter (m)	Distance into electrode bed (cm)
Pyramidal	$5 \times 10^{-6} - 8 \times 10^{-6}$	0.3
Cubic	$4 \times 10^{-6} - 5 \times 10^{-6}$	0.35
Rounded cuboids	$3 \times 10^{-6} - 4 \times 10^{-6}$	0.45
Spheres	2×10^{-6}	0.5

Anodised 4 hours at 8 ma cm^{-2}

Vermilyea (22) reports that Ag Cl has a definite orientation with the substrate and that changes in film composition can occur within the growing film. Lal et al state that the thickness of the film decreases almost inversely with the increase in the current density, but is almost independent of the concentration.

The difference in the Graph 4 Section 7 between the high and low current density film growth on the overpotential to time relationship is probably due, like lead in sulphuric acid polarisation, to concentration polarisation due to chloride ion depletion at the Ag/Ag Cl interface. The increase in chloride ion concentration, or decrease in the current density causes it to revert to a lower current density type growth mechanism.

Jaenicke, Tischer and Gerischer (29) used layers of silver chloride up to 30 microns thick and looked at the specific resistance to film thickness for various current densities of formation, as in Graph 2.

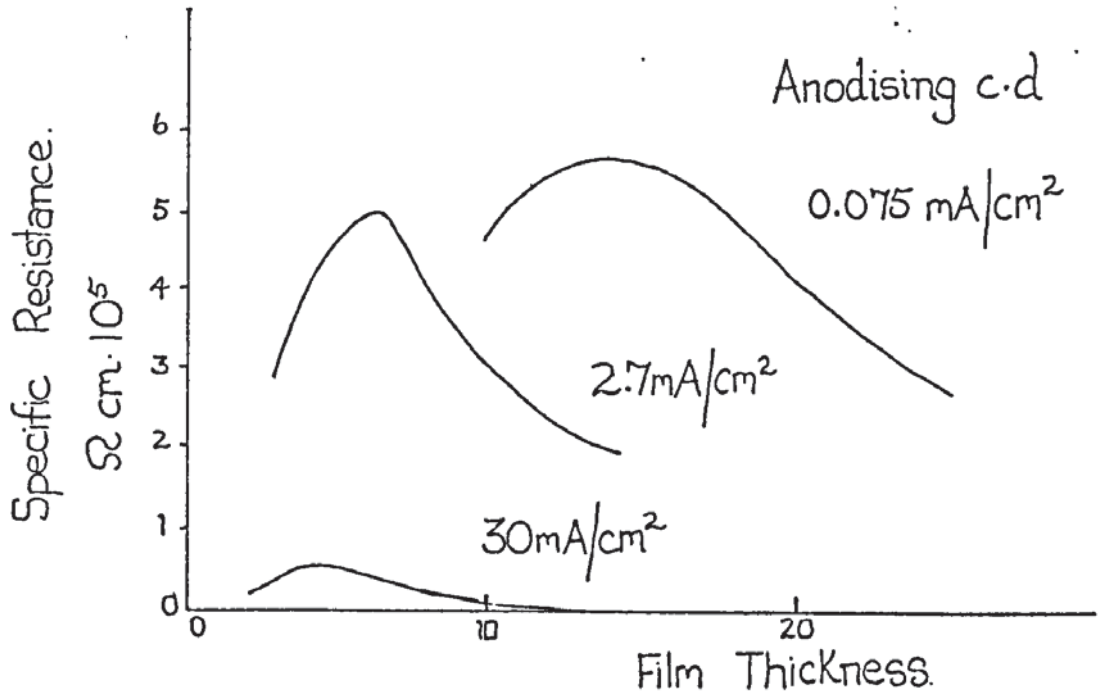

GRAPH 2

The resistance is larger the slower the film is formed. Slow anodising and low current density gives greater resistance, presumably changing the film morphology to a low porosity type film. They presume the silver chloride grows on the inner boundry interface between the silver and the chloride.

Gerisher states that at current densities less than 3 ma cm^{-2} the layer grows at only a few places on the silver surface; increase in current density causes the patches to grow together and cover the open areas. In these areas, crystal surfaces vary and differ in orientation.

Huber (30) looked at the growth of silver bromide films. He states that these films are non-porous with cup like depressions on the surface of the silver after anodising, thus showing that growth is not planar but proceeds into the metal by these depressions.

He states that there are three types of film, porous, open with large pores, or a locked structure with no pores. Huber states that anodic halide films on silver are locked structures with no pores.

SECTION (5)

TRANSPORT OF IONS AND COMPLEX FORMATION

The mode of transport of the metal or chloride ions is important in the way the film is structured, also the form in which the ions are transported dictates to an extent the mode of transport, so it is important to look at both of these points. Vijh (16) looked at the influence of chloride ions on the anodic behaviour of some metals and derived the process given below.

$M + nCl^- \rightarrow M(Cl)_n + ne$	Reaction and deposition.
$M(Cl)_n \rightarrow M^{n+} + nCl^-$	Dissolution.
$M^{n+} + m\,Cl^- \rightarrow (M_n\,Cl_m)^{(m-n)e}$	Complex formation and transport
$(M_n\,Cl_m)^{(m-n)e} \rightleftarrows M^{n+} + mCl^-$	Dissociation

In some metals like Mo, Zr and Ti the complex can be stable, but as in Fe or Al, the complex is unstable due to outer orbital hydridization, giving dissociation which provides free chloride ions to participate in the cycle of silver chloride dissolution again.

On (18) a cycled surface, where the silver has been anodised, then the film reduced, then a further anodisation carried out on the reduced silver surface, resulting in larger surface area, silver chloride crystallites form which grow together blocking off the silver surface with a rapid rise in over potential. This supports the theory that the formation of anodic silver chloride is mainly by solution phase diffusion of the $Ag\,Cl_{(n+1)}^{-n}$ ion complex, followed by crystal growth from supersaturated solution, (31).

When the concentration of potassium chloride was increased, the anodising solution for the cycled surfaces, lower overpotentials were found, this being attributed to higher solubility of the Ag Cl $_{(n+1)}^{-n}$ ion and smaller concentration overpotentials. The large difference in the maximum currents to reduce the silver chloride between curves a and c in Graph 3 supports the solution diffusion mechanism in the formation and reduction of silver chloride.

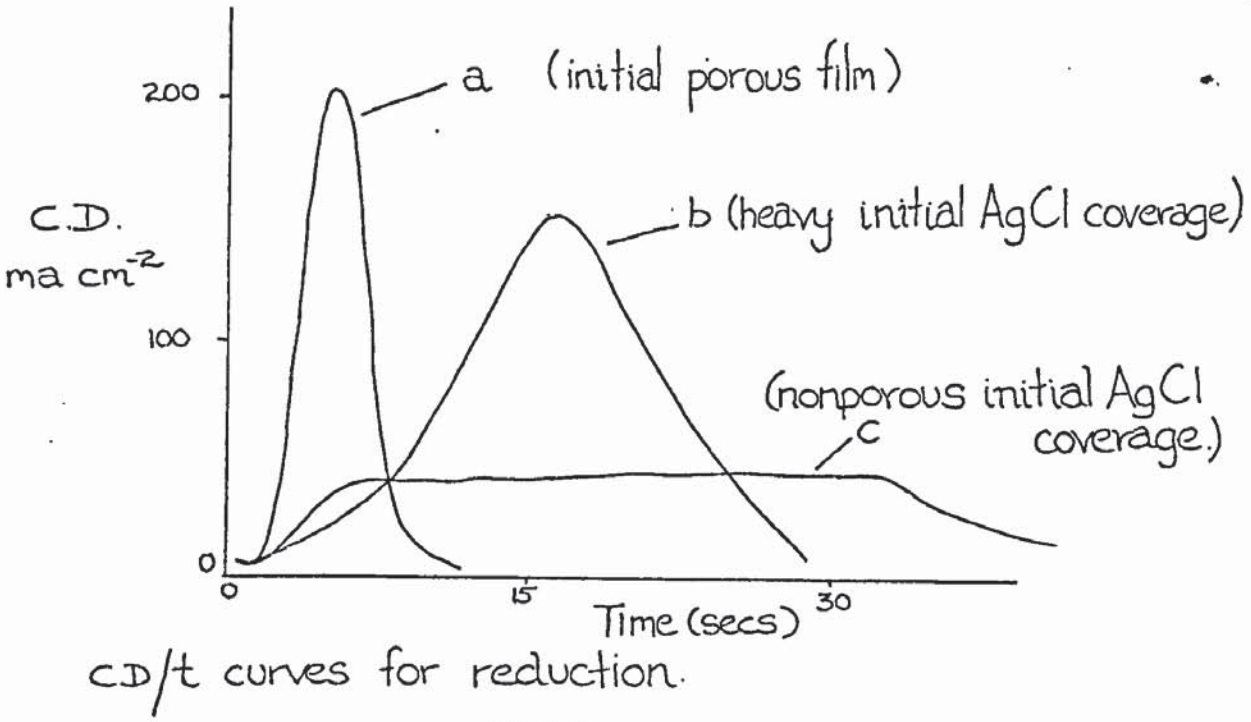

GRAPH 3

If significant solid phase transport had occured, then there would have been less difference in magnitude of the maximum currents. The decrease in the mass transport coefficient km^{o} at higher K Cl concentrations, is due to the increased portion of Ag Cl_4^{-3} present.

This ion has a larger ionic radius and a smaller diffusion coefficient than the other complexes; this means that at higher concentrations, the total diffusion coefficient of the Ag Cl $_{(n+1)}^{-n}$ ion is smaller than silver chloride and gets smaller at increased concentration of KCl.

Katan (19) suggests that the anodic process is that Ag is transported from pits in the Ag base (see Fig 1 Section 4) to sites on the Ag Cl and deposited. Not much of the silver is lost to the solution and the volume of the Ag Cl is larger than the pit volume (Ag removed) in the ratio 2.51:1 (molar volume).

Transport is presumed to be by bulk diffusion of the $AgCl_{(n+1)}^{-n}$ ion, where n = 0, 1, 2, 3, and this is a precursor to Ag Cl nucleation and precipitation. For the silver to dissolve, it must be oxidised to a stable singly charged state which can then combine with the chloride ion forming a complex species of the form $AgCl_{(n+1)}^{-n}$. The nearly constant Ag Cl thickness suggests that Ag Cl growth occurs along the growing edges of layers. The deposition of Ag Cl from the species takes place at the point nearest the dissolution pit, and the overhang suggests that the $AgCl_{(n+1)}^{-n}$ anions arrive from bulk solution at the growing edge of the Ag Cl.

This is strong evidence for bulk diffusion. With surface or ionic transport there should be no overhang, so bulk diffusion must be the main transport process. The complex formation is given below:

$Ag \rightarrow Ag^+ + e^-$	Dissolution
$Ag^+ + (n+1)\ Cl^- \rightarrow AgCl_{(n+1)}^{-n}$	Complex formation
$AgCl_{(n+1)}^{-n}{}_{(a)} \rightarrow AgCl_{(n+1)}^{-n}{}_{(b)}$	Solution Transport
$AgCl_{(n+1)}^{-n} \rightarrow AgCl_{(solid)} + n\ Cl^-$	Deposition and growth

It is suggested also that there can be swarm or embryo formation in solution (20). In the bed electrode (21), as the reaction surface moves deeper into the bed, a depletion of chloride ions occurs within the electrode. To make up for this, there is a proposed redistribution of the Ag Cl, in the form of the complex $AgCl_n^{-(n-1)}$ ion.

This ion diffuses down into the electrode body depositing as Ag Cl again and releasing chloride ions which can take part in a further reaction, see Fig 2.

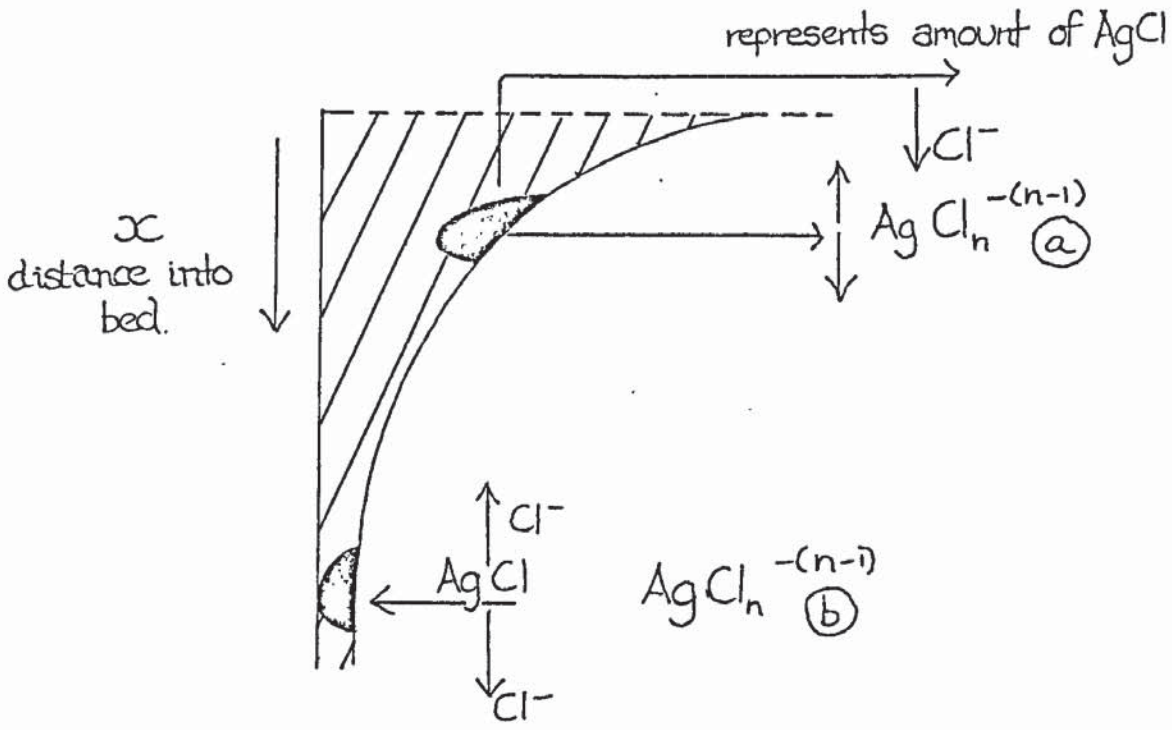

Fig 2

The formation of these complex ions is thought to increase the concentration gradient, also changing the morphology (see Section 4). There can be some loss of silver chloride, as some complex ions could be lost to solution and plated out on the counter electrode.

SECTION (6)

POROSITY OF FILM

It is suggested that pores (1) start where local rates of dissolution are high, and a higher temperature exists here which further increases the rate of dissolution, the film growing to a greater thickness mainly due to the presence of the pores.

Whichever is the mobile species, metal or anion, the pore stands a good chance, especially if the anion is mobile, of being blocked. This does not often happen to the extent to which it, in theory, should and this can be explained in several ways. One way would be that the increase in temperature at pore bases increases the rate of chemical dissolution in the pores and keeps them open, especially if a large current flow exists in the pore. Dissolution could also be field enhanced, expediting both growth and dissolution of the oxide.

Laws governing the blocking of pores in relation to film growth are summarised in Section 4. A pore (2) can exist where three grains meet, or along lines of disordered atoms, i.e. where slip planes meet or along axes of screw dislocations, or along lines representing edge dislocations.

If the pores are broad enough to admit the chloride ions, then oxidation at the pore bases could take place. This would tend to plug the pore in time and even if the metal ions are active and moving outward, such movement could bring the ions into positions to block previously active pores.

It is possible that the number of pores per unit area will therefore diminish as the amount of chloride absorbed per unit area increases, so the number of pores is probably proportional to the amount of chloride ion absorbed.

Needle like growths, as described in Section 4, are found in relation to the pores. It is reported that pores can be produced (6) by solutions that exhibit solvent action on the film, and initially a non-porous film is produced and then pores nucleate at nuclei on the film surface, producing pores $1 \times 10^{-8} - 3 \times 10^{-8}$ m diameter in films 7.2×10^{-5} m - 2.4×10^{-6} m thickness.

Lal et al (24) quote the value of the conductance of silver chloride at 25°C as being 1.2×10^{-7} $ohm^{-1}cm^{-1}$ which Kurtz suggests is 100 times less than the value of specific resistance for solid silver chloride. This therefore suggests porosity. Briggs and Thirsk (26) suggest the anodic film is porous and consists of fine crystalline material with a fine capillary network in it, this containing solution of bulk solution concentration. They assume that a film produced in 0.1N KCl has 0.1% of surface area as capillary area.

SECTION (7)

COLOUR AND AGING OF THE FILM

Silver chloride electrodes are variable in colour and in potential, needing after manufacture a period of time, known as the aging time, to adjust to normal equilibrium potential.

It is reported (6) that the silver chloride electrodes are uncertain in reliability with the equilibrium potentials differing between electrodes by 0.1 mV. They also need at least 24 hours to attain equilibrium and it is believed that the best electrodes are those pink or plum coloured. The electrodes are reported to suffer from a typical surface films and have potentials at equilibrium that vary with temperature.

0^{o} C - 0.2365V

25^{o} C - 0.2224V wrt SHE

50^{o} C - 0.2045V

Looking at the ratio of Ag to Cl in the Ag Cl films (7) formed at high current density, there tends to be an excess of Ag present, probably in the form of interstitial silver ions, causing high ionic conductivity and variation in colour, i.e. violet, black, grey at 2.5, 10, 20 ma cm^{-2} respectively. Colour differences probably correspond to energy levels of trapped electrons, energies corresponding to adsorbtion in the optical region. Trapped Ag^{+} ions will be due to the field during anodising causing migration.

Ag to Cl ratio

Precipitated Ag Cl = 1.01

Ag Cl, 10 ma cm^{-2}, 2MHCl = 1.075

Ag Cl, 20 ma cm^{-2}, 2MHCl = 1.1

Lal et al report a purplish grey film, with or without the presence of light. At high current densities in chloride solutions, a different behaviour to normal is seen as in Graph 4 below.

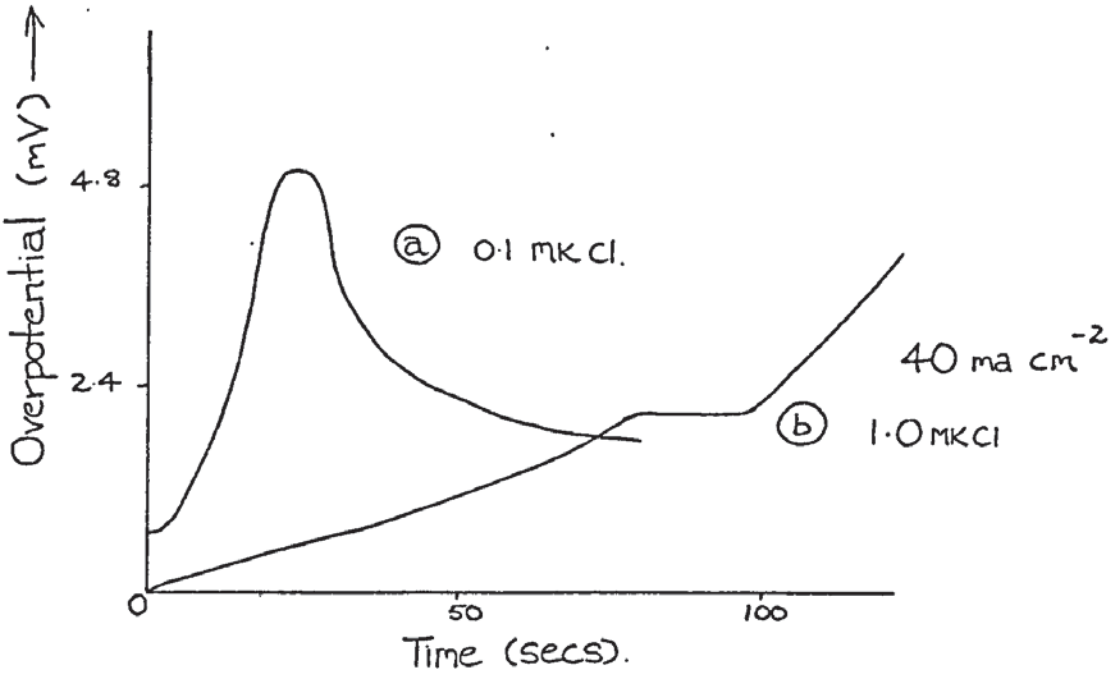

Graph 4

In plot a (a) of Graph 4 a dark film rapidly forms and is then covered by a loose white film whose spreading corresponds to the rapid rise in overpotential till oxygen is liberated. In plot (b) a dark firmly adherent layer is formed which grows till oxygen evolution at about 25 V or over. Sayer and Roberts (28) report that electrodes should be aged for 1 - 2 days before use, and the colour changes from sepia to pale tan or brown to greyish pink, pink or plum after washing.

The electrode (33) suffers an aging effect, where the old electrode is slightly more positive than the new, this being always in the same direction and magnitude, within 0.05 mV. This was first seen by Mac Innes and Parker (37) and has been studied by Smith and Taylor (38) and more recently by Taniguchi and Janz (39).

The aging effects are about the same for electrodes in or out of light, and neither composition solution nor impurities seem to affect it. Smith and Taylor (38) suggest the aging effect may be due to concentration polarisation within the pores of the deposit, this causing depletion of the chloride ions in the electrolyte, a depletion which persists when the electrode is transferred to the solution in which its bias potential is to be measured. They showed that the aging effect varied from a few minutes to 20 days, but Hornibrook, Janz and Gordon (40) disputed this, finding no aging after 25 to 40 minutes.

If there is linear diffusion, it should take only 10 minutes for concentration differences to fall to 10^{-4}N from 0.1N, but different manufacture and film morphology could lengthen this period. Smith and Taylor (38) used thickness and current densities 13.4 and 13.6 times, respectively, those of Gordon et al (40) so assuming 10 minutes aging for the thinly coated electrodes, a layer 13 times thicker would age over 28 hours, so for very thin coatings or very small current densities the aging time would be negligible.

SECTION (8)

STRESS IN FILM

It is known that the presence of internal tensile stress renders metal anodic towards unstressed metal. The stresses in a scratch or rolling line are represented below in Fig 3 this showing the way in which the silver probably dissolves and deposits.

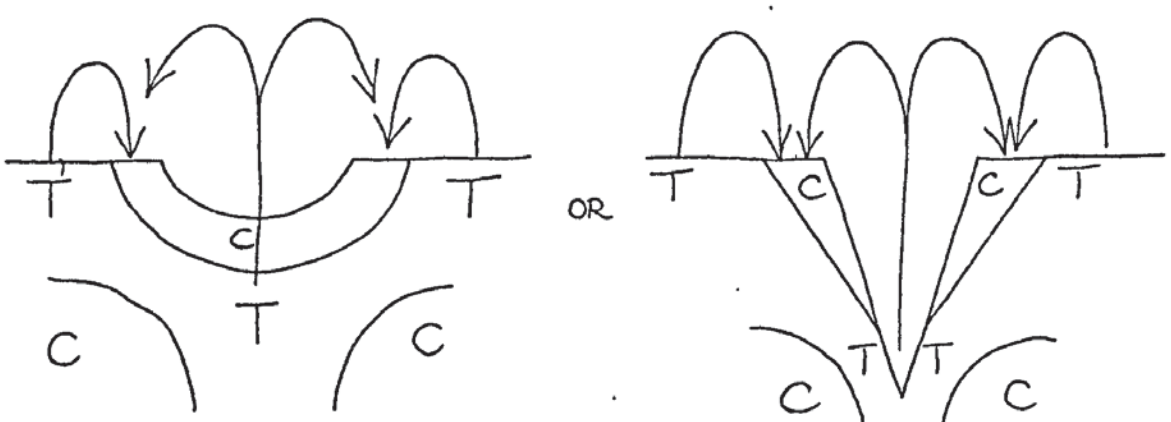

Fig 3

It is interesting that in rolled nickel pores occur at each side of the scratch line, probably in the area of tension boardering the area of compression as in Fig 4.

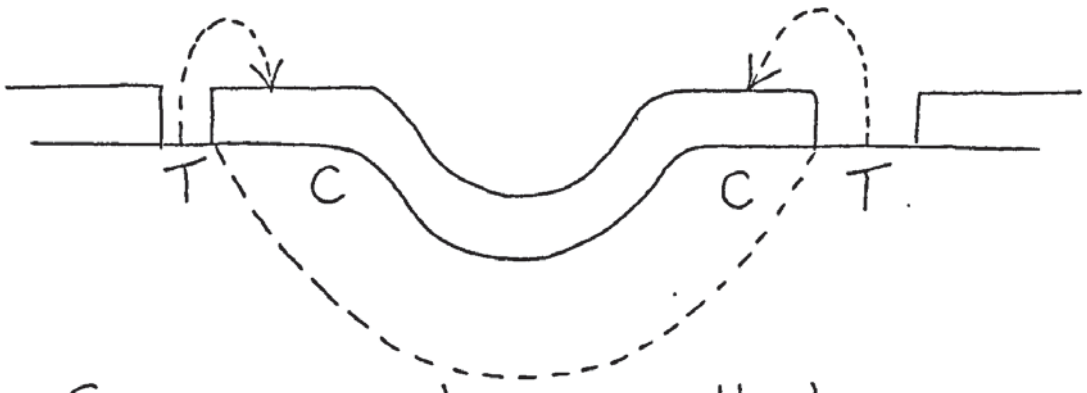

C = Compressional area = cathodic
T = Tensional area = anodic.

Fig 4

High current density films (7) develop compressive stresses which loosen the film, causing it to bulge out and detach. Complex ions have been found (8) to constitute the critical species in the embrittlement and stress corrosion of Ag Cl in certain aqueous environments. It is probably the chloride ion and/or the metal chloride complexes that cause this embrittlement.

SECTION (9):

REDUCTION OF FILM

The reduction of the Ag Cl film may be accomplished in various ways and is instructive insofar as it sheds light on the probable growth process. Katan, for instance, (19) found that if Ag Cl were left under the SEM beam, then it reduced by the path Ag Cl + $E(e^-) \rightarrow$ Ag + Cl$\uparrow$. He also reduced an Ag Cl film, anodised for 11 minutes at 5 ma cm^{-2} and reduced it at 5 ma cm^{-2} for 4 minutes.

When partially reduced, isolated Ag Cl mounds were formed with a smoothing out of the sharp angular edges of the pits in the silver base. The overhangs in the Ag Cl mounds were also generally lost. The retreating Ag Cl also left an increasingly wide band of pits beneath its growth edge, see Fig 1, and it is suggested that (19) when reduction is operating, there is deposition of Ag at the small nodules and the edges of pits, smoothing out their sharp angular contours. Briggs and Thirsk (26) found that the concentration of the solution had a marked effect on the Ag growth centre type on discharge, so they used different concentration for anodising and discharge. They found that the Ag growth on reduction starts at a number of points, giving circular spreading lateral patches as thick as the original Ag Cl film and attached to the Ag substrate. Cylindrical or inverted truncated cones are formed, and also dendrites of silver chloride can be formed within the Ag Cl in 0.1 N KCl.

In 1.0 N KCl, a diffuse form of Ag is produced, a granular type structure much like the original Ag Cl. Briggs and Thirsk also report that when reduction is undertaken, Ag is formed which must be porous eventually because its volume is much less than the original Ag Cl but the film has the same volume.

Schwab (27) reports that a fine granular mass of silver is produced with a pore radius of 2×10^{-6}m on reduction; in this reduction it is the chloride ion which diffuses away by the pores, whereas the silver ion is the mobile species in growth.

Dendrites (47) form at the metal - chloride interface and grow through the layer to the solution. Once the dendrites have reached the solution, the growth of the dendrites is assisted by plating out of Ag from the solution.

Ives and Janz (33), a reference work on the use of the Ag Cl film as a reference electrode, quote Fischbech's results (23) as indicating that formation of the Ag is at the Ag Cl surface, indicating non-porosity and current carriage by electronic conduction. They also quote Tubandt's work (35) as showing that ionic not electronic conduction transfers charge across the film and it is the Ag^+ ion that migrates.

SECTION (10)

DEGRADATION AND DISSOLUTION OF THE FILM

Silver chloride electrodes can degrade in a variety of conditions, causing the reproducibility of the electrode to suffer consequently. Matsuno (10) reports that electrodes stored in air had higher overpotential and less reproducibility than those stored in NaCl solution.

Gibbard (11) also reports on the solute and solvent activities of concentrated aqueous NaCl. When the Ag/Ag Cl electrode was placed in it, inconsistent results were gained. These results were attributed to the formation of a solid solution of NaCl and Ag Cl, proof of which has been gained from cell measurements and X-ray diffraction.

It is reported (12) that the silver chloride electrode loses silver chloride when in concentrated KCl solutions, especially at increased temperatures. To avoid this generation of blank spots on the electrode surface, then it is best to put the electrode in a closed cylinder with a small aperture to the environment covered with a porous material or carboxymethylcellulose or carboxymethylamylase. This tends to immobilise the Ag Cl/KCl complexes, keeping them in the container. Sayer and Roberts (28) report that unless the solution the electrode is kept in is saturated with Ag Cl, then the Ag Cl will dissolve by formation of complexes.

SECTION (II)

EFFECT OF LIGHT ON FILM

One author (I) quotes that transient species are formed by light, or UV, in silver chloride and that the change in electrode potential is probably due to these and to changes in composition produced by the light, in the solution.

Moody, Oke and Thomas (9) found that sunlight, as in Graph 5, caused a difference in potential of about 47 mV between a Ag/Ag Cl electrode and a calomel electrode, giving an average change of about 0.2 mV mt^{-1}. They found very little effect with artificial light or with UV light.

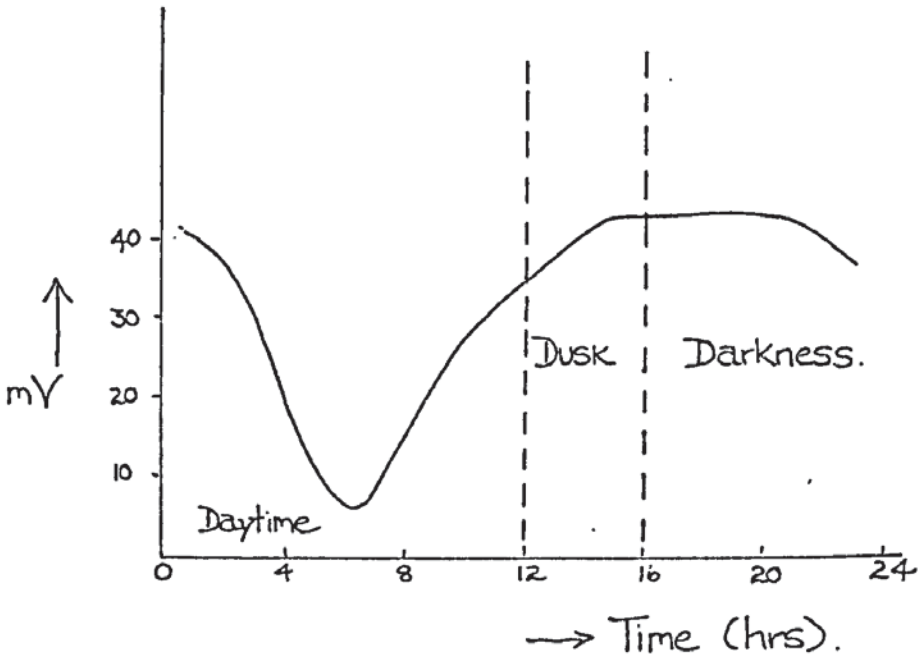

Graph 5

Ag/Ag Cl potential variation with sunlight during 24 hours.

Robinson and Frost (32) state that light can cause changes in the volume causing exfoliation of the Ag Cl film. Carmody (41) reports light changing the electrodes potential. Plum coloured electrodes seem immune to this but white ones, when exposed, change potential and the colour turns to brown.

Fresh hydrochloric acid solutions also gave brown electrodes of unstable potential, whereas old well used acid anodising solutions gave grey/white stable reproducible electrodes.

SECTION (12)

PERIODIC PHENOMENA

Lal, Thirsk and Wynne-Jones (25) looked at the periodic phenomena occurring during polarisation, where fluctuations were observed when the current was interrupted, as in Graph 6.

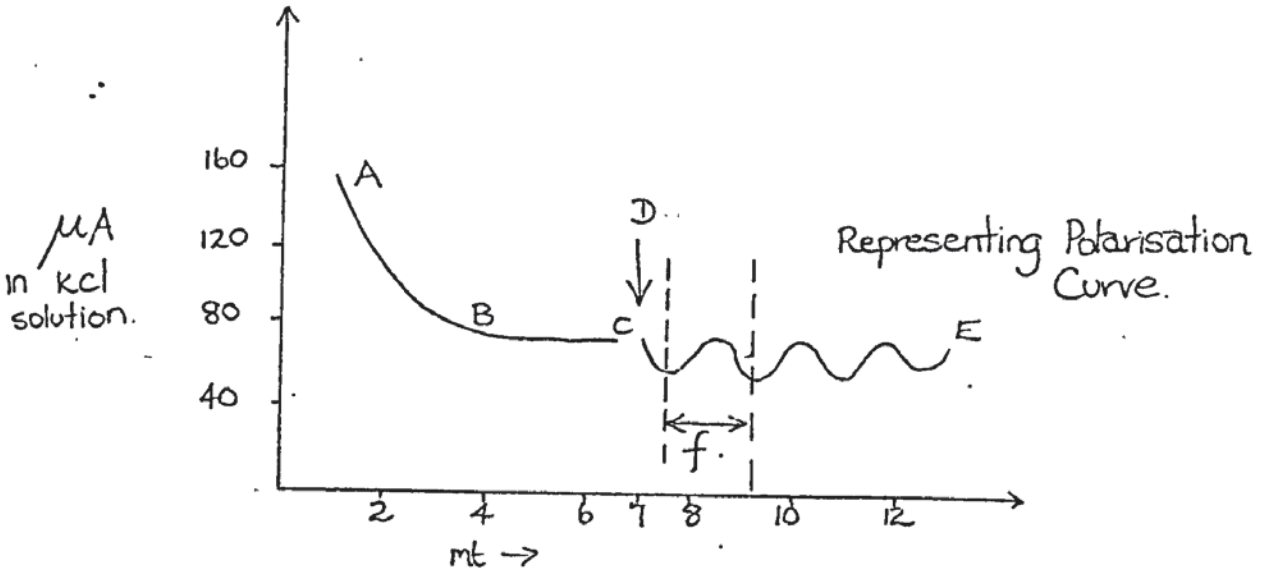

Graph 6

They used initial deposits of differing thickness in their experiments, as seen in Graph 7 below.

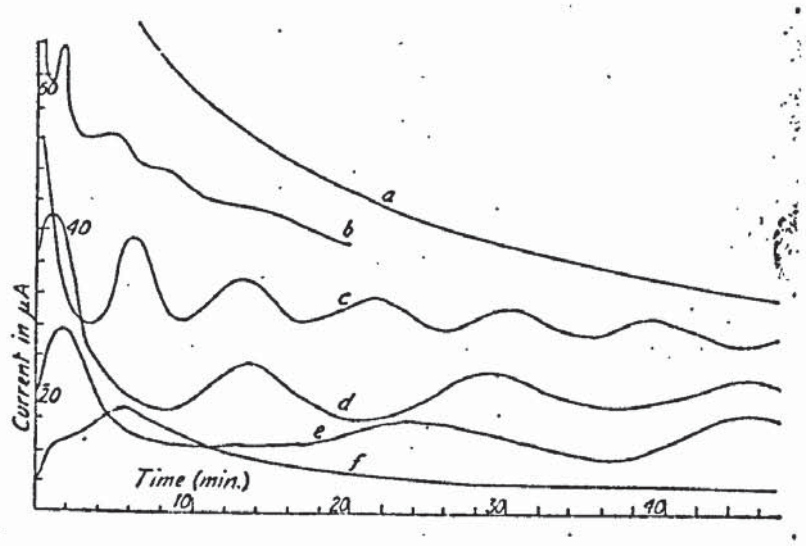

Graph 7

This shows how the thickness affects the periodicity of the phenomena. If the film thickness was kept constant and the time of interruption of the current was varied, then the set of graphs seen in Graph 8 is gained.

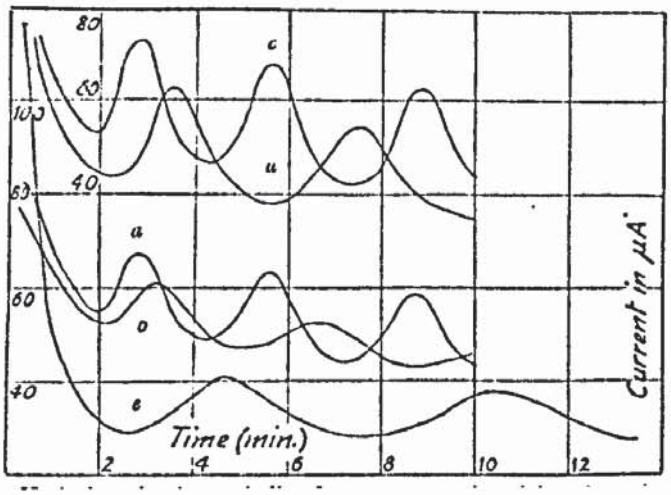

Graph 8

The concentration of HCl anodising solution was also varied to see the effect, which was roughly the same as in Graph 8. A layer of constant thickness was also produced and left for a set resting time, then anodising restarted at differing current densities to see the effect, as shown in Graph 9.

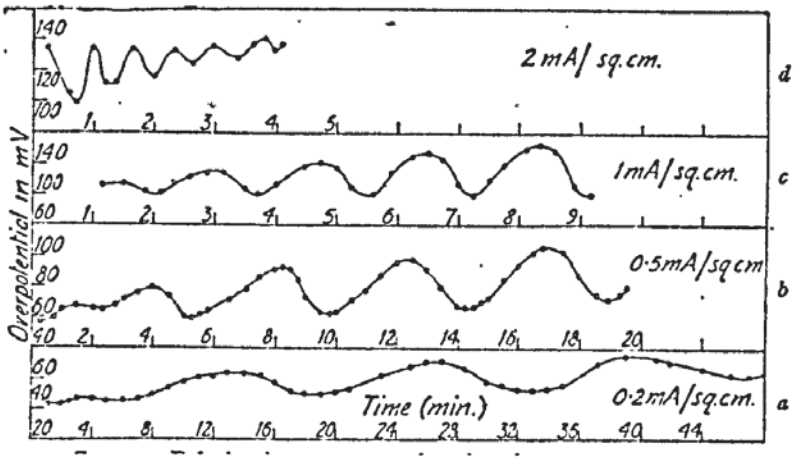

GRAPH 9

It can be seen that as the new current density increases, so the period of oscillation increases also. It is interesting that the periodicity phenomena does not occur in either bromide or iodide films, and that the film has to be greater than 5×10^{-7}m thick and less than 2×10^{-5}m thick for the periodicity to occur.

If anodising is being undertaken and periodicity occurs, when the film exceeds 2×10^{-5}m thick the phenomena will suddenly disappear. The best range for the phenomena is between 2×10^{-6}m to 5×10^{-6}m film thickness.

Graph 10 shows a straight line relationship between the current density and the frequency of oscillation; the Graph shows the relation between the charge passed during each oscillation, and the current density, and it shows that there is little relation between the two parameters. The charge passed during each oscillation is almost independent of the current density.

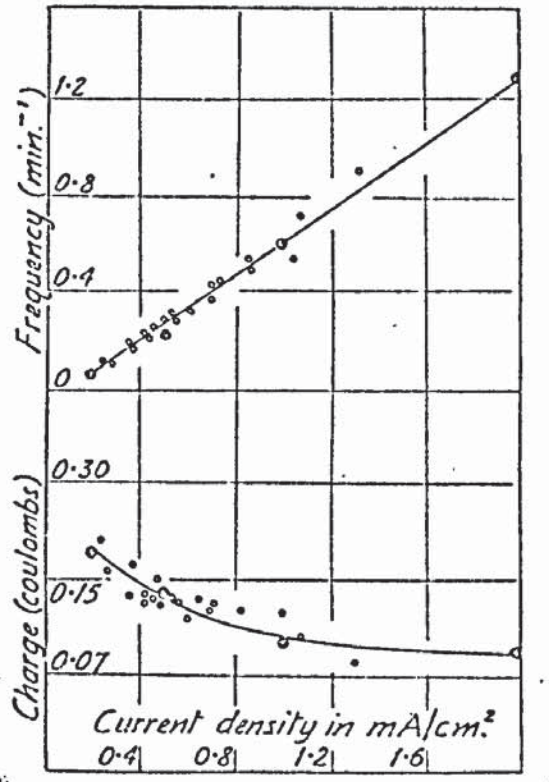

Graph 10

Graph 11 shows the relationship between the period of oscillation and temperature in 0.5 N KCl at various current densities, these also being straight line relationships the slope being different for different densities though. This periodic type behaviour is quite common, an example of this being precipitation by Liesegang rings (46). It is reported that the periodic behaviour could be from effects and processes occurring in the solid or in the solid film building.

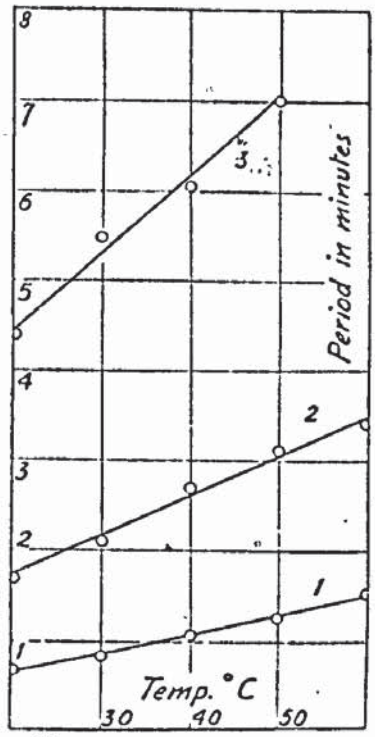

Graph II

One explanation for the periodic behaviour is by strain induced in the growing film, due in part to its adherence to the silver. The effect is produced by relief of the strain by breakdown in the uniform structure, lessening the restriction on the diffusion of chloride ions by the hitherto coherent layer. This appears as either an increase in the current on the chronogalvanic graphs or a decrease in the overpotential in the chronopotentiometric curves.

Another explanation of the change in overpotential effect would be that the change in concentration at the face of the electrode is a function of the rate of formation of crystallisation centres, the way in which they deposit on the silver chloride surface and the rate of deposition. The linear relationship between the frequency and the current density may be interpreted by the assumption that the quantity of electricity passed during each oscillation is equivalent to the form or morphology of the film up to the point of rupture. The linear relation of the temperature coefficient of periodicity, and the current density, supports this mechanism.

Lal, Thirsk and Wynne-Jones (25) assume that the periodic behaviour is seen only after stopping the current for more than 1 second, this being because there is a different type of crystal growth on restarting polarisation, due to change in the film structure during arrest.

SECTION (13)

SUMMARY

It is seen that growth of anodic oxide films on various metal surfaces can give films comprising of a number of layers, each porous, and a number of different particles such as needles growing eventually into platelets, nodules on particles, and spherical particles depositing in areas associated with irregularities or stresses in the metal surface.

It is pointed out that silver forms a film which slowly decreases in porosity as it grows. Formation of small nuclei occurs quickly after start of anodising, producing a layer that does not cover the whole surface in a monolayer. Some workers, like Huber, found no porosity probably due to use of very thick films.

Current density plays an important part in the growth mechanism and causes different morphologies. The film grows into bulbed mounds after the primary particle nucleation, and the slower the film is grown or the lower the current density conditions, then the greater the film resistance, presumably due to lower porosity.

Some authors suggest the film grows at the Ag/Ag Cl interface. Transport of material is mooted to be by complex ion formation and deposition from solution, the material transporting up the pores which can be self or mutually blocking, especially at higher temperatures where dissolution is greater. The number of pores will probably diminish as the film grows thicker.

The film takes a period of time after anodising to adjust to its equilibrium potential, some authors stating that light does not affect it during this period. This is not found to be the case in practice, and it is also suggested that the aging period is due to chloride ion depletion in the pores.

On reduction of the film granular masses are reported, much like the original chloride film structure. It is also found that interrupting the anodising, after a period, produces periodic waves in the potential/time curves. This is put down to either strain relief producing a chloride ion concentration rearrangement, or that the formation rate of the particles changes.

In none of the works reported has the film been looked at using the SEM, and this technique has been found extremely useful in examining the film morphologies. This obviates the necessity of delicate and unpredictable experiments involving electrochemical measurements to deduce the film structure.

Information gained in this work using the SEM can be used to enhance the properties and durability of the Ag/Ag Cl electrode, and also throws more light on the processes of anodic oxide film growth.

SECTION (14)

LIST OF LITERATURE SURVEY REFERENCES

(1) Young L. Anodic Oxide Films.
Academic Press, 1961.

(2) U.R. Evans. The Corrosion and Oxidation of Metals.
Scientific Principles & Practical Applications.
Edward Arnold Ltd., 1960.

(3) W.H.J. Vernon, E.I. Akeroyd, E.G. Stroud, J. Inst.
Met. 1939, 65, 310.

(4) B. Lustman. Trans. Electrochem. Soc.
1942, 81, 359.

(5) Pfefferhorn, . Naturwissenschaften.
1953, 40, 551.

(6) Encylopaedia of Electrochemistry.
Ed. C.A. Hampel.
Reinhold Pub. Corp. 1964.

(7) K.S. Indira, K.S.G. Doss, J. Electronal. Chem. and
Interfacial Electrochemistry. 17(½) 145-51, (1968)

(8) E.N. Pugh, A.R.C. Westwood
Amer. Soc. Test. Mater. Spec. Tech. Publ.
No. 425, 228-47, (1966).

(9) G.J. Moody, R.B. Oke, J.R.P. Thomas.
Analyst (London), 1969, 94(1122), 803-4.

(10) Hideo Onove, Takeski Hirakawa, Jaheo Matsuno.
Denki Kagaku 1970, 38(6), 437-43.

(11) F.H. Gibbard. J. Electrochem. Soc.
1973, 120(5), 624-7.

(12) Maatschappij von Electriscke Bedriffoaubomatisering
Electrofact N.V. Neth. Appl. 301, 617.
Oct 11, 1965, Ger. Appl. Jan 1963.

(13) E.M. Field, D.R. Holmes.
Corrosion Science 1965, Vol 5, pp 361-370.

(14) M. Turner, P.A. Brook.
Corrosion Science, 1973, Vol 13, pp 973-983.

(15) G.J. Bignold, R.Garnsey, G.M.W. Mann.
Corrosion Science, 1972, Vol 12, pp 325-332.

(16) Ashok K. Vijh, Corrosion Science, 1971, 11, 161-167.

(17) K. Grauer, W. Feitknecht.
Corrosion Science 1966, 6, 301-311.

(18) Hiram Gu, Douglas N. Bennion.
J. Electrochem. Soc.
Vo. 124, No 9, pp 1364, (1977).

(19) J. Katan, S. Szpak, D. Bennion.
J. Electrochem Soc. Vol 121, No 6, pp 757, (1974)

(20) A. Ziabriki - J. Chem. Phy. 48, 4368, (1968).

(21) S. Szpak, A. Nedolulla, J. Katan.
J. Electrochem. Soc. Vol 122, No 8, pp 1054.(1975)

(22) D.A. Vermilyea. Advances in Electrochemistry and Electrochemical Engineering. Anodic Films. Publ. Interscience Publ. Vol 3 1963.

(23) M. Fleischmann, H.R. Thirsk
J. Electrochem. Soc. Vol 110, No 6, 1963, pp 688-698

(24) H. Lal, H.R. Thirsk, W.F.F. Wynne-Jones.
Transactions of the Faraday Soc. 1951, Vol 47, pp 70-77.

(25) H. Lal, H.R. Thirsk, W.F.F. Wynne-Jones.
Trans. Far. Soc. 1951, Vol 47, pp 999-1006.

(26) G.W.D. Briggs, H.R. Thirsk.
Trans. Far. Soc. 1952, 48, pp 1171-1178.

(27) Schwab. J. Physic. Chem. 1950, 54, 576.

(28) D.J. Sayer, J.L. Roberts.
Experimental Electrochemistry for Chemists. pp 39-45.

(29) W.Jaenicke, R.P. Tischer, H. Gerischer.
Z. Elektrochem. 1955, 59, pp 448.

(30) Von K. Huber
Z. Elektrochem. 1955, 59, pp 693.

(31) R.D. Giles.
Electroanalytical Chemistry and Interfacial Electrochem.
Vol 27, 1970, 11-19.

(32) F.P.A. Robinson, F.A. Frost.
Corrosion, (N.A.C.E.) Vol 19, 1963, No 4, pp 115.

(33) Ives & Janz
"Reference Electrodes, Theory and Practice"
Academic Press 1969, pp 179-226.

(34) Fischbeck
Z. Anorg. Chem. (1925), 148, pp 97.

(35) Tubandt
"Handbuck der Experimatal Physik"
Vol 12 part 1.

(36) A.L. Afanasiev
J. Am. Chem. Soc. (1930), 52, 3477.

(37) D.A. MacInnes and K. Parker
J. Amer. Chem. Soc. (1915), 37, P, 1445.

(38) E.K. Smith, J.K. Taylor
J. Research Natl. Bur. Standards.
(1938), 20, 837.

(39) H. Taniguchi, G.T. Janz,
J. Electrochem. Soc. (1957), 104, p 123.

(40) W.J. Hornibrook, G.T. Janz, A.R. Gordon
J. Amer. Chem. Soc. (1942), 64, p 513

(41) W.R. Carmody
J. Amer. Chem. Soc. 1929, 51, p 2901

(42) W.R. Carmody
J. Amer. Chem. Soc. 1932, 54, p 3647

(43) W.J. Müller
Metallic Corrosion, Passivity and Protection,
1946, pp 51-54.

(44) A.D, Roberts. M.Sc. Dissertation. 1976. University of Aston In Birmingham. Dept. of Metallurgy.
"The Silver/Silver Chloride Electrode: It's Film Structure and Electrical Properties".

(45) M.J. Longster, D.J. Arrowsmith.
Proc. 5th ICML-NACE, 1974, pp 925.

(46) Hedges "Liesegang rings and other periodic structures"
Chapman & Hall, 1932.

(47) Kohlschutter & Stocker.
Helv. Chem. Acta. 1939, 22, 869.

CHAPTER 3

EXPERIMENTAL PROCEDURES

EXPERIMENTAL PROCEDURES

SECTION I

EXPERIMENTAL CONCEPT

The experimental concept was to produce a stable anodic silver chloride film on the surface of silver, to study the initial growth characteristics, and by varying the dependent and independent variables associated with the film formation, determine the conditions required to produce compact stable films with minimum porosity.

Many of the film variables, or experimental variables, were deemed impossible to measure quantitatively or keep stable, and these were eliminated. An example of this being light, which had been found in past experimental work (44) and in the literature (33) to affect the electrode potential and film characteristics. The equipment was placed therefore in a dark-room and kept completely sealed from extraneous light, the only illumination for all experiments being from a red photo safety light.

Oxygen was also deemed to be deleterious to the resulting film, so measures were taken to stop as much oxygen and other dissolved gases from remaining in the anodising, and other, solutions. Consequently dry pure white spot class nitrogen was bubbled through the solutions before each experiment, and a vacuum degassing technique used to remove, by boiling under reduced pressure, any remaining dissolved gases. Temperature in the latter experiment was also controlled, and a rig was designed to specifically enable all variables to be kept under control.

SECTION (2)

EQUIPMENT

The basic rig (see Figs 5 and 6 and pics 1 to 7) consisted of a stainless steel tank in which were placed two flasks of 1 ltr. volume which had exits and taps in their bases. To enable these exits to protrude from the tank base, two holes were cut in the tank. The flasks were then seated on specially moulded holders made of casting resin, and sealed into place with a flexible sealant (to allow for temperature induced dimensional changes) of silicone rubber.

The tanks were swathed in expanded polystyrene foam bricks to enable the control of temperature to be carried out accurately, so as to stop heat flow either out or in. The exits at the bases were to facilitate cleaning and solution removal after use. At the top of the flasks there were flanges to enable the lid to be clamped down firmly, and these lids, on either flask, contain a large number of ports to enable entry of instruments into the flask, and their use during experiments without having to disturb the equipment greatly.

The temperature control of the experiments was carried out by filling the tank up to the level of the flanges on the flask (the level of the liquid in the flasks) with a 50/50 mixture of anti-freeze and water. Anti-freeze was used as this allowed the greatest range of temperature, and croffles were spread on the surface to cut down temperature and fluid loss. Connected to this reservoir was a refrigeration unit which cooled the fluid down considerably, then pumped it through a heater/ thermostatic control unit which heated it up to the required temperature before returning it to be circulated round the tank. This enabled a very rigorous control of temperature to be carried out over a wide range.

The idea behind having two flasks was to enable the solution to be degassed and raised to the correct temperature in one, then transferred to the second for the experiment to proceed. This also enabled a second solution, of synthetic seawater B.S.1391 (1952) (Ref Part 2 "Atomic Research Establishment" salt droplet test) containing:

NaCl	23g/l	
$Na_2SO_4.10H_2O$	8.9g/l	ANALAR
$MgCl_2.6H_2O$	9.8g/l	
Ca Cl_2 (anhydrous)	1.2g/l	
in distilled water		

to be degassed and heated while the anodising experiment proceeded. This enabled the solution to be exchanged with the initial 0.1 N HCl anodising solution as soon after the anodising was complete, to ensure the least contamination or aging of the specimen before measurement could begin.

The degas flasks purpose was to remove traces of dissolved gases in the solutions by bubbling in white spot nitrogen gas, then evacuating the flask to boil out the gases, then again purging with nitrogen. The nitrogen gas could also be used to purge the anodising vessel to ensure the least contamination with air.

Solution could be transferred from one vessel to another using either a hand pump, or by letting the nitrogen gas build up to sufficient pressure above the solution to push it through, via the hand pump, to the adjacent flask. In the anodising flask the anode and cathode were built into the lid of the vessel, and these were constructed primarily of glass and nylon, these were modified for increased strength to stainless steel and nylon. The stainless steel was coated with an insulating layer of Lacomit stopping off solution to prevent solution contamination.

The assemblies were set into the lid at a set distance apart, using casting resin, and electrical contact to the lid exterior was achieved using two tungsten rods set into the glass. Pure copper cube connections were attached to the upper region of the lid for instrument and power connection.

Power in all cases came from a constant current supply source which would supply a constant current at a constant set potential. Recording of results was achieved using a twin pen recorder, this could be connected to the various measuring points on the flask, calibration of this being by a Vibron electronic voltmeter.

The most complicated parts of the assembly were the anode/cathode holders, (Fig 5 and 6). These were fitted onto the stainless steel or glass rods, and were constructed of machined nylon. The anode consisted of a threaded contact holder on to which threaded the silver specimen holder, this pressed the specimen onto the current contact and contained a seal to ensure that no solution penetrated. Onto the specimen holder threaded the KCl solution holder, open to solution via a sintered glass bridge.

The cathodic side consisted of a simple machined nylon block slotted onto the stainless steel rod, the cathode consisting of a platinum flat wire coil. The potential measurements were carried out using a saturated Calomel reference electrode, this being placed as near as possible to the anodic cell, and the conditions kept as constant as possible from experiment to experiment.

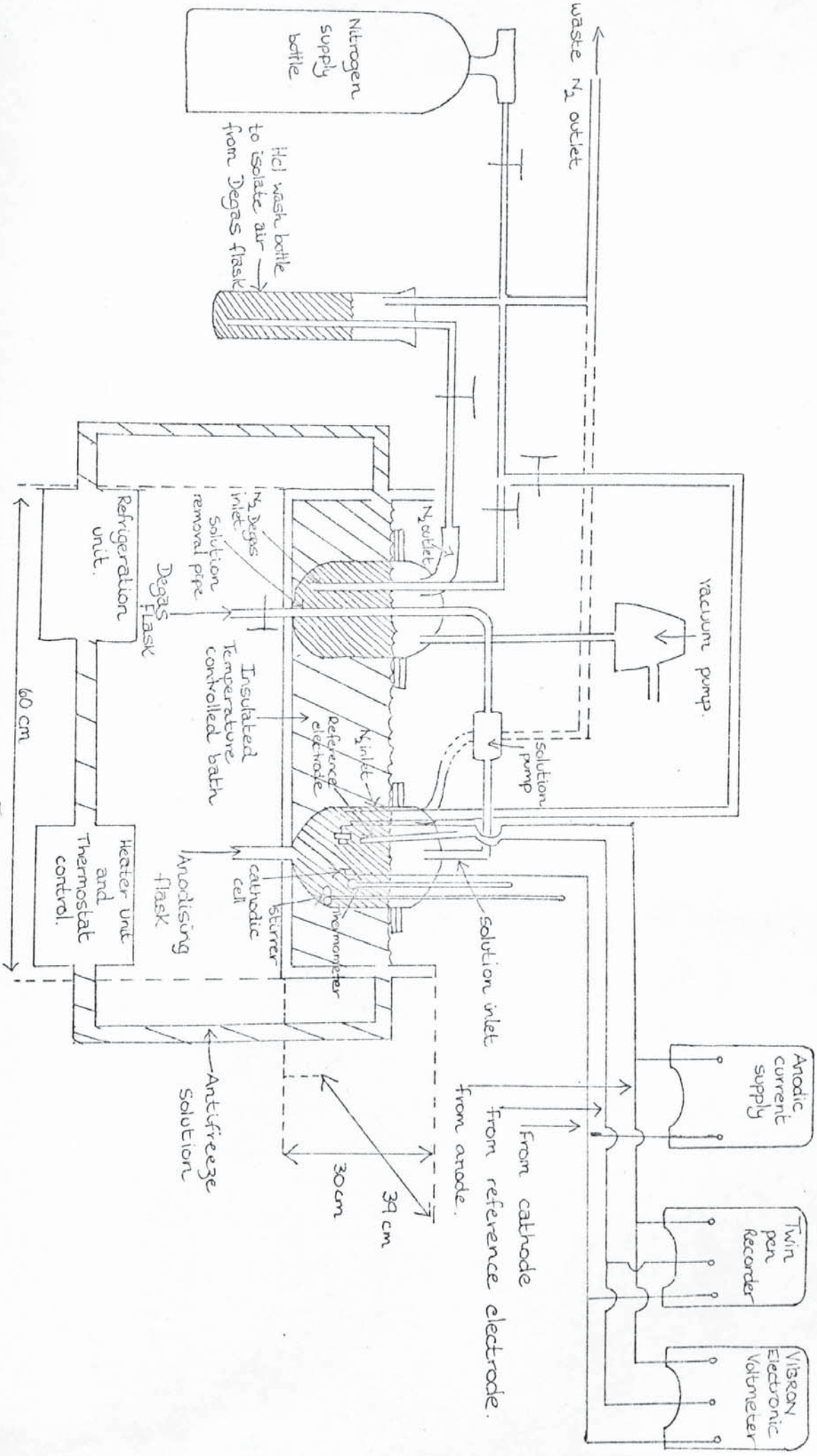

FIG 5 SCHEMATIC DIAGRAM OF EQUIPMENT

FIG 6 DIAGRAM OF CELLS

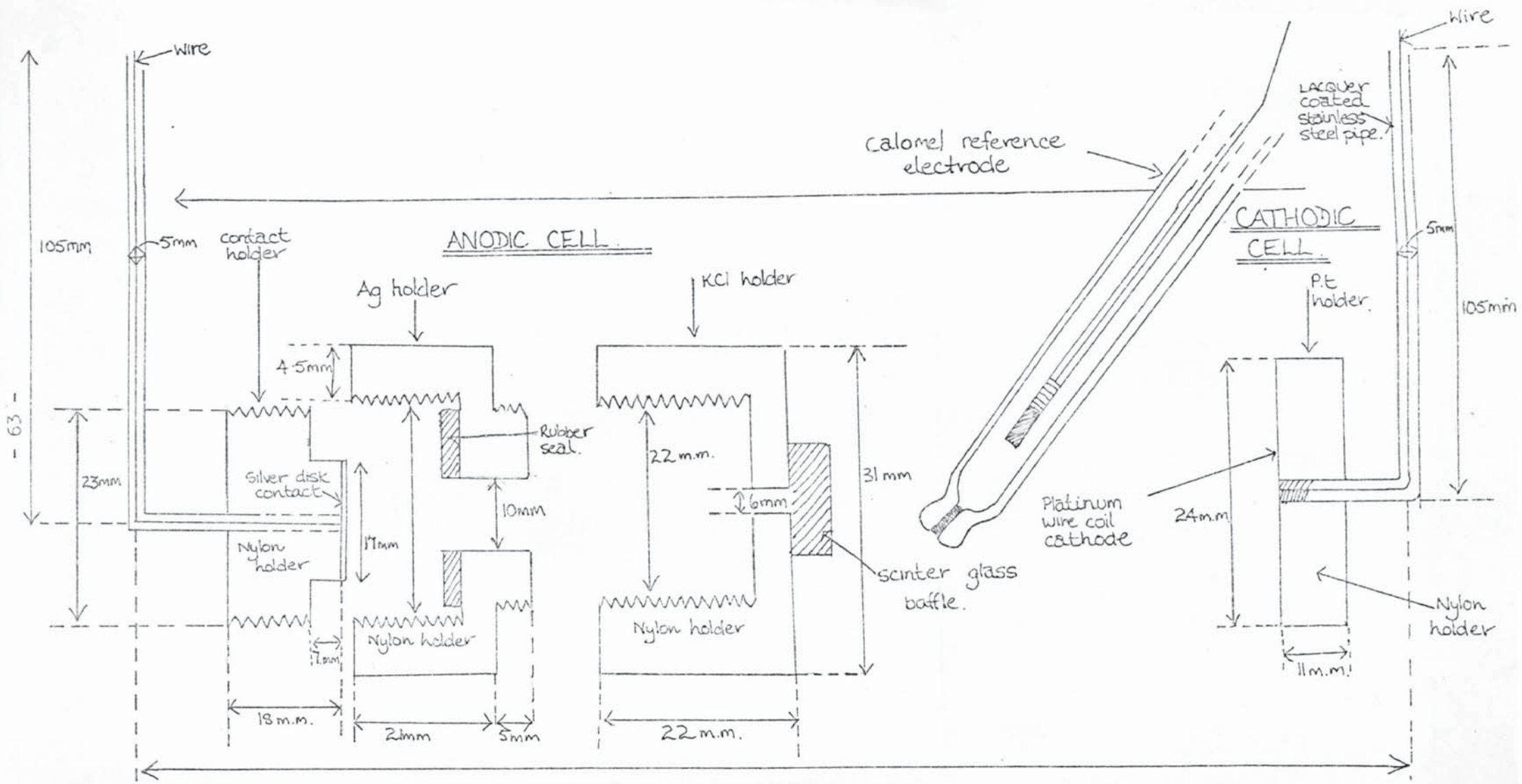

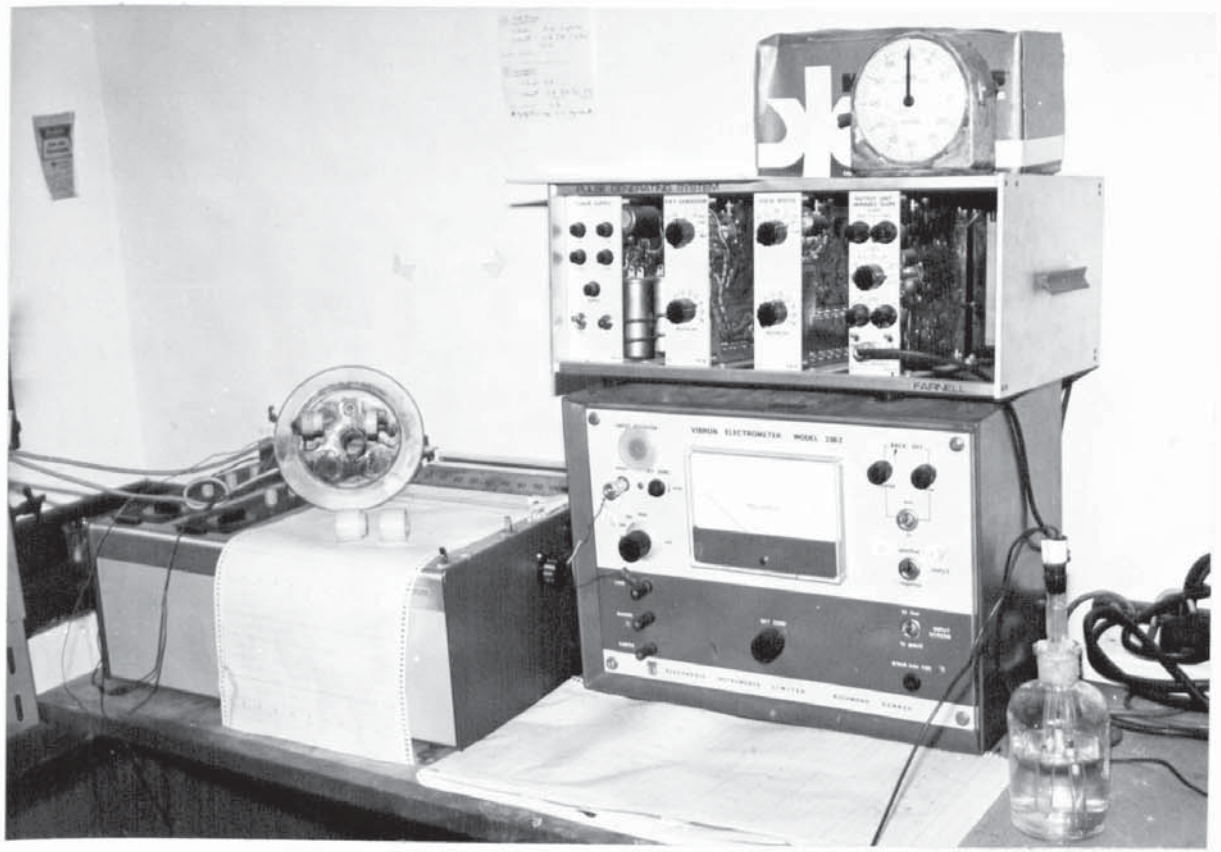

PIC 1 SHOWING THE RECORDING EQUIPMENT AND THE SPECIMEN HOLDER

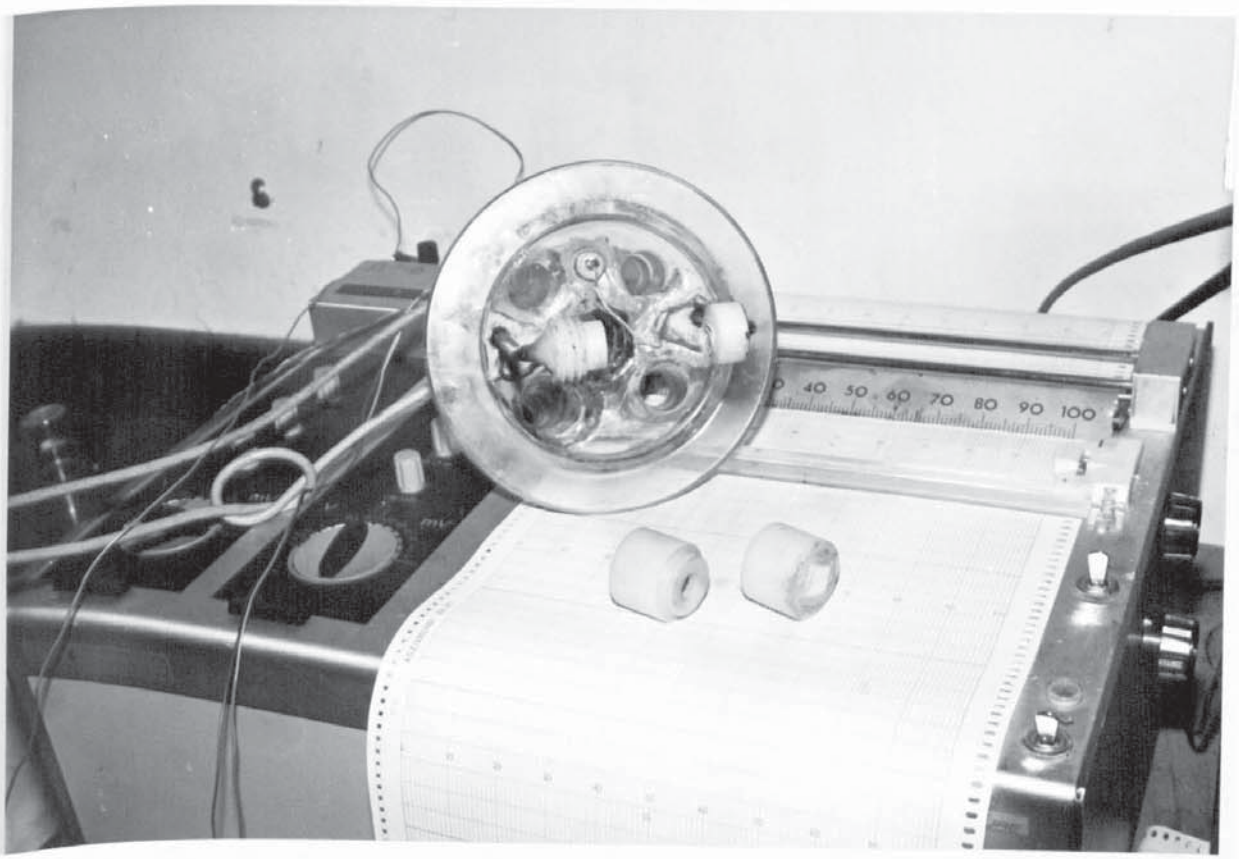

PIC 2 SHOWING THE SPECIMEN HOLDER DISMANTLED AND THE COUNTER ELECTRODE/CATHODE ASSEMBLY.

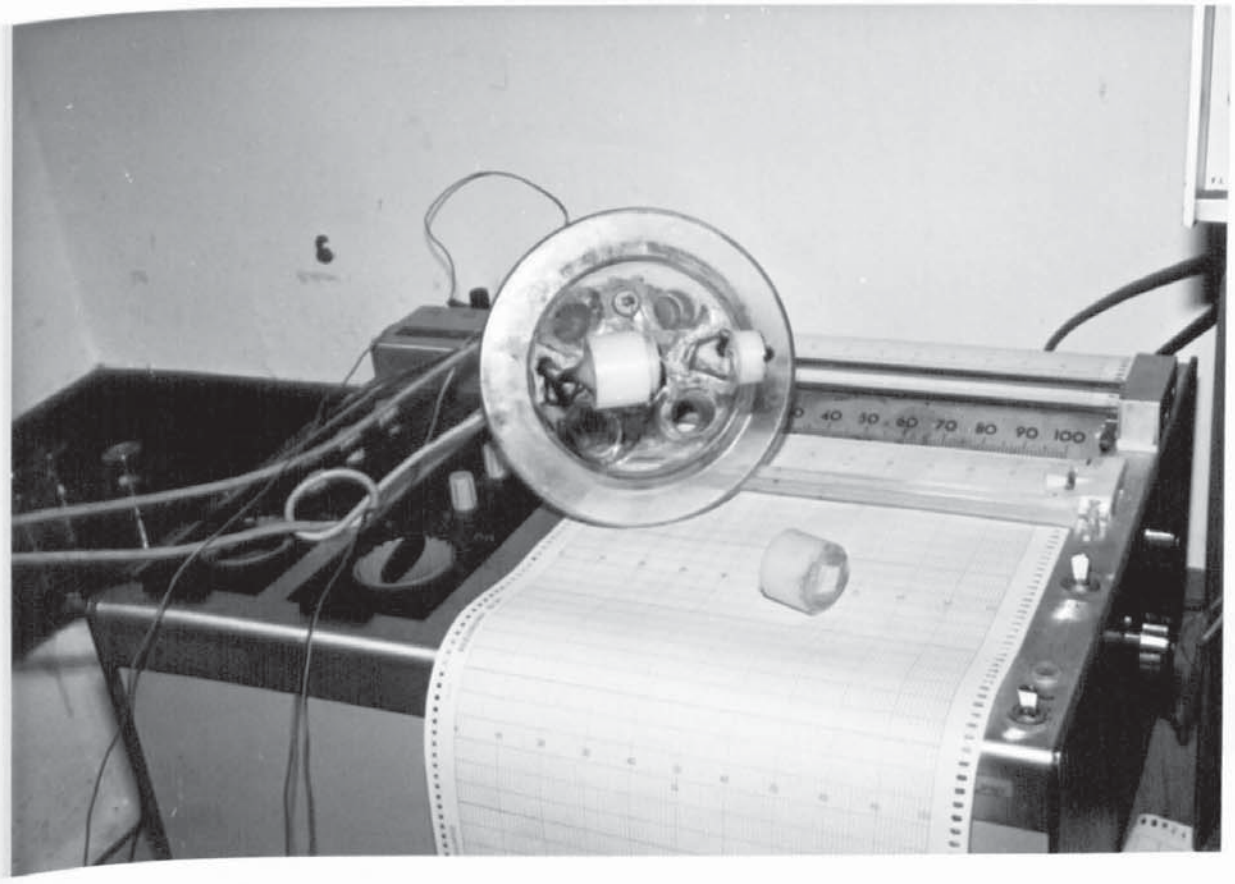

PIC 3 SHOWING THE SPECIMEN HOLDER CAP SCREWED IN PLACE

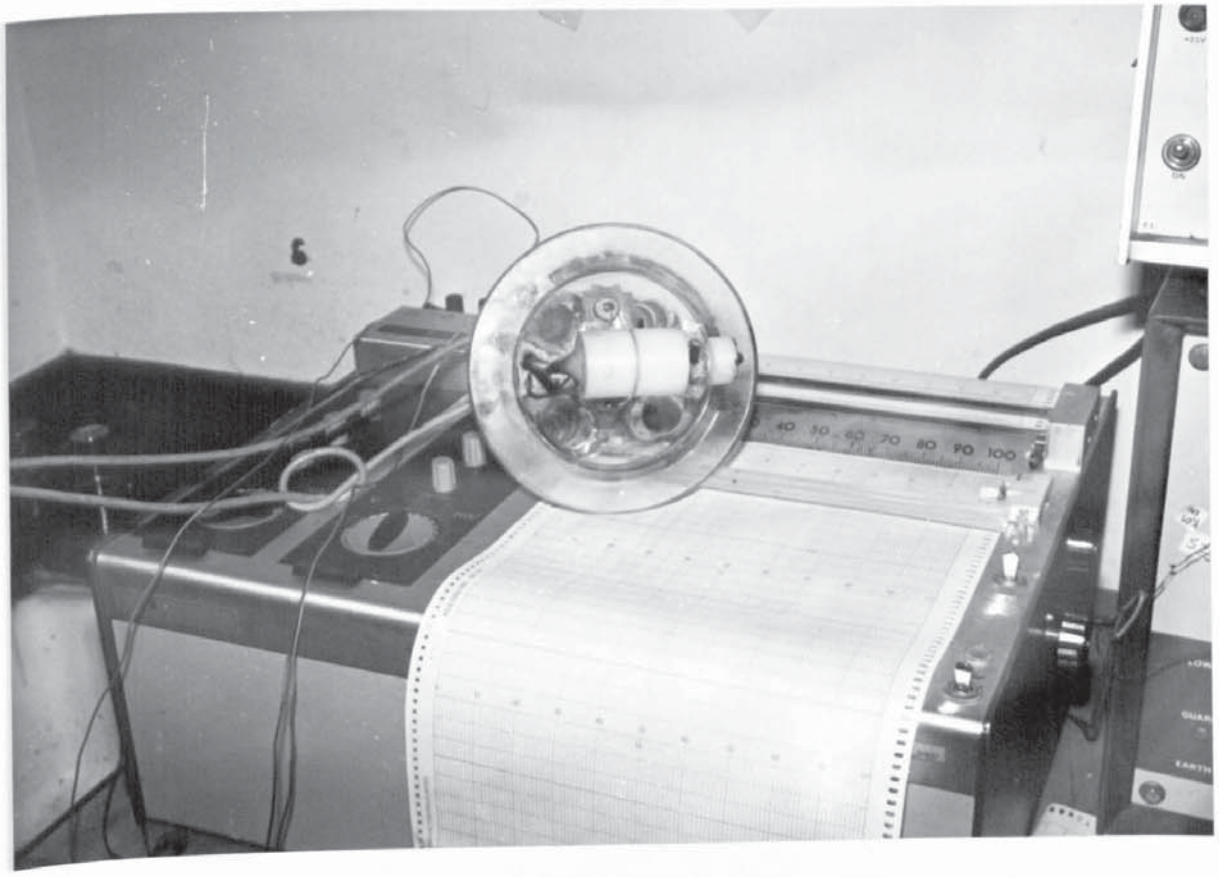

PIC 4 SHOWING THE PROTECTIVE CAP, FOR USE IN POTENTIOMETRIC TESTS, IN PLACE ON THE SPECIMEN HOLDER.

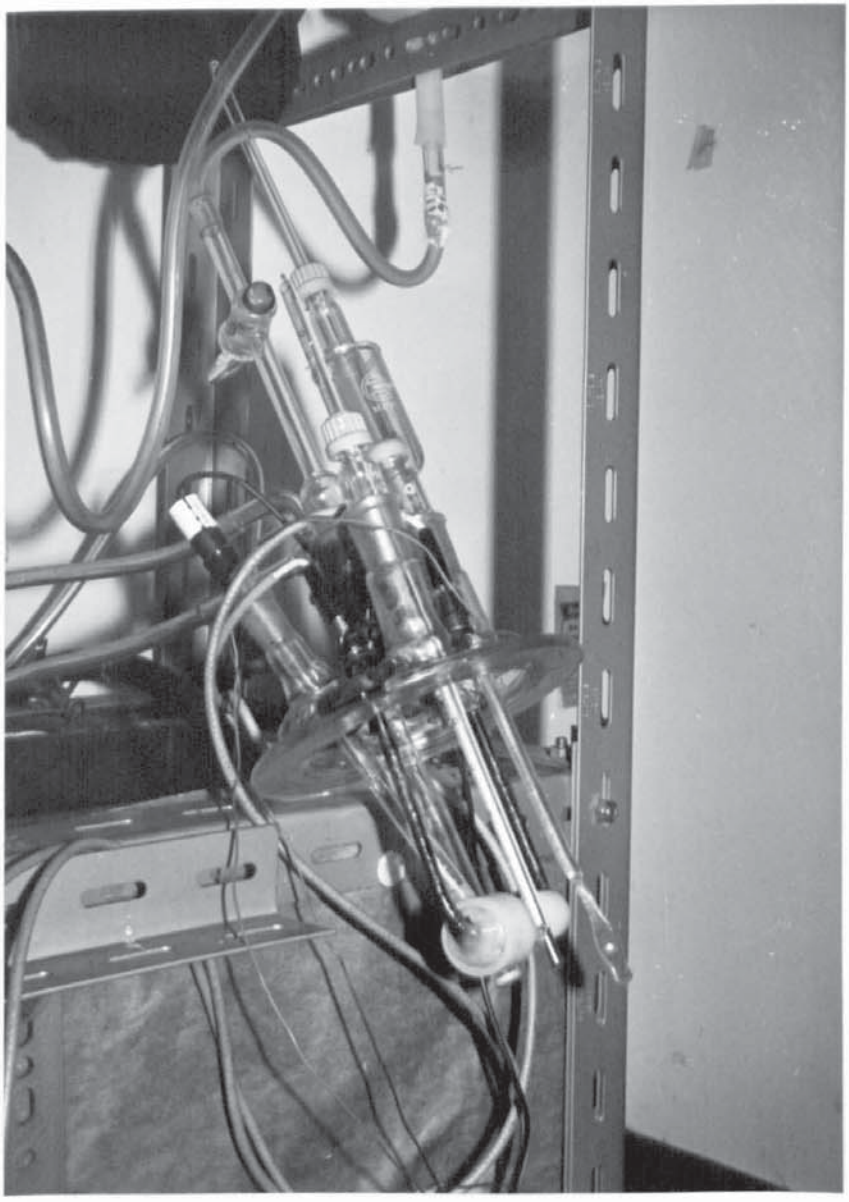

PIC 5 SHOWING THE FULL ANODISING AND TEST CELL COMPLETE WITH THERMOMETER, STIRER, REFERENCE ELECTRODE AND CAP ASSEMBLY.

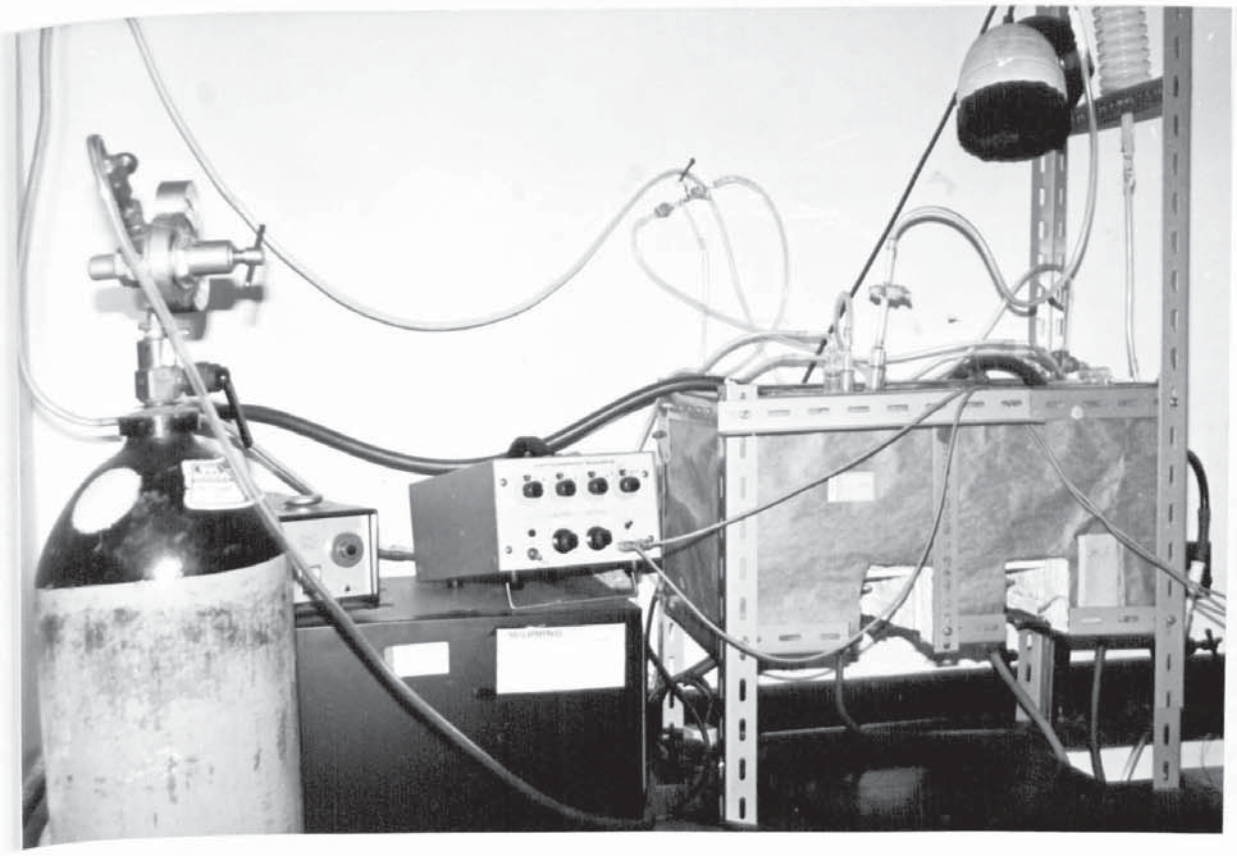

PIC 6 SHOWING THE CONSTANT TEMPERATURE BATH, AND SUPPLEMENTARY EQUIPMENT.

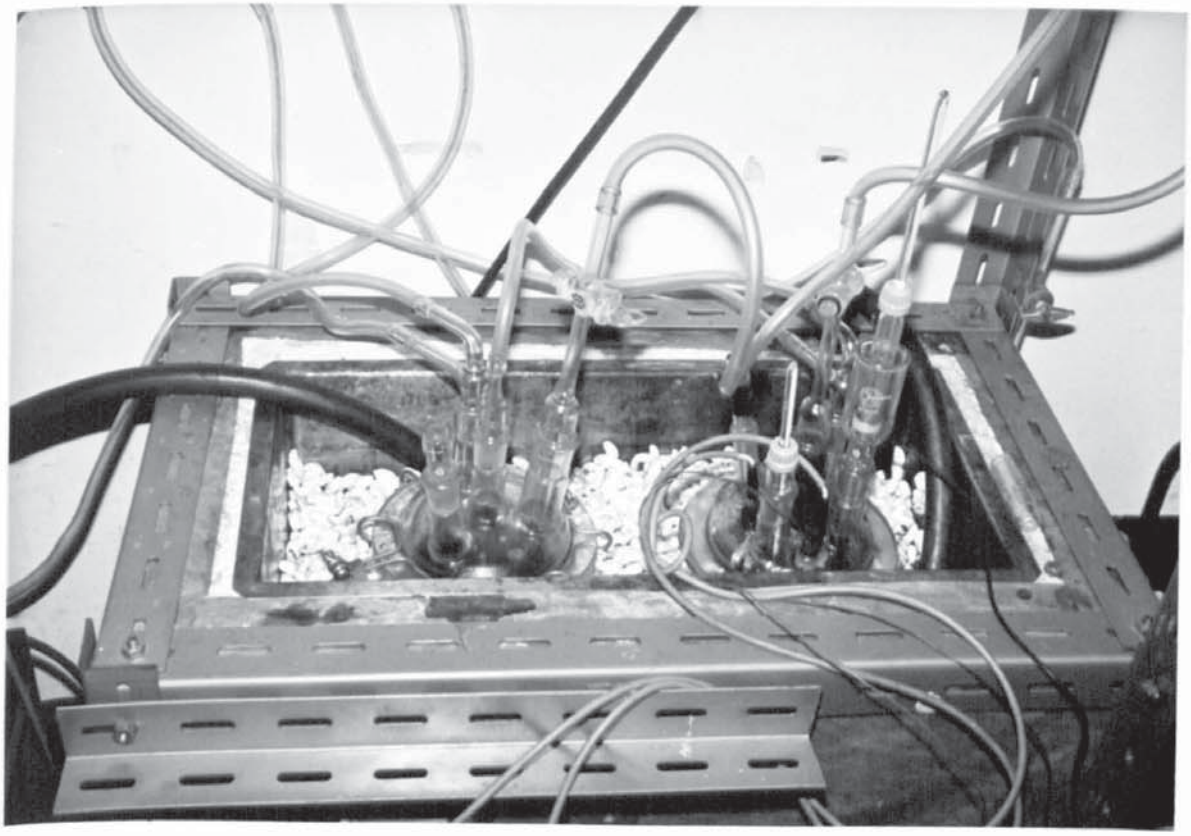

PIC 7 SHOWING THE SOLUTION GAS FLUSH, TEMPERATURE BATH AND ANODIC CELL ASSEMBLY

SECTION (3)

SPECIMEN PREPARATION

The specimens were all produced from pure silver sheet donated by Johnson Matthey Limited. They were cut by punch from the sheet, each having a diameter of 1 cm. Some of the specimens were prepared by abrading with Silvo proprietory silver cleaning compound, and others were left in their original scratched and rolled state, but abraded with a soft cloth.

They were all washed first in distilled water, then in Analar acetone, then again in distilled water before being placed in the anodising cell. Different treatments were given to a selection of specimens before, during and after anodising; for instance, specimen 4a was made cathodic before anodising, i.e. electrocleaned, to see what effect this would have on the resultant film. Several other specimens were annealed before anodising i.e. specimens 4d and 4b at 500°C for 2 hours under 1 atmosphere of nitrogen. In two cases, i.e. specimens 4d and 4c, the chloride film and basal silver were annealed after anodising also. Compression of the film was attempted as on specimen 4e, and then annealed under the above conditions, compression being at 2 tons/cm^2 for 5 minutes, or as in specimen 4f where the film was only compressed.

In some of the experiments the film was covered by a hydroplastic film which was then immersed in water to allow the gel film to thicken and become ionically conductive. This was to observe the effects of a protective film on the surface. Carbon black was in some cases mixed ultrasonically with the hydroplastic, and on one specimen the bare silver was coated in the hydroplastic and then anodising carried out through the film after the plastic had been impregnated with water.

Some of the specimens were sand blasted to see what effect this would have on the adherence and film layer formation of the chloride, as this would remove the Beilby layer and increase the surface area. Some specimens were vacuum annealed for 4 hours at 920°C (specimen 8.9).

Electropolishing and electrodeposition were other specimen preparation techniques tried, specimen 8.7 was electropolished and electrodeposited in silver cyanide/nitrate solution, at 50 V, 17°C, 1 ma/cm ^{2} for 15 minutes for polishing and 5 ma/cm ^{2} for 6 minutes for deposition. Specimen 8.8 had deposition at 1 ma/cm ^{2} for 3 hours and 9 ma/cm ^{2} for half of one hour successively. These specimens were subsequently examined and anodised to see the effect of the treatment.

Experiments were also carried out to observe the pore filling characteristics of the porous anodic layer. This was achieved by boiling the specimen in distilled water, or water plus silver chloride, or by filling with a mixture of Lacamit and acetone and drying the resulting film, then dissolving off the excess surface layer.

Several experiments were carried out to observe the partial dissolution of the film using a saturated solution of sodium thiosulphate, in which silver chloride readily dissolves. It was attempted to gradually cut layers through the film, to see the change in structure from the top to the base of the film.

A bright layer of silver was also deposited on the specimen then anodised. The deposition was at 20 ma/cm ^{2}, 50 V, 2 minutes, this being achieved using a TP solution additive donated by Ashton and Moore Limited, Birmingham.

To observe the way in which the film formed, i.e. from either solid or solution transport of the ions, a series of experiments was carried out using nylon thread attached to the silver surface, the idea was to see if any silver chloride was deposited on the thread and as to how the film would react to the presence of the thread, i.e. would it push the thread from the surface or would it form around it. This would thereby show if the film grew from the base downwards or from the top surface and upwards, which is in fact found to be the case.

SECTION (4)

EXPERIMENTAL ANALYSIS

Apart from these variations in experiments, the main purpose was to see the effect of the variation of the anodising parameters on the anodic film formation. The parameters were mainly the current density, potential, time and temperature, the solution concentration and light conditions being kept constant at 0.1 N HCl and red light from a dark-room safety light.

The variation in the parameters was used to give a quantitative and qualitative analysis of the film forming characteristics. When an anodic film had been gained it was analysed mainly on the Cambridge Mark II scanning electron microscope, and the results, mainly in pictorial form, were analysed to gain the 92 measurements taken from each specimen, these to be used in the computer analysis to show the way the variation in parameters effects the film morphology.

Regression analysis was carried out also to gain a general mathematical model for the film growth in respect to the porosity of the film. This porosity was the main characteristic looked at in the film, and the experiments guided by computer analysis were arranged so as to achieve the point at which the experimental parameters yielded the lowest porosity possible. The film gained would then hopefully be a thin stable film with good adherence to the basal silver.

Preparation of the films for analysis on the SEM was achieved in several ways. A specimen could be simply mounted on a stub and the film top surface examined, but to enable examination of film thickness it was necessary to fracture the film, and the underlying silver, as opposed to slicing or cutting the film, which tended to smear the malleable Ag Cl and disguise the real structure.

The film and silver could then be mounted in a special holder which enabled the side on view of the film thickness to be easily observed.

In other cases it was necessary to dissolve the silver from the film, using concentrated nitric acid solution, in which case the film detached and could be examined separately. To observe these detached films, and other detached films gained from cracking of the film laterally and detachment from the silver substrate, it was necessary to attach the film to the stub by either adhering the film side on, so that it stood at 90° to the stub surface, or by attaching the film to a copper grid. This was of the type used for transmission electron microscope and was itself then attached to a pure copper sheet and the whole examined in the SEM.

This arrangement was used to stop the degradation of the film found when in contact with the aluminium stub. It was found that the film resulting from the etching away of the silver, tended even after prolonged washing to destruct when placed on most metals after only a few minutes, turning to a fine white ashy substance with no relation to the original film structure. As even on the copper grid degradation was found to occur even though quite slow, a different medium was used, this being a woven carbon cloth of high purity. This allowed the film to be observed before final destruction set in in a matter of hours.

Using these techniques it was possible also to observe the base layer of the film, and the primary particles. It was also possible to dissolve the silver chloride away using concentrated sodium thiosulphate, thus enabling the deeply etched and pitted silver substrate to be examined.

SECTION (5)

EXPERIMENTAL PROCEDURES

Neglecting different specimen preparations, the same experimental procedure was carried out for each specimen, so that reproducibility would be guaranteed. The procedure was as follows after the specimen had been inserted.

(1) Temperature set for experiment.

(2) Solution placed in vessel.

(3) Degas by nitrogen for ½ hour.

(4) Vacuum degas for ½ hour.

(5) Degas by nitrogen for ½ hour.

(6) Anodic flask flushed by nitrogen.

(7) When temperature correct, liquid pumped into anodic flask.

(8) Solution left to temperature stabilise.

(9) Solution agitated to ensure no gas bubbles adhering to silver surface.

(10) Lights extinguished except for safety light.

(11) Recorder calibrated.

(12) Anodising carried out for set time.

(13) During anodising the change in potential with time is recorded.

(14) Flask is then emptied of anodising solution.

(15) Flask flushed with distilled water.

(16) KCl cap inserted onto the end of anodising cell cap.

(17) The synthetic sea water is placed in the anodising vessel after degassing in degas flask.

(18) Change in potential is measured against time until the specimen has reached a stable potential at about 222 mV.

The chronopotentiometric analysis in KCl and synthetic sea water were not taken for all the specimens. This was mainly due to the discovery that when undergoing these measurements, the structure of the chloride film tended to change with a renucleation process occurring on the surface. This increased the porosity and general particle size of the film, resulting in an end structure which could not satisfactorily correlate with the variation in the anodising parameters.

Removing the specimens after anodising and observing on the SEM, then returning to the solution for measurements tended not to be satisfactory as the specimen would now be contaminated, and the electron beam of the SEM tended to reduce the chloride back to silver, thus giving spurious results later.

CHAPTER 4

EXPERIMENTAL RESULTS

EXPERIMENTAL RESULTS

CONTENTS

SECTION (I)

TABLE OF RESULTS

The tables of results that follow contain the information used to programme the computer for statistical analysis. Explanations of particle and pore types, and abbreviations, are also given.

V	50	65	55
CD	1·0	1·5	2·5
l	0·79	1·18	1·97
t	25	30	30
T	600	630	630
INDEX NO.	1	2	3
V*F	$1·266\times10^{-10}$	$1·99\times10^{-10}$	$3·32\times10^{-10}$
WF	$7·04\times10^{-4}$	$11·03\times10^{-4}$	$18·43\times10^{-4}$
W*P	$6·83\times10^{-4}$	$1·1\times10^{-3}$	$1·82\times10^{-3}$
DF	$1·61\times10^{-6}$	$2·528\times10^{-6}$	$4·22\times10^{-6}$
Hi	$1·2\times10^{-6}$	$5·9\times10^{-6}$	$1·78\times10^{-6}$
H2	$4·174\times10^{-6}$	"	$9·03\times10^{-6}$
H3	—	—	$8·42\times10^{-6}$
H*	$5·38\times10^{-6}$	$5·9\times10^{-6}$	$1·92\times10^{-5}$
Z	2	2	3
VOL	$4·22\times10^{-10}$	$4·63\times10^{-10}$	$1·51\times10^{-9}$
A	324000	288000	259200
R	90·01	57·12	78·01
Yr	$2·96\times10^{-10}$	$2·65\times10^{-10}$	$1·18\times10^{-9}$
a_1	$8·91\times10^{5}$		—
r*1a	(M5) 8×10^{-7}	(M5)	(M5) $5·93\times10^{-7}$
b	—	—	—
c	—	—	—
r*2a	(M9) $2·69\times10^{-6}$	(M9) $2·53\times10^{-6}$	(M86) $3·23\times10^{-7}$
b	—	(M5) $2·53\times10^{-7}$	—
c	—	—	—
r*3a	—	—	(M9a) $3·16\times10^{-6}$
b	—	—	—
c	—	—	—
P1a	(M5) $2·15\times10^{-18}$	(M5)	(M5) $8·72\times10^{-19}$
b	—	—	—
c	—	—	—
P2a	(M9) $3·81\times10^{-17}$	(M9) $6·75\times10^{-17}$	(M86) $1·41\times10^{-17}$
b	—	(M5) $6·78\times10^{-20}$	—
c	—	—	—
P3a	—	—	(M9a) $1·32\times10^{-16}$
b	—	—	—
c	—	—	—
r1a	(Q3) 6×10^{-7}	(Q3)	(Q3) $2·97\times10^{-7}$
b	—	—	—
c	—	—	—
r2a	(Q3) $5·22\times10^{-7}$	(Q3) $1·26\times10^{-6}$	(Q7) $5·26\times10^{-7}$
b	(Q1) $2·0\times10^{-7}$	—	—
c	—	—	—
r3a	—	—	(Q3) $2·11\times10^{-6}$
b	—	—	—
c	—	—	—
Y1a	(Q3) $1·36\times10^{-18}$	(Q3)	(Q3) $4·91\times10^{-19}$
b	—	—	—
c	—	—	—
Y2a	(Q3) $3·59\times10^{-8}$	(Q3) $2·96\times10^{-17}$	(Q7) $7·87\times10^{-18}$
b	(Q1) $5·26\times10^{-19}$	—	—
c	—	—	—
Y3a	—	—	(Q3) $1·18\times10^{-16}$
b	—	—	—
c	—	—	—
G	9	9,7	9,8,7
VE	0·05	0·067	1·89
VS	210.	222	216.

V	55	55	65
CD	1·5	1·5	2·5
I	1·18	1·18	1·97
t	45	30	45
T	630	690	690
INDEX NO.	4	5	6
V*F	$1·99 \times 10^{-10}$	$2·17 \times 10^{-10}$	$3·63 \times 10^{-10}$
WF	$11·04 \times 10^{-4}$	$12·09 \times 10^{-4}$	$20·19 \times 10^{-4}$
W*P	$1·0 \times 10^{-3}$	$1·2 \times 10^{-3}$	$2·0 \times 10^{-3}$
DF	$2·53 \times 10^{-6}$	$2·77 \times 10^{-6}$	$4·62 \times 10^{-6}$
H1	$5·97 \times 10^{-7}$	$2·76 \times 10^{-7}$	$5·85 \times 10^{-7}$
H2	$5·37 \times 10^{-6}$	$2·76 \times 10^{-6}$	$6·61 \times 10^{-6}$
H3	—	—	—
H*	$5·97 \times 10^{-6}$	$5·035 \times 10^{-6}$	$7·2 \times 10^{-6}$
Z	2	2	2
VOL	$4·69 \times 10^{-10}$	$3·96 \times 10^{-10}$	$5·65 \times 10^{-10}$
A	82800	26640	216000
R	57·66	45·0	35·74
Yr	$2·7 \times 10^{-10}$	$1·75 \times 10^{-10}$	$2·02 \times 10^{-10}$
a_1	—	—	—
r*1a	(m5) $1·5 \times 10^{-7}$	(m5) $1·38 \times 10^{-7}$	(m5) $3·9 \times 10^{-7}$
b	—	—	—
c	—	—	—
r*2a	(m9) $2·09 \times 10^{-6}$	(m9) $1·64 \times 10^{-6}$	(m9) $5·07 \times 10^{-6}$
b	—	—	(M9) $1·56 \times 10^{-6}$
c	—	—	—
r*3a	—	—	—
b	—	—	—
c	—	—	—
P1a	(m5) $1·4 \times 10^{-20}$	(m5) $1·1 \times 10^{-20}$	(m5) $2·49 \times 10^{-19}$
b	—	—	—
c	—	—	—
P2a	(m9) $3·82 \times 10^{-17}$	(m9) $1·84 \times 10^{-17}$	(m9) $5·46 \times 10^{-16}$
b	—	—	(M9) $5·57 \times 10^{-14}$
c	—	—	—
P3a	—	—	—
b	—	—	—
c	—	—	—
r1a	(Q3) $1·5 \times 10^{-7}$	(Q3) $2·69 \times 10^{-7}$	(Q3) $2·93 \times 10^{-7}$
b	—	—	—
c	—	—	—
r2a	(Q3) $2·99 \times 10^{-7}$	(Q3) $3·64 \times 10^{-7}$	(Q3)
b	—	—	—
c	—	—	—
r3a	—	—	—
b	—	—	—
c	—	—	—
Y1a	(Q3) $4·18 \times 10^{-20}$	(Q3) $6·26 \times 10^{-20}$	(Q3) $1·94 \times 10^{-18}$
b	—	—	—
c	—	—	—
Y2a	(Q3) $1·51 \times 10^{-18}$	(Q3) $1·15 \times 10^{-18}$	(Q3)
b	—	—	—
c	—	—	—
Y3a	—	—	—
b	—	—	—
c	—	—	—
G	9	9	9
VF	0·051	0·035	0·29
VS	227	222	222

V	66.5	68.75	68
CD	2.16	1.64	1.47
i	1.7	1.29	1.16
t	46.5	49	50
T	702	719	725
INDEX NO.	7a	16e	17f
V*F	3.19×10^{-16}	2.48×10^{-16}	2.25×10^{-16}
WF	17.73×10^{-4}	13.78×10^{-4}	12.49×10^{-4}
W*P	—	—	—
DF	4.06×10^{-6}	3.16×10^{-6}	2.86×10^{-6}
H1	7.2×10^{-6}	5.99×10^{-6}	5.25×10^{-6}
H2			
H3	—	—	—
H*	7.2×10^{-6}	5.99×10^{-6}	5.25×10^{-6}
Z	2	2	2
VOL	5.66×10^{-10}	4.7×10^{-10}	4.12×10^{-10}
A	—	—	—
R	43.64	47.3	45.5
Yr	2.47×10^{-10}	2.23×10^{-10}	1.87×10^{-10}
a_1	8.42×10^{5}	—	—
r*1a	(m5)	(M5) 5.56×10^{-7}	(M1) 6.56×10^{-8}
b	—	(M1) 1.85×10^{-7}	(M5) 5.25×10^{-7}
c	—	—	—
r*2a	(m2a) 8.0×10^{-7}	(M19) 3.7×10^{-7}	(M19) 4.21×10^{-7}
b	—	—	(M5) 1.91×10^{-7}
c	—	—	—
r*3a	—	—	—
b	—	—	—
c	—	—	—
P1a	(m5)	(M5) 7.18×10^{-19}	(M1) 1.18×10^{-21}
b	—	(M1) 2.66×10^{-20}	(M5) 6.05×10^{-19}
c	—	—	—
P2a	(m2a) 2.15×10^{-18}	(M19) 2.13×10^{-19}	(M19) 3.13×10^{-19}
b	—	—	(M5) 2.94×10^{-20}
c	—	—	—
P3a	—	—	—
b	—	—	—
c	—	—	—
r1a	(Q3)	(Q3)	(Q3)
b	—	(Q3)	(Q3)
c	—	—	—
r2a	(Q3) 4.0×10^{-7}	(Q8) 6.67×10^{-7}	(Q8) 4.6×10^{-7}
b	—	—	—
c	—	—	—
r3a	—	—	—
b	—	—	—
c	—	—	—
Y11a	—	(Q3)	(Q3)
b	—	(Q3)	(Q3)
c	—	—	—
Y12a	(Q3) 3.67×10^{-18}	(Q8) 8.36×10^{-18}	(Q8) 3.48×10^{-18}
b	—	—	—
c	—	—	—
Y13a	—	—	—
b	—	—	—
c	—	—	—
G	5,6	5,8	5,87
VF	0.1	0.078	0.04
VS	—	—	—

V	68	68	57
CD	1·82	1·82	1·0
1	1·43	1·43	0·79
†	50	50	25
T	713	725	750
INDEX NO.	18g	19h	20
V*F	$2·42 \times 10^{-10}$	$2·77 \times 10^{-10}$	$1·58 \times 10^{-10}$
WF	$15·14 \times 10^{-4}$	$15·4 \times 10^{-4}$	$8·8 \times 10^{-4}$
W*P	—	—	—
DF	$3·47 \times 10^{-6}$	$3·53 \times 10^{-6}$	$2·01 \times 10^{-6}$
H1	} $7·55 \times 10^{-6}$	} $8·07 \times 10^{-6}$	$1·09 \times 10^{-6}$
H2			$2·18 \times 10^{-6}$
H3	—	—	—
H*	$7·55 \times 10^{-6}$	$8·07 \times 10^{-6}$	$3·26 \times 10^{-6}$
Z	2	2	2
VOL	$5·93 \times 10^{-10}$	$6·34 \times 10^{-10}$	$2·57 \times 10^{-10}$
A	—	—	—
R	54·1	56·3	38·3
Yr	$3·2 \times 10^{-10}$	$3·54 \times 10^{-10}$	$9·82 \times 10^{-11}$
a_1	—	—	$2·42 \times 10^{6}$
r*1a	(M5) $4·53 \times 10^{-7}$	(M1) $6·72 \times 10^{-8}$	(M5) $2·18 \times 10^{-7}$
b	(M1) $1·89 \times 10^{-7}$	(M2) $3·36 \times 10^{-7}$	—
c	—	—	—
r*2a	(M19)	(M19) $5·0 \times 10^{-7}$	(M19) $3·27 \times 10^{-7}$
b	—	—	(M15a) $2·5 \times 10^{-6}$
c	—	—	—
r*3a	—	—	—
b	—	—	—
c	—	—	—
P1a	(M5) $3·89 \times 10^{-19}$	(M5) $1·27 \times 10^{-21}$	(M5) $4·33 \times 10^{-20}$
b	(M1) $2·82 \times 10^{-20}$	(M2) $1·59 \times 10^{-19}$	—
c	—	—	—
P2a	(M19)	(M19) $5·24 \times 10^{-19}$	(M19) $1·47 \times 10^{-19}$
b	—	—	—
c	—	—	—
P3a	—	—	—
b	—	—	—
c	—	—	—
r1a	(Q3)	(Q3)	(Q3)
b	(Q3)	(Q3)	—
c	—	—	—
r2a	(Q8) $3·15 \times 10^{-7}$	(Q8) $4·81 \times 10^{-7}$	(Q8) $3·75 \times 10^{-7}$
b	—	—	—
c	—	—	—
r3a	—	—	—
b	—	—	—
c	—	—	—
Y1a	(Q3)	(Q3)	(Q3)
b	(Q3)	(Q3)	—
c	—	—	—
Y2a	(Q8) $2·36 \times 10^{-18}$	(Q8) $5·86 \times 10^{-18}$	(Q8) $9·62 \times 10^{-19}$
b	—	—	—
c	—	—	—
Y3a	—	—	—
b	—	—	—
c	—	—	—
G	5, 6, 8.	5, 6, 8.	7, 8.
VF	0·048	0·039	0·02
VS	—	—	—

V	57	57	68
CD	1·0	0·5	1·82
i	0·79	0·4	1·43
t	15	25	48
T	750	900	713
INDEX NO.	21	22	8a
V*F	$1·58 \times 10^{-10}$	$9·62 \times 10^{-11}$	$2·72 \times 10^{-10}$
WF	$8·8 \times 10^{-4}$	$5·35 \times 10^{-4}$	$15·14 \times 10^{-4}$
W*P	—	—	—
DF	$2·01 \times 10^{-6}$	$1·22 \times 10^{-6}$	$3·47 \times 10^{-6}$
H1	$2·32 \times 10^{-6}$	$3·76 \times 10^{-6}$	$7·4 \times 10^{-6}$
H2	$2·56 \times 10^{-6}$		
H3	—	—	—
H*	$4·86 \times 10^{-6}$	$3·76 \times 10^{-6}$	$7·4 \times 10^{-6}$
Z	2	2	2
VOL	$3·82 \times 10^{-10}$	$2·95 \times 10^{-10}$	$5·82 \times 10^{-10}$
A	—	—	136800
R	58·53	67·45	53·2
Yr	$2·23 \times 10^{-10}$	$1·99 \times 10^{-10}$	$3·1 \times 10^{-10}$
a_1	$2·62 \times 10^{6}$	$2·56 \times 10^{6}$	$7·76 \times 10^{5}$
r*1a	(M2a) $5·56 \times 10^{-7}$	(M5) $1·71 \times 10^{-7}$	(M5)
b	—	—	—
c	—	—	—
r*2a	(M19) $4·51 \times 10^{-7}$	(M19) $5·13 \times 10^{-7}$	(M2a) $1·25 \times 10^{-6}$
b	—	—	—
c	—	—	—
r*3a	—	—	—
b	—	—	—
c	—	—	—
P1a	(M2a) $7·18 \times 10^{-19}$	(M5) $2·1 \times 10^{-20}$	(M5)
b	—	—	—
c	—	—	—
P2a	(M19) $3·84 \times 10^{-19}$	(M19) $5·65 \times 10^{-19}$	(M2a) $8·18 \times 10^{-18}$
b	—	—	—
c	—	—	—
P3a	—	—	—
b	—	—	—
c	—	—	—
r1a	(Q3) $3·34 \times 10^{-7}$	(Q3)	—
b	—	—	—
c	—	—	—
r2a	(Q8) $2·82 \times 10^{-7}$	(Q8) $3·63 \times 10^{-7}$	(Q3) $5·84 \times 10^{-7}$
b	—	—	—
c	—	—	—
r3a	—	—	—
b	—	—	—
c	—	—	—
Y1a	(Q3) $8·11 \times 10^{-19}$	(Q3)	—
b	—	—	—
c	—	—	—
Y2a	(Q8) $6·32 \times 10^{-19}$	(Q8) $1·56 \times 10^{-18}$	(Q3) $7·93 \times 10^{-18}$
b	—	—	—
c	—	—	—
Y3a	—	—	—
b	—	—	—
c	—	—	—
G	8, 5	8, 6	5, 6
VF	0·022	0·007	0·69
VS	—	—	—

V	69·5	71	72·5
CD	1·47	1·13	0·78
I	1·16	0·89	0·61
t	50	51·5	53·0
T	725	736	747
INDEX NO.	9	10	11a
V*F	2·25 X10⁻¹⁰	1·75 X10⁻¹⁰	1·22 X10⁻¹⁰
WF	12·49 X10⁻⁴	9·73 X10⁻⁴	6·77 X10⁻⁴
W*p	1·18 X10⁻³	9·1 X10⁻⁴	—
DF	2·86 X10⁻⁶	2·23 X10⁻⁶	1·55 X10⁻⁶
H1	5·88 X10⁻⁷	1·23 X10⁻⁶	} 2·67 X10⁻⁶
H2	2·94 X10⁻⁶	3·05 X10⁻⁶	}
H3	—	—	—
H*	3·74 X10⁻⁶	4·28 X10⁻⁶	2·07 X10⁻⁶
Z	2	2	2
VOL	2·94 X10⁻¹⁰	3·36 X10⁻¹⁰	1·62 X10⁻¹⁰
A	93600	118800	1·26 X10⁵
R	23·5	48·0	25·11
Yr	6·9 X10⁻¹¹	1·61 X10⁻¹⁰	4·08 X10⁻¹¹
a	—	—	1·31 X10⁶
r*1a	(M1) 2·35 X10⁻⁷	(M5) 3·81 X10⁻⁷	(M5)
b	—	—	—
c	—	—	—
r*2a	(M9) 1·12 X10⁻⁶	(M9) 1·14 X10⁻⁶	(M19)
b	—	—	—
c	—	—	—
r*3a	—	—	—
b	—	—	—
c	—	—	—
P1a	(M1) 5·46 X10⁻²⁰	(M5) 2·32 X10⁻¹⁹	(M5)
b	—	—	—
c	—	—	—
P2a	(M9) 5·91 X10⁻¹⁸	(M9) 6·25 X10⁻¹⁸	(M19)
b	—	—	—
c	—	—	—
P3a	—	—	—
b	—	—	—
c	—	—	—
r1a	(Q3)	(Q3)	(Q3)
b	—	—	—
c	—	—	—
r2a	(Q1) 3·74 X10⁻⁷	(Q3)	(Q8) 7·18 X10⁻⁷
b	(Q3)	—	—
c	—	—	—
r3a	—	—	—
b	—	—	—
c	—	—	—
Yi1a	(Q3)	(Q3)	(Q3)
b	—	—	—
c	—	—	—
Yi2a	(Q1) 3·28 X10⁻¹⁹	(Q3)	(Q8) 3·35 X10⁻¹⁸
b	(Q3)	—	—
c	—	—	—
Yi3a	—	—	—
b	—	—	—
c	—	—	—
G	9	9	4, 6, 8
VE	0·08	0·055	0·011
VS	260	220	225

V	68	68	69·5
CD	1·47	1·82	1·47
i	1·16	1·43	1·16
t	48	48	48
T	713	725	713
INDEX NO.	12a	13b	14c
V*F	$2{\cdot}21 \times 10^{-10}$	$2{\cdot}77 \times 10^{-10}$	$2{\cdot}21 \times 10^{-10}$
WF	$12{\cdot}28 \times 12^{-4}$	$15{\cdot}4 \times 10^{-4}$	$12{\cdot}28 \times 10^{-4}$
W*P	—	—	—
DF	$2{\cdot}81 \times 10^{-6}$	$3{\cdot}52 \times 10^{-3}$	$2{\cdot}81 \times 10^{-6}$
H1	$4{\cdot}37 \times 10^{-6}$	$4{\cdot}93 \times 10^{-6}$	$7{\cdot}63 \times 10^{-6}$
H2	}	}	}
H3	—	—	—
H*	$4{\cdot}37 \times 10^{-6}$	$4{\cdot}93 \times 10^{-6}$	$7{\cdot}63 \times 10^{-6}$
Z	2	2	2
VOL	$3{\cdot}43 \times 10^{-10}$	$3{\cdot}87 \times 10^{-10}$	$5{\cdot}99 \times 10^{-10}$
A	—	—	—
R	35·55	28·4	63·13
Yr	$1{\cdot}22 \times 10^{-10}$	$1{\cdot}1 \times 10^{-10}$	$3{\cdot}79 \times 10^{-10}$
a J	—	$1{\cdot}5 \times 10^{6}$	$1{\cdot}2 \times 10^{6}$
r*1a	(M5)	(M5)	(M5)
b	—	—	—
c	—	—	—
r*2a	(M11) $6{\cdot}55 \times 10^{-7}$	(M11a) $7{\cdot}56 \times 10^{-7}$	(M19)
b	—	(M5) $1{\cdot}07 \times 10^{-7}$	—
c	—	—	—
r*3a	—	—	—
b	—	—	—
c	—	—	—
P1a	(M5)	(M5)	(M5)
b	—	—	—
c	—	—	—
P2a	(M11) $1{\cdot}18 \times 10^{-18}$	(M11a) $1{\cdot}81 \times 10^{-18}$	(M19)
b	—	(M5) $5{\cdot}08 \times 10^{-21}$	—
c	—	—	—
P3a	—	—	—
b	—	—	—
c	—	—	—
r1a	(Q3)	(Q3)	(Q3)
b	—	—	—
c	—	—	—
r2a	(Q3) $5{\cdot}82 \times 10^{-7}$	(Q3) $5{\cdot}34 \times 10^{-7}$	(Q8) $3{\cdot}74 \times 10^{-7}$
b	(Q6) $1{\cdot}09 \times 10^{-6}$	—	—
c	—	—	—
r3a	—	—	—
b	—	—	—
c	—	—	—
Y1a	(Q3)	(Q3)	(Q3)
b	—	—	—
c	—	—	—
Y2a	(Q3) $4{\cdot}65 \times 10^{-18}$	(Q3) $4{\cdot}41 \times 10^{-18}$	(Q8) $3{\cdot}35 \times 10^{-18}$
b	(Q6) $1{\cdot}64 \times 10^{-17}$	—	—
c	—	—	—
Y3a	—	—	—
b	—	—	—
c	—	—	—
G	5,8	6,7,8	5,6,8
VF	0·046	0·053	0·053
VS	—	—	—

V	68	57	63
CD	1·82	0·5	1·0
J	1·43	0·4	0·79
†	48	15	25
T	725	900	900
INDEX NO.	15d	23	24
V*F	$2·76 \times 10^{-10}$	$9·62 \times 10^{-11}$	$1·9 \times 10^{-10}$
WF	$15·4 \times 10^{-4}$	$5·35 \times 10^{-4}$	$1·06 \times 10^{-3}$
W*P	—	—	—
DF	$3·53 \times 10^{-6}$	$1·22 \times 10^{-6}$	$2·42 \times 10^{-6}$
H1	} $5·54 \times 10^{-6}$	} $3·0 \times 10^{-6}$	} $3·13 \times 10^{-6}$
H2			
H3	—	—	—
H*	$5·54 \times 10^{-6}$	$3·0 \times 10^{-6}$	$3·13 \times 10^{-6}$
Z	2	2	2
VOL	$4·35 \times 10^{-10}$	$2·36 \times 10^{-10}$	$2·46 \times 10^{-10}$
A	—	—	—
R	36·35	59·2	22·73
Yr	$1·58 \times 10^{-10}$	$1·4 \times 10^{-10}$	$5·59 \times 10^{-11}$
a	—	—	$3·79 \times 10^{b}$
r*1a	(M5) $9·23 \times 10^{-8}$	(M5) $2·0 \times 10^{-7}$	(M5)
b	—	—	—
c	—	—	—
r*2a	(M19) $3·61 \times 10^{-7}$	(M19) $5·0 \times 10^{-7}$	(M2a) $4·72 \times 10^{-7}$
b	—	—	—
c	—	—	—
r*3a	—	—	—
b	—	—	—
c	—	—	—
P1a	(M5) $3·3 \times 10^{-21}$	(M5) $3·35 \times 10^{-29}$	(M5)
b	—	—	—
c	—	—	—
P2a	(M19) $1·96 \times 10^{-19}$	(M19) $5·24 \times 10^{-19}$	(M2a) $4·4 \times 10^{-19}$
b	—	—	—
c	—	—	—
P3a	—	—	—
b	—	—	—
c	—	—	—
r1a	(Q3)	(Q3)	(Q3)
b	(Q8)	—	—
c	—	—	—
r2a	(Q8) $3·61 \times 10^{-7}$	(Q3) $3·64 \times 10^{-7}$	(Q3) $3·78 \times 10^{-7}$
b	—	(Q8) $8·89 \times 10^{-7}$	—
c	—	—	—
r3a	—	—	—
b	—	—	—
c	—	—	—
Y1a	(Q3)	(Q8)	(Q3)
b	(Q8)	—	—
c	—	—	—
Y2a	(Q8) $2·26 \times 10^{-18}$	(Q3) $1·25 \times 10^{-18}$	(Q3) $1·4 \times 10^{-18}$
b	—	(Q8) $7·45 \times 10^{-18}$	—
c	—	—	—
Y3a	—	—	—
b	—	—	—
c	—	—	—
G	5,6,8	8,6	8,6
VF	0·062	0·019	0·026
VS	—	—	—

V	63	63	63
CD	1·0	0·5	0·5
i	0·79	0·4	0·4
t	15	·25	15
T	900	750	750
INDEX NO.	25	26	27
V*F	$1·9 \times 10^{-10}$	$8·01 \times 10^{-11}$	$8·01 \times 10^{-11}$
WF	$1·06 \times 10^{-3}$	$4·46 \times 10^{-4}$	$4·46 \times 10^{-4}$
W*P	—	—	—
DF	$2·42 \times 10^{-6}$	$1·02 \times 10^{-6}$	$1·02 \times 10^{-6}$
H1	$3·59 \times 10^{-6}$	$5·58 \times 10^{-6}$	$5·14 \times 10^{-6}$
H2			
H3	—	—	—
H*	$3·59 \times 10^{-6}$	$5·38 \times 10^{-6}$	$5·14 \times 10^{-6}$
Z	2	2	2
VOL	$2·82 \times 10^{-10}$	$4·23 \times 10^{-10}$	$4·04 \times 10^{-10}$
A	—	—	—
R	32·53	81·04	80·14
Yr	$9·16 \times 10^{-11}$	$3·43 \times 10^{-10}$	$3·23 \times 10^{-10}$
a_L	—	$1·5 \times 10^{6}$	—
r*1a	(M5)	(M5)	(M5) $2·2 \times 10^{-7}$
b	—	—	—
c	—	—	—
r*2a	(M19) $3·64 \times 10^{-7}$	(M2a) $5·96 \times 10^{-7}$	(M2a) $4·41 \times 10^{-7}$
b	(M15a) $1·92 \times 10^{-6}$	—	(M15a) $1·47 \times 10^{-6}$
c	—	—	—
r*3a	—	—	—
b	—	—	—
c	—	—	—
P1a	(M5)	(M5)	(M5) $4·47 \times 10^{-20}$
b	—	—	—
c	—	—	—
P2a	(M19) $2·01 \times 10^{-19}$	(M2a) $8·84 \times 10^{-19}$	(M2a) $3·58 \times 10^{-19}$
b	(M15a)	—	(M15a)
c	—	—	—
P3a	—	—	—
b	—	—	—
c	—	—	—
r1a	(Q3)	(Q3)	(Q3)
b	—	—	(Q6) $3·67 \times 10^{-7}$
c	—	—	—
r2a	(Q8) $7·27 \times 10^{-7}$	(Q6) $1·29 \times 10^{-6}$	(Q3) $1·47 \times 10^{-7}$
b	(Q1) $4·36 \times 10^{-7}$	(Q3) $2·23 \times 10^{-7}$	(Q6) $3·6 \times 10^{-7}$
c	—	—	—
r3a	—	—	—
b	—	—	—
c	—	—	—
Y1a	(Q3)	(Q3)	(Q3)
b	—	—	(Q6) $1·86 \times 10^{-19}$
c	—	—	—
Y2a	(Q8) $5·96 \times 10^{-18}$	(Q6) $2·71 \times 10^{-19}$	(Q3) $3·48 \times 10^{-19}$
b	(Q1) $2·15 \times 10^{-18}$	(Q3) $8·43 \times 10^{-19}$	(Q6) $2·17 \times 10^{-19}$
c	—	—	—
Y3a	—	—	—
b	—	—	—
c	—	—	—
G	8, 7, 6	5, 3, 8	6, 7, 8
VF	0·045	0·043	0·011
VS	—	—	—

V	50	66.5	50
CD	1.0	2.16	0.4
l	0.79	1.7	0.32
t	25	46.5	23
T	600	702	5
INDEX NO.	1a	7	1.1
V*F	1.27×10^{-10}	3.19×10^{-10}	4.27×10^{-13}
VF	7.04×10^{-4}	17.72×10^{-4}	2.38×10^{-6}
V*P	—	1.75×10^{-3}	—
DF	1.61×10^{-6}	4.06×10^{-6}	5.44×10^{-9}
H1	}	4.49×10^{-7}	8.9×10^{-7}
H2	}	3.74×10^{-6}	—
H3	—	—	—
H*	-	4.19×10^{-6}	8.9×10^{-7}
Z	2.	2	1
VOl	—	3.29×10^{-10}	6.99×10^{-11}
A	—	162000	—
R	—	80.0	99.39
Yr	—	—	6.95×10^{-11}
a_1	—	—	—
r*1a	(M5)	(M5) 2.25×10^{-7}	(M5) 4.55×10^{-7}
b	—	—	(M1) 1.34×10^{-7}
c	—	—	—
r*2a	(M2a) 4.0×10^{-7}	(M9) 1.87×10^{-6}	—
b	—	—	—
c	—	—	—
r*3a	—	—	—
b	—	—	—
c	—	—	—
P1a	(M5)	(M5) 4.73×10^{-20}	(M5) 3.69×10^{-19}
b	—	—	(M1) 1.01×10^{-20}
c	—	—	—
P2a	(M2a) 2.68×10^{-19}	(M9) 2.74×10^{-17}	—
b	—	—	—
c	—	—	—
P3a	—	—	—
b	—	—	—
c	—	—	—
r1a	(Q3)	(Q3)	—
b	—	—	—
c	—	—	—
r2a	(Q6) 6.0×10^{-7}	(Q3)	—
b	(Q3) 2.0×10^{-7}	(Q2) 1.87×10^{-7}	—
c	—	—	—
r3a	—	—	—
b	—	—	—
c	—	—	—
Y11a	(Q3)	(Q3)	—
b	—	—	—
c	—	—	—
Y12a	(Q6)	(Q3)	—
b	(Q3)	(Q2) 4.11×10^{-19}	—
c	—	—	—
Y13a	—	—	—
b	—	—	—
c	—	—	—
G	5,8	9	1.
VE	—	0.114	—
VS	—	270.	—

V	50	50	50
CD	0·4	0·4	0·4
I	0·32	0·32	0·32
†	19	23	19
T	5	10	10
INDEX NO.	1·2	1·3	1·4
V*F	$4·28 \times 10^{-13}$	$8·55 \times 10^{-13}$	$8·55 \times 10^{-13}$
WF	$2·38 \times 10^{-6}$	$4·75 \times 10^{-6}$	$4·75 \times 10^{-6}$
W*P	—	—	—
DF	$5·44 \times 10^{-9}$	$1·09 \times 10^{-8}$	$1·09 \times 10^{-8}$
H1	$1·05 \times 10^{-6}$	$8·9 \times 10^{-7}$	$8·32 \times 10^{-7}$
H2	—	—	—
H3	—	—	—
H*	$1·05 \times 10^{-6}$	$8·9 \times 10^{-7}$	$8·32 \times 10^{-7}$
Z	1	1	1
VOL	$8·25 \times 10^{-11}$	$6·99 \times 10^{-11}$	$6·54 \times 10^{-11}$
A	—	—	—
R	99·48	98·78	98·7
Yr	$8·21 \times 10^{-11}$	$6·91 \times 10^{-11}$	$6·45 \times 10^{-11}$
a	—	—	—
r*1a	(M5) $5·26 \times 10^{-7}$	(M5) $4·45 \times 10^{-7}$	(M5) $4·16 \times 10^{-7}$
b	(M1) $1·05 \times 10^{-7}$ (M8) $1·63 \times 10^{-6}$	(M1) $4·45 \times 10^{-7}$	(M1,2) $2·08 \times 10^{-7}$
c	(M12,9) $1·05 \times 10^{-6}$	—	(M6) $8·32 \times 10^{-7}$
r*2a	—	—	—
b	—	—	—
c	—	—	—
r*3a	—	—	—
b	—	—	—
c	—	—	—
P1a	(M5) $6·11 \times 10^{-19}$	(M5) $3·68 \times 10^{-19}$	(M5) $3·02 \times 10^{-19}$
b	(M8) $1·82 \times 10^{-17}$ (M1) $4·89 \times 10^{-21}$	(M1) $3·68 \times 10^{-19}$	(M1,2) $3·79 \times 10^{-20}$
c	(M12,9) $4·89 \times 10^{-18}$	—	(M6) $2·41 \times 10^{-18}$
P2a	—	—	—
b	—	—	—
c	—	—	—
P3a	—	—	—
b	—	—	—
c	—	—	—
r1a	(Q5)	—	—
b	—	—	—
c	—	—	—
r2a	—	—	—
b	—	—	—
c	—	—	—
r3a	—	—	—
b	—	—	—
c	—	—	—
Y11a	—	—	—
b	—	—	—
c	—	—	—
Y12a	—	—	—
b	—	—	—
c	—	—	—
Y13a	—	—	—
b	—	—	—
c	—	—	—
G	I	1,2.	1,2.
VF	—	—	—
VS	—	—	—

V	50	50	50
CD	0.4	0.4	0.4
I	0.32	0.32	0.32
†	23	19	23
T	20	20	40
INDEX NO.	1.5	1.6	1.7
V*F	1.71×10^{-12}	1.71×10^{-12}	3.42×10^{-12}
WF	9.5×10^{-6}	9.5×10^{-6}	1.9×10^{-5}
W*P	—	—	—
DF	2.18×10^{-8}	2.18×10^{-8}	4.36×10^{-8}
H1	1.67×10^{-6}	—	8.89×10^{-7}
H2	—	—	—
H3	—	—	—
H*	1.67×10^{-6}		8.89×10^{-7}
Z	1.	1	1
VOL	1.31×10^{-10}	—	6.98×10^{-11}
A	—	—	—
R	98.69	—	95.1
Yr	1.29×10^{-10}	—	6.64×10^{-11}
a L	—	—	—
r*1a	(M5) 8.34×10^{-7}	(M5) 8.0×10^{-7}	(M5) 2.67×10^{-7}
b	(M1) 8.34×10^{-7}	(M1) 4.0×10^{-7}	—
c	—	—	—
r*2a	—	—	—
b	—	—	—
c	—	—	—
r*3a	—	—	—
b	—	—	—
c	—	—	—
P1a	(M5) 2.43×10^{-18}	(M5) 2.15×10^{-18}	(M5) 7.95×10^{-20}
b	(M1) 2.43×10^{-18}	(M1) 2.68×10^{-19}	—
c	—	—	—
P2a	—	—	—
b	—	—	—
c	—	—	—
P3a	—	—	—
b	—	—	—
c	—	—	—
r1a	—	—	(Q6) 3.56×10^{-7}
b	—	—	—
c	—	—	—
r2a	—	—	—
b	—	—	—
c	—	—	—
r3a	—	—	—
b	—	—	—
c	—	—	—
Y1a	—	—	(Q6) 3.54×10^{-19}
b	—	—	—
c	—	—	—
Y2a	—	—	—
b	—	—	—
c	—	—	—
Y3a	—	—	—
b	—	—	—
c	—	—	—
G	1	1	2.
VF	—	—	—
VS	—	—	—

V	50	50	50
CD	0.4	0.4	0.4
I	0.32	0.32	0.32
†	23	23	23
T	120	600	1,800
INDEX NO.	1.8	1.9	2.0
V*F	1.03×10^{-11}	5.15×10^{-11}	5.545×10^{-10}
WF	5.7×10^{-5}	1.85×10^{-4}	5.55×10^{-4}
W*P	—	—	—
DF	1.31×10^{-7}	6.55×10^{-7}	1.97×10^{-6}
H1	1.42×10^{-6}	2.0×10^{-6}	4.45×10^{-6}
H2	}	}	}
H3	—	—	—
H*	1.42×10^{-6}	2.6×10^{-6}	4.45×10^{-6}
Z	2	2	2
VOL	1.11×10^{-10}	1.57×10^{-10}	3.49×10^{-10}
A	—	—	—
R	90.73	67.22	55.75
Yr	1.01×10^{-10}	1.06×10^{-10}	1.95×10^{-10}
a	—	—	—
r*1a	(M1) 1.01×10^{-7}	(M5) 1.67×10^{-7}	(M5) 4.45×10^{-7}
b	—	—	—
c	—	—	—
r*2a	(M6a) 2.53×10^{-7}	(M6a) 5.56×10^{-7}	(M6a) 1.1×10^{-6}
b	—	—	—
c	—	—	—
r*3a	—	—	—
b	—	—	—
c	—	—	—
P1a	(M1) 4.32×10^{-21}	(M5) 1.94×10^{-20}	(M5) 3.68×10^{-19}
b	—	—	—
c	—	—	—
P2a	(M6a) 6.78×10^{-20}	(M6a) 7.18×10^{-19}	(M6a) 5.78×10^{-18}
b	—	—	—
c	—	—	—
P3a	—	—	—
b	—	—	—
c	—	—	—
r1a	(Q3)	(Q3)	(Q3)
b	—	—	—
c	—	—	—
r2a	(Q3) 1.52×10^{-7}	(Q3) 1.1×10^{-7}	(Q6) 1.1×10^{-6}
b	(Q6) 4.55×10^{-7}	(Q6) 3.89×10^{-7}	(Q3)
c	—	—	—
r3a	—	—	—
b	—	—	—
c	—	—	—
Y1a	(Q3)	(Q3)	(Q3)
b	—	—	—
c	—	—	—
Y2a	(Q3) 1.03×10^{-19}	(Q3) 7.76×10^{-20}	(Q6) 1.69×10^{-17}
b	(Q6) 9.22×10^{-19}	(Q6) 9.5×10^{-19}	(Q3)
c	—	—	—
Y3a	—	—	—
b	—	—	—
c	—	—	—
G	1, 2, 3.	4	4
VE	—	—	—
VS	—	—	—

V	50	50	50
CD	1·0	1·0	1·0
I	0·79	0·79	0·79
†	23	23	23
T	5	10	20
INDEX NO.	2·1	2·2	2·3
V*F	$1·06 \times 10^{-12}$	$2·16 \times 10^{-12}$	$4·32 \times 10^{-12}$
WF	$5·87 \times 10^{-6}$	$1·17 \times 10^{-5}$	$2·34 \times 10^{-5}$
W*P	—	—	—
DF	$1·35 \times 10^{-8}$	$2·7 \times 10^{-8}$	$5·4 \times 10^{-8}$
H1	$7·12 \times 10^{-7}$	$8·89 \times 10^{-7}$	$1·11 \times 10^{-6}$
H2	—	}	}
H3	—	—	—
H*	$7·12 \times 10^{-7}$	$8·89 \times 10^{-7}$	$1·11 \times 10^{-6}$
Z	1	2	2
VOL	$5·59 \times 10^{-11}$	$6·98 \times 10^{-11}$	$8·73 \times 10^{-11}$
A	—	—	—
R	98·11	96·91	95·05
Yr	$5·49 \times 10^{-11}$	$6·77 \times 10^{-11}$	$8·29 \times 10^{-11}$
a	—	—	—
r*1a	(M5) $3·56 \times 10^{-7}$	(M5) $1·78 \times 10^{-7}$	(M5) $1·11 \times 10^{-7}$
b	(M1) $3·56 \times 10^{-7}$	—	—
c	—	—	—
r*2a	—	(M6a) $4·45 \times 10^{-7}$	(M6a) $2·22 \times 10^{-7}$
b	—	—	—
c	—	—	—
r*3a	—	—	—
b	—	—	—
c	—	—	—
P1a	(M5) $1·88 \times 10^{-19}$	(M5) $2·35 \times 10^{-20}$	(M5) $5·75 \times 10^{-21}$
b	(M1) $1·88 \times 10^{-19}$	(—	—
c	—	—	—
P2a	—	(M6a) $3·68 \times 10^{-19}$	(M6a) $1·15 \times 10^{-20}$
b	—	—	—
c	—	—	—
P3a	—	—	—
b	—	—	—
c	—	—	—
r1a	—	(Q3)	(Q3)
b	—	—	—
c	—	—	—
r2a	—	(Q3) $2·23 \times 10^{-7}$	(Q6) $4·44 \times 10^{-7}$
b	—	(Q6) $3·34 \times 10^{-7}$	(Q3)
c	—	—	—
r3a	—	—	—
b	—	—	—
c	—	—	—
Y11a	—	(Q3)	(Q3)
b	—	—	—
c	—	—	—
Y12a	—	(Q3) $1·38 \times 10^{-19}$	(Q6) $6·88 \times 10^{-19}$
b	—	(Q6) $3·11 \times 10^{-19}$	(Q3)
c	—	—	—
Y13a	—	—	—
b	—	—	—
c	—	—	—
G	1, 2a	3,	3, 2, 2a, 1
VE	—	—	—
VS	—	—	—

V	50	50	50
CD	1.0	1.0	1.0
l	0.79	0.79	0.79
†	19	23	23
T	20	40	120
INDEX NO.	2.4	2.5	2.6
V*F	4.32×10^{-12}	8.64×10^{-12}	2.59×10^{-11}
VF	2.34×10^{-5}	4.68×10^{-5}	1.41×10^{-4}
W*P	—	—	—
DF	5.4×10^{-8}	1.08×10^{-8}	3.24×10^{-8}
H1	} 1.74×10^{-6}	} 1.34×10^{-6}	} 2.02×10^{-6}
H2			
H3	—	—	—
H*	1.74×10^{-6}	1.34×10^{-6}	2.02×10^{-6}
Z	2	2	2
VOL	1.37×10^{-10}	1.05×10^{-10}	1.59×10^{-10}
A	—	—	—
R	96.84	91.75	83.68
Yr	1.32×10^{-10}	9.61×10^{-11}	1.33×10^{-10}
a	—	—	—
r*1a	(M5) 2.3×10^{-7}	(M5) 2.23×10^{-7}	(M5) 1.62×10^{-7}
b	(M1) 3.45×10^{-7}	—	—
c	—	—	—
r*2a	(M6a) 4.14×10^{-7}	(M6a) 8.89×10^{-7}	(M6a) 4.45×10^{-7}
b	—	—	—
c	—	—	—
r*3a	—	—	—
b	—	—	—
c	—	—	—
P1a	(M5) 5.1×10^{-20}	(M5) 4.6×10^{-20}	(M5) 1.77×10^{-20}
b	(M1) 1.72×10^{-19}	—	—
c	—	—	—
P2a	(M6a) 2.98×10^{-19}	(M6a) 2.95×10^{-19}	(M6a) 3.68×10^{-19}
b	—	—	—
c	—	—	—
P3a	—	—	—
b	—	—	—
c	—	—	—
r1a	(Q3)	(Q3)	(Q3)
b	—	—	—
c	—	—	—
r2a	—	(Q6) 3.34×10^{-7}	(Q6) 3.3×10^{-7}
b	—	—	—
c	—	—	—
r3a	—	—	—
b	—	—	—
c	—	—	—
Y1a	—	(Q3)	(Q3)
b	—	—	—
c	—	—	—
Y2a	—	(Q6) 4.48×10^{-19}	(Q6) 6.91×10^{-19}
b	—	—	—
c	—	—	—
Y3a	—	—	—
b	—	—	—
c	—	—	—
G	3,2,2a,1	3	3,2
VF	—	—	—
VS	—	—	—

V	50	50	50
CD	1·0	1·0	1·0
I	0·79	0·79	0·79
+	23	19	19
T	600	600	1,200
INDEX NO.	2·7	2·8	2·9
V*F	1.3×10^{-10}	1.3×10^{-10}	2.53×10^{-10}
WF	7.02×10^{-4}	7.02×10^{-4}	1.41×10^{-3}
W*P	—	—	—
DF	1.62×10^{-7}	1.62×10^{-7}	3.22×10^{-6}
H1	} 5.56×10^{-6}	} 5.46×10^{-6}	} 7.32×10^{-6}
H2			
H3	—	—	—
H*	5.56×10^{-6}	5.46×10^{-6}	7.32×10^{-6}
Z	2	2	2
VOL	4.37×10^{-10}	4.29×10^{-10}	5.75×10^{-10}
A	—	—	—
R	70·23	69·66	56·0
Yr	3.07×10^{-10}	2.99×10^{-10}	3.22×10^{-10}
a_1	—	1.27×10^{6}	1.92×10^{6}
r*1a	(M5) 2.22×10^{-7}	(M5)	(M5)
b	—	—	—
c	—	—	—
r*2a	(M6a) 8.34×10^{-7}	(M2a) 1.26×10^{-7}	(M2a) 1.19×10^{-6}
b	—	(M4d) 5.82×10^{-6}	—
c	—	—	—
r*3a	—	—	—
b	—	—	—
c	—	—	—
P1a	(M5) 4.6×10^{-20}	(M5)	(M5)
b	—	—	—
c	—	—	—
P2a	(M6a) 2.42×10^{-18}	(M2a) 8.41×10^{-21}	(M2a) 6.98×10^{-18}
b	—	(M4)	—
c	—	—	—
P3a	—	—	—
b	—	—	—
c	—	—	—
r1a	(Q3)	(Q3)	(Q3)
b	—	—	—
c	—	—	—
r2a	(Q3) 2.78×10^{-7}	(Q1,3) 3.64×10^{-7}	(Q1,3) 5.92×10^{-7}
b	(Q6) 8.34×10^{-7}	(Q2) 1.82×10^{-7}	(Q2) 2.96×10^{-7}
c	—	—	—
r3a	—	—	—
b	—	—	—
c	—	—	—
Y1a	(Q3)	(Q3)	(Q3)
b	—	—	—
c	—	—	—
Y2a	(Q3) 1.35×10^{-18}	(Q1) 1.05×10^{-19}	(Q1) 2.62×10^{-18}
b	(Q6) 1.22×10^{-17}	(Q2) 2.62×10^{-20}	(Q2) 6.57×10^{-19}
c	—	(Q3) 2.27×10^{-18}	(Q3) 8.05×10^{-18}
Y3a	—	—	—
b	—	—	—
c	—	—	—
G	4,3	8,6	8,6
VE	—	—	—
VS	—	—	—

V	50	50	50
CD	1.0	1.0	5
I	0.79	0.79	3.93
†	23	19	23
T	1800	1800	5
INDEX NO.	3.0	3.1	3.2
V*F	3.89×10^{-10}	3.89×10^{-10}	5.25×10^{-12}
WF	2.11×10^{-3}	2.11×10^{-3}	2.92×10^{-5}
W*P	—	—	—
DF	4.95×10^{-6}	4.95×10^{-6}	6.68×10^{-8}
H1	} 7.78×10^{-6}	} 7.69×10^{-6}	} 1.0×10^{-6}
H2	}	}	}
H3	—	—	—
H*	7.78×10^{-6}	7.69×10^{-6}	1.0×10^{-6}
Z	2	2	2
VOL	6.11×10^{-10}	6.04×10^{-10}	7.86×10^{-11}
A	—	—	—
R	36.33	35.62	93.32
Yr	2.22×10^{-10}	2.15×10^{-10}	7.33×10^{-11}
a_1	—	—	—
r*1a	(M5)	(M5)	(M5) 1.11×10^{-7}
b	—	—	—
c	—	—	—
r*2a	(M11) 6.67×10^{-7}	(M3) 4.62×10^{-6}	(M6a) 2.78×10^{-7}
b	—	—	—
c	—	—	—
r*3a	—	—	—
b	—	—	—
c	—	—	—
P1a	(M5)	(M5)	(M5) 5.75×10^{-21}
b	—	—	—
c	—	—	—
P2a	(M11) 1.25×10^{-18}	(M3) 4.13×10^{-16}	(M6a) 8.98×10^{-20}
b	—	—	—
c	—	—	—
P3a	—	—	—
b	—	—	—
c	—	—	—
r1a	(Q3)	—	(Q3)
b	—	—	—
c	—	—	—
r2a	(Q3) 3.34×10^{-7}	—	(Q6) 1.67×10^{-7}
b	(Q1) 2.22×10^{-7}	—	—
c	—	—	—
r3a	—	—	—
b	—	—	—
c	—	—	—
Y11a	(Q3)	—	(Q3)
b	—	—	—
c	—	—	—
Y12a	(Q3) 2.72×10^{-18}	—	(Q6) 8.73×10^{-20}
b	(Q1) 1.21×10^{-18}	—	—
c	—	—	—
Y13a	—	—	—
b	—	—	—
c	—	—	—
G	5,8	9,6	1,2,3
VF	—	—	—
VS	—	—	—

V	50	50	50
CD	5	5	5
I	3.93	3.93	3.93
+	23	23	23
T	10	20	40
INDEX NO.	3.3	3.4	3.5
V*F	1.05×10^{-11}	2.1×10^{-11}	4.2×10^{-11}
WF	5.84×10^{-5}	1.17×10^{-4}	3.43×10^{-4}
W*P	—	—	—
DF	1.34×10^{-7}	2.67×10^{-7}	5.35×10^{-7}
H1	} 1.48×10^{-6}	} 2.43×10^{-6}	} 3.56×10^{-6}
H2	}	}	}
H3	—	—	—
H*	1.48×10^{-6}	2.43×10^{-6}	3.56×10^{-6}
Z	2	2	2
VOL	1.16×10^{-10}	1.91×10^{-10}	2.79×10^{-10}
A	—	—	—
R	90.98	88.98	84.96
Yr	1.06×10^{-10}	1.7×10^{-10}	2.37×10^{-10}
a	—	—	—
r*1a	(M5) 1.73×10^{-7}	(M5,)	(M5) 1.34×10^{-7}
b	—	—	—
c	—	—	—
r*2a	(M6a) 3.71×10^{-7}	(M6a) 2.96×10^{-7}	(M6a) 3.34×10^{-7}
b	—	—	—
c	—	—	—
r*3a	—	—	—
b	—	—	—
c	—	—	—
P1a	(M5) 2.16×10^{-20}	(M5,)	(M5) 9.93×10^{-21}
b	—	—	—
c	—	—	—
P2a	(M6a) 2.13×10^{-19}	(M6a,5) 1.09×10^{-19}	(M6a) 1.55×10^{-19}
b	—	—	—
c	—	—	—
P3a	—	—	—
b	—	—	—
c	—	—	—
r1a	(Q3)	(Q3)	(Q3)
b	—	—	—
c	—	—	—
r2a	(Q6) 2.47×10^{-7}	(Q6) 2.96×10^{-7}	(Q6a) 3.34×10^{-7}
b	—	—	(Q3) 1.67×10^{-7}
c	—	—	—
r3a	—	—	—
b	—	—	—
c	—	—	—
Y11a	(Q3)	(Q3)	(Q3)
b	—	—	—
c	—	—	—
Y12a	(Q6) 2.84×10^{-19}	(Q6) 6.69×10^{-19}	(Q6) 1.25×10^{-18}
b	—	—	(Q3) 3.12×10^{-19}
c	—	—	—
Y13a	—	—	—
b	—	—	—
c	—	—	—
G	1,2,3.	4,3	4
VF	—	—	—
VS	—	—	—

V	50	50	50
CD	5	5	5
I	3.93	3.93	3.93
†	23	23	19
T	120	600	600
INDEX NO.	3.6	3.4	5.8
V*F	1.26×10^{-10}	6.3×10^{-10}	6.3×10^{-10}
WF	7.01×10^{-4}	3.5×10^{-3}	3.5×10^{-3}
W*P	—	—	—
DF	1.61×10^{-6}	8.02×10^{-6}	8.02×10^{-6}
H1	6.67×10^{-6}	3.89×10^{-6}	1.32×10^{-5}
H2		1.0×10^{-5}	
H3	—	—	—
H*	6.67×10^{-6}	1.39×10^{-5}	3.32×10^{-5}
Z	2	2	2
VOL	5.24×10^{-10}	1.09×10^{-9}	1.04×10^{-9}
A	—	—	—
R	75.94	42.25	39.24
Yr	3.97×10^{-10}	4.61×10^{-10}	4.07×10^{-10}
a_1	—	—	3.82×10^{-5}
r*1a	(M5) 3.34×10^{-7}	(M5) 5.56×10^{-7}	(M5) 6.0×10^{-7}
b	—	—	—
c	—	—	—
r*2a	(M11) 5.56×10^{-7}	(M11,2a) 2.22×10^{-6}	(M11,2a) 2.55×10^{-6}
b	—	—	—
c	—	—	—
r*3a	—	—	—
b	—	—	—
c	—	—	—
P1a	(M5) 1.55×10^{-19}	(M5) 7.2×10^{-19}	(M5) 9.05×10^{-19}
b	—	—	—
c	—	—	—
P2a	(M11) 7.2×10^{-19}	(M11,2a) 4.6×10^{-17}	(M11,2a) 6.91×10^{-17}
b	—	—	—
c	—	—	—
P3a	—	—	—
b	—	—	—
c	—	—	—
r1a	(Q3)	(Q3)	(Q3)
b	—	—	—
c	—	—	—
r2a	(Q6) 6.67×10^{-7}	(Q1) 3.34×10^{-7}	(Q1) 3.64×10^{-7}
b	(Q3) 3.34×10^{-7}	(Q2) 1.67×10^{-7}	(Q2,5) 3.64×10^{-7}
c	(Q1) 1.78×10^{-7}	(Q3) 8.89×10^{-7}	(Q3) 7.28×10^{-7}
r3a	—	—	—
b	—	—	—
c	—	—	—
Y1a	(Q3)	(Q3)	(Q3)
b	—	—	—
c	—	—	—
Y2a	(Q6) 9.32×10^{-18}	(Q1) 1.55×10^{-18}	(Q1) 2.12×10^{-18}
b	(Q3) 2.33×10^{-18}	(Q2) 1.22×10^{-18}	(Q2,5) 1.06×10^{-18}
c	(Q1) 1.11×10^{-19}	(Q3) 3.45×10^{-17}	(Q3) 2.21×10^{-17}
Y3a	—	—	—
b	—	—	—
c	—	—	—
G	5,4,8.	6,8,	6,8.
VF	—	—	—
VS	—	—	—

V	50	50	50
CD	5	5	5
I	3.93	3.93	3.93
†	19	24	19
T	1200	1800	1800
INDEX NO.	3.9	4.0	4.1
V*F	1.26×10^{-9}	1.89×10^{-9}	1.89×10^{-9}
WF	7.0×10^{-3}	1.05×10^{-2}	1.05×10^{-2}
W*P	—	—	—
DF	1.60×10^{-5}	2.41×10^{-5}	2.41×10^{-5}
H1	2.4×10^{-5}		1.0×10^{-6}
H2			7.28×10^{-6}
H3	—	4.45×10^{-6}	2.76×10^{-5}
H*	2.4×10^{-5}	3.56×10^{-5}	3.59×10^{-5}
Z	2	3	3
VOL	1.89×10^{-9}	2.79×10^{-9}	2.82×10^{-9}
A	—	—	—
R	33.16	32.33	32.92
Yr	6.25×10^{-10}	9.03×10^{-10}	9.27×10^{-10}
a_1	6.05×10^{5}	—	4.79×10^{5}
r*1a	(M5) 6.15×10^{-7}	(M5)	(M5) 5.0×10^{-7}
b	—	—	—
c	—	—	—
r*2a	(M11) 2.48×10^{-6}	(M11) 7.78×10^{-7}	(M6a) 1.1×10^{-6}
b	—	—	—
c	—	—	—
r*3a	—	(M15) 5.34×10^{-6}	(M11) 4.83×10^{-6}
b	—	—	—
c	—	—	—
P1a	(M5) 9.76×10^{-19}	(M5)	(M5) 5.24×10^{-19}
b	—	—	—
c	—	—	—
P2a	(M11) 6.37×10^{-17}	(M11) 1.97×10^{-18}	(M6a) 5.58×10^{-18}
b	—	—	—
c	—	—	—
P3a	—	(M15)	(M11) 4.72×10^{-16}
b	—	—	—
c	—	—	—
r1a	(Q3) 6.15×10^{-7}	(Q3)	(Q3) 6.67×10^{-7}
b	(Q10) 1.2×10^{-6}	—	—
c	—	—	—
r2a	(Q1) 1.42×10^{-6}	(Q8) 4.45×10^{-7}	(Q3)
b	(Q3) 5.31×10^{-7}	—	(Q2) 5.0×10^{-7}
c	—	—	—
r3a	—	—	(Q3) 7.02×10^{-7}
b	—	—	—
c	—	—	—
Y1a	(Q3) 2.86×10^{-17}	(Q3)	(Q3) 1.16×10^{-17}
b	(Q10) 1.09×10^{-16}	—	—
c	—	—	—
Y2a	(Q1) 1.57×10^{-17}	(Q8) 1.94×10^{-17}	(Q3)
b	(Q3) 2.13×10^{-17}	—	(Q2) 1.73×10^{-18}
c	—	—	—
Y3a	—	—	(Q3) 4.27×10^{-17}
b	—	—	—
c	—	—	—
G	8, 6	8, 7, 6	8, 6
VE	—	—	—
VS			

V	50	50	50
CD	15	15	15
I	11·8	11·8	11·8
†	23	23	23
T	5	10	20
INDEX NO.	4·2	4·3	4·4
V*F	$1·58 \times 10^{-11}$	$3·16 \times 10^{-11}$	$6·32 \times 10^{-11}$
WF	$8·76 \times 10^{-5}$	$1·75 \times 10^{-4}$	$3·5 \times 10^{-4}$
W*P	—	—	—
DF	$2·01 \times 10^{-7}$	$4·01 \times 10^{-7}$	$8·03 \times 10^{-7}$
H1	} $1·11 \times 10^{-6}$	} $1·6 \times 10^{-6}$	
H2			$8·89 \times 10^{-7}$
H3	—	—	$1·11 \times 10^{-6}$
H*	$1·11 \times 10^{-6}$	$1·6 \times 10^{-6}$	$2·0 \times 10^{-6}$
Z	2	2	3
VOL	$8·73 \times 10^{-11}$	$1·26 \times 10^{-10}$	$1·57 \times 10^{-10}$
A	—	—	—
R	81·9	74·86	59·77
Yr	$7·15 \times 10^{-11}$	$9·41 \times 10^{-11}$	$9·39 \times 10^{-11}$
a_1	—	—	—
r*1a	(M5) $1·67 \times 10^{-7}$	(M5) $2·22 \times 10^{-7}$	(M5)
b	—	—	—
c	—	—	—
r*2a	(M6a) $2·78 \times 10^{-7}$	(M6a) $3·78 \times 10^{-7}$	(M6a) $3·34 \times 10^{-7}$
b	—	—	—
c	—	—	—
r*3a	—	—	(M8b) $4·45 \times 10^{-7}$
b	—	—	—
c	—	—	—
P1a	(M5) $1·94 \times 10^{-20}$	(M5) $4·6 \times 10^{-20}$	(M5)
b	—	—	—
c	—	—	—
P2a	(M6a) $8·98 \times 10^{-20}$	(M6a) $2·26 \times 10^{-19}$	(M6a) $1·56 \times 10^{-19}$
b	—	—	—
c	—	—	—
P3a	—	—	(M8b) $3·68 \times 10^{-19}$
b	—	—	—
c	—	—	—
r1a	(Q3)	(Q3)	(Q3)
b	—	—	—
c	—	—	—
r2a	(Q3) $1·11 \times 10^{-7}$	(Q6) $2·22 \times 10^{-7}$	(Q6) $4·45 \times 10^{-7}$
b	(Q6) $2·22 \times 10^{-7}$	(Q10) $3·34 \times 10^{-7}$	(—
c	—	—	—
r3a	—	—	—
b	—	—	—
c	—	—	—
Y1a	(Q3)	(Q3)	(Q3)
b	—	—	—
c	—	—	—
Y2a	(Q3) $4·31 \times 10^{-20}$	(Q6) $2·48 \times 10^{-19}$	(Q6) $5·52 \times 10^{-19}$
b	(Q6) $1·72 \times 10^{-19}$	(Q10) $2·8 \times 10^{-19}$	—
c	—	—	—
Y3a	—	—	—
b	—	—	—
c	—	—	—
G	2,3,4	4	5,7
VF	—	—	—
VS	—	—	—

V	50	50	50
CD	15	15	15
I	11·8	11·8	11·8
†	23	19	19
T	40	40	80
INDEX NO.	4·5	4·6	4·7
V*F	1.26×10^{-10}	1.26×10^{-10}	2.52×10^{-10}
WF	7.01×10^{-4}	7.01×10^{-4}	1.4×10^{-3}
W*P	—	—	—
DF	1.61×10^{-6}	1.61×10^{-6}	3.22×10^{-6}
H1	3.34×10^{-6}	8.0×10^{-7}	9.24×10^{-7}
H2		2.4×10^{-6}	2.16×10^{-6}
H3		9.6×10^{-6}	2.91×10^{-5}
H*	3.34×10^{-6}	1.28×10^{-5}	3.22×10^{-5}
Z	3	3	3
VOL	2.62×10^{-10}	1.01×10^{-9}	2.53×10^{-9}
A	—	—	—
R	51·88	87·47	90·03
Yr	1.36×10^{-10}	8.8×10^{-10}	2.28×10^{-9}
a	—	—	—
r*1a	(M5)	(M5) 4.0×10^{-7}	(M5) 4.62×10^{-7}
b	—	—	—
c	—	—	—
r*2a	(M6a) 3.34×10^{-7}	(M6a) 8.0×10^{-7}	(M6a) 1.15×10^{-6}
b	—	—	—
c	—	—	—
r*3a	(M8b) 4.45×10^{-7}	(M8a) 1.6×10^{-6}	(M8a) 1.54×10^{-6}
b	—	—	—
c	—	—	—
P1a	(M5)	(M5) 2.68×10^{-19}	(M5) 4.12×10^{-19}
b	—	—	—
c	—	—	—
P2a	(M6a) 1.56×10^{-19}	(M6a) 2.26×10^{-17}	(M6a) 6.44×10^{-18}
b	—	—	—
c	—	—	—
P3a	(M8b) 3.68×10^{-19}	(M8a) 1.72×10^{-17}	(M8a) 1.53×10^{-17}
b	—	—	—
c	—	—	—
r1a	(Q3)	(Q3)	(Q3)
b	—	—	—
c	—	—	—
r2a	(Q6)	(Q3) 6.4×10^{-7}	(Q3) 3.85×10^{-7}
b	—	—	—
c	—	—	—
r3a	(Q3) 3.34×10^{-7}	(Q7) 8.0×10^{-7}	(Q7) 9.52×10^{-7}
b	—	—	—
c	—	—	—
Y11a	(Q3)	(Q3)	(Q3)
b	—	—	—
c	—	—	—
Y12a	(Q6)	(Q3) 4.12×10^{-18}	(Q3) 1.43×10^{-18}
b	—	—	—
c	—	—	—
Y13a	(Q3) 1.17×10^{-18}	(Q7) 1.93×10^{-17}	(Q7) 8.3×10^{-17}
b	—	—	—
c	—	—	—
G	5,6	7,8	7,8
VE	—	—	—
VS	—	—	—

V	50	50	50
CD	15	15	15
I	11·8	11·8	7·8
†	23	19	19
T	120	120	360
INDEX NO.	4·8	4·9	5·0
V*F	$3{\cdot}78 \times 10^{-10}$	$3{\cdot}78 \times 10^{-10}$	$1{\cdot}13 \times 10^{-9}$
WF	$2{\cdot}1 \times 10^{-3}$	$2{\cdot}1 \times 10^{-3}$	$6{\cdot}3 \times 10^{-3}$
W*P	—	—	—
DF	$4{\cdot}83 \times 10^{-6}$	$4{\cdot}83 \times 10^{-6}$	$1{\cdot}45 \times 10^{-5}$
H1	$1{\cdot}0 \times 10^{-6}$	$1{\cdot}0 \times 10^{-6}$	$8{\cdot}0 \times 10^{-7}$
H2	$7{\cdot}96 \times 10^{-6}$	$6{\cdot}04 \times 10^{-6}$	$6{\cdot}47 \times 10^{-6}$
H3	$4{\cdot}45 \times 10^{-6}$	$2{\cdot}56 \times 10^{-5}$	$1{\cdot}09 \times 10^{-5}$
H*	$1{\cdot}34 \times 10^{-5}$	$3{\cdot}26 \times 10^{-5}$	$1{\cdot}82 \times 10^{-5}$
Z	3	3	3
VOL	$1{\cdot}05 \times 10^{-9}$	$2{\cdot}56 \times 10^{-9}$	$1{\cdot}43 \times 10^{-9}$
A	—	—	—
R	64·0	85·24	35·0
Yr	$6{\cdot}72 \times 10^{-10}$	$2{\cdot}18 \times 10^{-9}$	$2{\cdot}98 \times 10^{-10}$
a_1	—	$3{\cdot}45 \times 10^{5}$	—
r*1a	(m5)	(m5)	(m5) $4{\cdot}0 \times 10^{-7}$
b	—	—	—
c	—	—	—
r*2a	(m6a) $8{\cdot}34 \times 10^{-7}$	(m2a) $1{\cdot}85 \times 10^{-6}$	(m2a) $1{\cdot}46 \times 10^{-6}$
b	—	—	—
c	—	—	—
r*3a	(m8b) $8{\cdot}89 \times 10^{-7}$	(m8b) $8{\cdot}0 \times 10^{-7}$	(M11a) $6{\cdot}1 \times 10^{-6}$
b	(m15a) $1{\cdot}67 \times 10^{-5}$	—	(m5) $3{\cdot}81 \times 10^{-7}$
c	—	—	(m8) $1{\cdot}52 \times 10^{-6}$
P1a	(m5)	(m5)	(m5) $2{\cdot}68 \times 10^{-19}$
b	—	—	—
c	—	—	—
P2a	(m6a) $2{\cdot}43 \times 10^{-18}$	(m2a) $2{\cdot}64 \times 10^{-17}$	(m2a) $1{\cdot}29 \times 10^{-17}$
b	—	—	—
c	—	—	—
P3a	(m8b) $2{\cdot}95 \times 10^{-18}$	(m8b) $2{\cdot}15 \times 10^{-18}$	(m11a) $9{\cdot}5 \times 10^{-16}$
b	(m15a)	—	(m5) $2{\cdot}32 \times 10^{-19}$
c	—	—	(m8) $1{\cdot}48 \times 10^{-17}$
r1a	(Q3)	(Q3)	(Q3)
b	—	—	—
c	—	—	—
r2a	(Q6) $1{\cdot}67 \times 10^{-6}$	(Q3) $1{\cdot}56 \times 10^{-6}$	(Q3)
b	—	(Q5) $6{\cdot}25 \times 10^{-7}$	—
c	—	—	—
r3a	(Q10) $2{\cdot}78 \times 10^{-6}$	(Q7) $8{\cdot}0 \times 10^{-7}$	(Q5) $3{\cdot}81 \times 10^{-7}$
b	—	(Q6) $6{\cdot}25 \times 10^{-6}$	(Q12) $4{\cdot}76 \times 10^{-7}$
c	—	—	—
Y11a	(Q3)	(Q3)	(Q3)
b	—	—	—
c	—	—	—
Y12a	(Q6) $7{\cdot}82 \times 10^{-17}$	(Q3) $5{\cdot}4 \times 10^{-17}$	(Q3)
b	—	(Q5) $8{\cdot}64 \times 10^{-18}$	—
c	—	—	—
Y13a	(Q10) $1{\cdot}08 \times 10^{-16}$	(Q7) $5{\cdot}15 \times 10^{-17}$	(Q5) $2{\cdot}78 \times 10^{-18}$
b	—	(Q6) $3{\cdot}14 \times 10^{-15}$	(Q1) $8{\cdot}69 \times 10^{-18}$
c	—	—	(Q2) $4{\cdot}34 \times 10^{-18}$
G	8,7,5	8,7,5	6,7,8
VF	—	—	—
VS	—	—	—

V	50	50	50
CD	15	15	15
I	11·8	11·8	11·8
+	27	19	19
T	600	660	1260
INDEX NO.	5·1	5·2	5·3
V*F	$1·89 \times 10^{-9}$	$1·89 \times 10^{-9}$	$3·97 \times 10^{-9}$
VF	$1·05 \times 10^{-2}$	$1·05 \times 10^{-2}$	$2·21 \times 10^{-2}$
W*P	—	—	—
DF	$2·42 \times 10^{-5}$	$2·42 \times 10^{-5}$	$5·08 \times 10^{-5}$
H1	$4·44 \times 10^{-7}$	} $3·2 \times 10^{-5}$	} $5·6 \times 10^{-5}$
H2	$3·66 \times 10^{-5}$		
H3	$1·42 \times 10^{-5}$		
H*	$5·12 \times 10^{-5}$	$3·2 \times 10^{-5}$	$5·6 \times 10^{-5}$
Z	3	3	3
VOL	$4·02 \times 10^{-9}$	$2·52 \times 10^{-9}$	$4·4 \times 10^{-9}$
A	—	—	—
R	53·01	24·81	9·75
Yr	$2·13 \times 10^{-9}$	$6·24 \times 10^{-10}$	$4·29 \times 10^{-10}$
a_1	—	—	—
r*1a	(M5) $2·22 \times 10^{-7}$	(M5) $2·5 \times 10^{-7}$	(M5)
b	(M14) $5·56 \times 10^{-5}$	—	—
c	—	—	—
r*2a	(M8b) $1·77 \times 10^{-6}$	(M8) $8·42 \times 10^{-7}$	(M2a) $6·0 \times 10^{-7}$
b	—	—	—
c	—	—	—
r*3a	(M19) $8·89 \times 10^{-7}$	(M2a) $1·26 \times 10^{-6}$	(M8a) $1·0 \times 10^{-6}$
b	(M15a) $3·56 \times 10^{-6}$	—	—
c	—	—	—
P1a	(M5) $4·6 \times 10^{-20}$	(M5) $6·55 \times 10^{-20}$	(M5)
b	(M14)	—	—
c	—	—	—
P2a	(M8b) $2·31 \times 10^{-17}$	(M8) $2·5 \times 10^{-18}$	(M2a) $9·04 \times 10^{-19}$
b	—	—	—
c	—	—	—
P3a	(M19) $2·95 \times 10^{-18}$	(M2a) $8·38 \times 10^{-18}$	(M8a) $4·19 \times 10^{-18}$
b	(M15a)	—	—
c	—	—	—
r1a	(Q3) $2·22 \times 10^{-7}$	(Q3)	(Q3)
b	(Q6) $7·78 \times 10^{-7}$	—	—
c	—	—	—
r2a	(Q6) $1·11 \times 10^{-6}$	(Q3)	(Q3)
b	—	(Q6)	—
c	—	—	—
r3a	(Q8) $6·67 \times 10^{-7}$	(Q1) $1·68 \times 10^{-6}$	(Q2) $2·4 \times 10^{-7}$
b	(Q1) $2·22 \times 10^{-7}$	(Q2) $4·21 \times 10^{-7}$	(Q7) $1·12 \times 10^{-6}$
c	—	(Q3) $8·42 \times 10^{-7}$	(Q6) $4·17 \times 10^{-6}$
Y1a	(Q3) $3·1 \times 10^{-19}$	(Q3)	(Q3)
b	(Q6) $3·8 \times 10^{-18}$	—	—
c	—	—	—
Y2a	(Q6) $1·44 \times 10^{-16}$	(Q3)	(Q3)
b	—	(Q6)	—
c	—	—	—
Y3a	(Q8) $1·98 \times 10^{-17}$	(Q1) $2·24 \times 10^{-17}$	(Q2) $7·81 \times 10^{-19}$
b	(Q1) $2·2 \times 10^{-18}$	(Q2) $7·02 \times 10^{-19}$	(Q7) $2·21 \times 10^{-16}$
c	—	(Q3) $7·13 \times 10^{-17}$	(Q6) $3·06 \times 10^{-15}$
G	8, 7, 6	8, 7, 6	7
VF	—	—	—
VS	—	—	—

V	50	10	90
CD	15	5	5
J	11·8	3·93	3·93
†	23	19	19
T	1800	600	600
INDEX NO.	5·4	8·3	8·5
V*F	$5·67 \times 10^{-9}$	$6·3 \times 10^{-10}$	$6·3 \times 10^{-10}$
WF	$3·15 \times 10^{-2}$	$3·5 \times 10^{-3}$	$3·5 \times 10^{-3}$
W*P	—	—	—
DF	$7·25 \times 10^{-5}$	$8·02 \times 10^{-6}$	$8·02 \times 10^{-6}$
H1	$1·11 \times 10^{-6}$	$9·17 \times 10^{-6}$	$2·37 \times 10^{-6}$
H2	$2·13 \times 10^{-5}$	}	$8·0 \times 10^{-6}$
H3	$5·93 \times 10^{-5}$	—	—
T*	$8·17 \times 10^{-5}$	$9·17 \times 10^{-6}$	$1·04 \times 10^{-5}$
Z	3	2	2
VOL	$6·42 \times 10^{-9}$	$7·2 \times 10^{-10}$	$8·15 \times 10^{-10}$
A	—	—	—
R	11·65	12·54	22·66
Yr	$7·48 \times 10^{-10}$	$9·03 \times 10^{-11}$	$1·85 \times 10^{-10}$
a	—	$6·06 \times 10^{5}$	$8·85 \times 10^{5}$
r*1a	(M5) $1·01 \times 10^{-7}$	(M5)	(M5)
b	(M6a) $3·71 \times 10^{-7}$	—	—
c	—	—	—
r*2a	(M8b) $8·67 \times 10^{-7}$	(M2a) $1·67 \times 10^{-6}$	(M2a) $1·38 \times 10^{-6}$
b	(M15) $8·89 \times 10^{-6}$	—	—
c	—	—	—
r*3a	(M11b) $3·54 \times 10^{-6}$	—	—
b	(M9) $1·31 \times 10^{-5}$	—	—
c	—	—	—
P1a	(M5) $4·32 \times 10^{-4}$	(M5)	(M5)
b	(M6a) $2·14 \times 10^{-19}$	—	—
c	—	—	—
P2a	(M8b) $1·24 \times 10^{-18}$	(M2a) $1·95 \times 10^{-17}$	(M2a) $1·1 \times 10^{-17}$
b	(M15)	—	—
c	—	—	—
P3a	(M11b) $1·85 \times 10^{-16}$	—	—
b	(M9) $9·49 \times 10^{-15}$	—	—
c	—	—	—
r1a	(Q3) $2·11 \times 10^{-7}$	(Q3)	(Q3)
b	(Q6) $9·36 \times 10^{-7}$	—	—
c	—	—	—
r2a	(Q3) $4·45 \times 10^{-7}$	(Q3) $8·35 \times 10^{-7}$	(Q3) $4·14 \times 10^{-7}$
b	—	—	(Q6) $1·73 \times 10^{-6}$
c	—	—	—
r3a	(Q3) $8·34 \times 10^{-7}$	—	—
b	(Q1) $4·45 \times 10^{-7}$	—	—
c	—	—	—
Y1a	(Q3) $1·55 \times 10^{-19}$	(Q3)	(Q3)
b	(Q6) $3·05 \times 10^{-18}$	—	—
c	—	—	—
Y2a	(Q3) $1·32 \times 10^{-17}$	(Q3) $2·01 \times 10^{-17}$	(Q3) $4·3 \times 10^{-18}$
b	—	—	(Q6) $7·47 \times 10^{-17}$
c	—	—	—
Y3a	(Q3) $1·29 \times 10^{-16}$	—	—
b	(Q1) $1·11 \times 10^{-18}$	—	—
c	—	—	—
G	8, 7, 6	6, 8.	6, 8.
VF	—	—	—
VS	—	—	—

V	50	50	50
CD	5	5	5
I	3.93	3.93	3.93
†	19	19	19
T	600	600	600
INDEX NO.	9.0	9.1	9.2
V*F	6.3×10^{-10}	6.3×10^{-10}	6.3×10^{-10}
WF	3.5×10^{-3}	3.5×10^{-3}	3.5×10^{-3}
W*P	—	—	—
DF	8.02×10^{-6}	8.02×10^{-6}	8.02×10^{-6}
H1	} 1.04×10^{-5}	} 9.6×10^{-6}	} 1.3×10^{-5}
H2			
H3	—	—	—
H*	1.04×10^{-5}	9.6×10^{-6}	1.3×10^{-5}
Z	2	2	2
VOL	8.13×10^{-10}	7.54×10^{-10}	1.02×10^{-9}
A	—	—	—
R	22.5	16.46	38.31
Yr	1.83×10^{-10}	1.24×10^{-10}	3.9×10^{-10}
a_1	5.01×10^{5}	4.21×10^{5}	3.79×10^{5}
r*1a	(M2) 7.55×10^{-7}	(M5)	(M5)
b	(M9) 1.51×10^{-6}	—	—
c	(M5) 4.91×10^{-7}	—	—
r*2a	(M2a) 1.04×10^{-6}	(M2a) 1.6×10^{-6}	(M2a) 2.67×10^{-6}
b	(—	(M12) 2.4×10^{-6}	—
c	—	—	—
r*3a	—	—	—
b	—	—	—
c	—	—	—
P1a	(M2) 1.8×10^{-18}	(M5)	(M5)
b	(M9) 1.44×10^{-17}	—	—
c	(M5) 4.95×10^{-19}	—	—
P2a	(M2a) 4.64×10^{-18}	(M2a) 1.72×10^{-17}	(M2a) 7.95×10^{-17}
b	—	(M12) 5.79×10^{-17}	—
c	—	—	—
P3a	—	—	—
b	—	—	—
c	—	—	—
r1a	(Q3) 1.51×10^{-6}	(Q3)	(Q3)
b	—	—	—
c	—	—	—
r2a	(Q3) 7.69×10^{-7}	(Q5,12) 8.0×10^{-7}	(Q3) 3.34×10^{-7}
b	(Q1) 2.3×10^{-7}	(Q3) 1.0×10^{-6}	—
c	—	—	—
r3a	—	—	—
b	—	—	—
c	—	—	—
Y1a	(Q3) 1.7×10^{-17}	(Q3)	(Q3)
b	—	—	—
c	—	—	—
Y2a	(Q3) 1.93×10^{-17}	(Q5 12) 4.83×10^{-18}	(Q3) 4.54×10^{-18}
b	(Q1) 3.45×10^{-19}	(Q3) 2.02×10^{-17}	—
c	—	—	—
Y3a	—	—	—
b	—	—	—
c	—	—	—
G	6,8.	6,8.	6,8.
VF	—	—	—
VS	—	—	—

V	50	50	10
CD	5	15	0.04
I	3.93	11.8	0.032
t	19	25	25
T	600	1800	64800
INDEX NO.	10.3	11.0	11.2
V*F	6.3×10^{-10}	5.67×10^{-9}	5.44×10^{-10}
VF	3.5×10^{-3}	3.15×10^{-2}	3.02×10^{-3}
W*P	—	—	—
DF	8.02×10^{-6}	7.25×10^{-5}	6.92×10^{-6}
H1	6.15×10^{-7}	—	1.09×10^{-5}
H2	8.62×10^{-6}	7.73×10^{-5}	
H3	1.35×10^{-5}		—
H*	2.28×10^{-5}	7.73×10^{-5}	1.09×10^{-5}
Z	3	3	2
VOL	1.79×10^{-9}	6.07×10^{-9}	8.57×10^{-10}
A	—	—	2.88×10^{5}
R	64.78	6.62	36.52
Yr	1.16×10^{-9}	4.02×10^{-10}	3.13×10^{-10}
a_1	—	—	—
r*1a	(M5) 3.07×10^{-7}	(M5) 1.48×10^{-6}	(M5) 1.84×10^{-7}
b	—	—	—
c	—	—	—
r*2a	(M8b)	(M8b) 2.96×10^{-6}	(M16) 1.32×10^{-6}
b	—	—	(M17) 1.82×10^{-6}
c	—	—	(M9) 1.23×10^{-6}
r*3a	(M11a) 2.26×10^{-6}	(M2a) 1.0×10^{-5}	—
b	(M5) 3.23×10^{-7}	—	—
c	—	—	—
P1a	(M5) 1.22×10^{-19}	(M5) 1.36×10^{-17}	(M5) 2.59×10^{-20}
b	—	—	—
c	—	—	—
P2a	(M8b)	(M8b) 1.09×10^{-16}	(M16) 9.49×10^{-18}
b	—	—	(M17) 2.52×10^{-17}
c	—	—	(M9) 7.69×10^{-18}
P3a	(m11b) 4.82×10^{-17}	(M2a) 4.19×10^{-15}	—
b	(m5) 1.41×10^{-19}	—	—
c	—	—	—
r1a	(Q3)	(Q3)	(Q3)
b	—	—	—
c	—	—	—
r2a	(Q6) 6.15×10^{-7}	(Q6) 2.37×10^{-6}	(Q2a) 2.02×10^{-7}
b	—	—	(Q2b) 5.46×10^{-7}
c	—	—	—
r3a	(Q3) 4.84×10^{-7}	(Q3) 4.15×10^{-6}	—
b	—	—	—
c	—	—	—
Y1a	(Q3)	(Q3)	(Q3)
b	—	—	—
c	—	—	—
Y2a	(Q6) 1.03×10^{-17}	(Q6) 6.82×10^{-16}	(Q2a) 2.07×10^{-19}
b	—	—	(Q2b) 1.36×10^{-18}
c	—	—	—
Y3a	(Q3) 9.93×10^{-18}	(Q3) 2.09×10^{-15}	—
b	—	—	—
c	—	—	—
G	8, 7, 6	8, 6	4.
VF	—	—	.00015
VS	—	—	242.5

V	10	50,20,10.	50
CD	1·0	5·0	5·0, 2·0 1·0.
I	0·79	3·93	3·93, 1·58, 0·79.
†	25	25	25.
T	64800	200, 200, 200	200, 200, 200.
INDEX NO.	11·3	11·4.	11·5.
V*F	1.36×10^{-8}	6.3×10^{-10}.	3.37×10^{-10}
WF	7.56×10^{-2}	3.5×10^{-3}	1.87×10^{-3}
W*P	—	—	—
DF	1.73×10^{-4}	8.02×10^{-6}	3.32×10^{-6}
H1	5.52×10^{-6}	7.27×10^{-7}	} 1.4×10^{-6}
H2	7.93×10^{-5}	4.36×10^{-6}	
H3	1.0×10^{-4}	1.09×10^{-5}	—
H*	1.84×10^{-4}	1.6×10^{-5}	1.4×10^{-6}
Z	3	3	2
VOL	—	1.26×10^{-9}	1.1×10^{-10}
A	2.52×10^{5}	1.62×10^{5}	—
R	—	49·87	—
Yr	—	6.27×10^{-10}	—
a_1	—	3.8×10^{6}	8.72×10^{6}
r*1a	(M5) 6.9×10^{-7}	(M1,5) 3.72×10^{-7}	(M5) 1.78×10^{-7}
b	—	—	—
c	—	—	—
r*2a	(M9a) 6.9×10^{-6}	(M8b) 1.49×10^{-6}	(M11) 8.79×10^{-7}
b	—	(M15a) 3.35×10^{-6}	—
c	—	—	—
r*3a	(M8b) 4.48×10^{-6}	(M2a) 8.42×10^{-7}	—
b	—	(M14) 1.49×10^{-5}	—
c	—	—	—
P1a	(M5) 1.37×10^{-18}	(M1,5) 2.16×10^{-19}	(M5) 2.35×10^{-20}
b	—	—	—
c	—	—	—
P2a	(M9a) 9.51×10^{-11}	(M8b) 1.38×10^{-17}	(M11) 2.85×10^{-18}
b	—	(M15a)	—
c	—	—	—
P3a	(M8b) 3.78×10^{-16}	(M2a) 2.5×10^{-18}	—
b	—	(M14)	—
c	—	—	—
r1a	(Q3)	(Q3)	(Q3)
b	—	—	—
c	—	—	—
r2a	(Q1) 3.45×10^{-7}	(Q3) 5.58×10^{-7}	(Q3) 3.3×10^{-7}
b	—	—	—
c	—	—	—
r3a	(Q3) 1.79×10^{-7}	(Q3) 4.21×10^{-7}	—
b	(Q6) 3.57×10^{-7}	—	—
c	—	—	—
Y1a	(Q3)	(Q3)	(Q3)
b	—	—	—
c	—	—	—
Y2a	(Q1) 5.16×10^{-18}	(Q3) 4.27×10^{-18}	(Q3) 4.78×10^{-19}
b	—	—	—
c	—	—	—
Y3a	(Q3) 1.0×10^{-17}	(Q3) 6.07×10^{-18}	—
b	(Q6) 4.0×10^{-17}	—	—
c	—	—	—
G	9,8,7,6.	8,7,6	5,8.
VF	0·0015	0·1725	0·37
VS	230.	315.	—

V	50	50	50
CD	15·0	2·55	2·55
I	11·8	2·0	2·0
†	25	25	25
T	1800	1	5
INDEX NO.	11·7	11·6	11·6 (21·6)
V*F	5.67×10^{-9}	5.34×10^{-13}	2.67×10^{-12}
WF	3.15×10^{-2}	2.97×10^{-6}	1.49×10^{-5}
W*P	—	—	—
DF	7.22×10^{-5}	6.8×10^{-9}	3.4×10^{-8}
H1	5.26×10^{-7}	3.82×10^{-7}	3.78×10^{-7}
H2	1.47×10^{-5} (Q14) 5.53×10^{-6}	—	—
H3	1.85×10^{-5}	—	—
H*	3.92×10^{-5}	3.82×10^{-7}	3.78×10^{-7}
Z	3	1	1
VOL	3.08×10^{-9}	3.0×10^{-11}	2.97×10^{-11}
A	—	—	—
R	—	98·22	91·01
Yr	—	2.95×10^{-11}	2.7×10^{-11}
a_1	—	—	—
r*1a	(M5) 1.05×10^{-7}	(M5,1,2) 1.91×10^{-7}	(M5,2) 1.89×10^{-7}
b	—	—	—
c	—	—	—
r*2a	(M8b) 6.67×10^{-7}	—	—
b	(M14b) 2.67×10^{-5}	—	—
c	(M14a) 1.31×10^{-5}	—	—
r*3a	(M11) 3.04×10^{-6}	—	—
b	(M20) 4.85×10^{-6}	—	—
c	(M15a) 8.08×10^{-6}	—	—
P1a	(M5) 4.89×10^{-22}	(M5,1,2) 2.9×10^{-20}	(M5,2) 2.81×10^{-20}
b	—	—	—
c	—	—	—
P2a	(M8b) 1.24×10^{-18}	—	—
b	(M14b)	—	—
c	(M14a)	—	—
P3a	(M11) 1.19×10^{-16}	—	—
b	(M20)	—	—
c	(M15a)	—	—
r1a	(Q3)	(Q3)	(Q3)
b	—	—	—
c	—	—	—
r2a	(Q6)	—	—
b	—	—	—
c	—	—	—
r3a	(Q1) 3.81×10^{-7}	—	—
b	(Q8) 3.03×16^{-7}	—	—
c	—	—	—
Y1a	(Q3)	(Q3)	(Q3)
b	—	—	—
c	—	—	—
Y2a	(Q6)	—	—
b	—	—	—
c	—	—	—
Y3a	(Q1) 2.78×10^{-18}	—	—
b	(Q8) 5.34×10^{-18}	—	—
c	—	—	—
G	6,7,8	1	1,2a,4,6
VF	0·0706	1·27	—
VS	—	—	

V	50	50	50
CD	2·55	2·55	2·55
I	2·0	2·0	2·0
†	25	25	25
T	15	45	126
INDEX NO.	11·6 (31·6)	11·6 (41·6)	11·6 (51·6)
V*F	$8·01 \times 10^{-12}$	$2·4 \times 10^{-11}$	$6·41 \times 10^{-11}$
WF	$4·46 \times 10^{-5}$	$1·34 \times 10^{-4}$	$3·56 \times 10^{-4}$
W*P	—	—	—
DF	$1·02 \times 10^{-7}$	$3·06 \times 10^{-7}$	$8·16 \times 10^{-7}$
H1	$6·82 \times 10^{-7}$	} $1·45 \times 10^{-6}$	} $2·62 \times 10^{-6}$
H2	—		
H3	—	—	—
H*	$6·82 \times 10^{-7}$	$1·45 \times 10^{-6}$	$2·62 \times 10^{-6}$
Z	1	2	2
VOL	$5·35 \times 10^{-11}$	$1·14 \times 10^{-10}$	$2·06 \times 10^{-10}$
A	—	—	—
R	85·03	78·6	68·82
Yr	$4·55 \times 10^{-11}$	$9·02 \times 10^{-11}$	$1·42 \times 10^{-10}$
a_1	—	—	—
r*1a	(M5) $1·7 \times 10^{-7}$	(M5) $1·92 \times 10^{-7}$	(M5) $1·12 \times 10^{-7}$
b	(M6) $6·81 \times 10^{-7}$	—	—
c	—	—	—
r*2a	—	(M6a) $1·82 \times 10^{-7}$	(M6a) $2·01 \times 10^{-7}$
b	—	(M8b) $1·34 \times 10^{-6}$	(M15a) $3·6 \times 10^{-6}$
c	—	—	(M10) $1·44 \times 10^{-6}$
r*3a	—	—	—
b	—	—	—
c	—	—	—
P1a	(M5) $2·07 \times 10^{-20}$	(M5) $2·52 \times 10^{-20}$	(M5) $5·91 \times 10^{-21}$
b	(M6) $1·32 \times 10^{-18}$	—	—
c	—	—	—
P2a	—	(M6a) $2·52 \times 10^{-20}$	(M6a) $3·4 \times 10^{-20}$
b	—	(M8b) $9·93 \times 10^{-19}$	(M15a)
c	—	—	(M10) $1·26 \times 10^{-17}$
P3a	—	—	—
b	—	—	—
c	—	—	—
r1a	(Q3) $1·7 \times 10^{-7}$	(Q3)	(Q3)
b	—	—	—
c	—	—	—
r2a	—	(Q3) $1·09 \times 10^{-7}$	(Q3) $8·37 \times 10^{-8}$
b	—	(Q6) $3·64 \times 10^{-7}$	(Q6) $3·35 \times 10^{-7}$
c	—	—	—
r3a	—	—	—
b	—	—	—
c	—	—	—
Y1a	(Q3) $6·2 \times 10^{-20}$	(Q3)	(Q3)
b	—	—	—
c	—	—	—
Y2a	—	(Q3) $5·41 \times 10^{-20}$	(Q3) $5·77 \times 10^{-20}$
b	—	(Q6) $6·04 \times 10^{-19}$	(Q6) $9·22 \times 10^{-19}$
c	—	—	—
Y3a	—	—	—
b	—	—	—
c	—	—	—
G	3	4 2	5 2
VF	2·69	0.111	= 10.210
VS	—	—	—

V	50	50	50
CD	2·55	2·55	2·55
I	2·0	2·0	2·0
†	25	25	25
T	300	600	600
INDEX NO.	11·6 (61·6)	11·6 (71·6)	12·2
V*F	$1·6 \times 10^{-10}$	$3·2 \times 10^{-10}$	$3·21 \times 10^{-10}$
WF	$8·91 \times 10^{-4}$	$1·78 \times 10^{-3}$	$1·78 \times 10^{-3}$
W*P	—	—	—
DF	$2·04 \times 10^{-6}$	$4·08 \times 10^{-6}$	$4·08 \times 10^{-6}$
H1	$3·53 \times 10^{-6}$	$5·2 \times 10^{-6}$	$6·22 \times 10^{-6}$
H2			$9·33 \times 10^{-6}$
H3	—	—	—
H*	$3·53 \times 10^{-6}$	$5·2 \times 10^{-6}$	$1·55 \times 10^{-5}$
Z	2	2	2
VOL	$2·77 \times 10^{-10}$	$4·09 \times 10^{-10}$	$1·22 \times 10^{-9}$
A	—	—	—
R	42·29	21·66	73·08
Yr	$1·17 \times 10^{-10}$	$8·85 \times 10^{-11}$	$8·99 \times 10^{-10}$
a_L	$4·95 \times 10^{6}$	—	$2·58 \times 10^{6}$
r*1a	(M5) $1·57 \times 10^{-7}$	(M5)	(M5) $1·92 \times 10^{-7}$
b	—	—	—
c	—	—	—
r*2a	(M19) $3·9 \times 10^{-7}$	(M19) $2·0 \times 10^{-7}$	(M19)
b	—	(M15a) $3·2 \times 10^{-6}$	(M15a) $1·98 \times 10^{-6}$
c	—	—	—
r*3a	—	—	—
b	—	—	—
c	—	—	—
P1a	(M5) $1·62 \times 10^{-20}$	(M5)	(M5) $2·52 \times 10^{-20}$
b	—	—	—
c	—	—	—
P2a	(M19) $2·49 \times 10^{-19}$	(M19) $3·35 \times 10^{-20}$	(M19)
b	—	(M15a)	(M15a)
c	—	—	—
P3a	—	—	—
b	—	—	—
c	—	—	—
r1a	(Q3)	(Q3)	(Q3)
b	—	—	—
c	—	—	—
r2a	(Q3) $9·76 \times 10^{-8}$	(Q3) $1·0 \times 10^{-7}$	(Q8) $2·38 \times 10^{-7}$
b	(Q6) $1·95 \times 10^{-7}$	(Q6) $4·0 \times 10^{-7}$	—
c	—	—	—
r3a	—	—	—
b	—	—	—
c	—	—	—
Y11a	(Q3)	(Q3)	(Q3)
b	—	—	—
c	—	—	—
Y12a	(Q3) $1·06 \times 10^{-19}$	(Q3) $1·64 \times 10^{-19}$	(Q8) $2·75 \times 10^{-18}$
b	(Q6) $4·22 \times 10^{-19}$	(Q6) $2·62 \times 10^{-18}$	—
c	—	—	—
Y13a	—	—	—
b	—	—	—
c	—	—	—
G	5,6	7,8	6,7,8.
VE	−0·084	0·06	0·0184
VS	—	—	—

V	50	50	56
CD	2·55	2·55	2·55
l	2·0	2·0	2·0
t	25	25	25
T	600	600	600
INDEX NO.	12·3	12·4	12·5
V*F	$3·21 \times 10^{-10}$	$2·21 \times 10^{-10}$	$3·21 \times 10^{-10}$
WF	$1·78 \times 10^{-3}$	$1·78 \times 10^{-3}$	$1·78 \times 10^{-3}$
W*P	—	—	—
DF	$4·08 \times 10^{-6}$	$4·08 \times 10^{-6}$	$4·08 \times 10^{-6}$
H1	$6·22 \times 10^{-6}$	$8·0 \times 10^{-6}$	$7·14 \times 10^{-6}$
H2	$9·31 \times 10^{-6}$		
H3	—	—	—
H*	$1·55 \times 10^{-5}$	$8·0 \times 10^{-6}$	$7·14 \times 10^{-6}$
Z	2	2	2
VOL	$1·22 \times 10^{-9}$	$6·28 \times 10^{-10}$	$5·61 \times 10^{-10}$
A	—	—	—
R	73·08	48·92	42·79
Yr	$8·99 \times 10^{-10}$	$3·07 \times 10^{-10}$	$2·4 \times 10^{-10}$
a_l	$3·44 \times 10^{6}$	—	$2·43 \times 10^{6}$
r*1a	(M5) $3·89 \times 10^{-7}$	(M5)	(M5) $2·14 \times 16^{-7}$
b	(M8,9) $9·06 \times 10^{-7}$	—	—
c	—	—	—
r*2a	(M11) $8·91 \times 10^{-7}$	(M19)	(M19)
b	(M4) $1·19 \times 10^{-6}$	(M16) $8·34 \times 10^{-7}$	(M15a)
c	—	(M15a) $1·6 \times 10^{-6}$	—
r*3a	—	—	—
b	—	—	—
c	—	—	—
P1a	(M5) $2·45 \times 10^{-19}$	(M5)	(M5) $4·12 \times 10^{-20}$
b	(M8,9) $3·11 \times 10^{-18}$	—	—
c	—	—	—
P2a	(M11) $2·96 \times 10^{-18}$	(M19)	(M19)
b	(M4) $7·03 \times 10^{-18}$	(M16) $2·43 \times 10^{-18}$	(M15a)
c	—	(M15a) —	—
P3a	—	—	—
b	—	—	—
c	—	—	—
r1a	(Q3) $2·35 \times 10^{-7}$	(Q3)	(Q3)
b	—	—	—
c	—	—	—
r2a	(Q3) $3·96 \times 10^{-7}$	(Q8) $2·0 \times 10^{-7}$	(Q8) $2·86 \times 10^{-7}$
b	(Q1) $1·98 \times 10^{-7}$	(Q2a) $1·67 \times 10^{-7}$	—
c	(Q6) $3·96 \times 10^{-6}$	—	—
r3a	—	—	—
b	—	—	—
c	—	—	—
Y11a	(Q3) $5·46 \times 10^{-20}$	(Q3)	(Q3)
b	—	—	—
c	—	—	—
Y12a	(Q3) $4·6 \times 10^{-18}$	(Q8) $1·01 \times 16^{-18}$	(Q8) $1·83 \times 10^{-18}$
b	(Q1) $2·2 \times 10^{-19}$	(Q2a) $6·99 \times 10^{-19}$	—
c	(Q6) $4·6 \times 10^{-16}$	—	—
Y13a	—	—	—
b	—	—	—
c	—	—	—
G	6,7,8	6,8,7	7,8,5
VF	0·0184	0·044	0·044
VS	—	—	—

V	50	50	55
CD	2.55	10	1.5
J	2.0	7.86	1.18
†	25	25	45
T	600	250	630
INDEX NO.	12.6	12.8	4a
V*F	3.21×10^{-16}	6.68×10^{-10}	1.99×10^{-10}
WF	1.78×10^{-3}	3.71×10^{-3}	1.1×10^{-3}
W*P	—	—	—
DF	4.08×10^{-6}	8.5×10^{-6}	2.53×10^{-6}
H1	6.05×10^{-6}	7.51×10^{-7}	6.15×10^{-6}
H2		3.51×10^{-6}	
H3	—	—	—
H*	6.05×10^{-6}	4.26×10^{-6}	6.15×10^{-6}
Z	2	2	2
VOL	4.76×10^{-10}	3.35×10^{-10}	4.84×10^{-16}
A	—	—	6.12×10^{4}
R	32.5	—	58.83
Yr	1.55×10^{-10}	—	2.85×10^{-10}
a_1	1.26×10^{6}	—	7.12×10^{5}
r*1a	(M5) 2.16×10^{-7}	(M5) 1.18×10^{-7}	(M5) 1.54×10^{-7}
b	—	—	—
c	—	—	—
r*2a	(M19)	(M19) 8.51×10^{-7}	(M9) 2.15×10^{-6}
b	(M15a) 1.6×10^{-6}	—	(M5) 3.7×10^{-7}
c	—	—	—
r*3a	—	—	—
b	—	—	—
c	—	—	—
P1a	(M5) 4.24×10^{-20}	(M5) 6.82×10^{-21}	(M5) 1.53×10^{-20}
b	—	—	—
c	—	—	—
P2a	(M19)	(M19) 2.58×10^{-18}	(M9) 4.19×10^{-17}
b	(M15a)	—	(M5) 2.11×10^{-19}
c	(1 —	—	—
P3a	—	—	—
b	—	—	—
c	—	—	—
r1a	(Q3)	(Q3) 1.96×10^{-7}	(Q3)
b	—	—	—
c	—	—	—
r2a	(Q8) 2.8×10^{-7}	(Q8) 5.32×10^{-7}	(Q2) 6.15×10^{-7}
b	—	—	(Q3) 6.15×10^{-7}
c	—	—	—
r3a	—	—	—
b	—	—	—
c	—	—	—
Y1a	(Q3)	(Q3) 9.01×10^{-20}	(Q3)
b	—	—	—
c	—	—	—
Y2a	(Q8) 1.49×10^{-18}	(Q8) 3.12×10^{-18}	(Q2) 2.56×10^{-18}
b	—	—	(Q3) 7.32×10^{-18}
c	—	—	—
Y3a	—	—	—
b	—	—	—
c	—	—	—
G	6, 8, 7.	6, 8.	9
VE	—	—	0.114
VS	—	—	228.

V	55	55	55
CD	1·5	1·5	1·5
1	1·18	1·18	1·18
†	45	45	45
T	630	630	630
INDEX NO.	4b	4c	4d
V*F	$1·99 \times 10^{-10}$	$1·99 \times 10^{-10}$	$1·99 \times 10^{-10}$
WF	$1·1 \times 10^{-3}$	$1·1 \times 10^{-3}$	$1·1 \times 10^{-3}$
W*P	—	—	—
DF	$2·53 \times 10^{-6}$	$2·53 \times 10^{-6}$	$2·53 \times 10^{-6}$
H1	}		
H2	} $1·75 \times 10^{-5}$		
H3	}		
H*	$1·75 \times 10^{-5}$		
Z	3		
VOL	$1·38 \times 10^{-9}$		
A	$2·02 \times 10^{5}$	$7·2 \times 10^{4}$	$1·8 \times 10^{5}$
R	85·54		
Yr	$1·18 \times 10^{-9}$		
a1	—		
r*1a	(M5) $8·7 \times 10^{-7}$	(M9) $1·25 \times 10^{-6}$	(M18) $1·25 \times 10^{-7}$
b	—	—	—
c	—	—	—
r*2a	(M2a) $1·16 \times 10^{-6}$	—	—
b	—	—	—
c	—	—	—
r*3a	(M8b) $5·8 \times 10^{-7}$	—	—
b	—	—	—
c	—	—	—
P1a	(M5) $2·75 \times 10^{-18}$	(M9) $8·18 \times 10^{-18}$	(M18) $1·56 \times 10^{-20}$
b	—	—	—
c	—	—	—
P2a	(M2a) $6·53 \times 10^{-18}$	—	—
b	—	—	—
c	—	—	—
P3a	(M8b) $8·16 \times 10^{-19}$	—	—
b	—	—	—
c	—	—	—
r1a	(Q3)	—	(Q9) $1·25 \times 10^{-7}$
b	—	—	—
c	—	—	—
r2a	(Q3) $8·7 \times 10^{-7}$	—	—
b	(Q1) $2·9 \times 10^{-7}$	—	—
c	—	—	—
r3a	(Q7) $1·74 \times 10^{-7}$	—	—
b	—	—	—
c	—	—	—
Y11a	(Q3)	—	(Q9) $4·91 \times 10^{-20}$
b	—	—	—
c	—	—	—
Y12a	(Q3) $4·16 \times 10^{-17}$	—	—
b	(Q1) $6·13 \times 10^{-19}$	—	—
c	—	—	—
Y13a	(Q7) $1·35 \times 10^{-18}$	—	—
b	—	—	—
c	—	—	—
G	2,3	10	10
VF	0·095	0·073	0·014
VS	212·5.	227.	129

V	55	55	55
CD	1·5	1·5	1·5
I	1·18	1·18	1·18
†	45	45	45
T	630	630	630
INDEX NO.	4e	4f	4g
V*F	$1·99 \times 10^{-10}$	$1·99 \times 10^{-10}$	$1·99 \times 10^{-10}$
WF	$1·1 \times 10^{-3}$	$1·1 \times 10^{-3}$	$1·1 \times 10^{-3}$
W*P	—	—	—
DF	$2·53 \times 10^{-6}$	$2·53 \times 10^{-6}$	$2·53 \times 10^{-6}$
H1		$5·73 \times 10^{-6}$	$6·67 \times 10^{-6}$
H2			
H3			—
H*		$5·73 \times 10^{-6}$	$6·67 \times 10^{-6}$
Z		3	2
VOL		$4·5 \times 10^{-10}$	$5·24 \times 10^{-10}$
A	$1·08 \times 10^{5}$	$9·72 \times 10^{4}$	$3·6 \times 10^{4}$
R		55 - 75	62·0
Yr		$2·51 \times 10^{-10}$	$3·25 \times 10^{-10}$
a_1	$4·13 \times 10^{3}$	—	—
r*1a	(M5) $1·39 \times 10^{-6}$	(M5)	(M5) $3·7 \times 10^{-7}$
b	(M22)	—	—
c	—	—	—
r*2a	(M5) $1·72 \times 10^{-6}$	(M2a) $1·07 \times 10^{-6}$	(M9) $3·24 \times 10^{-7}$
b	—	—	(M5) $1·85 \times 10^{-7}$
c	—	—	—
r*3a	—	(M15) $4·3 \times 10^{-6}$	—
b	—	—	—
c	—	—	—
P1a	(M5) $1·12 \times 10^{-17}$	(M5)	(M5) $2·13 \times 10^{-19}$
b	(M22)	—	—
c	—	—	—
P2a	(M5) $2·11 \times 10^{-17}$	(M2a) $5·18 \times 10^{-18}$	(M9) $1·43 \times 10^{-19}$
b	—	—	(M5) $2·66 \times 10^{-20}$
c	—	—	—
P3a	—	(M15)	—
b	—	—	—
c	—	—	—
r1a	—	—	—
b	—	—	—
c	—	—	—
r2a	(Q8) $2·86 \times 10^{-6}$	—	—
b	—	—	—
c	—	—	—
r3a	—	—	—
b	—	—	—
c	—	—	—
Y1a	—	—	—
b	—	—	—
c	—	—	—
Y2a	(Q8)	—	—
b	—	—	—
c	—	—	—
Y3a	—	—	—
b	—	—	—
c	—	—	—
G	6	8·7	9.
VF	0·08	0·1081	0·065
VS	314	225	320.

V	55	55	
CD	1·5	1·5	
l	1·18	1·18	
t	45	45	
T	630	630	
INDEX NO.	4h.	4j	
V*F	1.99×10^{-10}	1.99×10^{-10}	
WF	1.1×10^{-3}	1.1×10^{-3}	
W*P	—	—	
DF	2.53×10^{-6}	2.53×10^{-6}	
H1	4.95×10^{-6}	3.52×10^{-7}	
H2		2.43×10^{-6}	
H3	—	6.26×10^{-6}	
H*	4.95×10^{-6}	9.04×10^{-6}	
Z	2	3	
VOL	3.89×10^{-10}	7.1×10^{-10}	
A	1.26×10^{5}	2.23×10^{5}	
R	48.8	71.99	
Yr	1.9×10^{-10}	5.12×10^{-10}	
a	—	—	
r*1a	(M5) 2.06×10^{-7}	(M5) 1.76×10^{-7}	
b	—	—	
c	—	—	
r*2a	(M9) 8.25×10^{-6}	(M9) 1.4×10^{-6}	
b	—	—	
c	—	—	
r*3a	—	(M5) 1.74×10^{-7}	
b	—	—	
c	—	—	
P1a	(M5) 3.67×10^{-20}	(M5) 2.26×10^{-20}	
b	—	—	
c	—	—	
P2a	(M9) 2.35×10^{-15}	(M9) 1.16×10^{-17}	
b	—	—	
c	—	—	
P3a	—	(M5) 2.21×10^{-20}	
b	—	—	
c	—	—	
r1a	(Q3) 1.03×10^{-7}	—	
b	—	—	
c	—	—	
r2a	(Q2) 4.13×10^{-7}	—	
b	—	—	
c	—	—	
r3a	—	—	
b	—	—	
c	—	—	
Y1a	(Q3) 1.65×10^{-19}	—	
b	—	—	
c	—	—	
Y2a	(Q2) 4.41×10^{-18}	—	
b	—	—	
c	—	—	
Y3a	—	—	
b	—	—	
c	—	—	
G	9	9	
VF	0·09	0·495	
VS	280.	261	

SECTION (1a)

TYPES OF PARTICLES AND PORES IN THE FILM

PARTICLES

M1

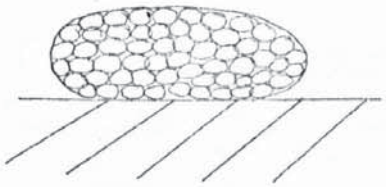

An oval particle made up of small K type nodules.

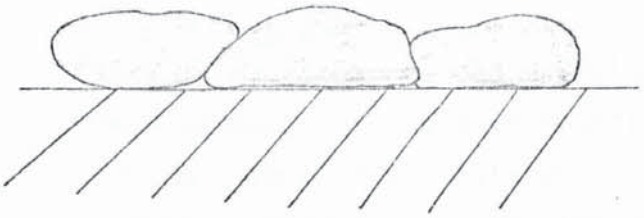

M2

Oval particles joined together in band.

M2a

As M2 but much larger and associated with second layer. Related to M11 or M19.

M3

Blocky particles of Ag Cl on surface
In redistributed film.

M4

Islands of large rounded or multiplanar regular particles in a surrounding matrix of small particles. Islands seem regularly spaced along troughs and are associated with pores.

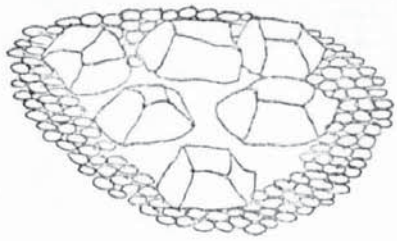

M5

Round nodules, again made up of K type particles, and much larger than the MI's.

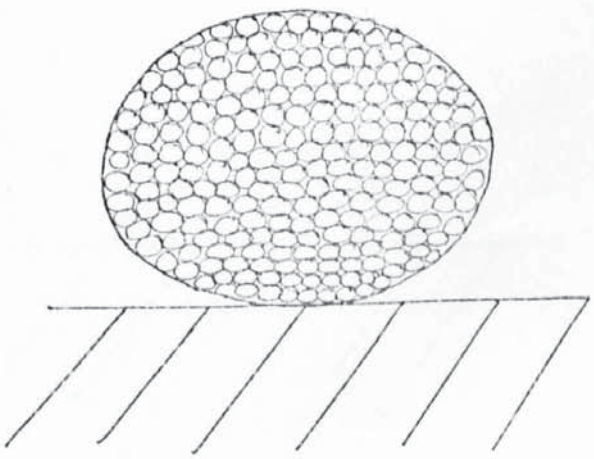

M6

Round agglomerates of particles on the base Ag.

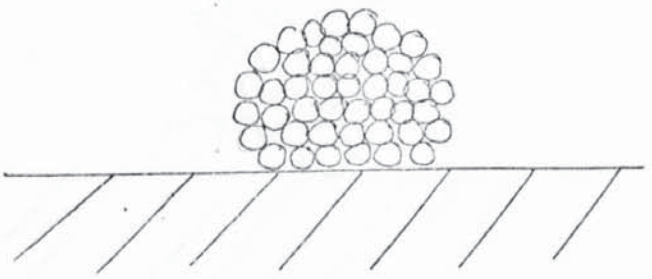

M6a

An extension of M6, the agglomerates have coalesced into bulbed mounds and ridges.

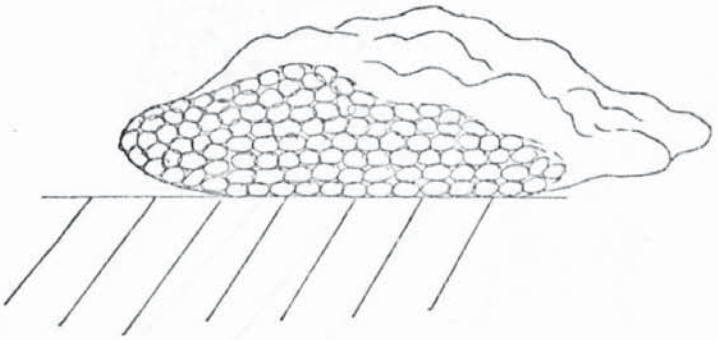

M7

Like M6 but made up of irregular particles.

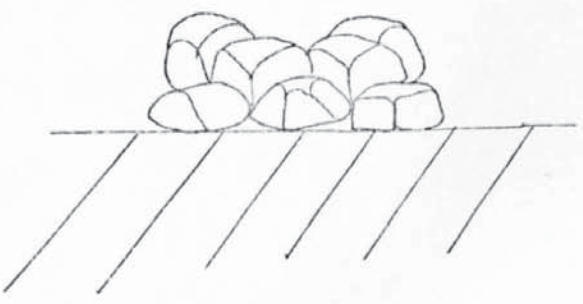

M8

Cactus particle, nodules joined together to form irregular arms.

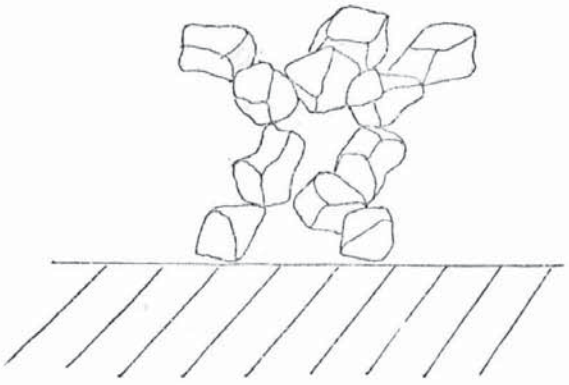

M8a

Extended type of M8, a thick layer being formed.

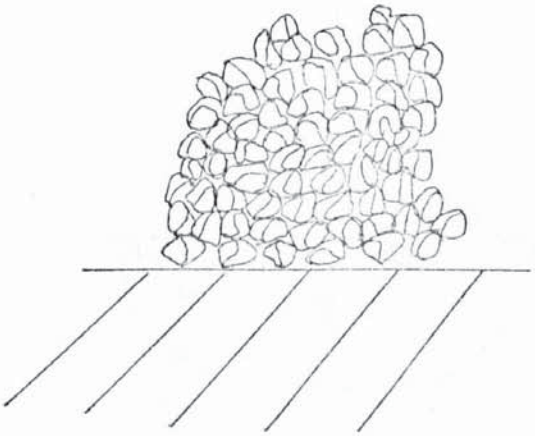

M8b

As M8a but nodules more rounded.

M9

Blocky type particle with flattish sides. Can be semi crystalline and facetted.

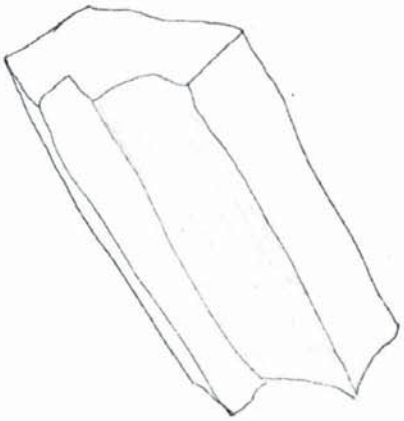

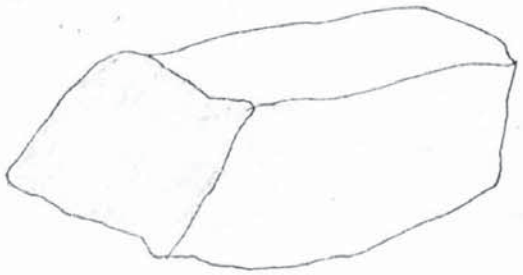

M10

Nodules growing on particles in higher layers. Generally associated with K type nodules.

M11

Very interlocked particles which fit together to form a coherent film. Looks almost like an Inca wall with very smooth surfaces and joints. Comes in three main shapes, as illustrated.

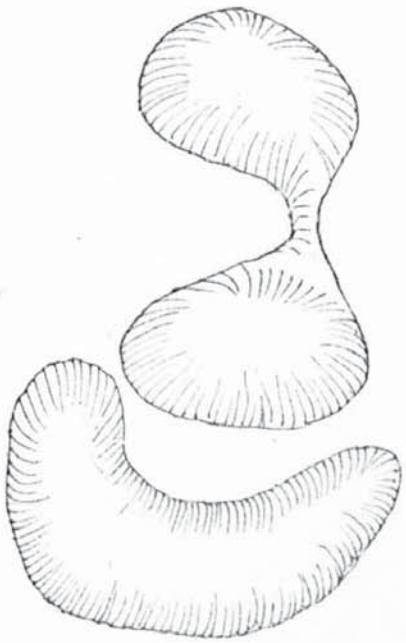

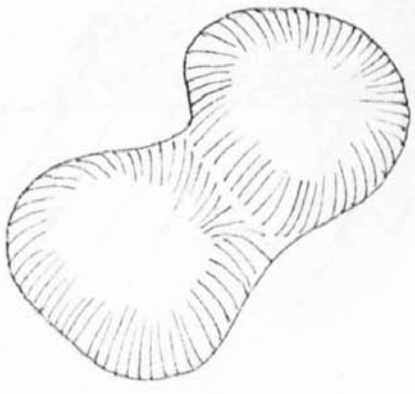

MI1b

Plate like particle, often pierced with pores.

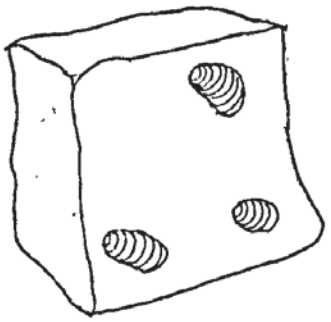

MI2

Particle with depression on the top and pore at centre. Channels run from side of particle to pore.

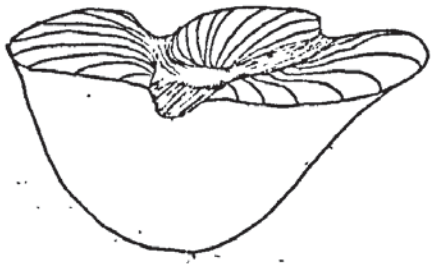

MI3

Almost fibrous porous clumps of material lying on the surface. Very little structure.

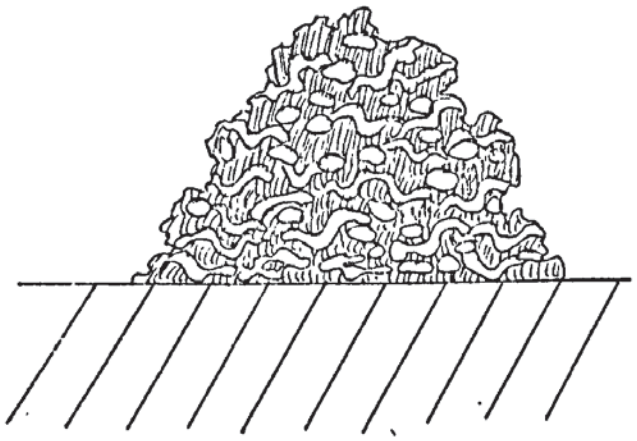

M14

Dendrite needle arms, nodular at the base, and finned.

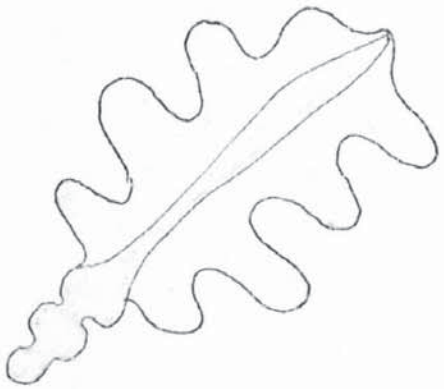

M14a

Needles made up of nodules, related to M8.

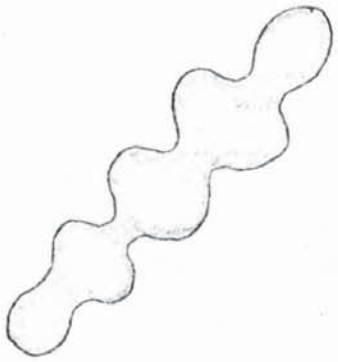

M15

Like 14a but not nodular.

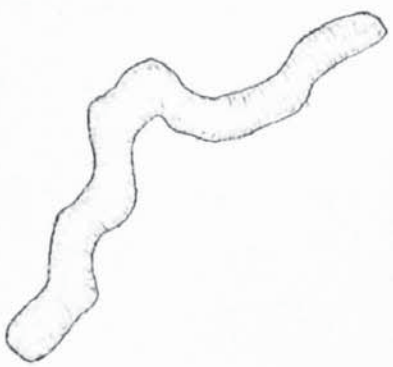

M15a

Straight needles, no fins and not nodular except at base. Associated with pore mouths and tends to grow in pairs.

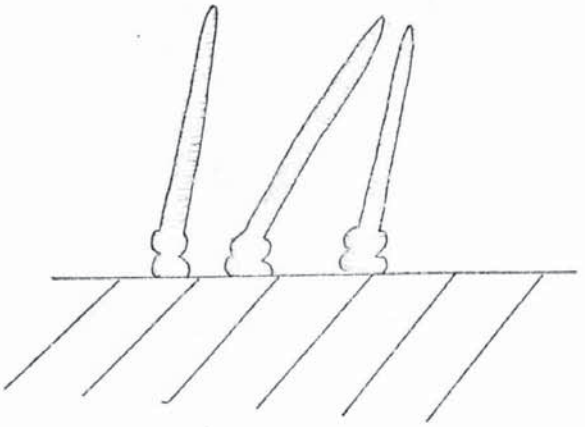

M16

Four sided pyramidal, particle and pore descending down from apex.

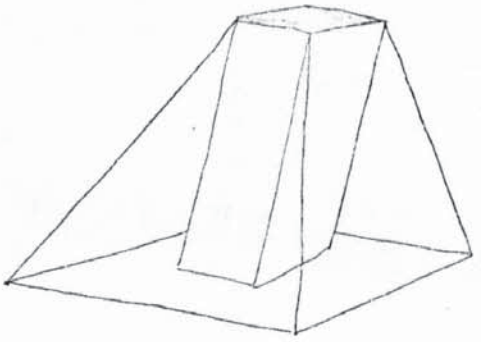

M17

As M16 but three sided pyramidal and three sided pore.

M18

Coral like structure of Ag Cl with pores descending down the arms of the particles.

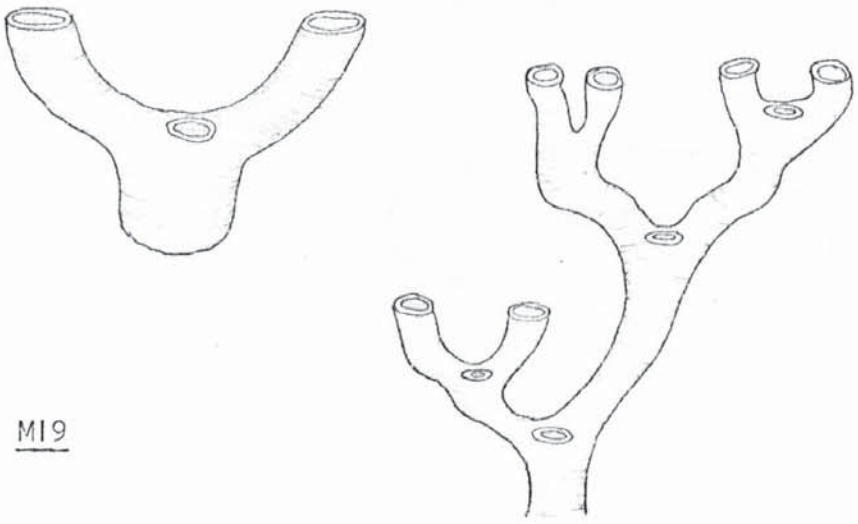

M19

Columnar type film of large particles.

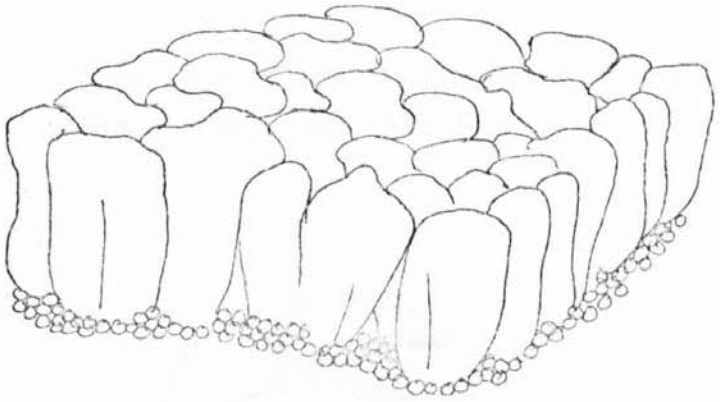

M20

Thin triangular platelets appearing out of the surface.

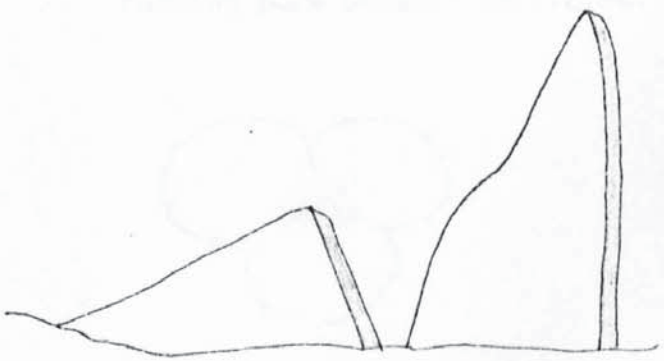

PORES

Q1

Pore in particle.

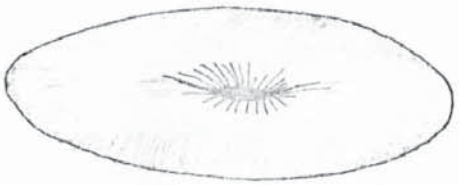

Q2

Pore in particle, but hole is square and channels run into it.

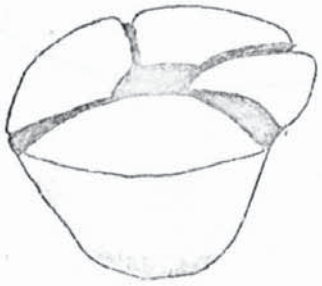

Q3

Packing pore between particles.

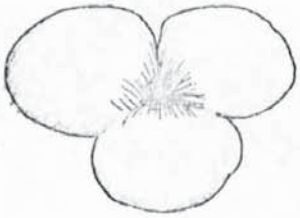

Q4

Very large Q3 type pore in Islands of very large particles surrounded by matrix of smaller particles. Related to Q6 pore.

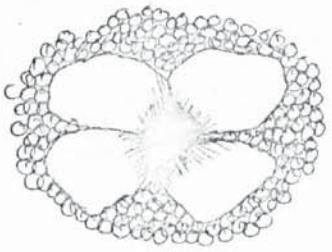

Q5

Rounded depression on particle surface.

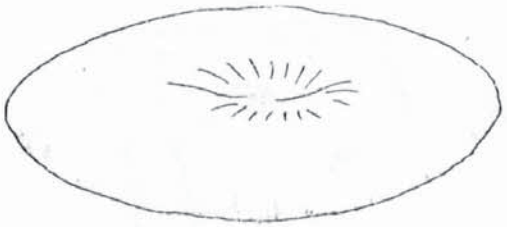

Q6

Very large pore extending through the film. Formed after layer growth.

Q7

Mini pores in semi amorphous mass or in very fine jumbled particles.

Q8

Pore in relatively flat surface of particle, like a platelet.

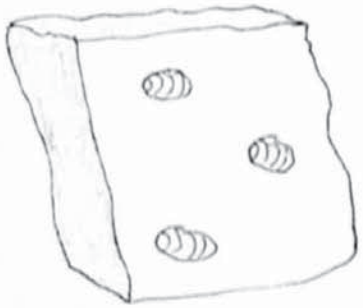

Q9

Pore down centre of arm.

Q10

Pores formed by closing of ridges over troughs.

SECTION (1b)

KEY TO ABBREVIATIONS

ABBREVIATIONS

V	Applied potential (volts)
CD	Current density (ma/cm^2)
CURNT (i)	Applied current (ma)
TEMP (t)	Anodising temperature (^oC)
TIME (T)	Anodising time (secs)
WF	Film weight from Faradays Laws (gms)
WSTRP (w*p)	Measured film weight (gms)
DF	Film thickness calculated
H1	Thickness of first layer (m)
H2	Thickness of second layer (m)
H3	Thickness of third layer (m)
HSTR (H*)	Film thickness (m)
Z	Number of layers in film.
VOL	Film volume (m^3)
A	Aging time (secs)
R (R*)	Percentage Porosity (%)
YR (yr)	Volume of pores in the film (m^3)(using Faradays Laws)
AI (ai)	Number of pores/unit area on film surface ($no./m^2$)
RST1A	Radius of (denoted) particle in first layer (m)
RST1B	Radius of (denoted) particle in first layer (m)
RST1C	Radius of (denoted) particle in first layer (m)
RST2A	Radius of (denoted) particle in second layer (m)
RST2B	Radius of (denoted) particle in second layer (m)
RST2C	Radius of (denoted) particle in second layer (m)
RST3A	Radius of (denoted) particle in thrid layer (m)
RST3B	Radius of (denoted) particle in third layer (m)
RST3C	Radius of (denoted) particle in third layer (m)

PI A	Volume of (denoted) particle in first layer (m^3)
PI B	Volume of (denoted) particle in first layer (m^3)
PI C	Volume of (denoted) particle in first layer (m^3)
P2 A	Volume of (denoted) particle in second layer (m^3)
P2 B	Volume of (denoted) particle in second layer (m^3)
P2 C	Volume of (denoted) particle in second layer (m^3)
P3 A	Volume of (denoted) particle in third layer (m^3)
P3 B	Volume of (denoted) particle in third layer (m^3)
P3 C	Volume of (denoted) particle in third layer (m^3)
RLTIA	Radius of (denoted) pore in first layer (m)
RLTIB	Radius of (denoted) pore in first layer (m)
RLTIC	Radius of (denoted) pore in first layer (m)
RLT2A	Radius of (denoted) pore in second layer (m)
RLT2B	Radius of (denoted) pore in second layer (m)
RLT2C	Radius of (denoted) pore in second layer (m)
RLT3A	Radius of (denoted) pore in third layer (m)
RLT3B	Radius of (denoted) pore in third layer (m)
RLT3C	Radius of (denoted) pore in third layer (m)
YI IA	Volume of (denoted) pore in first layer (m^3)
YI IB	Volume of (denoted) pore in first layer (m^3)
YI IC	Volume of (denoted) pore in first layer (m^3)
YI 2A	Volume of (denoted) pore in second layer (m^3)
YI 2B	Volume of (denoted) pore in second layer (m^3)
YI 2C	Volume of (denoted) pore in second layer (m^3)

YI 3A	Volume of (denoted) pore in third layer (m^3)
YI 3B	Volume of (denoted) pore in third layer (m^3)
YI 3C	Volume of (denoted) pore in third layer (m^3)
VF	Change in potential with time access cell when anodising - $\frac{dv}{dt}$
VS	Equilibrium potential of electrode w.r.t. saturated calomel electrode in KCl. (mV.)
G	Film geometry rating.

SECTION (IC)

FILM GEOMETRY RATING

A scale denoting the type of film structure.

1 = Scattered particles on surface.

2 = Occasional humped mounds.

2a = Occasional ridges.

3 = Broken part formed ridges and troughs.

4 = Well formed ridges and wide troughs

5 = Well formed ridges and closed troughs.

6 = Flat coherent, top surface.

7 = Thick film, evidence of nuclei on surface.

8 = Thick probably multilayer film.

9 = Disrupted film, evidence of renucleation or rearrangement.

10 = Etched particles, evidence of redissolution.

Can have two types quoted together, i.e. 8, 7. In this case this is a thick film of well formed particles, with needle nuclei on top.

SECTION (2)

REGRESSION ANALYSIS AND EQUATIONS ON FILM PARAMETERS AND VARIABLES

REGRESSION ANALYSIS COVA DATA1 CUT OFF PARAMETER .100000E- 5

DEPENDENT VARIABLE YR DEGREES OF FREEDOM 91

INDEPENDENT VARIABLES AT SIGNIFICANY LEVEL 5.00 %

V	CD	CURNT	TEMP	TIME	WF	WSTRP	DF	H1	H2	H3	HSTR	Z	VOL
A	R	AI	RST1A	RST1B	RST1C	RST2A	RST2B	RST2C	RST3A	RST3B	RST3C	P1A	P1B
P1C	P2A	P2B	P2C	P3A	P3B	P3C	RLT1A	RLT1B	RLT1C	RLT2A	RLT2B	RLT2C	RLT3A
RLT3B	RLT3C	YI1A	YI1B	YI1C	YI2A	YI2B	YI2C	YI3A	YI3B	YI3C	VF	VS	

VARIABLES IN THE REGRESSION SET

VAR NAME	REGRESSION COEFF	STANDARD ERROR	CONFIDENCE INTERVAL	T STAT	PART CORR	MULTIPLE CORRELATION	F S S
DF	0.6152501	.2762942E- 1	.5481644E- 1	22.27	-0.92	0.796	.6335968E 3
HSTR	0.5068685	.2962345E- 1	.5877377E- 1	19.14	0.89	0.845	.4935599E 3
Z	1.3151242	.2874406E 0	.5710990E 0	4.57	0.43	0.964	.1207826E 3
VOL	0.0852116	.1599119E- 1	.3172790E- 1	5.33	0.49	0.962	.1288609E 3
R	0.0414799	.5375906E- 2	.1066590E- 1	4.00	0.39	0.966	.1154481E 3
RST2C	1.5027943	.1258986E 0	.2458613E 0	12.77	0.80	0.917	.2744413E 3
P2A	0.4007211	.1168858E 0	.2318958E 0	3.43	0.34	0.967	.1109368E 3

VARIABLES NOT IN THE REGRESSION SET

VAR NAME	T STAT	PART CORR	MULTIPLE CORRELATION	F S S
V	1.83	0.19	0.972	.9472935E 2
CD	0.92	0.10	0.971	.9732108E 2
CURNT	0.92	0.10	0.971	.9752408E 2
TEMP	1.02	0.11	0.971	.9712492E 2
TIME	1.54	-0.16	0.972	.9573735E 2
WF	0.46	-0.05	0.971	.9801290E 2
WSTRP	1.05	0.11	0.971	.9704888E 2
H1	0.03	0.00	0.971	.9824446E 2
H2	1.23	0.13	0.972	.9661296E 2
H3	1.84	0.19	0.972	.9466846E 2

VAR NAME	T STAT	PART CORR	MULTIPLE CORRELATION	E S S	
A	0.60	-0.06	0.971	.9785A7E	2
AI	0.66	0.07	0.971	.977771E	2
RST1A	1.93	-0.20	0.972	.9435?2E	2
RST1B	1.91	0.20	0.972	.944076E	2
RST1C	0.73	0.08	0.971	.9747?7E	2
RST2A	1.42	-0.15	0.972	.9603?3E	2
RST2B	1.17	0.12	0.972	.9677?5E	2
RST3A	1.86	-0.19	0.972	.945?41E	2
RST3B	0.29	-0.03	0.971	.9815?0E	2
RST3C	1.64	0.17	0.972	.9540?7E	2
P1A	1.30	-0.14	0.972	.9643?9E	2
P1B	0.39	0.04	0.971	.9807?5E	2
P1C	0.29	0.03	0.971	.9815?8E	2
P2B	0.73	-0.08	0.971	.976648E	2
P2C	0.18	-0.02	0.971	.9820?9E	2
P3A	0.71	-0.07	0.971	.97697?E	2
P3B	0.10	0.01	0.971	.9823?1E	2
P3C	0.00		0.971	.982457E	2
RLY1A	0.61	0.06	0.971	.978?25E	2
RLY1B	1.11	0.12	0.972	.969?76E	2
RLY1C	0.00	0.00	0.971	.0000?0E	0
RLY2A	0.44	0.05	0.971	.9803?6E	2
RLY2B	0.11	-0.01	0.971	.9823?5E	2
RLY2C	0.90	0.09	0.971	.9736?5E	2
RLY3A	1.25	-0.13	0.972	.9655?0E	2
RLY3B	1.35	0.14	0.972	.9628?9E	2
RLY3C	0.67	-0.07	0.971	.977547E	2
VI1A	0.97	-0.10	0.971	.972?72E	2
VI1B	0.29	0.03	0.971	.9815?3E	2

16/57/54 22/09/78 ICL 1900 STATISTICAL ANALYSIS XDS3/26

VAR NAME	T STAT	PART CORR	MULTIPLE CORRELATION	E S S
YI1C	0.00	0.00	0.971	.000000E 0
YI2A	1.75	0.16	0.972	.9501488 2
YI2B	0.52	0.06	0.971	.9794848 2
YI2C	0.49	0.05	0.971	.9798688 2
YI3A	0.19	0.02	0.971	.9820408 2
YI3B	0.57	0.06	0.971	.9789758 2
YI3C	0.44	0.05	0.971	.9803108 2
VF	0.02	0.00	0.971	.9824538 2
VS	0.46	0.05	0.971	.9801838 2

E.S.S. .982457E 2

RESIDUAL ERROR .103905E 1

MULT CORR 0.971

INTERCEPT TERM 3.5855090

GET

NUMBER OF PAGES 27

REGRESSION ANALYSIS . COVA DATA1 CUT OFF PARAMETER .100000E- 5

DEPENDENT VARIABLE Z DEGREES OF FREEDOM 84

INDEPENDENT VARIABLES AT SIGNIFICANT LEVEL . 5.00 %

V	CD	CURNT	TEMP	TIMF	WF	WSTRP	DF	H1	H2	H3	HSTR	VOL	A
R	YR	AI	RST1A	RST1B	RST1C	RST2A	RST2B	RST2C	RST3A	RST3B	RST3C	P1A	P1B
P1C	P2A	P2B	P2C	P3A	P3B	P3C	RLT1A	RLT1B	RLT1C	RLT2A	RLT2B	RLT2C	RLT3A
RLT3B	RLT3C	YI1A	YI1B	YI1C	YI2A	YI2B	YI2C	YI3A	YI3B	YI3C	VF	VS	

VARIABLES IN THE REGRESSION SET

VAR NAME		REGRESSION COEFF	STANDARD ERROR	CONFIDENCE INTERVAL	T STAT	PART CORR	MULTIPLE CORRELATION	E S S	
CURNT		0.0113252	.555539E- 2	.110552E- 1	2.04	0.22	0.971	.168448E	1
H1	*	0.0804172	.186455E- 1	.371045E- 1	4.31	-0.43	0.966	.196061E	1
H2		0.0712425	.521237E- 2	.103726E- 1	13.67	0.83	0.908	.517471E	1
HSTR	*	0.0450305	.256061E- 2	.509562E- 2	9.78	-0.73	0.940	.343004E	1
R	*	0.0043744	.655861E- 3	.130516E- 2	6.67	-0.59	0.957	.245510E	1
YR		0.0794728	.515003E- 2	.102486E- 1	15.43	0.86	0.869	.615530E	1
RST1B	*	0.0044246	.379714E- 3	.755631E- 3	11.65	-0.79	0.926	.419961E	1
RST3A		0.2952837	.222162E- 1	.442101E- 1	13.29	0.82	0.911	.498072E	1
P3A	*	0.4518826	.457579E- 1	.910581E- 1	9.44	-0.72	0.942	.330729E	1
P3B		0.0960528	.449301E- 1	.894109E- 1	2.14	0.23	0.971	.169237E	1
RLT2A		0.0357560	.627044E- 2	.124782E- 1	5.70	0.53	0.961	.222640E	1
RLT3C		0.0544173	.452549E- 2	.900572E- 2	7.65	0.64	0.952	.272315E	1
YI2A	*	0.1706385	.332961E- 1	.662593E- 1	5.12	-0.49	0.963	.210695E	1
YI3B	*	0.2953879	.552829E- 1	.110012E 0	4.62	-0.45	0.965	.201287E	1

VARIABLES NOT IN THE REGRESSION SET

VAR NAME	T STAT	PART CORR	MULTIPLE CORRELATION	E S S	
V	1.05	0.11	0.973	.158400E	1
CD	0.78	-0.09	0.972	.159335E	1
TEMP	0.45	0.05	0.972	.160118E	1

VAR NAME	T STAT	PART CORR	MULTIPLE CORRELATION	E S S	
TIME	0.68	-0.07	0.972	.159626E	1
WT	0.00	0.00	0.972	.160507E	1
WSTRP	1.26	-0.14	0.973	.157509E	1
DF	0.04	0.00	0.972	.160504E	1
H3	0.84	0.09	0.973	.159148E	1
VOL	0.04	0.00	0.972	.160505E	1
A	0.78	-0.09	0.972	.159344E	1
AI	0.50	0.05	0.972	.160030E	1
RST1A	0.05	0.01	0.972	.160502E	1
RST1C	0.38	-0.04	0.972	.160231E	1
RST2A	1.06	0.12	0.973	.158352E	1
RST2B	0.77	-0.08	0.972	.159386E	1
RST2C	0.61	-0.07	0.972	.159706E	1
RST3B	0.95	-0.10	0.973	.158707E	1
RST3C	0.67	-0.07	0.972	.159640E	1
P1A	0.84	0.09	0.973	.159144E	1
P1B	0.11	0.01	0.972	.160483E	1
P1C	0.82	0.09	0.973	.159211E	1
P2A	0.35	0.04	0.972	.160275E	1
P2B	0.19	-0.02	0.972	.160438E	1
P2C	0.02	-0.00	0.972	.160506E	1
P3C	0.00		0.972	.160508E	1
RLY1A	1.66	0.18	0.973	.155375E	1
RLY1B	1.03	-0.11	0.973	.158498E	1
RLY1C	0.00	0.00	0.972	.000000E	0
RLY2B	1.00	-0.11	0.973	.158610E	1
RLY2C	0.67	0.07	0.972	.159640E	1
RLY3A	0.54	0.06	0.972	.159943E	1
RLY3B	0.92	-0.10	0.973	.158891E	1

VAR NAME	T STAT	PART CORR	MULTIPLE CORRELATION	F S S
YI1A	0.16	-0.02	0.972	.160445E 1
YI1B	1.10	-0.12	0.973	.138220E 1
YI1C	0.00	0.00	0.972	.000000E 0
YI2B	0.04	-0.00	0.972	.160565E 1
YI2C	0.98	0.11	0.973	.158669E 1
YI3A	0.70	0.08	0.972	.159574E 1
YI3C	1.48	0.16	0.973	.156353E 1
VF	0.97	-0.11	0.973	.158605E 1
VS	0.14	0.02	0.972	.160467E 1

E.S.S. .160507E 1

RESIDUAL ERROR .138232E 0

MULT CORR 0.972

INTERCEPT TERM = 11.2173649

REGRESSION ANALYSIS COVA DATA1 CUT OFF PARAMETER .100000E- 5

DEPENDENT VARIABLE WF DEGREES OF FREEDOM 96

INDEPENDENT VARIABLES AT SIGNIFICANT LEVEL 5.00 %

V	CD	CURNT	TEMP	TIME	WSTRP	DF	H1	H2	H3	HSTR	Z	VOL	A
R	YR	A1	RST1A	RST1B	RST1C	RST2A	RST2B	RST2C	RST3A	RST3B	RST3C	P1A	P1B
P1C	P2A	P2B	P2C	P3A	P3B	P3C	RLT1A	RLT1B	RLT1C	RLT2A	RLT2B	RLT2C	RLT3A
RLT3B	RLT3C	YI1A	YI1B	YI1C	YI2A	YI2B	YI2C	YI3A	YI3B	YI3C	VF	VS	

VARIABLES IN THE REGRESSION SET

VAR NAME	REGRESSION COEFF	STANDARD ERROR	CONFIDENCE INTERVAL	T STAT	PART CORR	MULTIPLE CORRELATION	E S S
DF	4.3036847	.477539E- 2	.947437E- 2	913.8	1.00	0.271	.806092E 6
YI2A	0.3274687	.140840E 0	.279029E 0	2.33	-0.23	1.000	.978901E 2

VARIABLES NOT IN THE REGRESSION SET

VAR NAME	T STAT	PART CORR	MULTIPLE CORRELATION	E S S
V	0.37	-0.04	1.000	.925343E 2
CD	1.36	-0.14	1.000	.909010E 2
CURNT	1.36	-0.14	1.000	.909019E 2
TEMP	0.09	-0.01	1.000	.926568E 2
TIME	0.63	0.06	1.000	.922649E 2
WSTRP	0.04	0.00	1.000	.926633E 2
H1	0.70	0.07	1.000	.921955E 2
H2	1.60	0.16	1.000	.902339E 2
H3	0.57	0.06	1.000	.923519E 2
HSTR	0.91	0.09	1.000	.918724E 2
Z	0.25	-0.03	1.000	.926045E 2
VOL	1.39	-0.14	1.000	.908211E 2
A	0.43	0.05	1.000	.924413E 2
R	1.01	0.10	1.000	.916788E 2
YR	0.53	0.05	1.000	.923946E 2

NAME		CORR	CORRELATION		
AI	0.87	-0.09	1.000	.919306E	2
RSY1A	0.29	0.03	1.000	.925856E	2
RSY1B	0.06	-0.01	1.000	.926611E	2
RSY1C	0.02	0.00	1.000	.926648E	2
RSY2A	0.33	0.03	1.000	.925570E	2
RSY2B	0.57	0.06	1.000	.923530E	2
RSY2C	0.24	-0.02	1.000	.926079E	2
RSY3A	0.75	-0.08	1.000	.921260E	2
RSY3B	0.48	-0.05	1.000	.924422E	2
RSY3C	0.18	-0.02	1.000	.926332E	2
P1A	0.44	0.05	1.000	.924736E	2
P1B	0.14	0.01	1.000	.926469E	2
P1C	0.06	0.01	1.000	.926616E	2
P2A	0.10	0.01	1.000	.926558E	2
P2B	0.32	-0.03	1.000	.925669E	2
P2C	0.13	-0.01	1.000	.926479E	2
P3A	0.33	-0.03	1.000	.925586E	2
P3B	0.94	-0.10	1.000	.918076E	2
P3C	0.00		1.000	.926652E	2
RLT1A	0.45	0.05	1.000	.924680E	2
RLT1B	0.44	-0.05	1.000	.924632E	2
RLT1C	0.00	0.00	1.000	.000000E	0
RLT2A	0.18	0.02	1.000	.926329E	2
RLT2B	1.42	0.14	1.000	.907387E	2
RLT2C	0.55	0.06	1.000	.923720E	2
RLT3A	0.69	-0.07	1.000	.922060E	2
RLT3B	0.10	0.01	1.000	.926550E	2
RLT3C	0.92	-0.09	1.000	.918425E	2
Y11A	0.47	0.05	1.000	.924502E	2

VAR NAME	T STAT	PART CORR	MULTIPLE CORRELATION	S S
YI1B	0.59	0.06	1.000	.923509E 2
YI1C	0.00	0.00	1.000	.000000E 0
YI2B	0.41	-0.04	1.000	.925063E 2
YI2C	1.46	-0.15	1.000	.906446E 2
YI3A	0.21	-0.02	1.000	.926209E 2
YI3B	0.85	0.09	1.000	.919717E 2
YI3C	0.28	-0.03	1.000	.925887E 2
VF	0.01	-0.00	1.000	.926652E 2
VS	0.54	-0.03	1.000	.925551E 2

E.S.S. .926652E 2

RESIDUAL ERROR .982478E 0

MULT CORR 1.000

INTERCEPT TERM = 5.7519087

[illegible] COVA DATA1 CUT OFF PARAMETER .100000E- 5

DEPENDENT VARIABLE VOL DEGREES OF FREEDOM 87

INDEPENDENT VARIABLES AT SIGNIFICANT LEVEL 5.00 %

V	CO	CURNT	TEMP	TIME	WF	WSTRP	DF	H1	H2	H3	HSTR	Z	A
R	YR	AI	RST1A	RST1B	RST1C	RST2A	RST2B	RST2C	RST3A	RST3B	RST3C	P1A	P1B
P1C	P2A	P2B	P2C	P3A	P3B	P3C	RLT1A	RLT1B	RLT1C	RLT2A	RLT2B	RLT2C	RLT3A
RLT3B	RLT3C	YI1A	YI1B	YI1C	YI2A	YI2B	YI2C	YI3A	YI3B	YI3C	VF	VS	

VARIABLES IN THE REGRESSION SET

VAR NAME		REGRESSION COEFF	STANDARD ERROR	CONFIDENCE INTERVAL	T STAT	PART CORR	MULTIPLE CORRELATION	E S S
H2	*	0.3565935	.399547E- 1	.179010E 0	3.96	-0.39	0.977	.585787E 3
H3	*	0.2346283	.527631E- 1	.104999E 0	4.45	-0.43	0.976	.608940E 3
HSTR		0.2369647	.460161E- 1	.915721E- 1	5.15	0.48	0.974	.647402E 3
R	*	0.0077795	.106930E- 1	.212790E- 1	6.34	-0.56	0.971	.725309E 3
YR		0.9569306	.834470E- 1	.166060E 0	11.47	0.78	0.950	.124614E 4
RST1B		0.0226748	.673497E- 2	.134026E- 1	3.37	0.34	0.978	.560810E 3
RST2B		0.6430644	.900047E- 1	.179109E 0	7.15	0.61	0.969	.787314E 3
RST3A		3.0831856	.298804E 0	.594621E 0	10.32	0.74	0.956	.110337E 4
P3B		7.8452095	.850124E 0	.169176E 1	9.23	0.70	0.961	.981843E 3
RLT1B		0.7111798	.183916E 0	.365997E 0	3.87	0.38	0.977	.581440E 3
RLT3C		0.5043803	.727943E- 1	.144861E 0	6.93	0.60	0.969	.769963E 3

VARIABLES NOT IN THE REGRESSION SET

VAR NAME	T STAT	PART CORR	MULTIPLE CORRELATION	E S S
V	0.46	0.05	0.980	.494949E 3
CO	0.82	0.09	0.981	.492340E 3
CURNT	0.82	0.09	0.981	.492343E 3
TEMP	0.39	-0.04	0.980	.495277E 3
TIME	1.49	-0.16	0.981	.483683E 3
WF	0.14	0.02	0.980	.496049E 3

VAR NAME	T STAT	PART CORR	MULTIPLE CORRELATION	E S S
MSTRP	1.18	-0.13	0.981	.488266E 3
DF	0.29	0.03	0.980	.495669E 3
H1	0.06	-0.01	0.980	.496146E 3
Z	0.13	0.01	0.980	.496069E 3
A	0.33	-0.04	0.980	.495554E 3
AI	0.74	-0.08	0.981	.493010E 3
RST1A	0.58	-0.06	0.981	.494244E 3
RST1C	0.02	-0.00	0.980	.496165E 3
RST2A	0.01	-0.00	0.980	.496165E 3
RST2C	0.23	0.02	0.980	.495869E 3
RST3B	1.54	0.16	0.981	.482869E 3
RST3C	0.05	-0.01	0.980	.496150E 3
P1A	1.60	-0.17	0.981	.481903E 3
P1B	0.36	-0.04	0.980	.495405E 3
P1C	0.15	0.02	0.980	.496032E 3
P2A	0.79	-0.08	0.981	.492630F 3
P2B	0.53	-0.06	0.980	.494560E 3
P2C	0.56	-0.06	0.980	.494386E 3
P3A	1.88	0.20	0.981	.476684E 3
P3C	0.00		0.980	.496166E 3
RLT1A	0.12	0.01	0.980	.496085E 3
RLT1C	0.00	0.00	0.980	.000000E 0
RLT2A	1.61	0.17	0.981	.481651E 3
RLT2B	0.83	0.09	0.981	.491732E 3
RLT2C	0.50	0.05	0.980	.494783E 3
RLT3A	1.30	0.14	0.981	.486542E 3
RLT3B	0.85	0.09	0.981	.492063E 3
YI1A	0.37	-0.04	0.980	.495371E 3
YI1B	0.45	-0.05	0.980	.495003E 3

VAR NAME	T STAT	PART CORR	MULTIPLE CORRELATION	E S S
YI1C	0.00	0.00	0.980	.000000E 0
YI2A	1.34	0.14	0.981	.486005E 3
YI2B	0.27	0.03	0.980	.495738E 3
YI2C	0.50	0.05	0.980	.496714E 3
YI3A	1.73	0.18	0.981	.479513E 3
YI3B	0.92	-0.10	0.981	.491308E 3
YI3C	0.93	0.10	0.981	.491202E 3
VF	0.09	0.01	0.980	.496119E 3
VS	0.42	0.05	0.980	.495139E 3

E.S.S. .496166E 3

RESIDUAL ERROR .258811E 1

MULT CORR 0.980

INTERCEPT TERM 141.5481476

REGRESSION ANALYSIS .COVA . DATA1 CUT OFF PARAMETER .100000E- 3

DEPENDENT VARIABLE A DEGREES OF FREEDOM 94

INDEPENDENT VARIABLES AT SIGNIFICANT LEVEL 5,00 %

V	CD	CURNT	TEMP	TIME	WF	WSTRP	DF	H1	H2	H3	HSTR	Z	VOL
R	YR	AI	RST1A	RST1B	RST1C	RST2A	RST2B	RST2C	RST3A	RST3B	RST3C	P1A	P1B
P1C	P2A	P2B	P2C	P3A	P3B	P3C	RLT1A	RLT1B	RLT1C	RLT2A	RLT2B	RLT2C	RLT3A
RLT3B	RLT3C	YI1A	YI1B	YI1C	YI2A	YI2B	YI2C	YI3A	YI3B	YI3C	VF	VS	

VARIABLES IN THE REGRESSION SET

VAR NAME		REGRESSION COEFF	STANDARD ERROR	CONFIDENCE INTERVAL	T STAT	PART CORR	MULTIPLE CORRELATION	E S S
TEMP	=	0,0386249	,205692E- 1	,566812E- 1	2,05	-0,21	0,550	,856054E 3
TIME		0,0001579	,320807E- 4	,652352E- 4	4,80	0,44	0,410	,102031E 4
YI1A		2,2066360	,836364E 0	,166331E 1	2,63	0,26	0,532	,879737E 3
VS	=	0,1125224	,370160E- 1	,746301E- 1	2,99	-0,29	0,518	,897347E 3

VARIABLES NOT IN THE REGRESSION SET

VAR NAME	T STAT	PART CORR	MULTIPLE CORRELATION	E S S
V	0,46	0,05	0,578	,817436E 3
CD	0,12	-0,01	0,576	,819231E 3
CURNT	0,12	-0,01	0,576	,819242E 3
WF	0,99	-0,10	0,582	,810728E 3
WSTRP	1,13	0,12	0,584	,808321E 3
DF	0,90	-0,10	0,582	,810789E 3
H1	0,75	0,08	0,580	,814454E 3
H2	0,50	-0,05	0,578	,817126E 3
H3	0,53	-0,05	0,578	,816913E 3
HSTR	0,84	-0,09	0,581	,813180E 3
Z	0,01	-0,00	0,576	,819349E 3
VOL	0,09	-0,01	0,576	,819281E 3
R	1,49	0,15	0,590	,806141E 3

VAR NAME	T STAT	PART CORR	MULTIPLE CORRELATION	E S S	
YR	0.67	0.07	0.579	.8154A2E	3
AI	1.08	0.11	0.584	.809124E	3
RST1A	1.18	0.12	0.585	.807350E	3
RST1B	0.12	0.01	0.576	.819232E	3
RST1C	0.05	-0.01	0.576	.819329E	3
RST2A	0.11	0.01	0.576	.819249E	3
RST2B	0.15	0.02	0.577	.819143E	3
RST2C	0.05	0.01	0.576	.819330E	3
RST3A	0.16	-0.02	0.577	.819133E	3
RST3B	0.19	0.02	0.577	.819024E	3
RST3C	0.04	-0.01	0.576	.819322E	3
P1A	0.87	0.09	0.581	.812709E	3
P1B	0.59	-0.06	0.579	.816294E	3
P1C	0.26	0.03	0.577	.818742E	3
P2A	0.85	-0.09	0.581	.813095E	3
P2B	0.17	-0.02	0.577	.819101E	3
P2C	0.68	-0.07	0.579	.815297E	3
P3A	0.32	-0.03	0.577	.818421E	3
P3B	0.32	0.03	0.577	.818470E	3
P3C	0.00		0.576	.819351E	3
RLT1A	0.95	-0.10	0.582	.811453E	3
RLT1B	0.83	-0.09	0.581	.813367E	3
RLT1C	0.00	0.00	0.576	.000000E	0
RLT2A	0.29	0.03	0.577	.818021E	3
RLT2B	0.84	-0.09	0.581	.813214E	3
RLT2C	0.69	0.07	0.579	.815224E	3
RLT3A	0.69	0.07	0.579	.815208E	3
RLT3B	0.13	-0.01	0.577	.819204E	3
RLT3C	0.16	-0.02	0.577	.819131E	3

NAME		CORR	CORRELATION	
YI1B	1.03	-0.11	0.583	,910021E 3
YI1C	0.00	0.00	0.576	,000000E 0
YI2A	0.96	0.10	0.582	,811367E 3
YI2B	1.68	-0.17	0.593	,795099E 3
YI2C	0.47	0.05	0.578	,817449E 3
YI3A	0.38	0.04	0.577	,818085E 3
YI3B	0.28	-0.03	0.577	,818640E 3
YI3C	0.03	=0.00	0.576	,819340E 3
VF	0.00	=0.00	0.576	,819350E 3

E.S.S. ,819350E 3

RESIDUAL ERROR ,295237E 1

MULT CORR 0.576

INTERCEPT TERM 85.1234873

DEPENDENT VARIABLE R DEGREES OF FREEDOM 88

INDEPENDENT VARIABLES AT SIGNIFICANT LEVEL 5.00 %

V	CD	CURNT	TEMP	TIME	WP	WSTRP	DF	H1	H2	H3	HSTR	Z	VOL
A	YR	AI	RST1A	RST1B	RST1C	RST2A	RST2B	RST2C	RST3A	RST3B	RST3C	P1A	P1B
P1C	P2A	P2B	P2C	P3A	P3B	P3C	RLT1A	RLT1B	RLT1C	RLT2A	RLT2B	RLT2C	RLT3A
RLT3B	RLT3C	YI1A	YI1B	YI1C	YI2A	YI2B	YI2C	YI3A	YI3B	YI3C	VF	VS	

VARIABLES IN THE REGRESSION SET

VAR NAME		REGRESSION COEFF	STANDARD ERROR	CONFIDENCE INTERVAL	T STAT	PART CORR	MULTIPLE CORRELATION	E S S
TEMP	=	0.5009684	.160648E 0	.319689E 0	3.12	-0.32	0.769	.260974E 5
Z	=	54.5131423	.525685E 1	.104611E 2	6.57	-0.57	0.672	.350114E 5
VOL	=	2.7789722	.350175E 0	.696844E 0	7.94	-0.65	0.608	.403192E 5
YR		5.5856313	.647924E 0	.128936E 1	8.62	0.68	0.567	.433473E 5
RST3A		9.9994201	.217769E 1	.433360E 1	4.59	0.44	0.738	.291310E 5
P1A	=	7.2426539	.232060E 1	.461799E 1	3.11	-0.31	0.769	.260875E 5
P3B		26.0712426	.634529E 1	.126271E 2	4.11	0.40	0.749	.260087E 5
RLT3A		2.2506503	.539639E 0	.107388E 1	4.19	0.41	0.748	.281456E 5
YI2B	=	10.2980946	.401403E 1	.798795E 1	2.55	-0.26	0.778	.252377E 5
YI3A	=	30.7914008	.697798E 1	.138862E 2	4.40	-0.42	0.743	.286699E 5

VARIABLES NOT IN THE REGRESSION SET

VAR NAME	T STAT	PART CORR	MULTIPLE CORRELATION	E S S
V	0.95	0.10	0.798	.232577E 5
CD	0.47	0.05	0.796	.234411E 5
CURNT	0.47	0.05	0.796	.234402E 5
TIME	1.31	-0.14	0.800	.230446E 5
WP	0.01	0.00	0.795	.235004E 5
WSTRP	0.50	-0.05	0.796	.234319E 5
DF	0.00	0.00	0.795	.235004E 5

15/46/30 22/09/78

VAR NAME		CORR	CORRELATION	
H1	0.60	-0.06	0.796	.234047E 5
H2	0.32	-0.03	0.795	.234721E 5
H3	0.17	-0.02	0.795	.234930E 5
HSTR	0.52	-0.06	0.796	.234272E 5
A	0.12	0.01	0.795	.234966E 5
AI	0.87	-0.09	0.797	.232980E 5
RST1A	0.15	-0.02	0.795	.234944E 5
RST1B	0.19	-0.02	0.795	.234906E 5
RST1C	0.12	0.01	0.795	.234965E 5
RST2A	1.33	-0.14	0.800	.230352E 5
RST2B	1.21	0.13	0.799	.231084E 5
RST2C	1.84	0.19	0.804	.226157E 5
RST3B	0.15	-0.02	0.795	.234944E 5
RST3C	1.86	0.20	0.804	.225974E 5
P1B	1.32	-0.14	0.800	.230365E 5
P1C	0.52	-0.06	0.796	.234285E 5
P2A	1.89	-0.20	0.804	.225736E 5
P2B	0.17	-0.02	0.795	.234922E 5
P2C	0.75	0.08	0.797	.233475E 5
P3A	0.11	-0.01	0.795	.234974E 5
P3C	0.00		0.795	.235004E 5
RLT1A	0.90	-0.10	0.797	.232835E 5
RLT1B	0.95	0.10	0.798	.232577E 5
RLT1C	0.00	0.00	0.795	.000000E 0
RLT2A	0.02	-0.00	0.795	.235003E 5
RLT2B	0.36	-0.04	0.796	.234645E 5
RLT2C	0.62	-0.07	0.796	.233981E 5
RLT3B	0.42	0.04	0.796	.234532E 5
RLT3C	0.13	0.01	0.795	.234956E 5

VAR NAME	T STAT	PART CORR	MULTIPLE CORRELATION	R S S
YI1A	0.24	0.03	0.795	.254842E 5
YI1B	0.01	-0.00	0.795	.235004E 5
YI1C	0.00	0.00	0.795	.000000E 0
YI2A	1.47	-0.16	0.801	.229296E 5
YI2C	0.77	-0.08	0.797	.233413E 5
YI3B	0.43	0.05	0.796	.234515E 5
YI3C	1.48	0.16	0.801	.229232E 5
VF	0.29	0.03	0.795	.234770E 5
VS	0.18	-0.02	0.795	.234921E 5

E.S.S. .235004E 5

RESIDUAL ERROR .163417E 2

MULT CORR 0.795

INTERCEPT TERM = 248.8697846

REGRESSION ANALYSIS 'COVA DATA1 CUT OFF PARAMETER .100000E- 5

DEPENDENT VARIABLE HSTR DEGREES OF FREEDOM 92

INDEPENDENT VARIABLES AT SIGNIFICANT LEVEL 5.00 %

V	CD	CURNT	TEMP	TIME	WF	WSTRP	DF	H1	H2	H3	Z	VOL	A
R	YR	AI	RST1A	RST1B	RST1C	RST2A	RST2B	RST2C	RST3A	RST3B	RST3C	P1A	P1B
P1C	P2A	P2B	P2C	P3A	P3B	P3C	RLT1A	RLT1B	RLT1C	RLT2A	RLT2B	RLT2C	RLT3A
RLT3B	RLT3C	YI1A	YI1B	YI1C	YI2A	YI2B	YI2C	YI3A	YI3B	YI3C	VF	VS	

VARIABLES IN THE REGRESSION SET

VAR NAME	REGRESSION COEFF	STANDARD ERROR	CONFIDENCE INTERVAL	T STAT	PART CORR	MULTIPLE CORRELATION	E S S
WF	0,2439445	,363874E- 2	,721927E- 2	61,54	0,99	0,910	,869951E 4
H3	0,0437871	,271403E- 1	,538468E- 1	3,46	0,34	0,908	,233044E 3
YR	1,1942778	,428850E- 1	,850839E- 1	27,15	0,94	0,981	,185807E 4
RST1A	0,2154372	,820140E- 1	,163906E 0	2,61	0,26	0,908	,221537E 3
RST3C	4,4094456	,208893E 0	,414444E 0	21,40	-0,91	0,908	,123276E 4
P3R	1,1962007	,419373E 0	,832036E 0	2,85	-0,29	0,908	,224532E 3

VARIABLES NOT IN THE REGRESSION SET

VAR NAME	T STAT	PART CORR	MULTIPLE CORRELATION	E S S
V	1,16	-0,12	0,908	,203305E 3
CD	0,52	-0,05	0,908	,205675E 3
CURNT	0,52	-0,05	0,908	,205679E 3
TEMP	1,21	-0,13	0,908	,203009E 3
TIME	0,44	0,05	0,908	,205856E 3
WSTRP	0,75	-0,08	0,908	,205066E 3
DF	0,06	0,01	0,908	,206280E 3
H1	1,51	0,16	0,908	,201214E 3
H2	1,49	0,15	0,908	,201400E 3
Z	0,48	-0,05	0,908	,205775E 3
VOL	1,39	0,14	0,908	,201982E 3

VAR NAME	T STAT	PART CORR	MULTIPLE CORRELATION	E S S
A	0.47	-0.05	0.998	.205783E 3
R	0.76	-0.08	0.998	.204997E 3
AI	0.68	0.07	0.998	.205234E 3
RST1B	1.16	0.12	0.998	.203277E 3
RST1C	0.42	-0.04	0.998	.205806E 3
RST2A	0.42	-0.04	0.998	.205809E 3
RST2B	0.53	-0.06	0.998	.205647E 3
RST2C	1.88	-0.19	0.998	.198540E 3
RST3A	0.46	0.05	0.998	.205816E 3
RST3B	0.56	0.06	0.998	.205534E 3
P1A	0.16	0.02	0.998	.206230E 3
P1B	0.20	-0.02	0.998	.206200E 3
P1C	0.39	0.04	0.998	.205987E 3
P2A	0.61	-0.06	0.998	.205452E 3
P2B	0.31	0.03	0.998	.206071E 3
P2C	0.08	-0.01	0.998	.206274E 3
P3A	0.31	0.03	0.998	.206076E 3
P3C	0.00		0.998	.206269E 3
RLT1A	1.17	-0.12	0.998	.203254E 3
RLT1B	0.99	0.10	0.998	.204086E 3
RLT1C	0.00	0.00	0.998	.000000E 0
RLT2A	1.03	-0.11	0.998	.203909E 3
RLT2B	0.10	-0.01	0.998	.206245E 3
RLT2C	0.36	0.04	0.998	.205902E 3
RLT3A	0.62	-0.07	0.998	.205408E 3
RLT3B	0.29	0.03	0.998	.206099E 3
RLT3C	1.07	0.11	0.998	.203703E 3
YI1A	0.07	-0.01	0.998	.206278E 3
YI1B	0.12	-0.01	0.998	.206258E 3

VAR NAME	T STAT	PART CORR	MULTIPLE CORRELATION	E S S
YI1C	0.00	0.00	0.998	,000000E 0
YI2A	0.82	-0.09	0.998	,204759E 3
YI2B	0.14	0.01	0.998	,206246E 3
YI2C	0.12	0.01	0.998	,206254E 3
YI3A	1.07	-0.11	0.998	,203707E 3
YI3B	0.66	-0.07	0.998	,205292E 3
YI3C	1.77	-0.18	0.998	,199387E 3
VF	0.10	0.01	0.998	,206287E 3
VS	0.75	-0.08	0.998	,205010E 3

E.S.S. ,2062898 3

RESIDUAL ERROR ,149742F 1

MULT CORR 0.998

INTERCEPT TERM = 20,9314349

DEPENDENT VARIABLE H1 DEGREES OF FREEDOM 93

INDEPENDENT VARIABLES AT SIGNIFICANT LEVEL 5.00 %

V	CD	CURNT	TEMP	TIME	WF	WSTRP	DF	H2	H3	HSTR	Z	VOL	A
R	YR	AI	RST1A	RST1B	RST1C	RST2A	RST2B	RST2C	RST3A	RST3B	RST3C	P1A	P1B
P1C	P2A	P2B	P2C	P3A	P3B	P3C	RLT1A	RLT1B	RLT1C	RLT2A	RLT2B	RLT2C	RLT3A
RLT3B	RLT3C	YI1A	YI1B	YI1C	YI2A	YI2B	YI2C	YI3A	YI3B	YI3C	VF	VS	

VARIABLES IN THE REGRESSION SET

VAR NAME	REGRESSION COEFF	STANDARD ERROR	CONFIDENCE INTERVAL	T STAT	PART CORR	MULTIPLE CORRELATION	E S S
H2	0.0001971	.807090E-2	.160127E-1	7.46	0.61	0.560	.519323E 2
Z	-0.3953073	.121749E 0	.241550E 0	-3.25	-0.32	0.733	.361785E 2
RST1B	-0.0048531	.114076E-2	.226328E-2	-4.08	-0.39	0.715	.383081E 2
RST3C	-0.1909379	.742734E-1	.147358E 0	-2.57	-0.26	0.745	.348040E 2
RLT2C	0.1116254	.143314E-1	.284331E-1	7.79	0.63	0.560	.536928E 2

VARIABLES NOT IN THE REGRESSION SET

VAR NAME	T STAT	PART CORR	MULTIPLE CORRELATION	E S S
V	0.39	-0.04	0.765	.324414E 2
CD	0.28	0.03	0.765	.324677E 2
CURNT	0.28	0.03	0.765	.324681E 2
TEMP	1.35	-0.14	0.770	.318601E 2
TIME	0.16	-0.02	0.765	.324838E 2
WF	0.47	-0.05	0.765	.324165E 2
WSTRP	0.34	-0.04	0.765	.324531E 2
DF	0.46	-0.05	0.765	.324202E 2
H3	1.95	-0.20	0.775	.312040E 2
HSTR	0.07	0.01	0.765	.324929E 2
VOL	0.30	0.03	0.765	.324627E 2
A	1.43	0.15	0.771	.317841E 2

VAR NAME	T STAT	PART CORR	MULTIPLE CORRELATION R_y	R S S
R	0.70	0.07	0.766	.323226E 2
YR	1.15	0.12	0.769	.320375E 2
AI	1.91	0.20	0.775	.312511E 2
RST1A	0.92	0.10	0.767	.322008E 2
RST1C	0.20	0.02	0.765	.324814E 2
RST2A	1.26	-0.13	0.769	.319403E 2
RST2B	0.51	-0.05	0.765	.324030E 2
RST2C	0.15	0.02	0.765	.324874E 2
RST3A	0.09	0.01	0.765	.324919E 2
RST3B	1.53	-0.16	0.771	.316969E 2
P1A	1.18	0.12	0.769	.320074E 2
P1B	0.19	0.02	0.765	.324821E 2
P1C	0.01	0.00	0.765	.324948E 2
P2A	1.23	-0.13	0.769	.319671E 2
P2B	0.64	-0.07	0.766	.323498E 2
P2C	0.00	0.00	0.765	.324949E 2
P3A	1.19	-0.12	0.769	.320000E 2
P3B	0.74	-0.08	0.766	.323002E 2
P3C	0.00		0.765	.324949E 2
RLY1A	0.05	0.01	0.765	.324939E 2
RLY1B	1.03	-0.11	0.768	.321253E 2
RLY1C	0.00	0.00	0.765	.000000E 0
RLY2A	0.56	-0.06	0.766	.323835E 2
RLY2C	0.13	0.01	0.765	.324890E 2
RLY3A	0.34	0.04	0.765	.324548E 2
RLY3B	0.29	-0.03	0.765	.324657E 2
RLY3C	0.80	0.08	0.767	.322791E 2
VI1A	1.03	0.11	0.768	.321228E 2
VI1B	0.09	0.01	0.765	.324919E 2

VAR NAME		T STAT	PART CORR	MULTIPLE CORRELATION	E S S
YI1C		0.00	0.00	0.765	.000000E 0
YI2A		0.26	0.03	0.765	.324704E 2
YI2B		0.96	0.10	0.767	.321740E 2
YI2C		0.85	0.09	0.767	.322406E 2
YI3A		0.66	-0.07	0.766	.323328E 2
YI3B		0.31	0.03	0.765	.324606E 2
YI3C		0.59	0.06	0.766	.323720E 2
VF		0.06	0.01	0.765	.324934E 2
VS		0.82	-0.08	0.767	.322007E 2
E.S.S.	.324949E 2				
RESIDUAL ERROR	.591107E 0				
MULT CORR	0.765				
INTERCEPT TERM	2.0146439				

REGRESSION ANALYSIS COVA - DATA1 CUT OFF PARAMETER .100000E- 5

DEPENDENT VARIABLE H2 DEGREES OF FREEDOM 83

INDEPENDENT VARIABLES AT SIGNIFICANT LEVEL 5.00 %

V	CD	CURNT	TEMP	TIME	WF	WSTRP	DF	H1	H3	HSTR	Z	VOL	A
R	YR	AI	RST1A	RST1B	RST1C	RST2A	RST2B	RST2C	RST3A	RST3B	RST3C	P1A	P1B
P1C	P2A	P2B	P2C	P3A	P3B	P3C	RLT1A	RLT1B	RLT1C	RLT2A	RLT2B	RLT2C	RLT3A
RLT3B	RLT3C	YI1A	YI1B	YI1C	YI2A	YI2B	YI2C	YI3A	YI3B	YI3C	VF	VS	

VARIABLES IN THE REGRESSION SET

VAR NAME		REGRESSION COEFF	STANDARD ERROR	CONFIDENCE INTERVAL	T STAT	PART CORR	MULTIPLE CORRELATION	E S S
WSTRP		0.2568563	.993310E- 1	.198066E 0	2.58	0.27	0.990	.1409A3E 3
H1		1.0097578	.170061E 0	.338421E 0	6.41	0.58	0.986	.1950S4E 3
HSYR		0.3728094	.979860E- 2	.194998E- 1	38.05	0.97	0.817	.2406288 4
Z		6.1589527	.427367E 0	.850440E 0	14.41	0.85	0.968	.4570236 3
VOL	*	0.2073584	.275030E- 1	.547322E- 1	7.54	-0.64	0.985	.2198A0E 3
A		0.0989157	.382217E- 1	.760611E- 1	2.59	0.27	0.990	.141024E 3
VR	*	0.4186125	.550954E- 1	.111232E 0	7.40	-0.64	0.985	.2186776 3
RST1B		0.0333598	.296103E- 2	.593224E- 2	17.90	0.89	0.955	.6541A1E 3
RST3A	*	2.1598635	.194763E 0	.387578E 0	11.09	-0.77	0.977	.323841E 3
RST3B		0.2402804	.737234E- 1	.146710E 0	3.26	0.34	0.990	.147195E 3
P1A	*	0.7939804	.184177E 0	.346513E 0	4.31	-0.43	0.989	.159712E 3
P2A		4.4003040	.444844E 0	.865244E 0	9.89	0.74	0.980	.284330E 3
RLT3C	*	0.4486074	.492095E- 1	.979269E- 1	8.71	-0.69	0.983	.249764E 3
YI3A	*	3.1540830	.492486E 0	.980052E 0	6.40	-0.58	0.986	.194980E 3
YI3B		1.5859367	.504064E 0	.100309E 1	3.15	0.33	0.990	.146058E 3

VARIABLES NOT IN THE REGRESSION SET

VAR NAME	T STAT	PART CORR	MULTIPLE CORRELATION	RESS
V	0.56	0.06	0.991	.129965E 3
CD	1.94	-0.21	0.991	.124777E 3
CURNT	1.94	-0.21	0.991	.124782E 3
TEMP	0.46	0.05	0.991	.130165E 3
TIME	1.26	-0.14	0.991	.128000E 3
WF	0.85	0.09	0.991	.129361E 3
DF	0.00	0.00	0.991	.129404E 3
H3	1.48	-0.16	0.991	.127107E 3
R	1.45	0.16	0.991	.127248E 3
AI	1.11	-0.12	0.991	.128556E 3
RST1A	1.58	0.17	0.991	.126635E 3
RST1C	0.32	-0.04	0.991	.130333E 3
RST2A	0.05	0.01	0.991	.130490E 3
RST2B	0.82	0.09	0.991	.129437E 3
RST2C	1.40	0.15	0.991	.127436E 3
RST3C	1.25	0.14	0.991	.128050E 3
P1B	0.95	-0.10	0.991	.129066E 3
P1C	0.87	-0.10	0.991	.129308E 3
P2A	1.24	-0.14	0.991	.128100E 3
P2B	1.09	-0.12	0.991	.128633E 5
P2C	0.96	0.11	0.991	.129030E 3
P3B	0.21	-0.02	0.991	.130422E 3
P3C	0.00		0.991	.130494E 3
RLY1A	0.82	-0.09	0.991	.129427E 3
RLY1B	0.74	-0.08	0.991	.129639E 3
RLY1C	0.00	0.00	0.991	.000000E 0
RLY2A	0.85	0.09	0.991	.129365E 3
RLY2B	0.74	0.08	0.991	.129633E 3

VAR NAME	T STAT	PART CORR	MULTIPLE CORRELATION	E S S
RLY2C	1.09	-0.12	0.991	.128636E 3
RLY3A	0.86	0.09	0.991	.129399E 3
RLY3B	0.51	0.06	0.991	.130087E 3
YI1A	0.16	-0.02	0.991	.130451E 3
YI1B	0.88	-0.10	0.991	.129263E 3
YI1C	0.00	0.00	0.991	.000000E 0
YI2A	0.79	0.09	0.991	.129504E 3
YI2B	0.21	-0.02	0.991	.130426E 3
YI2C	1.84	-0.20	0.991	.125333E 3
YI3C	1.32	0.14	0.991	.127793E 3
VF	0.46	-0.05	0.991	.130157E 3
VS	1.36	-0.15	0.991	.127008E 3

E.S.S. .130494E 3

RESIDUAL ERROR .125388E 1

MULY CORR 0.991

INTERCEPT TERM 19.2364911

REGRESSION ANALYSIS. COVA DATA1 CUT OFF PARAMETER .100000E- 5

DEPENDENT VARIABLE H3 DEGREES OF FREEDOM 83

INDEPENDENT VARIABLES AT SIGNIFICANT LEVEL 5.00 %

V	CD	CURNT	TEMP	TIME	WF	WSTHP	DF	H1	H2	HSTR	Z	VOL	A	
R	YR	AI	RST1A	RST1B	RST1C	RST2A	RST2B	RST2C	RST3A	RST3B	RST3C	P1A	P1B	
P1C	P2A	P2B	P2C	P3A	P3B	P3C	RLT1A	RLT1B	RLT1C	RLT2A	RLT2B	RLT2C	RLT3A	
RLT3B	RLT3C	YI1A	YI1B	YI1C	YI2A	YI2B	YI2C	YI3A	YI3B	YI3C	VF	VS		

VARIABLES IN THE REGRESSION SET

VAR NAME		REGRESSION COEFF	STANDARD ERROR	CONFIDENCE INTERVAL		T STAT	PART CORR	MULTIPLE CORRELATION	E S S
TIME	*	0,0000279	,520270E- 4	,103534E- 3	*	0.54	-0.06	0.972	,845263E 3
H1	*	1,2995532	,424841E 0	,845433E 0		3.06	-0.32	0.969	,937288E 3
H2	*	0,3146429	,104813E 0	,208578E 0		3.00	-0.31	0.969	,933784E 3
HSTR		0,6638626	,505055E- 1	,100506E 0		13.14	0.82	0.912	,259573E 4
Z		5.2930171	,100696E 1	,200386E 1		5.26	0.50	0.963	,112273E 4
VOL	*	0,5923001	,809769E- 1	,161144E 0		7.31	-0.63	0.954	,138528E 4
YR		0,6506401	,137781E 0	,274185E 0		4.72	0.46	0.965	,106864E 4
RST3B		1,0083781	,206975E 0	,411880E 0		5.16	0.49	0.963	,111273E 4
P2A	*	1,7001957	,767174E 0	,152667E 1		2.22	-0.24	0.971	,892172E 3
P3A		4.5407200	,966357E 0	,192703E 1		4.69	0.46	0.965	,106547E 4
P3B		5.5953524	,124329E 1	,247412E 1		4.50	0.44	0.966	,104788E 4
RLT2A	*	0,4592626	,118301E 0	,235420E 0		3.88	-0.39	0.967	,995277E 3
RLT3A	*	0,4091492	,968010E- 1	,192635E 0		4.23	-0.42	0.966	,102363E 4
RLT3B		0,2150262	,618424E- 1	,123066E 0		3.48	0.36	0.968	,965020E 3
RLT3C	*	0,2728148	,109071E 0	,217052E 0		2.50	-0.26	0.970	,905820E 3

VARIABLES NOT IN THE REGRESSION SET

VAR NAME	T STAT	PART CORR	MULTIPLE CORRELATION	R S S
V	1.47	0.16	0.973	.820589E 3
CD	1.57	0.17	0.973	.817747E 3
CURNT	1.57	0.17	0.973	.817761E 3
TEMP	0.43	0.05	0.973	.840444E 3
WS	0.14	-0.02	0.972	.842114E 3
WSTRP	0.33	0.04	0.973	.841218E 3
DF	0.07	-0.01	0.972	.842278E 3
A	1.42	0.15	0.973	.822216E 3
R	0.47	0.05	0.973	.840023E 3
AI	0.59	-0.07	0.973	.838783E 3
RST1A	0.35	-0.04	0.973	.841063E 3
RST1B	0.24	-0.03	0.972	.841758E 3
RST1C	0.74	0.08	0.973	.836727E 3
RST2A	1.86	-0.20	0.974	.808248E 3
RST2B	0.12	0.01	0.972	.842166E 3
RST2C	0.26	-0.03	0.972	.841618E 3
RST3A	0.01	-0.00	0.972	.842327E 3
RST3C	0.08	0.01	0.972	.842262E 3
P1A	0.08	-0.01	0.972	.842257E 3
P1B	0.59	-0.06	0.973	.838820E 3
P1C	0.23	-0.03	0.972	.841779E 3
P2A	1.39	-0.15	0.973	.822998E 3
P2C	0.55	-0.06	0.973	.839236E 3
P3C	0.00		0.972	.842398E 3
RLT1A	0.06	0.01	0.972	.842202E 3
RLT1B	0.03	0.01	0.972	.842260E 3
RLT1C	0.00	0.00	0.972	.000000E 0
RLT2B	0.92	0.10	0.973	.833798E 3

VAR NAME	T STAT	PART CORR	MULTIPLE CORRELATION	F S S	
RLY2C	0.48	-0.05	0.973	.8399??E	3
YI1A	0.81	0.09	0.973	.8355A1E	3
YI1B	0.11	-0.01	0.972	.842210E	3
YI1C	0.00	0.00	0.972	.000000E	0
YI2A	1.06	0.12	0.973	.830937E	3
YI2B	1.65	0.18	0.973	.815101E	3
YI2C	0.25	0.03	0.972	.8416A9E	3
YI3A	1.58	-0.17	0.973	.817309E	3
YI3B	1.40	-0.15	0.973	.822612E	3
YI3C	0.97	-0.11	0.973	.832609E	3
VF	0.77	0.08	0.973	.8562?8E	3
VS	0.62	-0.07	0.973	.838438E	3

E.S.S. .842328E 3

RESIDUAL ERROR .318568E 1

MULT CORR 0.972

INTERCEPT TERM 135.7920674

GET

NUMBER OF PAGES 24

REGRESSION ANALYSIS ' COVA ' DATA1 CUT OFF PARAMETER .100000E- 5

DEPENDENT VARIABLE YI1A DEGREES OF FREEDOM 90

INDEPENDENT VARIABLES AT SIGNIFICANT LEVEL 5.00 %

V	CD	CURNT	TEMP	TIME	WF	WSTRP	DF	H1	H2	H3	RSTR	Z	VOL	
A	R	YR	AI	RST1A	RST1B	RST1C	RST2A	RST2B	RST2C	RST3A	RST3B	RST3C	P1A	
P1B	P1C	P2A	P2B	P2C	P3A	P3B	P3C	RLT1A	RLT1B	RLT1C	RLT2A	RLT2B	RLT2C	
RLT3A	RLT3B	RLT3C	YI1B	YI1C	YI2A	YI2B	YI2C	YI3A	YI3B	YI3C	VF	VS		

VARIABLES IN THE REGRESSION SET

VAR NAME	REGRESSION COEFF	STANDARD ERROR	CONFIDENCE INTERVAL	T STAT	PART CORR	MULTIPLE CORRELATION	E S S
WSTRP	0.0413189	.164690E- 1	.326757E- 1	2.51	0.26	0.815	.426884E 1
A	0.0137653	.620004E- 2	.124199E- 1	2.20	0.23	0.818	.420479E 1
P1A	0.1321966	.302770E- 1	.600712E- 1	4.37	0.42	0.787	.483400E 1
RLT1A	0.1439042	.157674E- 1	.273145E- 1	9.00	0.69	0.635	.753050E 1
RLT1B	0.0488097	.135019E- 1	.267869E- 1	2.13	0.22	0.819	.419166E 1
RLT2C -	0.0451607	.513539E- 2	.101886E- 1	4.51	-0.43	0.784	.489152E 1
YI1B	0.4045269	.110125E 0	.230389E 0	3.48	0.34	0.802	.452779E 1
YI2A -	0.0017306	.323205E- 1	.641234E- 1	2.53	-0.26	0.815	.427330E 1

VARIABLES NOT IN THE REGRESSION SET

VAR NAME	T STAT	PART CORR	MULTIPLE CORRELATION	E S S
V	1.39	0.15	0.832	.390472E 1
CD	1.17	-0.12	0.831	.392987E 1
CURNT	1.16	-0.12	0.831	.392997E 1
TEMP	0.32	-0.03	0.828	.396533E 1
TIME	1.53	-0.16	0.833	.388806E 1
WF	1.29	-0.14	0.832	.391654E 1
DF	1.29	-0.14	0.832	.391628E 1
H1	0.43	0.05	0.829	.394140E 1
H2	1.34	-0.14	0.832	.391150E 1

VAR NAME	T STAT	PART CORR	MULTIPLE CORRELATION	E S S	
M3	1.31	-0.14	0.832	.391425E	1
MSYR	1.46	-0.15	0.833	.389666E	1
Z	0.90	-0.10	0.830	.395368E	1
VOL	0.75	-0.08	0.830	.396265E	1
R	0.01	-0.00	0.828	.398960E	1
YR	0.59	-0.06	0.829	.397419E	1
AI	1.55	-0.16	0.833	.388479E	1
RSY1A	0.44	0.05	0.829	.398097E	1
RST1B	1.05	-0.11	0.831	.394065E	1
RST1C	0.18	-0.02	0.828	.398828E	1
RST2A	0.55	-0.06	0.829	.397620E	1
RSY2B	0.12	0.01	0.828	.398992E	1
RST2C	0.65	0.07	0.829	.397070E	1
RST3A	0.43	-0.05	0.829	.398167E	1
RST3B	0.89	-0.09	0.830	.395486E	1
RST3C	0.67	0.07	0.829	.398950E	1
P1B	1.72	-0.18	0.834	.386077E	1
P1C	0.89	0.09	0.830	.395445E	1
P2A	0.73	-0.08	0.829	.396603E	1
P2B	0.87	-0.09	0.830	.395605E	1
P2C	0.68	0.07	0.829	.396894E	1
P3A	0.02	0.00	0.828	.398979E	1
P3B	1.87	-0.19	0.835	.383840E	1
P3C	0.00		0.828	.398984E	1
RLY1C	0.00	0.00	0.828	.000000E	0
RLT2A	0.34	0.04	0.829	.398469E	1
RLT2B	1.50	0.16	0.833	.389185E	1
RLT3A	1.03	-0.11	0.830	.394300E	1
RLT3B	0.28	0.03	0.828	.398639E	1

NAME	T STAT	PART CORR	MULTIPLE CORRELATION	E S S	
RLT3C	0.96	-0.01	0.828	.3988A4E	1
YI1C	0.00	0.00	0.828	.0000002	0
YI2B	1.63	0.17	0.834	.3874?1E	1
YI2C	0.24	-0.03	0.828	.3987?1E	1
YI3A	0.56	-0.06	0.829	.3975?4E	1
YI3B	1.10	0.12	0.831	.3986?4E	1
YI3C	0.21	0.02	0.828	.3987?9E	1
VF	0.34	0.04	0.829	.3984?0E	1
Vs	0.40	0.04	0.829	.3982?3E	1

E.S.S. .398981E 1

RESIDUAL ERROR .2105?0E 0

MULT CORR 0,828

INTERCEPT TERM = 11,2055613

REGRESSION ANALYSIS 'COVA DATA1 CUT OFF PARAMETER .100000E- 5

DEPENDENT VARIABLE YI2A DEGREES OF FREEDOM 88

INDEPENDENT VARIABLES AT SIGNIFICANT LEVEL 5.00 %

V	CD	CURNT	TEMP	TIME	WF	WSTRP	DF	H1	H2	H3	HSTR	Z	VOL	
A	R	YR	AI	RST1A	RST1B	RST1C	RST2A	RST2B	RST2C	RST3A	RST3B	RST3C	P1A	
P1B	P1C	P2A	P2B	P2C	P3A	P3B	P3C	RLT1A	RLT1B	RLT1C	RLT2A	RLT2B	RLT2C	
RLT3A	RLT3B	RLT3C	YI1A	YI1B	YI1C	YI2B	YI2C	YI3A	YI3B	YI3C	VF	VS		

VARIABLES IN THE REGRESSION SET

VAR NAME	REGRESSION COEFF	STANDARD ERROR	CONFIDENCE INTERVAL	T STAT	PART CORR	MULTIPLE CORRELATION	E S S
CURNT =	0.0457295	.120791E- 1	.240374E- 1	3.79	-0.37	0.882	.116952E 2
TIME =	0.0000203	.486782E- 5	.972676E- 5	4.15	-0.40	0.879	.120208E 2
VOL	0.0192425	.450290E- 2	.896077E- 2	4.27	0.41	0.877	.121442E 2
A	0.0453264	.107460E- 1	.213861E- 1	2.36	0.24	0.893	.106919E 2
RST2A =	0.2187932	.491655E- 1	.978393E- 1	4.45	-0.43	0.875	.123204E 2
P2A	0.3900219	.564469E- 1	.112329E 0	6.91	0.59	0.840	.155133E 2
P3A =	0.1841600	.778128E- 1	.154449E 0	2.37	-0.25	0.893	.107006E 2
RLT2A	0.1113596	.107344E- 1	.213615E- 1	10.37	0.74	0.759	.223568E 2
RLT2B =	0.0597930	.152724E- 1	.303917E- 1	3.92	-0.39	0.881	.118090E 2
YI2B	0.3150418	.108769E 0	.216451E 0	2.90	0.30	0.889	.110159E 2

VARIABLES NOT IN THE REGRESSION SET

VAR NAME	T STAT	PART CORR	MULTIPLE CORRELATION	E S S
V	0.81	0.09	0.900	.998229E 1
CD	0.49	0.05	0.900	.100293E 2
TEMP	0.91	0.10	0.901	.996240E 1
WF	0.66	-0.07	0.900	.100076E 2
WSTRP	1.28	0.14	0.902	.987251E 1
DF	0.66	-0.07	0.900	.100077E 2
H1	0.89	0.09	0.901	.996682E 1

NAME	T STAT	PART CORR	MULTIPLE CORRELATION	S S R	
M2	0.31	0.03	0.900	.100457E	2
M3	0.04	0.00	0.900	.100569E	2
MSTR	0.58	-0.06	0.900	.100189E	2
Z	0.87	-0.09	0.901	.997008E	1
R	0.11	-0.01	0.900	.100558E	2
YR	0.60	0.06	0.900	.100155E	2
AI	0.85	-0.09	0.900	.997476E	1
RST1A	0.30	0.03	0.900	.100469E	2
RST1B	1.22	0.13	0.901	.998908E	1
RST1C	1.55	0.16	0.902	.978620E	1
RST2B	0.11	-0.01	0.900	.100556E	2
RST2C	0.10	-0.01	0.900	.100560E	2
RST3A	1.00	0.11	0.901	.994318E	1
RST3B	1.05	0.11	0.901	.993172E	1
RST3C	0.18	0.02	0.900	.100533E	2
P1A	0.07	0.01	0.900	.100565E	2
P1B	0.65	0.07	0.900	.100080E	2
P1C	0.44	0.05	0.900	.100351E	2
P2B	0.29	-0.03	0.900	.100473E	2
P2C	1.48	-0.16	0.902	.981030E	1
P3B	0.20	-0.02	0.900	.100526E	2
P3C	0.00		0.900	.100571E	2
RLT1A	0.04	-0.00	0.900	.100569E	2
RLT1B	1.30	-0.14	0.902	.986024E	1
RLT1C	0.00	0.00	0.900	.000000E	0
RLT2C	0.99	0.11	0.901	.994450E	1
RLT3A	0.12	0.01	0.900	.100554E	2
RLT3B	0.98	-0.10	0.901	.994652E	1
RLT3C	1.59	-0.17	0.903	.977309E	1

VAR NAME	T STAT	PART CORR	MULTIPLE CORRELATION	E S S	
YI1A	1.66	-0.17	0.903	.974923E	1
YI1B	1.30	-0.14	0.902	.986689E	1
YI1C	0.00	0.00	0.900	.000000E	0
YI2C	0.63	-0.07	0.900	.100122E	2
YI3A	0.14	-0.01	0.900	.100549E	2
YI3B	1.52	-0.16	0.902	.979739E	1
YI3C	1.84	-0.19	0.904	.968114E	1
VF	0.71	0.08	0.900	.999559E	1
VS	1.14	0.12	0.901	.990807E	1

E.S.S. .100571E 2

RESIDUAL ERROR .338062E 0

MULT CORR 0.900

INTERCEPT TERM = 8.7879604

DEPENDENT VARIABLE YI2B DEGREES OF FREEDOM 93

INDEPENDENT VARIABLES AT SIGNIFICANT LEVEL 5.00 %

V	CD	CURNT	TEMP	TIME	WF	WSTRP	DF	H1	H2	H3	HSTR	Z	VOL
A	R	YR	AI	RST1A	RST1B	RST1C	RST2A	RST2B	RST2C	RST3A	RST3B	RST3C	P1A
P1B	P1C	P2A	P2B	P2C	P3A	P3B	P3C	RLT1A	RLT1B	RLT1C	RLT2A	RLT2B	RLT2C
RLT3A	RLT3B	RLT3C	YI1A	YI1B	YI1C	YI2A	YI2C	YI3A	YI3B	YI3C	VF	VS	

VARIABLES IN THE REGRESSION SET

VAR NAME	REGRESSION COEFF	STANDARD ERROR	CONFIDENCE INTERVAL	T STAT	PART CORR	MULTIPLE CORRELATION	E S S
RLT1A =	0.0356014	.103562E-1	.303790E-1	3.03	-0.30	0.720	.824421E 1
RLT2B	0.0953895	.105083E-1	.204516E-1	9.25	0.69	0.399	.144104E 2
RLT2C =	0.0377907	.869214E-2	.172452E-1	4.35	-0.41	0.688	.902731E 1
YI2A	0.2149558	.396410E-1	.786477E-1	5.42	0.49	0.651	.987450E 1
YI2C	0.2967621	.131716E 0	.261329E 0	2.03	0.21	0.737	.783331E 1

VARIABLES NOT IN THE REGRESSION SET

VAR NAME	T STAT	PART CORR	MULTIPLE CORRELATION	E S S
V	0.85	0.09	0.752	.744355E 1
CD	0.58	-0.06	0.751	.747527E 1
CURNT	0.58	-0.06	0.751	.747513E 1
TEMP	0.23	0.02	0.750	.749816E 1
TIME	0.30	-0.03	0.750	.749485E 1
WF	0.04	-0.00	0.750	.750230E 1
WSTRP	0.09	-0.01	0.750	.750180E 1
DF	0.03	-0.00	0.750	.750237E 1
H1	0.87	0.09	0.752	.744092E 1
H2	0.51	-0.05	0.751	.748092E 1
H3	0.13	0.02	0.750	.749985E 1
HSTR	0.26	-0.03	0.750	.749672E 1

VAR NAME	T STAT	PART CORR	MULTIPLE CORRELATION	B S D	
Z	0.86	-0.09	0.752	.744249E	1
VOL	0.68	-0.07	0.751	.744508E	1
A	1.79	-0.18	0.760	.724928E	1
R	1.12	-0.12	0.754	.740140E	1
YR	0.75	-0.08	0.752	.745655E	1
AI	0.15	-0.02	0.750	.750058E	1
RST1A	1.55	-0.16	0.757	.731129E	1
RST1B	1.05	-0.11	0.753	.741362E	1
RST1C	0.38	0.04	0.750	.749045E	1
RST2A	0.25	0.03	0.750	.749731E	1
RST2B	0.21	-0.02	0.750	.749890E	1
RST2C	0.30	0.03	0.750	.749532E	1
RST3A	0.89	-0.09	0.752	.743882E	1
RST3B	0.79	-0.08	0.752	.745293E	1
RST3C	0.54	0.06	0.751	.747851E	1
P1A	0.40	-0.04	0.750	.748913E	1
P1B	0.06	-0.01	0.750	.750212E	1
P1C	0.31	-0.03	0.750	.749464E	1
P2A	0.95	0.10	0.753	.743003E	1
P2B	0.05	-0.01	0.750	.750219E	1
P2C	0.38	0.04	0.750	.749084E	1
P3A	0.03	0.00	0.750	.750235E	1
P3B	0.36	-0.04	0.750	.749216E	1
P3C	0.00		0.750	.750243E	1
RLT1B	1.68	0.17	0.759	.727948E	1
RLT1C	0.00	0.00	0.750	.000000E	0
RLT2A	1.84	-0.19	0.760	.723489E	1
RLT3A	1.49	-0.15	0.757	.732534E	1
RLT3B	0.26	0.03	0.750	.749883E	1

VAR NAME	T STAT	PART CORR	MULTIPLE CORRELATION	E S S
RLT3C	0.50	0.05	0.751	.748218E 1
YI1A	1.01	0.10	0.753	.748021E 1
YI1B	1.86	0.19	0.760	.722977E 1
YI1C	0.00	0.00	0.750	.000000E 0
YI3A	0.66	-0.07	0.751	.748711E 1
YI3B	0.58	0.06	0.751	.748525E 1
YI3C	0.04	0.00	0.750	.750231E 1
VF	0.43	0.05	0.750	.748717E 1
VS	0.19	-0.02	0.750	.749958E 1

E.S.S. .750243E 1

RESIDUAL ERROR .284027E 0

MULT CORR 0.750

INTERCEPT TERM = 9.5140804

DEPENDENT VARIABLE YI2C DEGREES OF FREEDOM 97

INDEPENDENT VARIABLES AT SIGNIFICANT LEVEL 5.00 %

V CD CURNT TEMP TIME WF WSTRP DF H1 H2 H3 HSTR Z VOL

A R YR AI RST1A RST1B RST1C RST2A RST2B RST2C RST3A RST3B RST3C P1A

P1B P1C P2A P2B P2C P3A P3B P3C RLT1A RLT1B RLT1C RLT2A RLT2B RLT2C

RLT3A RLT3B RLT3C YI1A YI1B YI1C YI2A YI2B YI3A YI3B YI3C VF VS

VARIABLES IN THE REGRESSION SET

VAR NAME	REGRESSION COEFF	STANDARD ERROR	CONFIDENCE INTERVAL	T STAT	PART CORR	MULTIPLE CORRELATION	E S S
RLT2C	0.0400939	.531241E- 2	.105398E- 1	7.55	0.61	0.000	.741332E 1

VARIABLES NOT IN THE REGRESSION SET

VAR NAME	T STAT	PART CORR	MULTIPLE CORRELATION	E S S
V	0.37	0.04	0.609	.466415E 1
CD	0.15	0.02	0.608	.466950E 1
CURNT	0.15	0.02	0.608	.466949E 1
TEMP	0.68	0.07	0.611	.464834E 1
TIME	0.21	0.02	0.608	.466849E 1
WF	0.40	0.04	0.609	.466278E 1
WSTRP	0.00	0.00	0.608	.467063E 1
DF	0.42	0.04	0.609	.466166E 1
H1	0.56	0.06	0.610	.465544E 1
H2	0.04	0.00	0.608	.467056E 1
H3	0.40	0.04	0.609	.466302E 1
HSTR	0.37	0.04	0.609	.466402E 1
Z	0.18	0.02	0.608	.466902E 1
VOL	0.43	0.04	0.609	.466177E 1
A	0.00	0.00	0.608	.467063E 1
R	0.79	-0.08	0.612	.464030E 1

VAR NAME	T STAT	PART CORR	CORRELATION		
YR	0.02	0.00	0.608	.467062E	1
AI	0.13	0.01	0.608	.466978E	1
RST1A	0.15	0.02	0.608	.466955E	1
RST1B	0.15	0.02	0.608	.466955E	1
RST1C	0.47	0.05	0.609	.466008E	1
RST2A	0.71	0.07	0.611	.464657E	1
RST2B	0.39	-0.04	0.609	.466329E	1
RST2C	0.16	0.02	0.608	.466936E	1
RST3A	0.43	0.04	0.609	.466181E	1
RST3B	0.22	0.02	0.609	.466826E	1
RST3C	0.14	0.01	0.608	.466961E	1
P1A	0.14	-0.01	0.608	.466973E	1
P1B	0.12	0.01	0.608	.466993E	1
P1C	0.20	0.02	0.608	.466863E	1
P2A	1.14	0.12	0.615	.460836E	1
P2B	0.07	0.01	0.608	.467037E	1
P2C	0.00	-0.00	0.608	.467063E	1
P3A	0.00	-0.00	0.608	.467063E	1
P3B	0.00	0.00	0.608	.467063E	1
P3C	0.00		0.608	.467065E	1
RLT1A	0.01	-0.00	0.608	.467063E	1
RLT1B	0.23	0.03	0.609	.466757E	1
RLT1C	0.00	0.00	0.608	.000000E	0
RLT2A	0.57	-0.06	0.610	.465491E	1
RLT2B	0.60	-0.06	0.610	.465298E	1
RLT3A	0.38	0.04	0.609	.466363E	1
RLT3B	0.19	0.02	0.608	.466891E	1
RLT3C	0.16	0.02	0.608	.466937E	1
YI1A	0.13	-0.01	0.608	.466986E	1

VAR NAME	T STAT	PART CORR	MULTIPLE CORRELATION	E S S	
YI1B	0.00	-0.00	0.608	.4670636	1
YI1C	0.00	0.00	0.608	.0000000	0
YI2A	0.18	-0.02	0.608	.4669146	1
YI2B	0.94	0.10	0.613	.4428056	1
YI3A	0.00	-0.00	0.608	.4670636	1
YI3B	0.00	0.00	0.608	.4670636	1
YI3C	0.00	-0.00	0.608	.4670636	1
VF	0.01	-0.00	0.608	.4670636	1
VS	0.00	0.00	0.608	.4670636	1

E.S.S. .4670636 1

RESIDUAL ERROR .2194536 0

MULT CORR 0.608

INTERCEPT TERM = 17.05182D5

REGRESSION ANALYSIS - COVA DATA1 CUT OFF PARAMETER .100000E- 5

DEPENDENT VARIABLE YI3A DEGREES OF FREEDOM 88

INDEPENDENT VARIABLES AT SIGNIFICANT LEVEL 5.00 %

V	CD	CURNT	TEMP	TIME	WF	WSTRP	DF	H1	H2	H3	HSTR	Z	VOL	
A	R	YR	AI	RST1A	RST1B	RST1C	RST2A	RST2B	RST2C	RST3A	RST3B	RST3C	P1A	
P1B	P1C	P2A	P2B	P2C	P3A	P3B	P3C	RLT1A	RLT1B	RLT1C	RLT2A	RLT2B	RLT2C	
RLT3A	RLT3B	RLT3C	YI1A	YI1B	YI1C	YI2A	YI2B	YI2C	YI3B	YI3C	VF	VS		

VARIABLES IN THE REGRESSION SET

VAR NAME	REGRESSION COEFF	STANDARD ERROR	CONFIDENCE INTERVAL	T STAT	PART CORR	MULTIPLE CORRELATION	E S S
CURNT	0,0132726	,570278E- 2	,113485E- 1	2.33	0.24	0.945	,163918E 1
H3	-0,0055681	,144259E- 2	,287076E- 2	3.86	-0.38	0.939	,180555E 1
RST3A	-0,0354462	,190395E- 1	,378885E- 1	2.91	-0.30	0.943	,169295E 1
RST3C	-0,1430687	,181230E- 1	,360659E- 1	7.89	-0.64	0.909	,263760E 1
P3A	0,4481797	,457056E- 1	,909746E- 1	9.80	0.72	0.867	,322827E 1
P3B	0,1627693	,411049E- 1	,817988E- 1	4.45	0.43	0.936	,189105E 1
RLT3A	0,0384948	,377451E- 2	,751128E- 2	10.20	0.74	0.862	,336923E 1
RLT3B	0,0105598	,234900E- 2	,467451E- 2	4.50	0.43	0.935	,189873E 1
RLT3C	-0,0015252	,501662E- 2	,998307E- 2	12.26	-0.79	0.851	,418343E 1
YI3C	0,4414843	,108750E 0	,216424E 0	4.06	0.40	0.938	,183329E 1

VARIABLES NOT IN THE REGRESSION SET

VAR NAME	T STAT	PART CORR	MULTIPLE CORRELATION	E S S
V	0.50	0.05	0.948	,153975E 1
CD	0.75	-0.08	0.948	,153416E 1
TEMP	0.33	-0.04	0.948	,154218E 1
TIME	0.20	-0.02	0.948	,154343E 1
WF	0.92	-0.10	0.948	,152923E 1
WSTRP	0.42	-0.05	0.948	,154097E 1
DF	0.92	-0.10	0.948	,152922E 1

VAR NAME	T STAT	PART CORR	MULTIPLE CORRELATION	E S S	
H1	0.43	-0.05	0.948	.154082E	1
H2	1.17	-0.12	0.949	.152087E	1
HSTR	0.16	-0.02	0.948	.154366E	1
Z	0.52	-0.06	0.948	.153934E	1
VOL	0.90	0.10	0.948	.152997E	1
A	0.56	-0.06	0.948	.153061E	1
R	0.20	-0.02	0.948	.154346E	1
YR	1.58	0.17	0.949	.150119E	1
AI	0.31	0.03	0.948	.154240E	1
RST1A	1.40	-0.15	0.949	.151005E	1
RST1B	1.19	0.13	0.949	.151945E	1
RST1C	0.10	0.01	0.948	.154396E	1
RST2A	0.26	-0.03	0.948	.154294E	1
RST2B	0.26	-0.03	0.948	.154295E	1
RST2C	0.40	0.04	0.948	.154196E	1
RST3B	0.13	0.01	0.948	.154382E	1
P1A	0.78	-0.08	0.948	.153333E	1
P1B	0.22	-0.02	0.948	.154328E	1
P1C	0.09	-0.01	0.948	.154309E	1
P2A	0.31	-0.03	0.948	.154244E	1
P2B	0.33	-0.04	0.948	.154223E	1
P2C	0.14	-0.01	0.948	.154379E	1
P3C	0.00		0.948	.154413E	1
RLY1A	0.45	-0.05	0.948	.154049E	1
RLY1B	0.12	0.01	0.948	.154390E	1
RLY1C	0.00	0.00	0.948	.000000E	0
RLY2A	0.63	-0.07	0.948	.153716E	1
RLY2B	0.51	-0.05	0.948	.153959E	1
RLY2C	0.11	-0.01	0.948	.154394E	1

NAME		CORR	CORRELATION	
YI1A	0.24	-0.03	0.948	.154312E 1
YI1B	0.23	-0.02	0.948	.154320E 1
YI1C	0.00	0.00	0.948	.0000002 0
YI2A	0.68	-0.07	0.948	.153586E 1
YI2B	0.68	0.07	0.948	.153589E 1
YI2C	0.04	0.00	0.948	.154411E 1
YI3B	1.46	-0.15	0.949	.150733E 1
VF	0.01	-0.00	0.948	.154413E 1
VS	1.10	0.12	0.949	.152286E 1

E.S.S. .154413E 1

RESIDUAL ERROR .132465E 0

MULT CORR 0.948

INTERCEPT TERM 0.5515491

REGRESSION ANALYSIS ' COVA DATA1 CUT OFF PARAMETER .100000E- 5

DEPENDENT VARIABLE YI3B DEGREES OF FREEDOM 80

INDEPENDENT VARIABLES AT SIGNIFICANT LEVEL 5.00 %

V	CD	CURNT	TEMP	TIME	WF	WSTRP	DF	H1	H2	H3	HSTR	Z	VOL
A	R	YR	AI	RST1A	RST1B	RST1C	RST2A	RST2B	RST2C	RST3A	RST3B	RST3C	P1A
P1B	P1C	P2A	P2B	P2C	P3A	P3B	P3C	RLT1A	RLT1B	RLT1C	RLT2A	RLT2B	RLT2C
RLT3A	RLT3B	RLT3C	YI1A	YI1B	YI1C	YI2A	YI2B	YI2C	YI3A	YI3C	VF	VS	

VARIABLES IN THE REGRESSION SET

VAR NAME		REGRESSION COEFF	STANDARD ERROR	CONFIDENCE INTERVAL	T STAT	PART CORR	MULTIPLE CORRELATION	E S S	
CD		0.0090109	.350895E- 2	.698282E- 2	2.57	0.28	0.960	.847869E	0
TIME		0.0000050	.168287E- 5	.334891E- 5	2.96	0.31	0.959	.868929E	0
DF	-	0.0071374	.108004E- 2	.214927E- 2	6.61	-0.59	0.943	.121091E	1
H1		0.0436437	.130672E- 1	.260038E- 1	3.34	0.35	0.956	.892523E	0
VOL	-	0.0470942	.253387E- 2	.504201E- 2	10.69	-0.77	0.909	.190207E	1
A	-	0.0067825	.329977E- 2	.656654E- 2	2.05	-0.22	0.962	.824494E	0
YR		0.0119450	.407519E- 2	.810964E- 2	2.93	0.31	0.960	.867423E	0
RST1A		0.0700624	.144717E- 1	.287987E- 1	4.84	0.48	0.953	.101279E	1
RST2A		0.0420468	.950812E- 2	.189212E- 1	2.32	0.25	0.961	.855945E	0
RST3A		0.1037522	.188236E- 1	.374594E- 1	8.70	0.70	0.928	.152409E	1
RST3B		0.0347997	.729682E- 2	.145207E- 1	4.77	0.47	0.953	.100600E	1
P1A	-	0.0971248	.324633E- 1	.646020E- 1	2.99	-0.32	0.959	.870943E	0
P3A		0.1393264	.309413E- 1	.703296E- 1	4.51	0.45	0.954	.982206E	0
P3C	-	0.0930003	.378909E- 1	.748058E- 1	2.47	-0.27	0.961	.843230E	0
RLT2A		0.0116917	.380664E- 2	.757522E- 2	3.07	0.32	0.959	.875066E	0
RLT3A	-	0.0460588	.349535E- 2	.695574E- 2	7.46	-0.64	0.937	.132751E	1
RLT3B		0.0430254	.169550E- 2	.337205E- 2	22.70	0.93	0.883	.582804E	1
YI3C		1.2599747	.750730E- 1	.149396E 0	16.52	0.88	0.827	.345440E	1

VARIABLES NOT IN THE REGRESSION SET

VAR NAME	T STAT	PART CORR	MULTIPLE CORRELATION	F S S
V	0.27	0.03	0.964	.782562E 0
CURNT	0.60	-0.07	0.964	.779066E 0
TEMP	0.26	-0.03	0.964	.782617E 0
WF	0.77	0.09	0.964	.777522E 0
WSTRP	1.31	0.15	0.964	.766038E 0
H2	0.73	-0.08	0.964	.777965E 0
H3	0.57	0.06	0.964	.780103E 0
HSTR	1.05	0.12	0.964	.772469E 0
Z	0.64	0.07	0.964	.779109E 0
R	1.51	-0.17	0.965	.761310E 0
AI	0.83	0.09	0.964	.776503E 0
RSY1B	1.31	-0.15	0.964	.766739E 0
RSY1C	1.13	-0.13	0.964	.770080E 0
RST2B	0.62	-0.07	0.964	.779507E 0
RST2C	0.93	-0.10	0.964	.774764E 0
RST3C	0.66	-0.07	0.964	.778981E 0
P1B	1.11	-0.12	0.964	.771369E 0
P1C	0.20	0.02	0.964	.782917E 0
P2A	0.16	-0.02	0.964	.782976E 0
P2B	0.50	0.06	0.964	.780803E 0
P2C	0.49	0.05	0.964	.780947E 0
P3C	0.00		0.964	.783301E 0
RLY1A	0.29	-0.03	0.964	.782490E 0
RLY1B	1.48	0.16	0.965	.762116E 0
RLY1C	0.00	0.00	0.964	.000000E 0
RLY2B	0.38	0.04	0.964	.781660E 0
RLY2C	0.66	-0.07	0.964	.779069E 0
RLY3C	1.30	0.14	0.964	.767000E 0

VAR NAME	T STAT	PART CORR	MULTIPLE CORRELATION	E S S
YI1A	0.00	0.00	0.964	.783600E 0
YI1B	0.77	0.09	0.964	.777442E 0
YI1C	0.00	0.00	0.964	.000000E 0
YI2A	1.20	-0.13	0.964	.769553E 0
YI2B	1.61	0.18	0.965	.758412E 0
YI2C	0.16	-0.02	0.964	.782906E 0
YI3A	1.17	-0.13	0.964	.769942E 0
VF	0.09	0.01	0.964	.783212E 0
VS	0.42	-0.05	0.964	.781591E 0

E.S.S. .783301E 0

RESIDUAL ERROR .989508E-1

MULT CORR 0.964

INTERCEPT TERM 2.0567002

GET

NUMBER OF PAGES 24

REGRESSION ANALYSIS COVA DATA1 CUT OFF PARAMETER .100000E- 5

DEPENDENT VARIABLE YI3C DEGREES OF FREEDOM 77

INDEPENDENT VARIABLES AT SIGNIFICANT LEVEL 5.00 %

V	CD	CURNT	TEMP	TIME	WF	WSTRP	DF	H1	H2	H3	HSTR	Z	VOL
A	R	YR	AI	RST1A	RST1B	RST1C	RST2A	RST2B	RST2C	RST3A	RST3B	RST3C	P1A
P1B	P1C	P2A	P2B	P2C	P3A	P3B	P3C	RLT1A	RLT1B	RLT1C	RLT2A	RLT2B	RLT2C
RLT3A	RLT3B	RLT3C	YI1A	YI1B	YI1C	YI2A	YI2B	YI2C	YI3A	YI3B	VF	VS	

VARIABLES IN THE REGRESSION SET

VAR NAME		REGRESSION COEFF	STANDARD ERROR	CONFIDENCE INTERVAL	T STAT	PART CORR	MULTIPLE CORRELATION	E S S
CURNT	-	0.0083495	.240294E- 2	.478184E- 2	3.47	-0.37	0.967	.262119E 0
TIME	-	0.0000070	.168749E- 5	.335811E- 5	4.13	-0.43	0.966	.276798E 0
WF		0.0025364	.409541E- 3	.814986E- 3	6.19	0.58	0.958	.339463E 0
H1	-	0.0418381	.758321E- 2	.150906E- 1	2.88	-0.31	0.969	.250905E 0
HSTR	-	0.0045762	.192766E- 2	.383605E- 2	2.37	-0.26	0.970	.243174E 0
VOL		0.0137622	.219470E- 2	.436745E- 2	6.27	0.58	0.957	.342302E 0
R		0.0010646	.279079E- 3	.555368E- 3	3.81	0.40	0.966	.269414E 0
RST1A	-	0.0223445	.758925E- 2	.151026E- 1	2.94	-0.32	0.967	.252099E 0
RST2C		0.1414942	.293673E- 1	.584410E- 1	4.82	0.48	0.963	.294902E 0
RST3A	-	0.0794022	.107040E- 1	.213010E- 1	7.42	-0.65	0.951	.338518E 0
RST3B	-	0.0105434	.350527E- 2	.697549E- 2	3.01	-0.32	0.969	.253214E 0
RST3C	-	0.2350228	.445696E- 1	.962555E- 1	5.27	-0.52	0.962	.308302E 0
P1A		0.0405682	.180577E- 1	.359347E- 1	2.25	0.25	0.970	.241442E 0
P2A	-	0.0152346	.656386E- 2	.130617E- 1	2.32	-0.26	0.970	.242443E 0
P2C	-	1.8962923	.652196E 0	.129787E 1	2.91	-0.31	0.969	.251467E 0
P3A	-	0.1372449	.236320E- 1	.470288E- 1	5.81	-0.55	0.959	.325841E 0
RLT1B	-	0.0145004	.490441E- 2	.975977E- 2	2.96	-0.32	0.969	.252314E 0
RLT3B	-	0.0195695	.187260E- 2	.372647E- 2	10.45	-0.77	0.931	.547971E 0
RLT3C		0.0185845	.278261E- 2	.553740E- 2	6.68	0.61	0.955	.357855E 0
YI3A		0.1388671	.311317E- 1	.619520E- 1	4.46	0.45	0.964	.285142E 0

VAR NAME	REGRESSION COEFF	STANDARD ERROR	CONFIDENCE INTERVAL	T STAT	PART CORR	MULTIPLE CORRELATION	E S S	
Y13B	0.4020198	.390054E- 1	.696607E- 1	11.48	0.79	0.972	.614719E	0

VARIABLES NOT IN THE REGRESSION SET

VAR NAME	T STAT	PART CORR	MULTIPLE CORRELATION	E S S	
V	0.40	0.05	0.972	.226115E	0
CD	0.55	-0.06	0.972	.225696E	0
TEMP	0.40	0.05	0.972	.226106E	0
WSTRP	0.13	0.02	0.972	.225536E	0
DF	0.89	0.10	0.972	.224245E	0
H2	0.65	0.10	0.972	.224437E	0
H3	0.92	0.10	0.972	.224008E	0
Z	0.36	0.04	0.972	.226214E	0
A	1.01	0.12	0.972	.225569E	0
YR	0.81	0.09	0.972	.224652E	0
AI	0.46	-0.05	0.972	.225965E	0
RST1B	0.32	0.04	0.972	.226277E	0
RST1C	0.20	0.02	0.972	.226475E	0
RST2A	0.16	-0.02	0.972	.226517E	0
RST2B	0.43	0.05	0.972	.226068E	0
P1B	0.62	0.07	0.972	.225457E	0
P1C	0.08	-0.01	0.972	.226569E	0
P2B	0.85	-0.10	0.972	.224472E	0
P3B	0.48	0.05	0.972	.225915E	0
P3C	0.00		0.972	.226593E	0
RLT1A	0.69	0.08	0.972	.225186E	0
RLT1C	0.00	0.00	0.972	.000000E	0
RLT2A	0.07	-0.01	0.972	.226575E	0
RLT2B	0.25	0.03	0.972	.226309E	0
RLT2C	0.12	-0.01	0.972	.226547E	0

NAME			CORR	CORRELATION	
RLT3A	1.41	0.16	0.973	.2207?6E	0
Y11A	1.55	0.18	0.974	.219614E	0
Y11B	0.16	-0.02	0.972	.226516E	0
Y11C	0.00	0.00	0.972	.000000E	0
Y12A	0.74	0.09	0.972	.224953E	0
Y12B	0.33	0.04	0.972	.226270E	0
Y12C	0.45	0.05	0.972	.225980E	0
VF	0.17	0.02	0.972	.226506E	0
VS	0.65	-0.07	0.972	.225319E	0

E.S.S. .226590E 0

RESIDUAL ERROR .542459E-1

MULT CORR 0.972

INTERCEPT TERM = 40.9417502

17/05/13. 22/09/78 ICL 1900 STATISTICAL ANALYSIS XDS3/2A

REGRESSION ANALYSIS COVA DATA1 CUT OFF PARAMETER .100000E- 5

DEPENDENT VARIABLE RLT1A DEGREES OF FREEDOM 93

INDEPENDENT VARIABLES AT SIGNIFICANT LEVEL 5.00 %

V	CD	CURNT	TEMP	TIME	WF	WSTRP	DF	H1	H2	H3	HSTR	Z	VOL
A	R	YR	AI	RST1A	RST1B	RST1C	RST2A	RST2B	RST2C	RST3A	RST3B	RST3C	P1A
P1B	P1C	P2A	P2B	P2C	P3A	P3B	P3C	RLT1B	RLT1C	RLT2A	RLT2B	RLT2C	RLT3A
RLT3B	RLT3C	YI1A	YI1B	YI1C	YI2A	YI2B	YI2C	YI3A	YI3B	YI3C	VF	VS	

VARIABLES IN THE REGRESSION SET

VAR NAME	REGRESSION COEFF	STANDARD ERROR	CONFIDENCE INTERVAL	T STAT	PART CORR	MULTIPLE CORRELATION	E S S
WSTRP	- 0.1913669	.765495E- 1	.155843E 0	2.44	-0.24	0.779	.988245E 2
Z	0.5261539	.186432E 0	.369882E 0	2.83	0.28	0.773	.100912E 3
P1B	1.8380490	.289507E 0	.574382E 0	6.35	0.55	0.685	.133159E 3
P1C	1.1415402	.477080E 0	.946526E 0	2.39	0.24	0.779	.986148E 2
YI1A	2.7722389	.285130E 0	.565698E 0	9.72	0.71	0.504	.167321E 3

VARIABLES NOT IN THE REGRESSION SET

VAR NAME	T STAT	PART CORR	MULTIPLE CORRELATION	F S S
V	1.11	0.11	0.797	.916721E 2
CD	0.86	-0.09	0.796	.921478E 2
CURNT	0.87	-0.09	0.796	.921427E 2
TEMP	1.77	0.18	0.801	.896430E 2
TIME	0.32	-0.03	0.794	.927921E 2
WF	0.72	-0.08	0.795	.923689E 2
DF	0.73	-0.08	0.795	.923654E 2
H1	0.86	-0.09	0.796	.921569E 2
H2	0.10	-0.01	0.794	.928857E 2
H3	0.57	-0.06	0.795	.925641E 2
HSTR	1.10	-0.11	0.797	.916954E 2
VOL	1.09	-0.11	0.797	.917219E 2

VAR NAME	T STAT	PART CORR	MULTIPLE CORRELATION	E R S	
A	0.34	-0.09	0.796	.9219686	2
R	1.17	-0.12	0.797	.9152726	2
YR	1.29	-0.13	0.798	.9124426	2
AI	0.74	-0.08	0.795	.9234056	2
RST1A	1.53	-0.16	0.800	.9059366	2
RST1B	0.35	-0.04	0.794	.9277286	2
RST1C	0.15	0.02	0.794	.9287246	2
RST2A	0.80	-0.08	0.795	.9225346	2
RST2B	0.22	-0.02	0.794	.9284866	2
RST2C	0.47	-0.05	0.794	.9267136	2
RST3A	1.33	-0.14	0.798	.9113866	2
RST3B	0.14	-0.02	0.794	.9287476	2
RST3C	0.58	-0.06	0.795	.9255426	2
P1A	1.40	-0.15	0.799	.9071186	2
P2A	1.04	-0.11	0.796	.9181826	2
P2B	0.16	0.02	0.794	.9286366	2
P2C	0.00	0.00	0.794	.9289586	2
P3A	0.45	0.05	0.794	.9269276	2
P3B	0.98	0.10	0.796	.9193266	2
P3C	0.00		0.794	.9289606	2
RLT1B	0.69	-0.07	0.795	.9241376	2
RLT1C	0.00	0.00	0.794	.0000006	0
RLT2A	0.37	0.04	0.794	.9275426	2
RLT2B	0.20	0.02	0.794	.9285716	2
RLT2C	0.53	-0.06	0.794	.9261196	2
RLT3A	0.98	-0.10	0.796	.9193926	2
RLT3B	0.68	-0.07	0.795	.9243456	2
RLT3C	0.65	-0.07	0.795	.9247256	2
YI1B	1.19	-0.12	0.797	.9149636	2

VAR NAME	T STAT	PART CORR	MULTIPLE CORRELATION	E S S
YI1C	0.00	0.00	0.794	.000000E 0
YI2A	0.03	-0.00	0.794	.928949E 2
YI2B	1.34	-0.14	0.798	.911073E 2
YI2C	0.34	-0.04	0.794	.927783E 2
YI3A	0.56	0.06	0.795	.926814E 2
YI3B	0.42	-0.04	0.794	.927147E 2
YI3C	0.00	-0.00	0.794	.928958E 2
VF	0.39	0.04	0.794	.927458E 2
VS	0.36	-0.04	0.794	.927644E 2

E.S.S. .928958E 2

RESIDUAL ERROR .999440E 0

MULT CORR 0.794

INTERCEPT TERM 109.7903083

REGRESSION ANALYSIS - COVA DATA1 CUT OFF PARAMETER .100000E- 5

DEPENDENT VARIABLE RLY1B DEGREES OF FREEDOM 91

INDEPENDENT VARIABLES AT SIGNIFICANT LEVEL 5.00 %

V	CD	CURNT	TEMP	TIME	WF	WSTRP	DF	H1	H2	H3	HSTR	Z	VOL
A	R	YR	AI	RST1A	RST1B	RST1C	RST2A	RST2B	RST2C	RST3A	RST3B	RST3C	P1A
P1B	P1C	P2A	P2B	P2C	P3A	P3B	P3C	RLT1A	RLT1C	RLT2A	RLT2B	RLT2C	RLT3A
RLT3B	RLT3C	YI1A	YI1B	YI1C	YI2A	YI2B	YI2C	YI3A	YI3B	YI3C	VF	VS	

VARIABLES IN THE REGRESSION SET

VAR NAME	REGRESSION COEFF	STANDARD ERROR	CONFIDENCE INTERVAL	T STAT	PART CORR	MULTIPLE CORRELATION	F S S
VOL	0.0763631	.207740E- 1	.412168E- 1	3.68	0.36	0.759	.124847E 3
RST1B	0.0096639	.228473E- 2	.453291E- 2	4.23	0.41	0.747	.130076E 3
RST3A -	0.3887201	.141330E 0	.280399E 0	2.75	-0.28	0.774	.117745E 3
P3B	1.6115823	.346721E 0	.687895E 0	4.65	0.44	0.737	.134514E 3
YI1A	1.0131552	.334814E 0	.664267E 0	3.03	0.30	0.770	.119644E 3
YI1B	2.1019777	.609814E 0	.120987E 1	3.45	0.34	0.763	.122899E 3
YI3C -	2.2446629	.664885E 0	.131913E 1	3.38	-0.33	0.764	.122321E 3

VARIABLES NOT IN THE REGRESSION SET

VAR NAME	T STAT	PART CORR	MULTIPLE CORRELATION	E S S
V	0.09	0.01	0.794	.108606E 3
CD	0.96	-0.10	0.796	.107611E 3
CURNT	0.96	-0.10	0.796	.107612E 3
TEMP	0.67	-0.07	0.795	.108166E 3
TIME	0.51	0.05	0.795	.108304E 3
WF	1.35	0.14	0.799	.106536E 3
WSTRP	0.30	-0.03	0.794	.108600E 3
DF	1.35	0.14	0.799	.106533E 3
H1	0.13	-0.01	0.794	.108667E 3
H2	1.24	0.13	0.798	.106873E 3

VAR NAME	T STAY	PART CORR	MULTIPLE CORRELATION	E S S	
RB	1.00	0.11	0.796	.1075038	3
RSTR	1.32	0.14	0.796	.1066279	3
Z	0.60	-0.06	0.795	.1082718	3
A	0.78	-0.08	0.795	.1079718	3
R	0.76	0.08	0.795	.1080218	3
YR	0.90	-0.09	0.796	.1077318	3
AI	0.20	0.02	0.794	.1086598	3
RST1A	1.21	-0.13	0.798	.1069588	3
RST1C	0.39	-0.04	0.794	.1085268	3
RST2A	0.23	0.02	0.794	.1086438	3
RST2B	0.43	-0.05	0.794	.1084828	3
RST2C	1.06	-0.11	0.797	.1073868	3
RST3B	0.59	0.06	0.795	.1082838	3
RST3C	0.86	-0.09	0.796	.1078198	3
P1A	0.89	-0.09	0.796	.1077488	3
P1B	0.87	-0.09	0.796	.1078048	3
P1C	0.11	-0.01	0.794	.1086928	3
P2A	0.26	0.03	0.794	.1086278	3
P2B	0.32	-0.03	0.794	.1085858	3
P2C	0.32	0.03	0.794	.1085828	3
P3A	0.94	0.10	0.796	.1076458	3
P3C	0.00		0.794	.1087068	3
RLT1A	1.34	-0.14	0.798	.1065828	3
RLT1C	0.00	0.00	0.794	.0000008	0
RLT2A	0.18	-0.02	0.794	.1086658	3
RLT2B	0.16	-0.02	0.794	.1086748	3
RLT2C	0.26	-0.03	0.794	.1086258	3
RLT3A	1.48	-0.15	0.799	.1061138	3
RLT3B	1.32	-0.14	0.798	.1066448	3

VAR NAME	T STAT	PART CORR	MULTIPLE CORRELATION	F < S
RLT3C	0.36	0.04	0.794	.108546E 3
YI1C	0.00	0.00	0.794	.000000E 0
YI2A	0.65	-0.07	0.795	.108201E 3
YI2B	1.68	0.17	0.801	.105404E 3
YI2C	0.06	0.01	0.794	.108702E 3
YI3A	0.89	-0.09	0.796	.107753E 3
YI3B	0.59	-0.06	0.795	.108200E 3
VF	0.05	0.01	0.794	.108703E 3
VS	0.30	0.03	0.794	.108565E 3

R.S.S. .108706E 3

RESIDUAL ERROR .109297E 1

MULT CORR 0.794

INTERCEPT TERM 46.7457372

REGRESSION ANALYSIS COVA DATA1 CUT OFF PARAMETER .100000E- 5

DEPENDENT VARIABLE RLT2A DEGREES OF FREEDOM 69

INDEPENDENT VARIABLES AT SIGNIFICANT LEVEL 5.00 %

V	CD	CURNT	TEMP	TIME	WF	WSTRP	DF	H1	H2	H3	HSTR	Z	VOL	
A	R	YR	AI	RST1A	RST1B	RST1C	RST2A	RST2B	RST2C	RST3A	RST3B	RST3C	P1A	
P1B	P1C	P2A	P2B	P2C	P3A	P3B	P3C	RLT1A	RLT1B	RLT1C	RLT2B	RLT2C	RLT3A	
RLT3B	RLT3C	YI1A	YI1B	YI1C	YI2A	YI2B	YI2C	YI3A	YI3B	YI3C	VF	VS		

VARIABLES IN THE REGRESSION SET

VAR NAME	REGRESSION COEFF	STANDARD ERROR	CONFIDENCE INTERVAL	T STAT	PART CORR	MULTIPLE CORRELATION	F S S
H2	0.0074793	.342251E- 1	.691029E- 1	2.52	0.26	0.904	.269463E 3
H3 *	0.1315367	.244791E- 1	.487135E- 1	5.37	-0.49	0.880	.333165E 3
Z	4.0328020	.424495E 0	.844745E 0	9.50	0.71	0.911	.506050E 3
YR *	0.2405272	.589753E- 1	.117361E 0	3.74	-0.37	0.896	.291076E 3
RLY1B	0.3456345	.122470E 0	.243715E 0	2.82	0.29	0.903	.274067E 3
YI1B	1.9956172	.937248E 0	.186512E 1	2.10	0.22	0.906	.263967E 3
YI2A	3.1566457	.267947E 0	.533215E 0	11.79	0.78	0.751	.644331E 3
YI3A	3.1933741	.471270E 0	.937827E 0	6.78	0.58	0.861	.381496E 3
YI3B	3.3911908	.579940E 0	.115409E 1	5.78	0.52	0.875	.345932E 3

VARIABLES NOT IN THE REGRESSION SET

VAR NAME	T STAT	PART CORR	MULTIPLE CORRELATION	F S S
V	0.27	0.03	0.911	.251349E 3
CD	0.86	0.09	0.912	.249448E 3
CURNT	0.86	0.09	0.912	.249439E 3
TEMP	0.08	0.01	0.911	.251537E 3
TIME	0.32	0.03	0.911	.251268E 3
WF	0.53	-0.06	0.911	.250741E 3
WSTRP	1.74	-0.18	0.914	.243214E 3
DF	0.54	-0.06	0.911	.250717E 3

VAR NAME	T STAT	PART CORR	MULTIPLE CORRELATION	E S S
R1	1.35	-0.14	0.913	.244439E 3
RSTR	0.86	-0.09	0.912	.249429E 3
VOL	0.82	-0.09	0.912	.249645E 3
A	0.20	0.02	0.911	.251445E 3
R	0.94	0.10	0.912	.249061E 3
AI	0.53	-0.06	0.911	.250760E 3
RST1A	0.56	0.06	0.911	.250665E 3
RST1B	0.04	-0.00	0.911	.251551E 3
RST1C	0.41	-0.04	0.911	.251069E 3
RST2A	1.00	-0.11	0.912	.248716E 3
RST2B	1.08	0.11	0.912	.248286E 3
RST2C	0.75	0.08	0.912	.249962E 3
RST3A	1.37	-0.14	0.913	.246321E 3
RST3B	0.87	0.09	0.912	.249306E 3
RST3C	0.85	0.09	0.912	.249512E 3
P1A	0.15	0.02	0.911	.251440E 3
P1B	0.29	0.03	0.911	.251314E 3
P1C	0.03	-0.00	0.911	.251553E 3
P2A	0.78	-0.08	0.912	.249816E 3
P2B	0.42	-0.04	0.911	.251058E 3
P2C	0.08	0.01	0.911	.251536E 3
P3A	0.35	-0.04	0.911	.251210E 3
P3B	0.80	-0.08	0.912	.249749E 3
P3C	0.00		0.911	.251555E 3
RLT1A	0.80	0.09	0.912	.249735E 3
RLT1C	0.00	0.00	0.911	.000000E 0
RLT2B	1.58	0.17	0.914	.244615E 3
RLT2C	0.14	-0.01	0.911	.251502E 3
RLT3A	0.84	0.09	0.912	.249537E 3

VAR NAME	T STAT	PART CORR	MULTIPLE CORRELATION	E S S
RLT3B	0.82	0.09	0.912	.249644E 3
RLT3C	0.85	-0.06	0.911	.250596E 3
YI1A	0.55	0.06	0.911	.250678E 3
YI1C	0.00	0.00	0.911	.000000E 0
YI2B	1.07	-0.11	0.912	.248310E 3
YI2C	0.90	-0.10	0.912	.249237E 3
YI3C	0.80	-0.09	0.912	.249719E 3
VF	0.40	-0.04	0.911	.251062E 3
VS	0.36	-0.04	0.911	.251192E 3

E.S.S. .251595E 3

RESIDUAL ERROR .168121E 1

MULT CORR 0.911

INTERCEPT TERM 196.4002292

REGRESSION ANALYSIS COVA DATA1 CUT OFF PARAMETER .100000E- 5

DEPENDENT VARIABLE RLT2B DEGREES OF FREEDOM 93

INDEPENDENT VARIABLES AT SIGNIFICANT LEVEL 5.00 %

V	CD	CURNT	TEMP	TIME	WF	WSTRP	DF	H1	H2	H3	HSTR	Z	VOL
A	R	YR	AI	RST1A	RST1B	RST1C	RST2A	RST2B	RST2C	RST3A	RST3B	RST3C	P1A
P1B	P1C	P2A	P2B	P2C	P3A	P3B	P3C	RLT1A	RLT1B	RLT1C	RLT2A	RLT2C	RLT3A
RLT3B	RLT3C	YI1A	YI1B	YI1C	YI2A	YI2B	YI2C	YI3A	YI3B	YI3C	VF	VS	

VARIABLES IN THE REGRESSION SET

VAR NAME	REGRESSION COEFF	STANDARD ERROR	CONFIDENCE INTERVAL	T STAT	PART CORR	MULTIPLE CORRELATION	E S S
RLT1A	0.3401764	.133064E 0	.263998E 0	2.56	0.26	0.702	.402653E 3
RLT2A	0.2495971	.797948E- 1	.158313E 0	2.88	0.29	0.695	.409706E 3
RLT2C	0.1939789	.504417E- 1	.100076E 0	3.05	0.30	0.692	.413911E 3
YI2A	2.1399217	.420734E 0	.834736E 0	5.09	-0.47	0.628	.466863E 3
YI2B	4.9129792	.526823E 0	.104522E 1	9.33	0.70	0.287	.728029E 3

VARIABLES NOT IN THE REGRESSION SET

VAR NAME	T STAT	PART CORR	MULTIPLE CORRELATION	E S S
V	0.48	0.05	0.726	.375266E 3
CD	0.99	-0.10	0.729	.372214E 3
CURNT	0.99	-0.10	0.729	.372222E 3
TEMP	1.17	-0.12	0.730	.370662E 3
TIME	0.64	0.07	0.727	.374583E 3
WF	0.59	-0.06	0.726	.374807E 3
WSTRP	0.13	0.01	0.725	.376151E 3
DF	0.61	-0.06	0.726	.374699E 3
H1	0.08	0.01	0.725	.376191E 3
H2	0.28	0.03	0.725	.375891E 3
H3	0.22	-0.02	0.725	.376023E 3
HSTR	0.35	-0.04	0.726	.375714E 3

VAR NAME	T STAT	PART CORR	MULTIPLE CORRELATION	F S S	
Z	0.63	-0.07	0.727	.3745892	3
VOL	0.25	-0.03	0.725	.3759516	3
A	1.40	0.14	0.732	.3684146	3
R	0.16	0.02	0.725	.3761088	3
YR	0.41	0.04	0.726	.3755296	3
AI	1.09	-0.10	0.737	.3621396	3
RST1A	0.65	0.07	0.727	.3745116	3
RST1B	0.49	0.05	0.726	.3752336	3
RST1C	0.27	-0.03	0.725	.3759086	3
RST2A	0.37	-0.04	0.726	.3756486	3
RST2B	0.10	-0.01	0.725	.3761776	3
RST2C	0.57	-0.06	0.726	.3748476	3
RST3A	0.71	-0.07	0.727	.3741756	3
RST3B	0.43	-0.04	0.726	.3754436	3
RST3C	0.90	-0.09	0.728	.3729366	3
P1A	0.24	0.02	0.725	.3759826	3
P1B	0.12	0.01	0.725	.3761566	3
P1C	0.14	0.01	0.725	.3761326	3
P2A	0.23	-0.02	0.725	.3759946	3
P2B	1.22	0.13	0.730	.3701926	3
P2C	0.77	-0.08	0.727	.3737946	3
P3A	0.26	-0.03	0.725	.3759296	3
P3B	0.53	0.06	0.726	.3750676	3
P3C	0.00		0.725	.3762156	3
RLT1B	1.09	-0.11	0.729	.3714096	3
RLT1C	0.00	0.00	0.725	.0000006	0
RLT3A	0.95	-0.10	0.728	.3725336	3
RLT3B	0.35	0.04	0.726	.3757256	3
RLT3C	0.85	-0.09	0.728	.3733176	3

VAR NAME	T STAT	PART CORR	MULTIPLE CORRELATION	E S S
YI1A	0.13	0.01	0.725	.376145E 3
YI1B	1.48	-0.15	0.733	.367516E 3
YI1C	0.00	0.00	0.725	.000000E 0
YI2C	1.71	-0.18	0.735	.364004E 3
YI3A	0.03	-0.00	0.725	.376210E 3
YI3B	0.05	0.01	0.725	.376202E 3
YI3C	0.06	-0.01	0.725	.376202E 3
VF	0.19	-0.02	0.725	.376061E 3
VS	0.25	0.03	0.725	.375958E 3

E.S.S. .376215E 3

RESIDUAL ERROR .201130E 1

MULT CORR 0.725

INTERCEPT TERM 49.6212326

REGRESSION ANALYSIS COVA DATA1 CUT OFF PARAMETER .100000E- 5

DEPENDENT VARIABLE RLT2C DEGREES OF FREEDOM 92

INDEPENDENT VARIABLES AT SIGNIFICANT LEVEL 5.00 %

V	CD	CURNT	TEMP	TIME	WF	WSTRP	DF	H1	H2	H3	HSTR	Z	VOL
A	R	YR	AI	RST1A	RST1B	RST1C	RST2A	RST2B	RST2C	RST3A	RST3B	RST3C	P1A
P1B	P1C	P2A	P2B	P2C	P3A	P3B	P3C	RLT1A	RLT1B	RLT1C	RLT2A	RLT2B	RLT3A
RLT3B	RLT3C	YI1A	YI1B	YI1C	YI2A	YI2B	YI2C	YI3A	YI3B	YI3C	VF	VS	

VARIABLES IN THE REGRESSION SET

VAR NAME	REGRESSION COEFF	STANDARD ERROR	CONFIDENCE INTERVAL	T STAT	PART CORR	MULTIPLE CORRELATION	E S S	
H1	1.1016951	.310077E 0	.615102E -0	3.81	0.37	0.739	.6429368	3
RST1C	0.6023102	.147294E 0	.292227E 0	4.09	0.39	0.744	.6562058	3
P1B	2.1003277	.795474E 0	.157822E 1	2.64	0.27	0.666	.5973558	3
P1C	7.7130400	.132404E 1	.2626858 1	5.83	0.52	0.745	.7601058	3
YI1A	1.9078808	.704240E 0	.139721E 1	2.79	-0.28	0.804	.6024068	3
YI2C	4.0484900	.106140E 1	.210593E 1	3.81	0.37	0.739	.6430808	3

VARIABLES NOT IN THE REGRESSION SET

VAR NAME	T STAT	PART CORR	MULTIPLE CORRELATION	E S S	
V	0.71	0.07	0.822	.5521918	3
CD	0.55	0.06	0.822	.5534078	3
CURNT	0.55	0.06	0.822	.5534138	3
TEMP	0.11	-0.01	0.821	.5551988	3
TIME	1.64	-0.17	0.827	.5593368	3
WF	1.41	-0.15	0.826	.5434348	3
WSTRP	0.43	0.05	0.822	.5541348	3
DF	1.42	-0.15	0.826	.5432198	3
H2	1.15	-0.12	0.824	.5473038	3
H3	1.32	-0.14	0.825	.5448628	3
HSTR	1.08	-0.11	0.824	.5482738	3

NAME	T STAT	PART CORR	MULTIPLE CORRELATION	F S S	
Z	1.01	0.10	0.823	.5491698	3
VOL	0.86	0.09	0.823	.5506411	3
A	0.07	-0.01	0.821	.5552458	3
R	0.43	-0.04	0.822	.5541548	3
YR	1.60	0.17	0.827	.5400008	3
AI	0.44	0.05	0.822	.5540648	3
RST1A	0.56	0.06	0.822	.5532618	3
RST1B	0.22	0.02	0.821	.5549858	3
RST2A	0.21	-0.02	0.821	.5550218	3
RST2B	0.71	0.07	0.822	.5522298	3
RST2C	0.31	0.03	0.822	.5547008	3
RST3A	0.23	-0.02	0.821	.5549668	3
RST3B	0.16	0.02	0.821	.5551248	3
RST3C	0.41	0.04	0.822	.5542478	3
P1A	1.10	0.11	0.824	.5480428	3
P2A	0.87	-0.09	0.823	.5506718	3
P2B	1.16	0.12	0.824	.5471598	3
P2C	0.00	-0.00	0.821	.5552788	3
P3A	0.05	-0.01	0.821	.5552638	3
P3B	0.34	-0.04	0.822	.5545598	3
P3C	0.00		0.821	.5552788	3
RLT1A	0.11	-0.01	0.821	.5552088	3
RLT1B	0.92	0.10	0.823	.5502068	3
RLT1C	0.00	0.00	0.821	.0000008	0
RLT2A	1.33	0.14	0.825	.5446348	3
RLT2B	0.93	0.10	0.823	.5500588	3
RLT3A	0.01	0.00	0.821	.5552778	3
RLT3B	0.01	0.00	0.821	.5552778	3
RLT3C	0.10	-0.02	0.821	.5550628	3

NAME	T STAT	PART CORR	MULTIPLE CORRELATION	E S S	
YI1B	1.12	0.12	0.824	.547747E	3
YI1C	0.00	0.00	0.821	.000000E	0
YI2A	0.20	0.02	0.821	.555028E	3
YI2B	1.43	-0.15	0.826	.542242E	3
YI3A	0.20	0.02	0.821	.555029E	3
YI3B	0.24	-0.03	0.821	.554923E	3
YI3C	0.28	-0.03	0.821	.554805E	3
VF	0.12	-0.01	0.821	.555195E	3
VS	0.00	0.00	0.821	.555276E	3

```
E.S.S.           .555278E  3
RESIDUAL ERROR   .245675E  1
MULT CORR        0.821
INTERCEPT TERM        212.3551978
GET
```

```
NUMBER OF PAGES   24
```

DATA: CUT OFF PARAMETER .100000E- 5

DEPENDENT VARIABLE RLT3A DEGREES OF FREEDOM 59

INDEPENDENT VARIABLES AT SIGNIFICANT LEVEL 5.00 %

V	CD	CURNT	TEMP	TIME	WF	USTRP	DF	H1	H2	H3	HSTR	Z	VOL
A	R	YR	AI	RST1A	RST1B	RST1C	RST2A	RST2B	RST2C	RSTXA	RST3B	RST3C	P1A
P1B	P1C	P2A	P2B	P2C	P3A	P3B	P3C	RLT1A	RLT1B	RLT1C	RLT2A	RLT2B	RLT2C
RLT3B	RLT3C	YI1A	YI1B	YI1C	YI2A	YI2B	YI2C	YI3A	YI3B	YI3C	VF	VS	

VARIABLES IN THE REGRESSION SET

VAR NAME	REGRESSION COEFF	STANDARD ERROR	CONFIDENCE INTERVAL	T STAT	PART CORR	MULTIPLE CORRELATION	E S S
RST1A	0.4421799	.124155E 0	.247069E 0	3.40	0.34	0.926	.477529E 3
RST2C	0.5485010	.190970E 0	.380046E 0	2.87	0.29	0.929	.461742E 3
RST3A	1.8342395	.221755E 0	.441289E 0	8.27	0.66	0.882	.747511E 3
RST3B	0.6053439	.130973E 0	.260636E 0	5.03	0.47	0.915	.545166E 3
P3A	-4.3436024	.634523E 0	.126270E 1	6.81	-0.59	0.899	.643097E 3
P3B	-4.0391916	.690863E 0	.137442E 1	5.88	-0.53	0.909	.586647E 3
RLT3C	0.5554683	.692110E- 1	.137731E 0	8.03	0.65	0.835	.728505E 3
YI3A	11.6144777	.902025E 0	.179503E 1	12.88	0.81	0.800	.120989E 4
YI3B	-1.8658007	.746155E 0	.148486E 1	2.50	-0.26	0.930	.452314E 3

VARIABLES NOT IN THE REGRESSION SET

VAR NAME	T STAT	PART CORR	MULTIPLE CORRELATION	E S S
V	0.18	0.02	0.935	.422472E 3
CD	0.72	0.10	0.936	.418558E 3
CURNT	0.93	0.10	0.936	.418547E 3
TEMP	1.06	0.11	0.936	.417343E 3
TIME	0.12	0.01	0.935	.422556E 3
WF	0.02	0.00	0.935	.422620E 3
USTRP	1.88	0.20	0.938	.406381E 3
DF	0.02	0.00	0.935	.422620E 3

NAME		CORR	CORRELATION	
H1	0.27	0.03	0.935	.422273E 3
H2	0.29	0.03	0.935	.422214E 3
H3	0.24	-0.03	0.935	.422336E 3
HSTR	0.22	-0.02	0.935	.422383E 3
Z	1.76	0.18	0.937	.408266E 3
VOL	1.43	-0.15	0.937	.413071E 3
A	0.36	0.04	0.935	.421987E 3
R	1.09	0.11	0.936	.417033E 3
YR	0.56	-0.06	0.935	.421069E 3
AI	0.63	0.07	0.935	.420718E 3
RST1B	1.61	-0.17	0.937	.410519E 3
RST1C	0.77	-0.08	0.935	.419824E 3
RST2A	0.00	0.00	0.935	.422622E 3
RST2B	0.52	-0.06	0.935	.421339E 3
RST3C	0.01	-0.00	0.935	.422622E 3
P1A	1.92	-0.20	0.938	.405669E 3
P1B	0.37	-0.04	0.935	.421982E 3
P1C	0.16	0.02	0.935	.422409E 3
P2A	0.52	-0.06	0.935	.421322E 3
P2B	0.29	-0.03	0.935	.422214E 3
P2C	0.06	0.01	0.935	.422604E 3
P3C	0.00		0.935	.422622E 3
RLT1A	0.66	-0.07	0.935	.420530E 3
RLT1B	1.69	-0.18	0.937	.409284E 3
RLT1C	0.00	0.00	0.935	.000000E 0
RLT2A	1.56	0.16	0.937	.411275E 3
RLT2B	0.13	0.01	0.935	.422537E 3
RLT2C	0.42	-0.04	0.935	.421702E 3
RLT3B	0.49	0.05	0.935	.421469E 3

NAME	T STAT	PART CORR	MULTIPLE CORRELATION	E S S
YI1A	1.33	-0.14	0.936	.414261E 3
YI1B	0.51	-0.05	0.935	.421305E 3
YI1C	0.00	0.00	0.935	.000000E 0
YI2A	0.05	0.01	0.935	.422609E 3
YI2B	0.17	-0.02	0.935	.422476E 3
YI2C	0.23	-0.02	0.935	.422379E 3
YI3C	0.21	-0.02	0.935	.422402E 3
VF	0.10	0.01	0.935	.422572E 3
VS	0.89	-0.09	0.936	.418863E 3

E.S.S. .422622E 3

RESIDUAL ERROR .217912E 1

MULT CORR 0.935

INTERCEPT TERM 20.3412533

REGRESSION ANALYSIS , COVA , DATA1 CUT OFF PARAMETER .100000E- 5

DEPENDENT VARIABLE RLT3B DEGREES OF FREEDOM 85

INDEPENDENT VARIABLES AT SIGNIFICANT LEVEL 5.00 %

V	CD	CURNT	TEMP	TIME	WF	WSTRD	DF	H1	H2	H3	HSTR	Z	VOL
A	R	YR	AI	RST1A	RST1B	RST1C	RST2A	RST2B	RST2C	RST3A	RST3B	RST3C	P1A
P1B	P1C	P2A	P2B	P2C	P3A	P3B	P3C	RLT1A	RLT1B	RLT1C	RLT2A	RLT2B	RLT2C
RLT3A	RLT3C	YI1A	YI1B	YI1C	YI2A	YI2B	YI2C	YI3A	YI3B	YI3C	VF	VS	

VARIABLES IN THE REGRESSION SET

VAR NAME		REGRESSION COEFF	STANDARD ERROR	CONFIDENCE INTERVAL	T STAT	PART CORR	MULTIPLE CORRELATION	E S S
DF		0.1497832	.191682E- 1	.381447E- 1	6.77	0.60	0.925	.561341E 3
H1	-	0.9943805	.274719E 0	.546686E 0	3.62	-0.37	0.945	.433612E 3
Z	-	1.7033698	.717190E 0	.142721E 1	2.49	-0.26	0.949	.402396E 3
VOL		0.5279804	.403139E- 1	.921641E- 1	11.40	0.78	0.873	.960888E 3
RST1A	-	1.4712176	.291150E 0	.579389E 0	5.05	-0.49	0.937	.439706E 3
RST2A	-	0.4920046	.201345E 0	.400677E 0	2.45	-0.26	0.949	.401504E 3
RST3A	-	3.0020685	.438909E 0	.873422E 0	6.84	-0.60	0.924	.585590E 3
RST3B	-	0.7377426	.150650E 0	.299793E 0	4.90	-0.47	0.938	.482700E 3
P1A		2.0477303	.663983E 0	.132133E 1	3.08	0.32	0.947	.417410E 3
P3A	-	3.1350700	.729514E 0	.145173E 1	4.30	-0.43	0.941	.457626E 3
P3B		2.7673240	.782960E 0	.155809E 1	3.56	0.36	0.945	.431679E 3
RLT1B	-	0.4921161	.174871E 0	.347994E 0	2.81	-0.30	0.948	.410229E 3
RLT3A		0.3945489	.692344E- 1	.137776E 0	5.70	0.53	0.933	.521028E 3
YI3B		18.5152770	.773234E 0	.153873E 1	23.95	0.93	0.514	.296158E 4
YI3C	-	23.5060400	.100521E 1	.331378E 1	14.12	-0.84	0.827	.127356E 4

VAR NAME	T STAT	PART CORR	MULTIPLE CORRELATION	F.S.S
V	0.72	0.08	0.953	.372135E 3
CD	0.86	-0.09	0.953	.371170E 3
CURNT	0.86	-0.09	0.953	.371133E 3
TEMP	0.43	-0.05	0.952	.373636E 3
TIME	1.87	-0.20	0.954	.359178E 3
WF	0.40	-0.04	0.952	.373781E 3
WSTRP	0.82	-0.09	0.953	.371474E 3
H2	0.49	0.05	0.952	.373414E 3
H3	0.13	0.01	0.952	.374230E 3
HSTR	0.86	-0.09	0.953	.371128E 3
A	1.06	0.12	0.953	.369423E 3
R	1.40	0.15	0.953	.365771E 3
YR-L	0.57	-0.06	0.953	.373034E 3
AI	0.76	-0.08	0.953	.371883E 3
RST1B	0.10	-0.02	0.952	.374335E 3
RST1C	0.73	0.08	0.953	.372049E 3
RST2B	0.77	0.09	0.953	.371780E 3
RST2C	0.66	0.07	0.953	.372514E 3
RST3C	0.71	0.08	0.953	.372239E 3
P1B	0.61	0.07	0.953	.372786E 3
P1C	0.36	-0.04	0.952	.373890E 3
P2A	1.81	-0.20	0.954	.360105E 3
P2B	0.87	-0.10	0.953	.371107E 3
P2C	1.33	0.15	0.953	.366577E 3
P3C	0.00		0.952	.374406E 3
RLT1A	0.53	0.06	0.953	.373105E 3
RLT1C	0.00	0.00	0.952	.000000E 0
RLT2A	0.24	-0.03	0.952	.374296E 3

RLT2B	0.12	0.01	0.952	.374429E 3
RLT2C	0.01	-0.00	0.952	.374496E 3
RLT3C	0.27	0.03	0.952	.374159E 3
YI1A	1.57	0.17	0.954	.363612E 3
YI1B	0.62	-0.07	0.953	.372771E 3
YI1C	0.00	0.00	0.952	.000000E 0
YI2A	0.00	-0.00	0.952	.374496E 3
YI2B	0.56	-0.04	0.953	.373049E 3
YI2C	0.33	0.04	0.952	.373901E 3
YI3A	0.15	0.02	0.952	.374396E 3
VF	0.30	-0.03	0.952	.374076E 3
VS	0.42	-0.05	0.952	.373700E 3

E.S.S. .374496E 3

RESIDUAL ERROR .212415E 1

MULT CORR 0.952

INTERCEPT TERM = 22.1541573

REGRESSION ANALYSIS COVA DATA1 CUT OFF PARAMETER .100000E- 5

DEPENDENT VARIABLE RLT3C DEGREES OF FREEDOM 89

INDEPENDENT VARIABLES AT SIGNIFICANT LEVEL 5.00 %

V	CD	CURNT	TEMP	TIME	WF	WSTRP	DF	H1	H2	H3	HSTR	Z	VOL	
A	R	YR	AI	RST1A	RST1B	RST1C	RST2A	RST2B	RST2C	RST3A	RST3B	RST3C	P1A	
P1B	P1C	P2A	P2B	P2C	P3A	P3B	P3C	RLT1A	RLT1B	RLT1C	RLT2A	RLT2B	RLT2C	
RLT3A	RLT3B	YI1A	YI1B	YI1C	YI2A	YI2B	YI2C	YI3A	YI3B	YI3C	VF	VS		

VARIABLES IN THE REGRESSION SET

VAR NAME		REGRESSION COEFF	STANDARD ERROR	CONFIDENCE INTERVAL	T STAT	PART CORR	MULTIPLE CORRELATION	E S S
CURNT		0.2517590	.619029E- 1	.143186E 0	3.74	0.37	0.926	.257790E 3
H3	-	0.0763306	.150760E- 1	.300025E- 1	5.06	-0.47	0.917	.266856E 3
RST2C	-	1.0092649	.133474E 0	.269590E 0	7.89	-0.64	0.809	.378606E 3
P3A		4.3063135	.436929E 0	.8726678 0	10.00	0.73	0.859	.473074E 3
RLT3A		0.2482042	.448124E- 1	.891746E- 1	5.60	0.48	0.917	.267608E 3
RLT3B		0.2409037	.455294E- 1	.906043E- 1	5.28	0.47	0.915	.262536E 3
YI3A	-	9.2080003	.613529E 0	.122490E 1	15.09	-0.85	0.748	.792406E 3
YI3B	-	3.0433127	.840833E 0	.168420E 1	3.64	-0.36	0.926	.255927E 3
YI3C		13.7100576	.938190E 0	.186701E 1	14.61	0.84	0.761	.757001E 3

VARIABLES NOT IN THE REGRESSION SET

VAR NAME	T STAT	PART CORR	MULTIPLE CORRELATION	E S S
V	0.06	0.01	0.936	.222706E 3
CD	1.46	-0.15	0.938	.217481E 3
TEMP	0.04	-0.00	0.936	.222710E 3
TIME	1.08	0.11	0.937	.219785E 3
WF	0.15	0.02	0.936	.222654E 3
WSTRP	0.16	-0.02	0.936	.222646E 3
DF	0.15	0.02	0.936	.222654E 3
H1	0.15	0.02	0.936	.222653E 3

VOL	0.42	-0.04	0.936	.222271E 3
A	0.18	0.02	0.936	.222634E 3
R	0.75	-0.08	0.937	.221315E 3
YR	0.94	-0.10	0.937	.220517E 3
AI	0.75	0.08	0.937	.221315E 3
RST1A	1.43	-0.15	0.938	.217610E 3
RST1B	1.09	-0.12	0.937	.219732E 3
RST1C	0.08	0.01	0.936	.222697E 3
RST2A	0.39	-0.04	0.936	.222535E 3
RST2B	0.41	-0.04	0.936	.222494E 3
RST3A	0.92	-0.10	0.937	.220601E 3
RST3B	1.40	0.15	0.938	.217643E 3
RST3C	1.19	0.13	0.937	.219167E 3
P1A	0.69	-0.07	0.937	.221507E 3
P1B	0.33	-0.03	0.936	.222443E 3
P1C	0.13	-0.01	0.936	.222670E 3
P2A	0.33	-0.04	0.936	.222434E 3
P2B	0.12	-0.01	0.936	.222679E 3
P2C	0.10	-0.01	0.936	.222687E 3
P3B	0.01	-0.00	0.936	.222713E 3
P3C	0.00		0.936	.222714E 3
RLT1A	0.79	-0.08	0.937	.221151E 3
RLT1B	0.86	-0.09	0.937	.220857E 3
RLT1C	0.00	0.00	0.936	.000000E 0
RLT2A	1.62	-0.17	0.938	.216300E 3
RLT2B	0.63	-0.07	0.936	.221664E 3

VAR NAME	T STAT	PART CORR	MULTIPLE CORRELATION	S S	
RLT2C	0.21	-0.02	0.936	.222663E	3
YI1A	0.60	-0.06	0.936	.221801E	3
YI1B	0.36	-0.04	0.936	.222302E	3
YI1C	0.00	0.00	0.936	.000000E	0
YI2A	1.79	-0.19	0.938	.214684E	3
YI2B	0.42	0.05	0.936	.222259E	3
YI2C	0.06	0.01	0.936	.222705E	3
VF	0.17	-0.02	0.936	.222640E	3
VS	0.70	0.07	0.937	.221481E	3

E.S.S. .222714E 3

RESIDUAL ERROR .158190E 1

MULT CORR 0.936

INTERCEPT TERM 84.5933506

DEPENDENT VARIABLE P1A DEGREES OF FREEDOM 95

INDEPENDENT VARIABLES AT SIGNIFICANT LEVEL 5.00 %

V	CD	CURNT	TEMP	TIME	WF	WSTRP	DF	H1	H2	H3	HSTR	Z	VOL
A	R	YR	AI	RST1A	RST1B	RST1C	RST2A	RST2B	RST2C	RST3A	RST3B	RST3C	P1B
P1C	P2A	P2B	P2C	P3A	P3B	P3C	RLT1A	RLT1B	RLT1C	RLT2A	RLT2B	RLT2C	RLT3A
RLT3B	RLT3C	YI1A	YI1B	YI1C	YI2A	YI2B	YI2C	YI3A	YI3B	YI3C	VF	VS	

VARIABLES IN THE REGRESSION SET

VAR NAME	REGRESSION COEFF	STANDARD ERROR	CONFIDENCE INTERVAL	T STAT	PART CORR	MULTIPLE CORRELATION	E S S
TEMP	0,0078858	,324865E- 2	,644531E- 2	2,43	-0,24	0,903	,115319E 2
RST1A	0,3031602	,161074E- 1	,3592518- 1	20,06	0,90	0,297	,568341E 2
RLT3A	0,0433230	,651495E- 2	,129257E- 1	3,58	-0,34	0,906	,123232E 2

VARIABLES NOT IN THE REGRESSION SET

VAR NAME	T STAT	PART CORR	MULTIPLE CORRELATION	E S S
V	1,10	0,11	0,910	,107216E 2
CD	0,06	0,01	0,909	,108580E 2
CURNT	0,06	0,01	0,909	,108580E 2
TIME	0,28	-0,03	0,909	,108405E 2
WF	1,71	-0,17	0,912	,105305E 2
WSTRP	1,67	0,17	0,911	,105460E 2
DF	1,71	-0,17	0,912	,105298E 2
H1	0,01	0,00	0,909	,108304E 2
H2	0,79	-0,08	0,909	,107876E 2
H3	0,07	-0,01	0,909	,108579E 2
HSTR	1,06	-0,11	0,910	,107304E 2
Z	0,71	0,07	0,909	,107968E 2
VOL	1,47	-0,15	0,911	,106148E 2
A	0,49	-0,05	0,909	,108310E 2

NAME	T STAT	PART CORR	MULTIPLE CORRELATION	R S S	
R	0.56	0.06	0.909	.108299E	2
YR	1.86	0.19	0.912	.104741E	2
AI	1.20	0.12	0.910	.106953E	2
RSY1B	0.60	0.06	0.909	.108173E	2
RSY1C	0.41	0.04	0.909	.108395E	2
RSY2A	0.32	0.03	0.909	.108466E	2
RSY2B	1.54	-0.16	0.911	.105926E	2
RSY2C	1.26	-0.13	0.910	.106785E	2
RSY3A	1.68	-0.17	0.912	.105432E	2
RSY3B	0.74	0.08	0.909	.107952E	2
RSY3C	0.95	-0.10	0.910	.107549E	2
P1B	1.29	-0.13	0.910	.106683E	2
P1C	0.22	0.02	0.909	.108529E	2
P2A	0.76	0.08	0.909	.107920E	2
P2B	1.01	0.10	0.910	.107422E	2
P2C	0.79	-0.08	0.909	.107860E	2
P3A	1.47	-0.15	0.911	.106136E	2
P3B	1.42	-0.15	0.911	.106291E	2
P3C	0.00		0.909	.108584E	2
RLY1A	0.34	-0.04	0.909	.108451E	2
RLY1B	0.34	-0.04	0.909	.108447E	2
RLY1C	0.00	0.00	0.909	.000000E	0
RLY2A	0.93	-0.10	0.910	.107600E	2
RLY2B	0.70	-0.07	0.909	.108018E	2
RLY2C	0.57	0.06	0.909	.108211E	2
RLY3B	0.25	0.03	0.909	.108514E	2
RLY3C	0.22	0.02	0.909	.108528E	2
YI1A	0.52	0.05	0.909	.108278E	2
YI1B	0.09	-0.01	0.909	.108575E	2

VAR NAME	T STAT	PART CORR	MULTIPLE CORRELATION	E S S
YI1C	0.00	0.00	0.909	,000000E 0
YI2A	0.05	-0.01	0.909	,108581E 2
YI2B	0.53	0.05	0.909	,108242E 2
YI2C	0.08	0.01	0.909	,108577E 2
YI3A	0.56	-0.06	0.909	,108228E 2
YI3B	0.25	-0.03	0.909	,108510E 2
YI3C	0.71	-0.07	0.909	,108009E 2
VF	0.08	-0.01	0.909	,108577E 2
VS	0.94	0.10	0.910	,107577E 2

E.S.S. ,108584E 2

RESIDUAL ERROR ,358081E 0

MULT CORR 0.909

INTERCEPT TERM = 20.0370343

REGRESSION ANALYSIS' COVA DATA1 CUT OFF PARAMETER ,1OUGOVEM #

DEPENDENT VARIABLE P1B DEGREES OF FREEDOM 94

INDEPENDENT VARIABLES AT SIGNIFICANT LEVEL 5,00 %

V	CD	CURNT	TEMP	TIME	WF	WSTRP	DF	H1	H2	H3	HSTP	Z	VOL
A	R	YR	AI	RST1A	RST1B	RST1C	RST2A	RST2B	RST2C	RST3A	RST3B	RST3C	P1A
P1C	P2A	P2B	P2C	P3A	P3B	P3C	RLT1A	RLT1B	RLT1C	RLY2A	RLT2B	RLT2C	RLT3A
RLT3B	RLT3C	YI1A	YI1B	YI1C	YI2A	YI2B	YI2C	YI3A	YI3B	YI3C	VP	VS	

VARIABLES IN THE REGRESSION SET

VAR NAME		REGRESSION COEFF	STANDARD ERROR	CONFIDENCE INTERVAL	T STAT	PART CORR	MULTIPLE CORRELATION	E S S
P1C	=	0,8472253	,131004E 0	,259920E 0	6,47	-0,55	0,521	,993733E 1
RLT1A		0,1281565	,227887E- 1	,452128E- 1	5,62	0,50	0,571	,919135E 1
RLT2C		0,0366153	,749834E- 2	,148767E- 1	4,88	0,45	0,607	,802205E 1
YI1A	=	0,2129636	,104817E 0	,207957E 0	2,03	-0,21	0,688	,717948E 1

VARIABLES NOT IN THE REGRESSION SET

VAR NAME	T STAT	PART CORR	MULTIPLE CORRELATION	E S S
V	1,17	-0,12	0,709	,677686E 1
CD	0,07	0,01	0,704	,687713F 1
CURNT	0,07	0,01	0,704	,687713E 1
TEMP	1,77	-0,18	0,716	,665245E 1
TIME	0,08	0,01	0,704	,687645F 1
WF	0,22	-0,07	0,704	,687403E 1
WSTRP	0,86	0,09	0,707	,682317F 1
DF	0,21	-0,02	0,704	,687411E 1
H1	0,27	0,03	0,705	,687224E 1
H2	0,45	-0,05	0,705	,686264E 1
H3	0,59	-0,06	0,706	,685186E 1
HSTR	0,25	-0,03	0,704	,687284E 1
Z	1,09	-0,11	0,709	,679145E 1

NAME	T STAT	PART CORR	MULTIPLE CORRELATION	E S S	
VOL	0.51	-0.05	0.705	.685790E	1
A	0.21	-0.02	0.704	.687408E	1
R	0.57	0.06	0.706	.685317E	1
YR	0.31	-0.03	0.705	.687022E	1
AI	0.31	0.03	0.705	.687047E	1
RST1A	0.36	0.04	0.705	.686774E	1
RST1B	0.29	0.03	0.705	.687122E	1
RST1C	1.70	0.17	0.715	.667067E	1
RST2A	0.28	0.03	0.705	.687169E	1
RST2B	0.11	-0.01	0.704	.687649E	1
RST2C	0.12	0.01	0.704	.687699E	1
RST3A	0.17	-0.02	0.704	.687527E	1
RST3B	0.37	-0.04	0.705	.686741E	1
RST3C	0.11	0.01	0.704	.687661E	1
P1A	0.16	-0.02	0.704	.687558E	1
P2A	0.50	0.05	0.705	.685885E	1
P2B	0.13	-0.01	0.704	.687617E	1
P2C	0.00	0.00	0.704	.687746E	1
P3A	0.41	-0.04	0.705	.686505E	1
P3B	0.74	-0.08	0.706	.683714E	1
P3C	0.00		0.704	.687746E	1
RLT1B	0.66	-0.07	0.706	.684563E	1
RLT1C	0.00	0.00	0.704	.000000E	0
RLT2A	0.60	-0.06	0.706	.685197E	1
RLT2B	0.09	0.01	0.704	.687689E	1
RLT3A	0.02	0.00	0.704	.687744E	1
RLT3B	0.08	0.01	0.704	.687700E	1
RLT3C	0.12	0.01	0.704	.687641E	1
Y11B	0.14	-0.01	0.704	.687597E	1

NAME	PART CORR	MULTIPLE CORRELATION	E.S.S.
YI1C	0.00	0.704	.000000E 0
YI2A	0.17	-0.02 0.704	.687528E 1
YI2B	0.02	-0.00 0.704	.687743E 1
YI2C	0.27	0.03 0.705	.687216E 1
YI3A	0.31	-0.03 0.705	.687051E 1
YI3B	0.29	0.03 0.705	.687154E 1
YI3C	0.00	0.00 0.704	.687746E 1
VF	0.23	0.02 0.704	.687366E 1
VS	0.69	0.07 0.706	.684264E 1

E.S.S. .687746E 1

RESIDUAL ERROR .270489E 0

MULT CORR 0.704

INTERCEPT TERM = 38.3456459

REGRESSION ANALYSIS COVA DATA1 CUT OFF PARAMETER .10000E- 5

DEPENDENT VARIABLE P1C DEGREES OF FREEDOM 94

INDEPENDENT VARIABLES AT SIGNIFICANT LEVEL 5.00 %

V	CD	CURNT	TEMP	TIME	WF	WSTRP	DF	H1	H2	H3	HSTR	Z	VOL
A	R	YR	AI	RSY1A	RST1B	RST1C	RST2A	RST2B	RST2C	RST3A	RST3B	RST3C	P1A
P1B	P2A	P2B	P2C	P3A	P3B	P3C	RLT1A	RLT1B	RLT1C	RLT2A	RLT2B	RLT2C	RLT3A
RLT3B	RLT3C	YI1A	YI1B	YI1C	YI2A	YI2B	YI2C	YI3A	YI3B	YI3C	VF	VS	

VARIABLES IN THE REGRESSION SET

VAR NAME	REGRESSION COEFF	STANDARD ERROR	CONFIDENCE INTERVAL	T STAT	PART CORR	MULTIPLE CORRELATION	E S S
RST1C =	0.0436079	.9357426- 2	.1856516- 1	4.66	-0.43	0.645	.2969546 1
P1B =	0.2476789	.5491196- 1	.1089456 0	4.51	-0.42	0.648	.2934296 1
RLT1A	0.0487460	.1130092- 1	.2242116- 1	2.54	0.25	0.701	.2578266 1
RLT2C	0.0957391	.4290036- 2	.8432066- 2	8.41	0.66	0.406	.4226866 1

VARIABLES NOT IN THE REGRESSION SET

VAR NAME	T STAT	PART CORR	MULTIPLE CORRELATION	E S S
V	0.47	-0.05	0.724	.2406606 1
CD	0.01	0.00	0.724	.2412216 1
CURNT	0.01	0.00	0.724	.2412216 1
TEMP	0.57	-0.06	0.725	.2403756 1
TIME	0.02	0.00	0.724	.2412216 1
WF	0.12	-0.01	0.724	.2411656 1
WSTRP	0.19	0.02	0.724	.2411296 1
DF	0.11	-0.01	0.724	.2411886 1
H1	0.04	0.00	0.724	.2412176 1
H2	0.33	-0.03	0.724	.2409406 1
H3	0.23	-0.02	0.724	.2410886 1
HSTR	0.19	-0.02	0.724	.2411276 1
Z	0.79	-0.08	0.726	.2396096 1

VAR NAME	T STAT	PART CORR	MULTIPLE CORRELATION	F S S	
VOL	0.36	-0.04	0.724	.2408656	1
A	0.37	-0.04	0.724	.2408656	1
R	0.49	0.05	0.724	.2406066	1
YR	0.34	-0.03	0.724	.2409268	1
AI	0.43	0.04	0.724	.2407548	1
RST1A	0.30	-0.03	0.724	.2409848	1
RST1B	0.26	0.03	0.724	.2410438	1
RST2A	0.26	-0.03	0.724	.2410168	1
RST2B	0.08	-0.01	0.724	.2412038	1
RST2C	0.06	0.01	0.724	.2412138	1
RST3A	0.13	-0.01	0.724	.2411798	1
RST3B	0.04	-0.00	0.724	.2412188	1
RST3C	0.05	0.01	0.724	.2412148	1
P1A	0.51	-0.05	0.724	.2405598	1
P2A	0.02	0.00	0.724	.2412218	1
P2B	0.00	-0.00	0.724	.2412228	1
P2C	0.00	0.00	0.724	.2412228	1
P3A	0.25	-0.03	0.724	.2410578	1
P3B	0.18	-0.02	0.724	.2411378	1
P3C	0.00		0.724	.2412228	1
RLT1B	0.51	-0.05	0.725	.2405568	1
RLT1C	0.00	0.00	0.724	.0000008	0
RLY2A	0.40	-0.04	0.724	.2406818	1
RLY2B	0.33	-0.03	0.724	.2409418	1
RLY3A	0.01	0.00	0.724	.2412218	1
RLY3B	0.06	0.01	0.724	.2412148	1
RLY3C	0.06	0.01	0.724	.2412138	1
YI1A	0.36	-0.04	0.724	.2408048	1
YI1B	0.45	-0.05	0.724	.2407018	1

VAR NAME	T STAT	PART CORR	MULTIPLE CORRELATION	F S S
Y11C	0.00	0.00	0.724	.000000E 0
Y12A	0.26	0.03	0.724	.241053E 1
Y12B	0.20	-0.02	0.724	.241116E 1
Y12C	0.56	0.06	0.725	.240345E 1
Y13A	0.13	-0.01	0.724	.241178E 1
Y13B	0.05	0.01	0.724	.241214E 1
Y13C	0.00	0.00	0.724	.241222E 1
VF	0.06	0.01	0.724	.241211E 1
VS	0.35	0.04	0.724	.240906E 1

E.S.S. .241222E 1

RESIDUAL ERROR .1601938E 0

MULT CORR 0.724

INTERCEPT TERM = 23.0917295

GET

NUMBER OF PAGES 24

DEPENDENT VARIABLE P2A DEGREES OF FREEDOM 87

INDEPENDENT VARIABLES AT SIGNIFICANT LEVEL 5.00 %

V	CD	CURNT	TEMP	TIME	WF	WSTRP	DF	H1	H2	H3	HSTR	Z	VOL
A	R	YR	AI	RST1A	RST1B	RST1C	RST2A	RST2B	RST2C	RST3A	RST3B	RST3C	P1A
P1B	P1C	P2B	P2C	P3A	P3B	P3C	RLT1A	RLT1B	RLT1C	RLT2A	RLT2B	RLT2C	RLT3A
RLT3B	RLT3C	YI1A	YI1B	YI1C	YI2A	YI2B	YI2C	YI3A	YI3B	YI3C	VF	VS	

VARIABLES IN THE REGRESSION SET

VAR NAME	REGRESSION COEFF	STANDARD ERROR	CONFIDENCE INTERVAL	T STAT	PART CORR	MULTIPLE CORRELATION	F S S
CD	0.0383207	.124157E- 1	.247073E- 1	3.09	0.31	0.942	.177819E 2
TIME	0.0000318	.688482E- 5	.157008E- 4	4.62	0.44	0.934	.199588E 2
HS	0.0219704	.562140E- 2	.111867E- 1	3.91	0.39	0.938	.168409E 2
Z -	0.6564686	.133902E 0	.2664658 0	4.90	-0.47	0.933	.204548E 2
A -	0.0445046	.144660E- 1	.287685E- 1	3.03	-0.31	0.942	.177704E 2
RST2A	0.6779271	.442810E- 1	.841392E- 1	16.03	0.86	0.773	.633805E 2
P1A	0.1439031	.628477E- 1	.1250675 0	2.61	0.27	0.943	.172709E 2
P3B -	0.3209476	.126152E 0	.2510435 0	2.54	-0.26	0.944	.172143E 2
RLT2A -	0.0417320	.198035E- 1	.3940895- 1	2.11	-0.22	0.945	.168450E 2
YI2A	0.5288230	.907130E- 1	.1964405 0	5.86	0.52	0.926	.219307E 2
VS -	0.0165902	.624444E- 2	.1242645- 1	2.66	-0.27	0.943	.173273E 2

VARIABLES NOT IN THE REGRESSION SET

VAR NAME	T STAT	PART CORR	MULTIPLE CORRELATION	F S S
V	0.08	0.01	0.948	.160259E 2
CURNT	0.06	-0.01	0.948	.160264E 2
TEMP	0.01	-0.00	0.948	.160249E 2
WF	0.32	0.03	0.948	.160084E 2
WSTRP	1.21	-0.13	0.949	.157576E 2
DF	0.33	0.04	0.948	.160064E 2

VAR NAME	STAT	PART CORR	MULTIPLE CORRELATION	F	
R1	0.50	-0.05	0.948	.159801E	2
R2	0.86	-0.09	0.948	.159806E	2
RSTR	0.37	0.04	0.948	.160015E	2
VOL	0.21	-0.02	0.948	.160191E	2
R	0.26	-0.03	0.948	.160146E	2
YR	0.53	0.06	0.948	.159656E	2
A1	0.53	-0.06	0.948	.159764E	2
RST1A	0.66	-0.07	0.948	.159453E	2
RST1B	0.51	-0.05	0.948	.159745E	2
RST1C	0.13	-0.01	0.948	.160240E	2
RST2B	0.80	-0.09	0.948	.159075E	2
RST2C	0.12	0.01	0.948	.160241E	2
RST3A	0.49	-0.05	0.948	.159821E	2
RST3B	0.44	-0.05	0.948	.159916E	2
RST3C	0.14	0.02	0.948	.160232E	2
P1A	0.52	0.06	0.948	.159762E	2
P1C	0.11	0.01	0.948	.160246E	2
P2B	0.49	-0.05	0.948	.159816E	2
P2C	0.09	-0.01	0.948	.160255E	2
P3A	0.33	-0.04	0.948	.160071E	2
P3C	0.00		0.948	.160270E	2
RLT1A	0.52	0.06	0.948	.159770E	2
RLT1B	0.10	-0.01	0.948	.160251E	2
RLT1C	0.00	0.00	0.948	.000000E	0
RLT2B	1.51	0.16	0.949	.156136E	2
RLT2C	0.47	0.05	0.948	.159859E	2
RLT3A	0.72	-0.08	0.948	.159307E	2
RLT3B	0.01	0.00	0.948	.160270E	2
RLT3C	0.45	0.05	0.948	.159886E	2

VAR NAME	T STAT	PART CORR	MULTIPLE CORRELATION	F S S
YI1A	0.30	0.03	0.948	.160165E 2
YI1B	0.19	0.02	0.948	.160264E 2
YI1C	0.00	0.00	0.948	.000000E 0
YI2B	1.35	0.14	0.949	.156936E 2
YI2C	1.53	0.17	0.949	.155755E 2
YI3A	0.67	-0.07	0.948	.159442E 2
YI3B	0.03	-0.00	0.948	.160269E 2
YI3C	0.12	0.01	0.948	.160242E 2
VF	0.27	0.03	0.948	.160136E 2

E.S.S. .160270E 2

RESIDUAL ERROR .429206E 0

MULT CORR 0.948

INTERCEPT TERM = 4.9902256

REGRESSION ANALYSIS , COVA SATAT CUT OFF PARAMETER ,1000000E 5

DEPENDENT VARIABLE P2C DEGREES OF FREEDOM 95

INDEPENDENT VARIABLES AT SIGNIFICANT LEVEL 5,00 %

V	CD	CURNT	TEMP	TIME	WF	WSTRP	DF	H1	H2	H3	HSTR	Z	VOL
A	R	YR	A1	RST1A	RST1B	RST1C	RST2A	RST2B	RST2C	RST3A	RST3B	RST3C	P1A
P1B	P1C	P2A	P2B	P3A	P3B	P3C	RLT1A	RLT1B	RLT1C	RLT2A	RLT2B	RLT2C	RLT3A
RLT3B	RLT3C	YI1A	YI1B	YI1C	YI2A	YI2B	YI2C	YI3A	YI3B	YI3C	VF	VS	

VARIABLES IN THE REGRESSION SET

VAR NAME		REGRESSION COEFF	STANDARD ERROR	CONFIDENCE INTERVAL	T STAT	PART CORR	MULTIPLE CORRELATION	E S S
TIME	=	0,0000015	,109362E- 6	,336914E- 6	8,91	-0,67	0.000	,229869E- 1
H2		0,0011179	,190470E- 3	,377908E- 3	5,87	0,52	0,568	,170547E- 1
RST1B	=	0,0000628	,231843E- 4	,459977E- 4	2,71	-0,27	0,643 .	,134835E- 1

VARIABLES NOT IN THE REGRESSION SET

VAR NAME	T STAT	PART CORR	MULTIPLE CORRELATION	E S S
V	0,52	-0,05	0.676	,124606E- 1
CD	1,13	-0,12	0,630	,123460E- 1
CURNT	1,13	-0,12	0,660	,123477E- 1
TEMP	0,29	-0,03	0,675	,125049E- 1
WF	0,27	-0,03	0,675	,125069E- 1
WSTRP	0,23	-0,03	0,675	,125055E- 1
DF	0,27	-0,03	0,675	,125069E- 1
H1	0,24	0,02	0,675	,125067E- 1
H3	0,01	0,00	0,675	,125163E- 1
HSTR	0,13	-0,01	0,675	,125140E- 1
Z	1,63	-0,17	0,686	,121714E- 1
VOL	1,76	-0,18	0,688	,121186E- 1
A	0,32	-0,03	0,675	,125031E- 1
R	1,35	0,14	0,683	,122775E- 1

VAR NAME	T STAT	PART CORR	MULTIPLE CORRELATION	E N S
YR	0.90	-0.09	0.676	.124601E- 1
AI	0.00	-0.00	0.675	.125163E- 1
RSY1A	0.07	0.01	0.675	.125156E- 1
RSY1C	0.36	0.04	0.675	.124989E- 1
RSY2A	0.41	-0.04	0.676	.124942E- 1
RSY2B	0.73	-0.08	0.677	.124445E- 1
RSY2C	0.42	-0.04	0.676	.124929E- 1
RSY3A	0.48	-0.05	0.676	.124856E- 1
RSY3B	1.43	-0.15	0.683	.123512E- 1
RSY3C	1.34	-0.14	0.682	.123820E- 1
P1A	0.03	-0.00	0.675	.125162E- 1
P1B	0.12	0.01	0.675	.125145E- 1
P1C	0.35	-0.04	0.675	.124906E- 1
P2A	0.28	-0.03	0.675	.125089E- 1
P2B	0.30	-0.03	0.675	.125045E- 1
P3A	0.16	-0.02	0.675	.125127E- 1
P3B	0.94	-0.10	0.679	.123969E- 1
P3C	0.00		0.675	.125165E- 1
RLY1A	0.50	-0.05	0.676	.124629E- 1
RLY1B	1.01	-0.10	0.679	.123817E- 1
RLY1C	0.00	0.00	0.675	.000000E 0
RLY2A	1.53	-0.16	0.685	.122102E- 1
RLY2B	0.13	-0.02	0.675	.125131E- 1
RLY2C	0.50	-0.05	0.676	.124827E- 1
RLY3A	0.62	-0.06	0.677	.124651E- 1
RLY3B	0.25	-0.03	0.675	.125077E- 1
RLY3C	0.16	-0.02	0.675	.125126E- 1
YI1A	0.03	-0.00	0.675	.125162E- 1
YI1B	0.11	0.01	0.675	.125147E- 1

VAR NAME	T TEST	PART CORR	MULTIPLE CORRELATION	E S S
Y11C	0.00	0.00	0.675	.3040A0E 0
Y12A	1.26	-0.20	0.691	.120233E- 1
Y12B	0.34	-0.04	0.675	.125008E- 1
Y12C	0.09	-0.01	0.675	.125151E- 1
Y13A	0.02	-0.00	0.675	.125162E- 1
Y13B	0.79	0.08	0.678	.124344E- 1
Y13C	0.02	0.00	0.675	.125162E- 1
VF	0.33	0.03	0.675	.125017E- 1
VS	0.04	-0.00	0.675	.125161E- 1

E.S.S. .125163E- 1

RESIDUAL ERROR .114763E- 1

MULT CORR 0.675

INTERCEPT TERM - 17.0119237

REGRESSION ANALYSIS , COVA DATA1 CUT OFF PARAMETER .1000000E-5

DEPENDENT VARIABLE P3A DEGREES OF FREEDOM 87

INDEPENDENT VARIABLES AT SIGNIFICANT LEVEL 5.00 %

V	CD	CURNT	TEMP	TIME	WF	WSTRP	DF	H1	H2	H3	HSTR	Z	VOL
A	R	YR	AI	RST1A	RST1B	RST1C	RST2A	RST2B	RST2C	RST3A	RST3B	RST3C	P1A
P1B	P1C	P2A	P2B	P2C	P3B	P3C	RLT1A	RLT1B	RLT1C	RLT2A	RLT2B	RLT2C	RLT3A
RLT3B	RLT3C	YI1A	YI1B	YI1C	YI2A	YI2B	YI2C	YI3A	YI3B	YI3C	VF	VS	

VARIABLES IN THE REGRESSION SET

VAR NAME	REGRESSION COEFF	STANDARD ERROR	CONFIDENCE INTERVAL	T STAT	PART CORR	MULTIPLE CORRELATION	E S S	
CURNT	= 0.0315721	.889504E- 2	.177011E- 1	3.55	-0.36	0.903	.458362E	1
H2	0.0120769	.307501E- 2	.612523E- 2	3.92	0.39	0.900	.471252E	1
Z	= 0.2069230	.666164E- 1	.132566E 0	3.11	-0.32	0.906	.444867E	1
RST2B	0.0592534	.914709E- 2	.181629E- 1	6.49	0.57	0.873	.594373E	1
RST3A	0.2021521	.262158E- 1	.521694E- 1	7.71	0.64	0.854	.674059E	1
RLT3A	= 0.0917824	.769623E- 2	.153155E- 1	4.13	-0.40	0.899	.478888E	1
RLT3B	= 0.0486020	.659703E- 2	.126107E- 1	4.51	-0.44	0.895	.494157E	1
RLT3C	0.0934080	.108268E- 1	.215452E- 1	7.70	0.64	0.854	.673547E	1
YI3A	1.0065575	.115409E 0	.229646E 0	8.74	0.68	0.836	.751933E	1
YI3B	0.4096826	.124870E 0	.248490E 0	3.28	0.33	0.909	.449942E	1
YI3C	= 1.2472766	.193743E 0	.385540E 0	6.44	-0.56	0.870	.603576E	1

VARIABLES NOT IN THE REGRESSION SET

VAR NAME	T STAT	PART CORR	MULTIPLE CORRELATION	E S S	
V	0.85	0.09	0.917	.397091E	1
CD	1.20	0.13	0.916	.393828E	1
TEMP	0.42	0.05	0.916	.399571E	1
TIME	0.91	-0.10	0.917	.396551E	1
WF	0.04	-0.00	0.916	.400303E	1
WSTRP	0.11	0.01	0.916	.400342E	1

VAR NAME	T STAT	PART CORR	PARTIAL CORRELATION	P
DF	0.01	-0.00	0.916	.4004011E 1
R1	1.18	-0.13	0.918	.3939835E 1
R3	0.57	0.06	0.916	.3998919E 1
RSTR	0.91	-0.10	0.917	.3965746E 1
VOL	0.52	0.06	0.916	.3991596E 1
A	0.43	-0.05	0.916	.3995335E 1
R	0.52	-0.06	0.916	.3991238E 1
VR	0.26	-0.03	0.916	.4000818E 1
AI	0.85	-0.09	0.917	.3970316E 1
RST1A	0.43	-0.05	0.916	.3995465E 1
RST1B	1.68	-0.18	0.919	.3877177E 1
RST1C	0.63	-0.07	0.917	.3985681E 1
RST2A	0.80	0.09	0.917	.3974346E 1
RST2C	1.31	0.14	0.918	.3926228E 1
RST3B	1.87	-0.20	0.920	.3848816E 1
RST3C	1.70	0.18	0.919	.3874577E 1
P1A	0.25	-0.03	0.916	.4001186E 1
P1B	0.06	0.01	0.916	.4000387E 1
P1C	0.21	0.02	0.916	.4001465E 1
P2A	0.76	0.08	0.917	.3977086E 1
P2B	0.43	-0.05	0.916	.3995529E 1
P2C	0.14	-0.02	0.916	.4000967E 1
P3B	1.43	-0.15	0.918	.3911548E 1
P3C	0.00		0.916	.4004402E 1
RLT1A	1.77	0.19	0.919	.3862792E 1
RLT1B	0.20	-0.02	0.916	.4002238E 1
RLT1C	0.00	0.00	0.916	.0000000E 0
RLT2A	0.20	0.02	0.916	.4002238E 1
RLT2B	1.03	0.11	0.917	.3955555E 1

VAR NAME	'T STAT	PART CORR	MULTIPLE CORRELATION	E S S	
RLT2C	0.10	-0.01	0.916	.400350E	1
YI1A	1.17	0.12	0.918	.394158E	1
YI1B	0.66	0.07	0.917	.398412E	1
YI1C	0.00	0.00	0.916	.000000E	0
YI2A	0.38	-0.04	0.916	.399729E	1
YI2B	0.23	0.03	0.916	.400148E	1
YI2C	0.01	0.00	0.916	.400401E	1
VF	0.32	-0.03	0.916	.399925E	1
VS	0.13	0.01	0.916	.400321E	1

E.S.S. .400401E 1

RESIDUAL ERROR .214550E 0

MULT CORR 0.916

INTERCEPT TERM = 13.1256248

REGRESSION ANALYSIS , COVA DAY=1 CUT OFF PARAMETER ,10000E-3

DEPENDENT VARIABLE P3B DEGREES OF FREEDOM 86

INDEPENDENT VARIABLES AT SIGNIFICANT LEVEL 5.00 %

V	CD	CURNT	TEMP	TIME	WF	WSTRP	DF	H1	H2	H3	RST1	Z	VOL
A	R	YR	AI	RST1A	RST1B	RST1C	RST2A	RST2B	RST2C	RST3A	RST3B	RST3C	P1A
P1B	P1C	P2A	P2B	P2C	P3A	P3C	RLT1A	RLT1B	RLT1C	RLT2A	RLT2B	RLT2C	RLT3A
RLT3B	RLT3C	YI1A	YI1B	YI1C	YI2A	YI2B	YI2C	YI3A	YI3B	YI3C	VF	VS	

VARIABLES IN THE REGRESSION SET

VAR NAME		REGRESSION COEFF	STANDARD ERROR	CONFIDENCE INTERVAL	T STAT	PART CORR	MULTIPLE CORRELATION	F S S
H1		0.0999578	.277474E- 1	.552173E- 1	2.16	0.23	0.859	.390896E 1
H2	-	0.0186569	.471103E- 2	.937496E- 2	3.96	-0.39	0.840	.438381E 1
H3		0.0156672	.328295E- 2	.653310E- 2	4.77	0.46	0.827	.468953E 1
YR	-	0.0520999	.642210E- 2	.127801E- 1	5.00	-0.47	0.824	.478473E 1
RST2B		0.0231779	.212830E- 1	.423543E- 1	2.97	0.30	0.852	.408763E 1
RST2C	-	0.1956364	.442457E- 1	.880489E- 1	3.52	-0.35	0.846	.424109E 1
RST3B		0.0315304	.117802E- 1	.234426E- 1	2.68	0.26	0.854	.401851E 1
RLT1B		0.0442883	.152970E- 1	.304423E- 1	2.90	0.30	0.852	.406901E 1
RLT3B		0.0807617	.624934E- 2	.124361E- 1	4.93	0.47	0.825	.475364E 1
RLT3C	-	0.0353619	.654303E- 2	.130224E- 1	5.40	-0.50	0.816	.496647E 1
YI3B	-	0.6822967	.124582E 0	.247918E 0	5.48	-0.51	0.815	.500077E 1
YI3C		1.3020254	.151802E 0	.302121E 0	8.58	0.68	0.733	.667857E 1

VARIABLES NOT IN THE REGRESSION SET

VAR NAME	T STAT	PART CORR	MULTIPLE CORRELATION	F S S
V	0.18	0.02	0.867	.370626E 1
CD	0.09	0.01	0.866	.370731E 1
CURNT	0.09	0.01	0.866	.370730E 1
TEMP	1.55	0.17	0.870	.366632E 1
TIME	0.24	0.03	0.867	.370510E 1

VAR NAME	T STAT	PART CORR	MULTIPLE CORRELATION		
WF	0.03	-0.00	0.866	.3707616	1
WSTRP	0.49	0.05	0.867	.3697159	1
DF	0.00	-0.00	0.866	.3707466	1
WSTR	0.00	-0.00	0.866	.3707466	1
Z	0.56	0.06	0.867	.3694208	1
VOL	1.61	0.17	0.871	.3596388	1
A	0.30	0.03	0.867	.3703826	1
R	0.59	-0.06	0.867	.3692356	1
AI	0.05	0.01	0.866	.3707546	1
RST1A	0.15	0.02	0.866	.3706716	1
RST1B	0.01	-0.00	0.866	.3707656	1
RST1C	0.59	-0.06	0.867	.3692286	1
RST2A	0.72	0.08	0.867	.3685126	1
RST3A	0.24	0.03	0.867	.3705146	1
RST3C	0.99	-0.11	0.868	.3665466	1
P1A	0.62	-0.07	0.867	.3690766	1
P1B	0.12	-0.01	0.866	.3707016	1
P1C	0.22	0.02	0.867	.3705576	1
P2A	0.29	0.03	0.867	.3703876	1
P2B	0.13	0.01	0.866	.3706836	1
P2C	0.46	-0.05	0.867	.3698496	1
P3A	0.36	0.04	0.867	.3701036	1
P3C	0.00		0.866	.3707466	1
RLY1A	0.10	0.01	0.866	.3707216	1
RLY1C	0.00	0.00	0.866	.0000006	0
RLY2A	0.24	-0.03	0.867	.3705106	1
RLY2B	0.13	0.01	0.866	.3706046	1
RLY2C	0.14	0.02	0.866	.3706766	1
RLY3A	0.76	-0.08	0.867	.3682586	1

VAR NAME			CORR	CORRELATION	
YI1A	1.42	-0.15	0.870	,3e2279E	1
YI1B	0.92	-0.10	0.868	,3e7146E	1
YI1C	0.00	0.00	0.866	,000000E	0
YI2A	0.06	-0.01	0.866	,370739E	1
YI2B	0.76	-0.08	0.867	,368245E	1
YI2C	0.06	-0.01	0.866	,370736E	1
YI3A	0.76	0.08	0.867	,3e9148E	1
VF	0.70	-0.08	0.867	,3e8619E	1
VS	0.24	-0.03	0.867	,370504E	1

E,S,S, ,370706E 1

RESIDUAL ERROR ,207635E 0

MULT CORR 0.866

INTERCEPT TERM =- 7,7805252

REGRESSION ANALYSIS , CONA DATA1 CUT OFF PARAMETER .100000E- 5

DEPENDENT VARIABLE RST1A DEGREES OF FREEDOM 38

INDEPENDENT VARIABLES AT SIGNIFICANT LEVEL 5.00 %

V	CD	CURNT	TEMP	TIME	WF	WSTRP	DF	H1	H2	H3	HSTR	Z	VOL
A	R	YR	AI	RST1B	RST1C	RST2A	RST2B	RST2C	RST3A	RST3B	RST3C	P1A	P1B
P1C	P2A	P2B	P2C	P3A	P3B	P3C	RLT1A	RLT1B	RLT1C	RLT2A	RLT2B	RLT2C	RLT3A
RLT3B	RLT3C	YI1A	YI1B	YI1C	YI2A	YI2B	YI2C	YI3A	YI3B	YI3C	VF	VS	

VARIABLES IN THE REGRESSION SET

VAR NAME	REGRESSION COEFF	STANDARD ERROR	CONFIDENCE INTERVAL	T STAT	PART CORR	MULTIPLE CORRELATION	E S S
TEMP	0.0134951	.702403E- 2	.139778E- 1	2.63	0.27	0.947	.443659E 2
H2 =	0.0066397	.171169E- 1	.340619E- 1	5.06	-0.47	0.937	.531265E 2
H3 =	0.0035391	.145384E- 1	.289313E- 1	4.37	-0.42	0.940	.500748E 2
HSTR	0.0772339	.104254E- 1	.207465E- 1	7.41	0.62	0.920	.668045E 2
A	0.0438383	.219201E- 1	.436210E- 1	2.23	0.23	0.948	.434652E 2
YR =	0.0489390	.198539E- 1	.395093E- 1	2.46	-0.25	0.948	.439851E 2
P1A	1.8095041	.103008E 0	.204986E 0	18.34	0.89	0.736	.198463E 3
RLT2A	0.0334868	.224491E- 1	.442758E- 1	2.40	0.25	0.948	.438443E 2
RLY3C =	0.0834433	.197024E- 1	.392077E- 1	4.24	-0.41	0.941	.495306E 2
VS =	0.0416718	.906221E- 2	.180338E- 1	2.39	-0.25	0.948	.438182E 2

VARIABLES NOT IN THE REGRESSION SET

VAR NAME	T STAT	PART CORR	MULTIPLE CORRELATION	E S S
V	0.25	0.03	0.951	.411157E 2
CD	0.32	0.03	0.951	.410967E 2
CURNT	0.32	0.03	0.951	.410963E 2
TIME	1.67	-0.18	0.953	.394650E 2
WF	0.42	-0.04	0.951	.410621E 2
WSTRP	0.71	-0.08	0.952	.409104E 2
DF	0.42	-0.04	0.951	.410621E 2

VAR NAME	T STAT	PART CORR	MULTIPLE CORRELATION	R S S	
H1	0.48	-0.05	0.951	.4103458	2
Z	0.64	-0.07	0.951	.4095428	2
VOL	0.27	0.03	0.951	.4110908	2
R	1.20	0.13	0.952	.4046078	2
AI	1.59	-0.17	0.953	.3998038	2
RSY1B	0.37	0.04	0.951	.4107898	2
RSY1C	0.77	0.08	0.952	.4086788	2
RSY2A	0.44	-0.05	0.951	.4105188	2
RSY2B	0.34	-0.04	0.951	.4108848	2
RSY2C	0.06	-0.01	0.951	.4114278	2
RSY3A	0.61	0.07	0.951	.4096948	2
RSY3B	0.96	-0.10	0.952	.4071038	2
RSY3C	0.02	-0.00	0.951	.4114408	2
P1A	1.72	0.18	0.953	.3979068	2
P1C	0.71	-0.08	0.952	.4090738	2
P2A	1.08	-0.11	0.952	.4060468	2
P2B	1.22	-0.13	0.952	.4044748	2
P2C	1.60	0.17	0.953	.3997428	2
P3A	0.11	0.01	0.951	.4113878	2
P3B	0.28	-0.03	0.951	.4110678	2
P3C	0.00		0.951	.4114438	2
RLY1A	0.58	0.06	0.951	.4098518	2
RLY1B	0.94	-0.10	0.952	.4073018	2
RLY1C	0.00	0.00	0.951	.0000008	0
RLY2A	0.50	0.05	0.951	.4102478	2
RLY2C	0.23	-0.02	0.951	.4111868	2
RLY3A	1.00	0.11	0.952	.4067768	2
RLY3B	0.03	0.00	0.951	.4114398	2
YI1A	0.68	0.07	0.952	.4092728	2

VAR NAME	T STAT	PART CORR	MULTIPLE CORRELATION	P S S
YI1B	0.69	-0.07	0.952	.409104E 2
YI1C	0.00	0.00	0.951	.000000E 0
YI2A	0.01	-0.00	0.951	.411442E 2
YI2B	1.27	-0.14	0.952	.403977E 2
YI2C	0.17	0.02	0.951	.411303E 2
YI3A	0.15	-0.02	0.951	.411339E 2
YI3B	1.13	0.12	0.952	.405503E 2
YI3C	0.41	0.04	0.951	.410657E 2
VF	0.54	-0.06	0.951	.410067E 2

E.S.S. .411443E 2

RESIDUAL ERROR .603775E 0

MULT CORR 0.951

INTERCEPT TERM 43.0194085

REGRESSION ANALYSIS COV4 DATA1 CUT OFF PARAMETER .100000E- 5

DEPENDENT VARIABLE RST1B DEGREES OF FREEDOM 87

INDEPENDENT VARIABLES AT SIGNIFICANT LEVEL 5.00 %

V	CD	CURNT	TEMP	TIME	WF	WSTRP	DF	H1	H2	H3	HSTR	Z	VOL
A	R	YR	AI	RST1A	RST1C	RST2A	RST2B	RST2C	RST3A	RST3B	RST3C	P1A	P1B
P1C	P2A	P2B	P2C	P3A	P3B	P3C	RLT1A	RLT1B	RLT1C	RLT2A	RLT2B	RLT2C	RLT3A
RLT3B	RLT3C	YI1A	YI1B	YI1C	YI2A	YI2B	YI2C	YI3A	YI3B	YI3C	VF	VS	

VARIABLES IN THE REGRESSION SET

VAR NAME		REGRESSION COEFF	STANDARD ERROR		CONFIDENCE INTERVAL		T STAT	PART CORR	MULTIPLE CORRELATION	E S S	
CURNT		3.7394570	.989381E	0	.196887E	1	3.78	0.38	0.883	.673035E	5
H1	=	22.3069199	.352204E	1	.700884E	1	6.35	-0.56	0.890	.646099E	5
H2		10.5956720	.796893E	0	.158980E	1	13.21	0.82	0.657	.173818E	6
H3	=	3.2051880	.521787E	0	.103836E	1	6.14	-0.55	0.854	.828842E	5
HSTR	=	1.5943662	.491725E	0	.978529E	0	3.16	-0.32	0.888	.644508E	5
Z	=	64.4423559	.799072E	1	.159015E	2	8.06	-0.65	0.818	.101002E	6
VOL		2.2445696	.573069E	0	.114041E	1	3.95	0.39	0.881	.681674E	5
YR		7.9911789	.928374E	0	.184746E	1	8.61	0.68	0.806	.107045E	6
RST2A	=	4.8923519	.240754E	1	.479101E	1	2.01	-0.21	0.896	.604880E	5
RST2C	=	8.8797396	.213433E	1	.424732E	1	4.16	-0.41	0.879	.693198E	5
YI3B	=	21.6110395	.898679E	1	.178837E	2	2.40	-0.25	0.893	.616536E	5

VARIABLES NOT IN THE REGRESSION SET

VAR NAME	T STAT	PART CORR	MULTIPLE CORRELATION	E S S	
V	0.77	0.08	0.901	.574110E	5
CD	1.31	-0.14	0.903	.566842E	5
TEMP	0.52	0.06	0.901	.576283E	5
TIME	0.11	-0.01	0.900	.578033E	5
WF	0.17	-0.02	0.901	.577908E	5
WSTRP	1.29	-0.14	0.902	.567040E	5

VAR NAME	T STAT	PART CORR	MULTIPLE CORRELATION	E S S
DF	0.02	-0.00	0.900	.578107E 5
A	0.56	-0.06	0.901	.575849E 5
R	0.12	-0.01	0.900	.578017E 5
AI	1.36	0.15	0.903	.565861E 5
RST1A	0.82	0.09	0.901	.573614E 5
RST1C	1.12	0.12	0.902	.569867E 5
RST2B	1.64	-0.17	0.904	.560491E 5
RST3A	1.40	0.15	0.903	.565203E 5
RST3B	1.41	-0.15	0.903	.564993E 5
RST3C	0.94	0.10	0.902	.572286E 5
P1A	1.75	0.19	0.904	.558143E 5
P1B	0.38	0.04	0.901	.577123E 5
P1C	0.08	0.01	0.900	.578066E 5
P2A	1.18	0.13	0.902	.568526E 5
P2B	0.56	-0.06	0.901	.576015E 5
P2C	0.13	0.01	0.900	.578001E 5
P3A	1.84	-0.19	0.904	.556290E 5
P3B	1.56	-0.17	0.903	.562141E 5
P3C	0.00		0.900	.578110E 5
RLT1A	0.59	-0.06	0.901	.575787E 5
RLT1B	0.68	-0.07	0.901	.575016E 5
RLT1C	0.00	0.00	0.900	.000000E 0
RLT2A	1.17	-0.13	0.902	.569023E 5
RLT2B	1.46	-0.16	0.903	.564180E 5
RLT2C	0.26	0.03	0.901	.577652E 5
RLT3A	0.79	-0.08	0.901	.573986E 5
RLT3B	0.47	-0.05	0.901	.576646E 5
RLT3C	0.93	0.10	0.902	.572367E 5
YI1A	0.43	-0.05	0.901	.576859E 5

VAR NAME	T STAT	PART CORR	MULTIPLE CORRELATION	E S S
YI1B	0.92	-0.10	0.901	.572443E 5
YI1C	0.00	0.00	0.900	.000000E 0
YI2A	0.50	0.05	0.901	.576445E 5
YI2B	0.31	0.03	0.901	.577445E 5
YI2C	1.61	0.17	0.904	.561118E 5
YI3A	1.60	-0.17	0.904	.561310E 5
YI3C	0.03	0.00	0.900	.578102E 5
VF	0.36	0.04	0.901	.577240E 5
VS	0.76	0.08	0.901	.574281E 5

E.S.S. .578110E 5

RESIDUAL ERROR .257778E 2

MULT CORR 0.900

INTERCEPT TERM = 283.7448249

REGRESSION ANALYSIS ' COVA DATA1 CUT OFF PARAMETER ,100000E- 5

DEPENDENT VARIABLE RST1C DEGREES OF FREEDOM 94

INDEPENDENT VARIABLES AT SIGNIFICANT LEVEL 5,00 %

V	CD	CURNT	TEMP	TIME	WF	WSTRP	DF	H1	H2	H3	HSTR	Z	VOL
A	R	YR	AI	RST1A	RST1B	RST2A	RST2B	RST2C	RST3A	RST3B	RST3C	P1A	P1B
P1C	P2A	P2B	P2C	P3A	P3B	P3C	RLT1A	RLT1B	RLT1C	RLT2A	RLT2B	RLT2C	RLT3A
RLT3B	RLT3C	YI1A	YI1B	YI1C	YI2A	YI2B	YI2C	YI3A	YI3B	YI3C	VF	VS	

VARIABLES IN THE REGRESSION SET

VAR NAME	REGRESSION COEFF	STANDARD ERROR	CONFIDENCE INTERVAL	T STAT	PART CORR	MULTIPLE CORRELATION	F S S
Z	0,7377664	,2060108E 0	,567444E 0	2,58	-0,26	0.664	,2164876E 3
P1B	1,1031824	,4981408E 0	,9883309E 0	2,21	0,22	0.671	,234363E 3
P1C	3,9984424	,867481E -0	,172108E 1	4,56	-0,43	0,601	,272082E 3
RLT2C	0,2535540	,455074E- 1	,902866E- 1	5,57	0,50	0,552	,296309E 3

VARIABLES NOT IN THE REGRESSION SET

VAR NAME	T STAT	PART CORR	MULTIPLE CORRELATION	E S S
V	0,39	-0,04	0,691	,222383E 3
CD	0,87	0,09	0,694	,220937E 3
CURNT	0,87	0,09	0,694	,220929E 3
TEMP	0,74	-0,08	0,693	,221426E 3
TIME	0,06	0,01	0,691	,222734E 3
WF	0,78	0,08	0,693	,221206E 3
WSTRP	0,20	0,02	0,691	,222650E 3
DF	0,79	0,08	0,693	,221265E 3
H1	0,08	-0,01	0,691	,222725E 3
H2	0,05	-0,01	0,691	,222736E 3
H3	1,00	0,10	0,695	,220370E 3
HSTR	0,90	0,09	0,694	,220833E 3
VOL	1,07	0,11	0,695	,220011E 3

VAR NAME	T STAT	PART CORR	MULTIPLE CORRELATION	E S S	
A	0.27	0.03	0.691	.2225726	3
R	1.02	0.11	0.695	.2202816	3
YR	0.01	0.08	0.693	.2211786	3
AI	0.05	-0.01	0.691	.2227366	3
RSY1A	1.28	0.13	0.697	.2188646	3
RSY1B	0.37	0.04	0.691	.2224116	3
RSY2A	0.75	-0.08	0.693	.2213866	3
RSY2B	0.13	0.01	0.691	.2226096	3
RSY2C	0.24	0.02	0.691	.2226046	3
RSY3A	1.32	0.14	0.698	.2186246	3
RSY3B	0.66	0.07	0.693	.2217126	3
RSY3C	0.36	0.04	0.691	.2224376	3
P1A	1.47	0.15	0.699	.2176566	3
P2A	0.16	0.02	0.691	.2226346	3
P2B	0.24	0.02	0.691	.2226066	3
P2C	0.00	0.00	0.691	.2227426	3
P3A	0.03	0.00	0.691	.2227406	3
P3B	0.12	0.01	0.691	.2227056	3
P3C	0.00		0.691	.2227426	3
RLY1A	1.06	0.11	0.695	.2199786	3
RLY1B	0.23	0.02	0.691	.2226106	3
RLY1C	0.00	0.00	0.691	.0000006	0
RLY2A	0.04	0.00	0.691	.2227686	3
RLY2B	0.92	-0.10	0.694	.2207136	3
RLY3A	1.11	0.11	0.696	.2198546	3
RLY3B	0.48	0.05	0.692	.2221876	3
RLY3C	0.40	0.04	0.691	.2223426	3
YI1A	1.11	0.11	0.696	.2198456	3
YI1B	0.04	-0.00	0.691	.2227386	3

VAR NAME	T STAT	PART CORR	MULTIPLE CORRELATION	E S S
YI1C	0.00	0.00	0.691	.000000E 0
YI2A	1.37	0.14	0.698	.218317E 3
YI2B	0.13	-0.01	0.691	.222702E 3
YI2C	0.71	0.07	0.693	.221533E 3
YI3A	0.03	0.00	0.691	.222739E 3
YI3B	0.05	-0.01	0.691	.222735E 3
YI3C	0.00	0.00	0.691	.222742E 3
VF	0.59	-0.06	0.692	.221906E 3
VS	0.23	-0.02	0.691	.222610E 3

E.S.S. .222742E 3

RESIDUAL ERROR .153935E 1

MULT CORR 0.691

INTERCEPT TERM = 50.8640348

REGRESSION ANALYSIS . COVA DATA1 CUT OFF PARAMETER .100000E- 5

DEPENDENT VARIABLE RST2A DEGREES OF FREEDOM 90

INDEPENDENT VARIABLES AT SIGNIFICANT LEVEL 5.00 %

V	CD	CURNT	TEMP	TIME	WF	WSTRP	DF	H1	H2	H3	HSTR	Z	VOL
A	R	YR	AI	RST1A	RST1B	RST1C	RST2B	RST2C	RST3A	RST3B	RST3C	P1A	P1B
P1C	P2A	P2B	P2C	P3A	P3B	P3C	RLT1A	RLT1B	RLT1C	RLT2A	RLT2B	RLT2C	RLT3A
RLT3B	RLT3C	YI1A	YI1B	YI1C	YI2A	YI2B	YI2C	YI3A	YI3B	YI3C	VF	VS	

VARIABLES IN THE REGRESSION SET

VAR NAME	REGRESSION COEFF	STANDARD ERROR	CONFIDENCE INTERVAL	T STAT	PART CORR	MULTIPLE CORRELATION	E S S
CURNT *	0.0021103	.199269E- 1	.395341E- 1	3.12	-0.31	0.897	.322077E 2
H3 *	0.0300136	.689607E- 2	.156818E- 1	4.35	-0.42	0.887	.352545E 2
Z	0.9968910	.158944E 0	.315342E 0	6.27	0.55	0.864	.418536E 2
P2A	1.0448580	.653493E- 1	.129653E 0	15.68	0.86	0.585	.108712E 3
P2C	7.6845043	.381924E 1	.757758E 1	2.01	0.21	0.903	.304338E 2
P3B	0.3917466	.197199E 0	.391715E 0	2.34	0.24	0.902	.309063E 2
YI2A *	0.2857017	.955384E- 1	.1895468 0	2.97	-0.30	0.898	.319773E 2
VS	0.0494070	.747084E- 2	.148222E- 1	3.94	0.38	0.891	.341376E 2

VARIABLES NOT IN THE REGRESSION SET

VAR NAME	T STAT	PART CORR	MULTIPLE CORRELATION	E S S
V	0.19	0.02	0.908	.291116E 2
CD	0.24	0.03	0.908	.291055E 2
TEMP	0.52	0.06	0.908	.290367E 2
TIME	0.75	-0.08	0.908	.289441E 2
WF	0.09	-0.01	0.908	.291209E 2
WSTRP	1.07	0.11	0.909	.287543E 2
DF	0.11	-0.01	0.908	.291108E 2
H1	0.16	0.02	0.908	.291152E 2
H2	1.77	0.18	0.911	.281325E 2

VAR NAME	T STAT	PART CORR	MULTIPLE CORRELATION	F & S
HSYR	0.35	-0.04	0.908	.290843E 2
VOL	0.52	-0.06	0.908	.290353E 2
A	1.57	0.16	0.910	.283419E 2
R	0.33	-0.03	0.908	.290881E 2
YR	0.84	-0.09	0.908	.288951E 2
AI	0.47	-0.05	0.908	.290523E 2
RSY1A	0.22	-0.02	0.908	.291060E 2
RSY1B	0.23	0.02	0.908	.291060E 2
RSY1C	0.86	-0.09	0.908	.288839E 2
RSY2B	0.57	0.06	0.908	.290139E 2
RSY2C	0.27	-0.03	0.908	.290901E 2
RSY3A	0.42	-0.04	0.908	.290651E 2
RSY3B	0.04	-0.00	0.908	.291252E 2
RSY3C	0.09	-0.01	0.908	.291214E 2
P1A	0.93	-0.10	0.909	.288495E 2
P1B	0.47	-0.05	0.908	.290516E 2
P1C	0.01	0.00	0.908	.291258E 2
P2B	0.64	0.07	0.908	.289696E 2
P3A	0.83	0.09	0.908	.288990E 2
P3C	0.00		0.908	.291256E 2
RLY1A	0.37	-0.04	0.908	.290783E 2
RLY1B	0.52	0.05	0.908	.290370E 2
RLY1C	0.00	0.00	0.908	.000000E 0
RLY2A	1.60	0.17	0.910	.283117E 2
RLY2B	0.86	-0.09	0.908	.288842E 2
RLY2C	0.53	-0.06	0.908	.290313E 2
RLY3A	0.09	0.01	0.908	.291209E 2
RLY3B	0.52	0.05	0.908	.290365E 2
RLY3C	0.99	-0.10	0.909	.288095E 2

VAR NAME	T STAT	PART CORR	MULTIPLE CORRELATION	F S S
YI1A	0.17	0.02	0.908	.291141E 2
YI1B	0.51	0.05	0.908	.290374E 2
YI1C	0.00	0.00	0.908	.000000E 0
YI2B	0.91	-0.10	0.909	.288534E 2
YI2C	1.05	-0.11	0.909	.287680E 2
YI3A	1.12	0.12	0.909	.287186E 2
YI3B	0.53	0.06	0.908	.290327E 2
YI3C	0.54	-0.06	0.908	.290303E 2
VF	0.36	-0.04	0.908	.290803E 2

E.S.S. .291238E 2

RESIDUAL ERROR .568856E 0

MULT CORR 0.908

INTERCEPT TERM 142.9394174

REGRESSION ANALYSIS COVA DATA1 CUT OFF PARAMETER .0000002- 5

DEPENDENT VARIABLE RST2B DEGREES OF FREEDOM 90

INDEPENDENT VARIABLES AT SIGNIFICANT LEVEL 5.00 %

V	CO	CURNT	TEMP	TIME	WF	WSTRP	DF	R1	R2	R3	RST3	Z	VOL
A	R	YR	AI	RSY1A	RST1B	RST1C	RST2A	RST2C	RST3A	RST3B	RST3C	P1A	P1B
P1C	P2A	P2B	P2C	P3A	P3B	P3C	RLT1A	RLT1B	RLT1C	RLT2A	RLT2B	RLT2C	RLT3A
RLT3B	RLT3C	YI1A	YI1B	YI1C	YI2A	YI2B	YI2C	YI3A	YI3B	YI3C	VF	VS	

VARIABLES IN THE REGRESSION SET

VAR NAME	REGRESSION COEFF	STANDARD ERROR	CONFIDENCE INTERVAL	T STAT	PART CORR	MULTIPLE CORRELATION	F S S
R3	0.0467021	.902567E- 2	.179069E- 1	2.96	0.30	0.956	.716337E 2
R	0.0073158	.361440E- 2	.717108E- 2	2.02	-0.21	0.958	.682583E 2
RST2A	0.2062928	.122244E 0	.248483E 0	2.13	0.22	0.958	.685640E 2
RST2C	1.0169437	.261290E 0	.518398E 0	3.89	0.38	0.953	.762727E 2
RST3C	1.5916166	.420845E 0	.846860E 0	3.64	0.36	0.954	.748699E 2
P2A	0.5785473	.138420E 0	.274636E 0	4.18	-0.40	0.952	.779557E 2
P2B	0.4402022	.197825E 0	.392484E 0	2.23	0.23	0.958	.688745E 2
P3A	1.7431822	.258854E 0	.509504E 0	6.79	0.58	0.939	.988957E 2

VARIABLES NOT IN THE REGRESSION SET

VAR NAME	T STAT	PART CORR	MULTIPLE CORRELATION	F S S
V	0.49	-0.05	0.960	.651075E 2
CO	1.76	-0.18	0.962	.630848E 2
CURNT	1.76	-0.18	0.962	.630847E 2
TEMP	1.17	-0.12	0.961	.643001E 2
TIME	0.22	-0.02	0.960	.652500E 2
WF	0.23	-0.02	0.960	.652457E 2
WSTRP	0.09	-0.01	0.960	.652787E 2
DF	0.31	-0.03	0.960	.652150E 2
R1	1.12	0.12	0.961	.643803E 2

VAR NAME	F STAT	PART CORR	MULTIPLE CORRELATION	R S S
H2	0.30	-0.03	0.960	.6521792E 2
HSTR	0.25	-0.03	0.960	.6523872E 2
Z	1.03	-0.21	0.962	.6252694E 2
VOL	0.08	-0.01	0.960	.6529052E 2
A	0.16	0.02	0.960	.6526538E 2
YR	0.11	0.01	0.960	.6527566E 2
AI	0.30	-0.03	0.960	.6522016E 2
RST1A	0.24	-0.03	0.960	.6524216E 2
RST1B	0.33	-0.04	0.960	.6520386E 2
RST1C	0.81	0.09	0.960	.6480456E 2
RST3A	0.85	-0.09	0.960	.6475586E 2
RST3B	0.70	0.07	0.960	.6493206E 2
P1A	0.02	-0.00	0.960	.6528456E 2
P1B	0.57	0.06	0.960	.6504526E 2
P1C	0.20	0.02	0.960	.6525526F 2
P2C	1.06	0.11	0.961	.6444196E 2
P2A	0.91	0.10	0.961	.6468276E 2
P3C	0.00		0.960	.6528476E 2
RLY1A	0.92	-0.10	0.961	.6467296E 2
RLY1B	0.90	0.09	0.961	.6470006E 2
RLY1C	0.00	0.00	0.960	.0000006E 0
RLY2A	0.53	-0.06	0.960	.6508306E 2
RLY2B	0.15	0.02	0.960	.6526016E 2
RLY2C	1.44	0.15	0.961	.6379656E 2
RLY3A	0.98	-0.10	0.961	.6458866E 2
RLY3B	0.59	-0.06	0.960	.6502696E 2
RLY3C	1.18	-0.12	0.961	.6427316E 2
YI1A	0.94	-0.10	0.961	.6463696E 2
YI1B	0.92	-0.10	0.961	.6466326E 2

VAR NAME	T STAT	PART CORR	MULTIPLE CORRELATION*	E S S
YI1C	0.00	0.00	0.960	.000000E 0
YI2A	0.47	-0.05	0.960	.651233E 2
YI2B	1.49	-0.16	0.961	.636883E 2
YI2C	0.32	-0.03	0.960	.652078E 2
YI3A	0.24	0.02	0.960	.652442E 2
YI3B	0.82	-0.09	0.960	.647898E 2
YI3C	0.61	-0.06	0.960	.650168E 2
VF	0.29	0.03	0.960	.652221E 2
VS	0.49	-0.05	0.960	.651055E 2

E.S.S.	.652847E 2
RESIDUAL ERROR	.651696E 0
MULT CORR	0.960
INTERCEPT TERM	27.9929401

DEPENDENT VARIABLE RST2C DEGREES OF FREEDOM 38

INDEPENDENT VARIABLES AT SIGNIFICANT LEVEL 5.00 %

V CD CURNT TEMP TIME WF WSTRP DF H1 H2 H3 WSTR Z VOL

A R YR AI RST1A RST1B RST1C RST2A RST2B RST3A RST3B RST3C P1A P1B

P1C P2A P2B P2C P3A P3B P3C RLT1A RLT1B RLT1C RLT2A RLT2B RLT2C RLT3A

RLT3B RLT3C YI1A YI1B YI1C YI2A YI2B YI2C YI3A YI3B YI3C VF VS

VARIABLES IN THE REGRESSION SET

VAR NAME	REGRESSION COEFF	STANDARD ERROR	CONFIDENCE INTERVAL	T STAT	PART CORR	MULTIPLE CORRELATION	E S S	
TIME	0.0000378	.370404E- 5	.737103E- 5	10.20	0.74	0.982	.609561E	1
H2 -	0.0147154	.405404E- 2	.806932E- 2	3.63	-0.36	0.991	.321215E	1
H3 -	0.0112456	.270109E- 2	.537508E- 2	4.16	-0.41	0.990	.334435E	1
YR	0.0110297	.549974E- 2	.109451E- 1	2.03	0.21	0.992	.292452E	1
RST3C	1.6273425	.250960E- 1	.499611E- 1	70.46	0.99	0.286	.190419E	3
P2C	12.4927740	.162965E 1	.324299E 1	7.65	0.63	0.987	.465033E	1
RLT3B	0.0194469	.503464E- 2	.100190E- 1	3.86	0.38	0.991	.326789E	1
RLT3C -	0.0558054	.558004E- 2	.111043E- 1	9.64	-0.72	0.983	.574662E	1
YI3B -	0.4993510	.921744E- 1	.183427E 0	5.42	-0.50	0.989	.372532E	1
YI3C	1.7320158	.124879E 0	.248509E 0	13.87	0.83	0.974	.890158E	1

VARIABLES NOT IN THE REGRESSION SET

VAR NAME	T STAT	PART CORR	MULTIPLE CORRELATION	E S S	
V	0.06	-0.01	0.992	.279386E	1
CD	0.37	0.04	0.992	.278961E	1
CURNT	0.37	0.04	0.992	.278947E	1
TEMP	0.02	0.00	0.992	.279398E	1
WF	0.96	-0.10	0.992	.276492E	1
WSTRP	0.17	0.02	0.992	.279310E	1
DF	0.95	-0.10	0.992	.276535E	1

VAR NAME	T STAT	PART CORR	MULTIPLE CORRELATION	E S S	
R1	0.46	-0.05	0.992	.2787196	1
RSTR	1.01	-0.11	0.992	.2761026	1
Z	1.32	0.14	0.992	.2739236	1
VOL	0.48	0.05	0.992	.2786676	1
A	0.39	0.04	0.992	.2789636	1
R	1.10	-0.12	0.992	.2755676	1
AI	0.36	-0.04	0.992	.2789876	1
RST1A	0.91	-0.10	0.992	.2767756	1
RST1B	0.83	-0.09	0.992	.2772076	1
RST1C	0.72	-0.08	0.992	.2777346	1
RST2A	0.41	-0.04	0.992	.2788666	1
RST2B	1.22	0.13	0.992	.2746966	1
RST3A	0.03	-0.00	0.992	.2793966	1
RST3B	0.40	0.04	0.992	.2788776	1
P1A	1.13	-0.12	0.992	.2753366	1
P1B	0.26	-0.03	0.992	.2791796	1
P1C	0.09	0.01	0.992	.2793766	1
P2A	1.26	-0.13	0.992	.2744936	1
P2B	0.39	0.04	0.992	.2789196	1
P3A	0.42	0.05	0.992	.2788226	1
P3B	0.53	0.06	0.992	.2784866	1
P3C	0.00		0.992	.2794066	1
RLT1A	0.62	0.07	0.992	.2781596	1
RLT1B	0.29	-0.03	0.992	.2791416	1
RLT1C	0.00	0.00	0.992	.0000006	0
RLT2A	0.42	-0.04	0.992	.2788466	1
RLT2B	0.32	0.03	0.992	.2792436	1
RLT2C	0.42	-0.04	0.992	.2788486	1
RLT3A	0.04	-0.00	0.992	.2793956	1

NAME		COEF	CORRELATION	
YI1A	0.48	0.04	0.992	,2788558 1
YI1B	0.25	-0.03	0.992	,2792628 1
YI1C	0.00	0.00	0.992	,0000008 0
YI2A	1.20	-0.13	0.992	,2748818 1
YI2B	0.43	-0.05	0.992	,2783118 1
YI2C	0.14	-0.02	0.992	,2793348 1
YI3A	0.20	0.02	0.992	,2792738 1
VF	0.59	-0.06	0.992	,2782828 1
VS	0.06	0.01	0.992	,2793888 1

E,S,S. ,279399E 1

RESIDUAL ERROR ,178185E 0

MULT CORR 0.992

INTERCEPT TERM 231.3485190

GF?

NUMBER OF PAGES 24

DEPENDENT VARIABLE RST3A DEGREES OF FREEDOM 89

INDEPENDENT VARIABLES AT SIGNIFICANT LEVEL 5.00 %

V	CD	CURNT	TEMP	TIME	WF	MSTRP	DF	H1	H2	H3	MSTR	Z	VOL
A	R	YR	AI	RST1A	RST1B	RST1C	RST2A	RST2B	RST2C	RST3B	RST3C	P1A	P1B
P1C	P2A	P2B	P2C	P3A	P3B	P3C	RLT1A	RLT1B	RLT1C	RLT2A	RLT2B	RLT2C	RLT3A
RLT3B	RLT3C	YI1A	YI1B	YI1C	YI2A	YI2B	YI2C	YI3A	YI3B	YI3C	VF	VS	

VARIABLES IN THE REGRESSION SET

VAR NAME	REGRESSION COEFF	STANDARD ERROR	CONFIDENCE INTERVAL	T STAT	PART CORR	MULTIPLE CORRELATION	E S S
CURNT	0.0995067	.225461E- 1	.444688E- 1	3.11	0.31	0.917	.364556E 2
TIME	0.0000091	.757223E- 5	.150687E- 4 *	1.20	0.13	0.924	.353926E 2
Z	1.3726608	.170857E 0	.339965E 0	8.03	0.65	0.867	.567018E 2
RST1A	0.1803134	.350864E- 1	.698219E- 1	5.14	0.48	0.902	.426152E 2
RST2A -	0.1405329	.552269E- 1	.109901E 0	2.54	-0.26	0.920	.352541E 2
P3A	1.7965927	.129236E 0	.257179E 0	13.90.	0.83	0.738	.104223E 3
RLT1A -	0.1420501	.404529E- 1	.805006E- 1	3.51	-0.35	0.915	.374162E 2
YI2A	0.2130689	.103674E 0	.206307E 0	2.06	0.21	0.922	.344298E 2
VF	0.0103025	.508509E- 2	.101193E- 1	2.03	0.21	0.922	.343788E 2

VARIABLES NOT IN THE REGRESSION SET

VAR NAME	T STAT	PART CORR	MULTIPLE CORRELATION	E S S
V	1.30	-0.14	0.927	.322415E 2
CD	0.15	-0.02	0.925	.326549E 2
TEMP	0.50	-0.05	0.926	.327698E 2
WF	1.49	0.16	0.927	.320545E 2
MSTRP	0.33	0.03	0.926	.328235E 2
DF	1.49	0.16	0.927	.320518E 2
H1	0.61	-0.07	0.926	.327230E 2
H2	1.09	-0.12	0.926	.324261E 2

VAR NAME	T STAT	PART CORR	MULTIPLE CORRELATION	R S Q
M3	0.02	0.00	0.925	.328630E 2
MGYR	1.31	0.14	0.927	.322359E 2
VOL	1.21	0.13	0.927	.322384E 2
A	1.18	-0.12	0.927	.323566E 2
R	0.92	0.10	0.926	.325482E 2
YR	1.16	-0.12	0.927	.323555E 2
AI	0.24	0.03	0.926	.328410E 2
RSY1B	0.10	-0.01	0.925	.328504E 2
RSY1C	1.03	0.11	0.926	.324731E 2
RSY2B	0.78	-0.08	0.926	.326346E 2
RSY2C	0.45	-0.05	0.926	.327860E 2
RSY3B	0.95	-0.10	0.926	.325302E 2
RSY3C	0.20	-0.02	0.926	.328476E 2
P1A	1.78	-0.19	0.928	.317249E 2
P1B	0.96	0.10	0.926	.325111E 2
P1C	0.97	-0.10	0.926	.325136E 2
P2A	0.27	0.03	0.926	.328349E 2
P2B	0.03	-0.00	0.925	.328627E 2
P2C	0.76	0.08	0.926	.326409E 2
P3B	0.80	-0.09	0.926	.326256E 2
P3C	0.00		0.925	.328631E 2
RLY1B	1.01	0.11	0.926	.324648E 2
RLY1C	0.00	0.00	0.925	.000000E 0
RLY2A	1.91	-0.20	0.929	.315504E 2
RLY2B	1.45	-0.15	0.927	.321063E 2
RLY2C	1.42	-0.15	0.927	.321305E 2
RLY3A	1.10	0.12	0.927	.324153E 2
RLY3B	0.14	0.01	0.925	.328560E 2
RLY3C	0.14	-0.01	0.925	.328558E 2

VAR NAME	T STAT	PART CORR	MULTIPLE CORRELATION	E S S
YI1A	0.01	-0.00	0.925	,328630E 2
YI1B	0.67	-0.07	0.926	,326966E 2
YI1C	0.00	0.00	0.925	,000000E 0
YI2D	0.42	-0.04	0.926	,327942E 2
YI2C	0.12	-0.01	0.925	,328575E 2
YI3A	0.26	-0.03	0.926	,326380E 2
YI3B	0.43	0.05	0.926	,327945E 2
YI3C	1.01	-0.11	0.926	,324846E 2
VS	1.19	0.13	0.927	,323400E 2

E.S.S. ,328631E 2

RESIDUAL ERROR ,607658E 0

MULT CORR 0.925

INTERCEPT TERM 31.0105981

DEPENDENT VARIABLE RST3B DEGREES OF FREEDOM 91

INDEPENDENT VARIABLES AT SIGNIFICANT LEVEL 5.00 %

V	CD	CURNT	TEMP	TIME	WF	WSTRP	DF	H1	H2	H3	HSTR	Z	VOL
A	R	VR	AI	RST1A	RST1B	RST1C	RST2A	RST2B	RST2C	RST3A	RST3C	P1A	P1B
P1C	P2A	P2B	P2C	P3A	P3B	P3C	RLT1A	RLT1B	RLT1C	RLT2A	RLT2B	RLT2C	RLT3A
RLT3B	RLT3C	YI1A	YI1B	YI1C	YI2A	YI2B	YI2C	YI3A	YI3B	YI3C	VF	VS	

VARIABLES IN THE REGRESSION SET

VAR NAME	REGRESSION COEFF	STANDARD ERROR	CONFIDENCE INTERVAL	T STAT	PART CORR	MULTIPLE CORRELATION	E S S
TIME	0.0000043	.169185E- 4	.335683E- 4	0.25	0.03	0.749	.207305E 3
RST1A	0.7561560	.180295E 0	.369609E 0	3.95	-0.38	0.697	.242704E 3
RST2B	0.1042801	.551974E- 1	.109512E 0	2.98	0.30	0.720	.227322E 3
P1A	1.0016062	.452569E 0	.897500E 0	2.35	0.24	0.731	.219604E 3
P3B	2.1377215	.410670E 0	.814770E 0	5.21	0.48	0.656	.268841E 3
RLT3A	0.1709551	.340204E- 1	.675284E- 1	5.96.	0.53	0.624	.288117E 3
YI2A	0.6920903	.291850E 0	.499685E 0	2.75	0.28	0.724	.224347E 3

VARIABLES NOT IN THE REGRESSION SET

VAR NAME	T STAT	PART CORR	MULTIPLE CORRELATION	E S S
V	0.61	-0.06	0.750	.206325E 3
CD	0.63	0.07	0.750	.206255E 3
CURNT	0.63	0.07	0.750	.206263E 3
TEMP	0.46	-0.05	0.750	.206646E 3
WF	0.43	-0.04	0.749	.206740E 3
WSTRP	1.67	-0.17	0.756	.200925E 3
DF	0.43	-0.05	0.749	.206746E 3
H1	0.84	-0.09	0.751	.205561E 3
H2	0.87	0.09	0.751	.205426E 3
H3	0.68	0.07	0.750	.206091E 3

VAR NAME	T STAT	PART CORR	MULTIPLE CORRELATION	E S S	
HSTR	0.50	-0.05	0.750	.2045746	3
Z	0.33	-0.03	0.749	.2069046	3
VOL	1.50	-0.16	0.756	.2021018	3
A	0.19	0.02	0.749	.2070702	3
R	0.54	0.06	0.750	.2044896	3
YR	1.05	-0.11	0.752	.2048366	3
AI	0.00	-0.00	0.749	.2071576	3
RST1B	0.45	0.05	0.750	.2060966	3
RST1C	0.36	0.04	0.749	.2066296	3
RST2A	0.65	-0.07	0.750	.2041066	3
RST2C	1.03	-0.11	0.753	.2045086	3
RST3A	1.59	-0.16	0.757	.2015316	3
RST3C	0.08	-0.01	0.749	.2071416	3
P1B	0.44	0.05	0.749	.2067206	3
P1C	0.37	-0.04	0.749	.2068496	3
P2A	0.26	+0.03	0.749	.2070006	3
P2B	0.05	0.01	0.749	.2071516	3
P2C	0.20	0.03	0.749	.2069686	3
P3A	1.47	-0.15	0.756	.2023036	3
P3C	0.00		0.749	.2071576	3
RLT1A	0.17	0.02	0.749	.2070646	3
RLT1B	1.44	0.15	0.755	.2024646	3
RLT1C	0.00	0.00	0.749	.0000006	0
RLT2A	0.17	0.02	0.749	.2070896	3
RLT2B	0.62	+0.07	0.750	.2062776	3
RLT2C	0.09	-0.01	0.749	.2071476	3
RLT3B	1.58	-0.16	0.757	.2015356	3
RLT3C	0.52	-0.06	0.750	.2065276	3
YI1A	0.49	0.05	0.750	.2066026	3

VAR NAME		PART CORR	CORRELATION	
YI1B	0.19	0.02	0.749	.207078E 3
YI1C	0.00	0.00	0.749	.000000E 0
YI2B	1.11	-0.12	0.753	.204342E 3
YI2C	0.32	0.03	0.749	.206928E 3
YI3A	1.15	-0.12	0.753	.204161E 3
YI3B	1.01	-0.11	0.752	.204847E 3
YI3C	1.33	-0.14	0.754	.203172E 3
VF	0.21	-0.02	0.749	.207053E 3
VS	0.36	-0.04	0.749	.206865E 3

E.S.S. .207157E 3

RESIDUAL ERROR .150879E 1

MULT CORR 0.749

INTERCEPT TERM 71.5025704

REGRESSION ANALYSIS , CONV DATA1 CUT OFF PARAMETER ,10000E+ 5

DEPENDENT VARIABLE RST3C DEGREES OF FREEDOM 87

INDEPENDENT VARIABLES AT SIGNIFICANT LEVEL 5.00 %

V	CD	CURNT	TEMP	TIME	WF	WSTRP	DF	H1	H2	H3	HSTR	Z	VOL
A	R	YR	AI	RST1A	RST1B	RST1C	RST2A	RST2B	RST2C	RST3A	RST3B	P1A	P1B
P1C	P2A	P2B	P2C	P3A	P3B	P3C	RLT1A	RLT1B	RLT1C	RLT2A	RLT2B	RLT2C	RLT3A
RLT3B	RLT3C	YI1A	YI1B	YI1C	YI2A	YI2B	YI2C	YI3A	YI3B	YI3C	VF	VS	

VARIABLES IN THE REGRESSION SET

VAR NAME	REGRESSION COEFF	STANDARD ERROR	CONFIDENCE INTERVAL	T STAT	PART CORR	MULTIPLE CORRELATION	E S S	
TIME	= 0.0000246	.213329E- 5	.428407E- 5	11.41	-0.77	0.984	.217258E	1
WF	0.0021134	.226741E- 3	.455195E- 3	9.24	0.70	0.987	.172419E	1
VOL	= 0.0102101	.198201E- 2	.394420E- 2	5.15	-0.48	0.991	.113575E	1
YR	0.0124437	.378529E- 2	.753270E- 2	3.29	0.33	0.993	.9783A1E	0
RST2B	0.0311824	.956567E- 2	.190755E- 1	3.25	0.33	0.993	.9761328	0
RST2C	0.5493761	.193595E- 1	.384852E- 1	27.37	0.95	0.935	.836563E	1
P2C	= 0.1577901	.927089E 0	.184491E 1	8.76	-0.69	0.988	.164102E	1
RLT3B	= 0.0057145	.296987E- 2	.591005E- 2	2.93	-0.30	0.993	.956406E	0
RLT3C	0.0327756	.346022E- 2	.688703E- 2	9.47	0.71	0.987	.176747E	1
YI3B	0.2408223	.590579E- 1	.117525E 0	3.74	0.37	0.992	.1010135	1
YI3C	= 1.0322726	.710674E- 1	.142619E 0	14.68	-0.84	0.977	.302676E	1

VARIABLES NOT IN THE REGRESSION SET

VAR NAME	T STAT	PART CORR	MULTIPLE CORRELATION	E S S	
V	0.75	0.08	0.993	.864627E	0
CD	0.02	-0.00	0.993	.870274E	0
CURNT	0.01	-0.00	0.993	.870275E	0
TEMP	0.68	0.07	0.993	.865554E	0
WSTRP	0.50	-0.05	0.993	.867769E	0
DF	1.20	0.13	0.994	.855829E	0

VAR NAME	T STAT	PART CORR	MULTIPLE CORRELATION	E S S
H1	0.85	-0.09	0.994	.869949E 0
H2	0.85	0.09	0.994	.869881E 0
H3	0.14	0.02	0.993	.870072E 0
HSTR	1.74	-0.18	0.994	.840663E 0
Z	0.28	-0.03	0.993	.869463E 0
A	0.30	-0.03	0.993	.869345E 0
R	0.63	0.07	0.993	.866233E 0
AI	0.08	0.01	0.993	.870211E 0
RST1A	0.23	-0.02	0.993	.869763E 0
RST1B	1.99	0.21	0.994	.832079E 0
RST1C	0.06	0.01	0.993	.870237E 0
RST2A	0.06	0.01	0.993	.870244E 0
RST3A	0.01	-0.00	0.993	.870275E 0
RST3B	0.31	0.03	0.993	.869201E 0
P1A	0.11	-0.01	0.993	.870145E 0
P1B	0.15	-0.02	0.993	.870048E 0
P1C	0.18	-0.02	0.993	.869933E 0
P2A	0.50	0.05	0.993	.869712E 0
P2B	1.17	-0.13	0.994	.856538E 0
P3A	0.35	-0.04	0.993	.869049E 0
P3B	0.64	-0.07	0.993	.866122E 0
P3C	0.00		0.993	.870365E 0
RLT1A	0.11	-0.01	0.993	.870155E 0
RLT1B	0.73	0.08	0.993	.864926E 0
RLT1C	0.00	0.00	0.993	.000000E 0
RLT2A	0.70	0.07	0.993	.865411E 0
RLT2B	0.29	-0.03	0.993	.869446E 0
RLT2C	0.36	-0.04	0.993	.869053E 0
RLT3A	0.59	-0.06	0.993	.868826E 0

VAR NAME	T STAT	PART CORR	MULTIPLE CORRELATION	E S S
YI1A	0.15	0.07	0.993	.870964E 0
YI1B	0.24	0.03	0.993	.869702E 0
YI1C	0.00	0.00	0.993	.870802E 0
YI2A	1.31	0.14	0.994	.858180E 0
YI2B	1.24	0.13	0.994	.858348E 0
YI2C	0.14	0.02	0.993	.870881E 0
YI3A	1.20	-0.13	0.994	.859638E 0
VF	0.26	0.03	0.993	.869607E 0
VS	0.02	0.00	0.993	.870272E 0

E.S.S. .870277E 0

RESIDUAL ERROR .100016E 0

MULT CORR 0.993

INTERCEPT TERM = 151.5412940

SECTION (3)

CDR MODELS

CDR, computer derived relations, are regression "models" derived from statistical analysis.

Each "model" is part of a true regression equation, but to analyse the effects of different film parameters on each other, they have been broken down.

The CDR's used in analysis are listed.

Where the CDR is quoted, an example might be

↑v M8b (3) or ↓l M15a (2)

The key to any of these is

↑↓ ,	x ,	X Number ,	(Number)
This denotes the trend, i.e. ↑ increases with ↓ decreases with	Denotes property v = volume r = radius l = length	Denotes the particle, pore or parameter that varies	Denotes film layer

An example of a CDR could be

↑v/r M5(1) => ↓r Q3(2)

This means that an increase in the volume or radius of the M5 particle in the first layer would result in Q3 pores of smaller radius in the second layer. This does not refer to change after the film has grown, but to change trends in different specimens during anodising.

MODELS

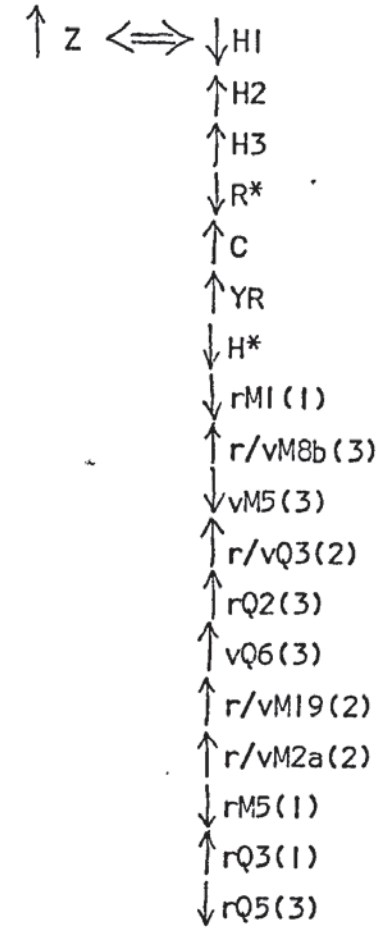
Z
H1
H2
H3
R*
C
YR
H*
rM1(1)
r/vM8b(3)
vM5(3)
r/vQ3(2)
rQ2(3)
vQ6(3)
r/vM19(2)
r/vM2a(2)
rM5(1)
rQ3(1)
rQ5(3)

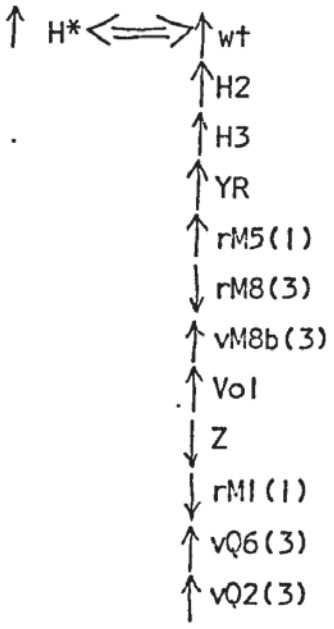
H*
wt
H2
H3
YR
rM5(1)
rM8(3)
vM8b(3)
Vol
Z
rM1(1)
vQ6(3)
vQ2(3)

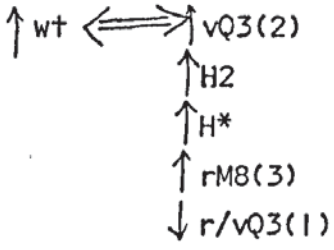
wt
vQ3(2)
H2
H*
rM8(3)
r/vQ3(1)

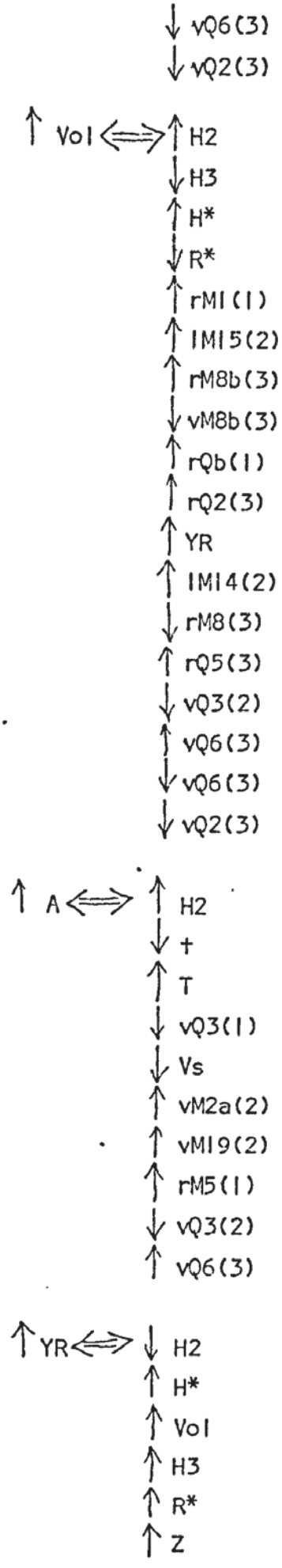
vQ6(3)
vQ2(3)
Vol
H2
H3
H*
R*
rMI(1)
IMI5(2)
rM8b(3)
vM8b(3)
rQb(1)
rQ2(3)
YR
IMI4(2)
rM8(3)
rQ5(3)
vQ3(2)
vQ6(3)
vQ6(3)
vQ2(3)
A
H2
t
T
vQ3(1)
Vs
vM2a(2)
vMI9(2)
rM5(1)
vQ3(2)
vQ6(3)
YR
H2
H*
Vol
H3
R*
Z

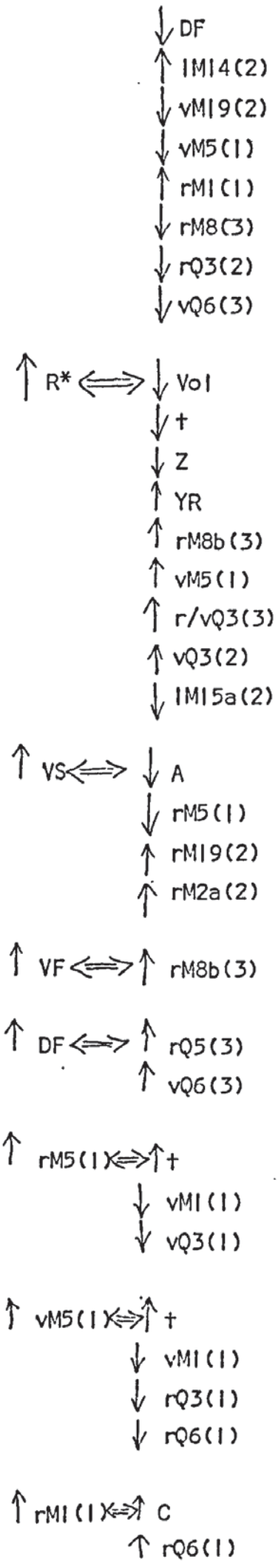
DF
IMI4(2)
vMI9(2)
vM5(1)
rMI(1)
rM8(3)
rQ3(2)
vQ6(3)
R*
VoI
t
Z
YR
rM8b(3)
vM5(1)
r/vQ3(3)
vQ3(2)
IMI5a(2)
VS
A
rM5(1)
rMI9(2)
rM2a(2)
VF
rM8b(3)
DF
rQ5(3)
vQ6(3)
rM5(1)X
t
vMI(1)
vQ3(1)
vM5(1)X
t
vMI(1)
rQ3(1)
rQ6(1)
rMI(1)X
C
rQ6(1)

↑vM1(1)⟺ ↓vM5(1)
↓vQ3(1)
↓rM5(1)
↓rQ3(1)

↑ rQ3(1)⟺ ↓vM5(1)
↓vM1(1)

↑ vQ3(1)⟺ ↓vM1(1)
↑vM5(1)
↓rQ6(1)

↑ rQ6(1)⟺ ↓vQ3(1)

↑rM19/2a(2)⟺ ↓rM1(1)
↓C
↑vQ3(2)
↑IM15a(2)
↑rQ6(1)
↑rQ6(3)

↑vM19/2a(2)⟺ ↓YR
↑vM5(1)
↑rQ3(2)
↑IM15a(2)
↑vQ3(2)
↑rQ6(2)

↑IM15a(2)⟺ ↑r/vM19/2a(2)
↑IM14(2)
↑r/vQ3(2)
↑rQ3(1)

↑vM15a(2)⟺ ↑vQ3(2)

↑IM14(2)⟺ ↑YR
↓rM1(1)
↑IM15a(2)
↑T
↑rQ6(1)

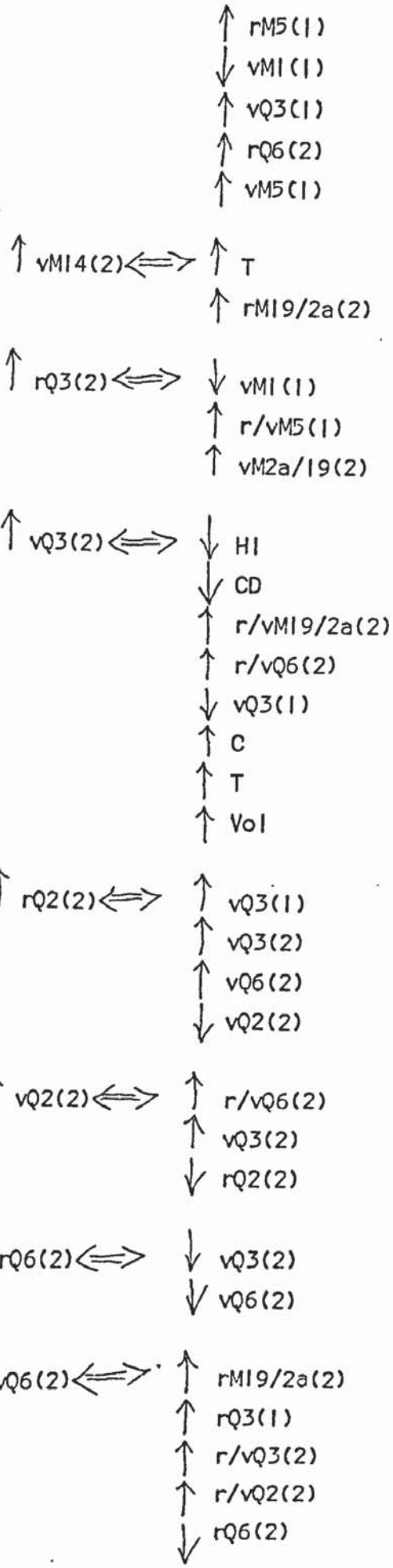
↑ rM5(1)
↓ vM1(1)
↑ vQ3(1)
↑ rQ6(2)
↑ vM5(1)
↑ vMI4(2) ⟺ ↑ T
↑ rMI9/2a(2)
↑ rQ3(2) ⟺ ↓ vM1(1)
↑ r/vM5(1)
↑ vM2a/19(2)
↑ vQ3(2) ⟺ ↓ HI
↓ CD
↑ r/vMI9/2a(2)
↑ r/vQ6(2)
↓ vQ3(1)
↑ C
↑ T
↑ Vol
↑ rQ2(2) ⟺ ↑ vQ3(1)
↑ vQ3(2)
↑ vQ6(2)
↓ vQ2(2)
↑ vQ2(2) ⟺ ↑ r/vQ6(2)
↑ vQ3(2)
↓ rQ2(2)
↑ rQ6(2) ⟺ ↓ vQ3(2)
↓ vQ6(2)
↑ vQ6(2) ⟺ ↑ rMI9/2a(2)
↑ rQ3(1)
↑ r/vQ3(2)
↑ r/vQ2(2)
↓ rQ6(2)

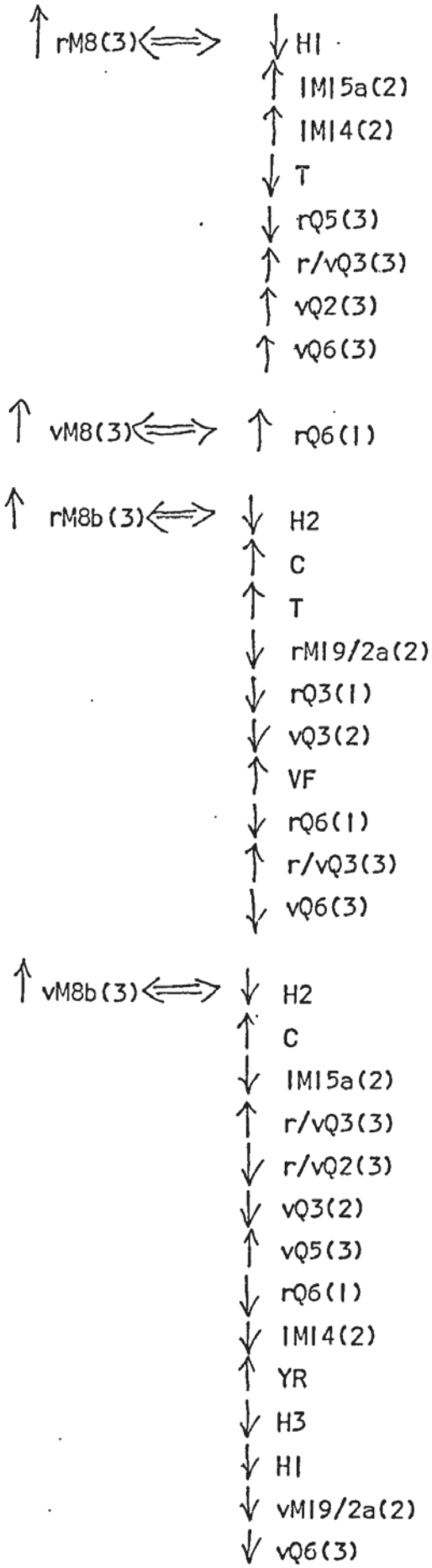
rM8(3)
H1
IM15a(2)
IM14(2)
T
rQ5(3)
r/vQ3(3)
vQ2(3)
vQ6(3)
vM8(3)
rQ6(1)
rM8b(3)
H2
C
T
rM19/2a(2)
rQ3(1)
vQ3(2)
VF
rQ6(1)
r/vQ3(3)
vQ6(3)
vM8b(3)
H2
C
IM15a(2)
r/vQ3(3)
r/vQ2(3)
vQ3(2)
vQ5(3)
rQ6(1)
IM14(2)
YR
H3
H1
vM19/2a(2)
vQ6(3)

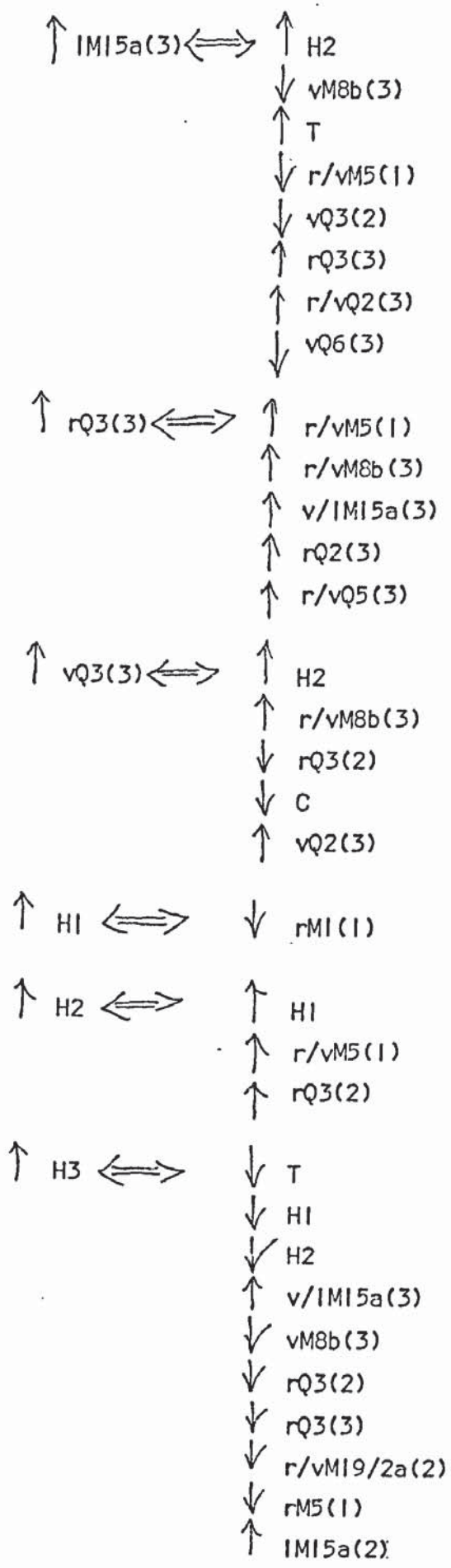
↑ IMI5a(3) ⟺
↑ H2
↓ vM8b(3)
↑ T
↓ r/vM5(1)
↓ vQ3(2)
↑ rQ3(3)
↑ r/vQ2(3)
↓ vQ6(3)
↑ rQ3(3) ⟺
↑ r/vM5(1)
↑ r/vM8b(3)
↑ v/IMI5a(3)
↑ rQ2(3)
↑ r/vQ5(3)
↑ vQ3(3) ⟺
↑ H2
↑ r/vM8b(3)
↓ rQ3(2)
↓ C
↑ vQ2(3)
↑ H1 ⟺
↓ rM1(1)
↑ H2 ⟺
↑ H1
↑ r/vM5(1)
↑ rQ3(2)
↑ H3 ⟺
↓ T
↓ H1
↓ H2
↑ v/IMI5a(3)
↓ vM8b(3)
↓ rQ3(2)
↓ rQ3(3)
↓ r/vMI9/2a(2)
↓ rM5(1)
↑ IMI5a(2)

SECTION (4)

OPTIMUM FILM REGRESSION EQUATION - USING COMPUTER ASSISTED MODELING AND CHOICE OF PROGRESSIVE EXPERIMENTAL PARAMETERS.

A series of experiments were run to find the optimum film parameters in terms of minimum porosity (R*).

To accomplish this the computer was used to calculate, using a hill climb and multiple regression approach, the next experimental parameters for a new series of experiments which would find the line of greatest slope, eventually leading to the point of experimental least porosity in the film.

The eventual nearest approach to this point was recorded on the regression equation model for the film, as below:

$$R^*(\min) = -162.145762 + 9.2989278V - 2.376195\ C.D. - 0.0773171\ T - 0.0806665V^2 + 0.0000257\ T^2$$

and as seen in the following printout.

[illegible] FOR [illegible] STATISTICAL ANALYSIS ANS3/26

REGRESSION ANALYSIS   COVA   DATA2   CUT OFF PARAMETER .100000E- 5

DEPENDENT VARIABLE   9   DEGREES OF FREEDOM   58

INDEPENDENT VARIABLES AT SIGNIFICANT LEVEL   20,00 %

V   CD   TEMP   TIME   VSQ   COS2   TEMPSQ   TIMESQ

VARIABLES IN THE REGRESSION SET

VAR NAME		REGRESSION COEFF	STANDARD ERROR	CONFIDENCE INTERVAL	T STAT	PART CORR	MULTIPLE CORRELATION	E S S
V		0,2959275	.5843492E 1	.7573173E 1	1,59	0,20	0.890	.7773.1E 4
CD	-	2,3763956	.3437958 0	.4555334 0	6,91	-0,67	0.796	.1358?5E 5
TIME	-	0,0773171	.1094531- 1	.1420882- 1	7,05	-0,68	0,793	.1343435E 5
VSQ	-	0,0000665	.4007142E- 1	.5307818- 1	1,66	-0,24	0,889	.7800068E 4
TIMESQ		0,0000257	.6124126E- 5	.7936862- 5	4,20	0,48	0.860	.9708165E 4

VARIABLES NOT IN THE REGRESSION SET

VAR NAME	T STAT	PART CORR	MULTIPLE CORRELATION	F S S
TEMP	0,36	0,05	0.895	.7430.4E 4
COSQ	0,51	0,07	0.895	.7413.7E 4
TEMPSQ	0,39	0,05	0,895	.742825E 4

E.S.S.   .7447?7E 4

RESIDUAL ERROR   .1133196 2

MULT CORR   0,895

INTERCEPT TERM   - 162,1457026
60-

FFFFFFFFFFFFFFFFFFFFFFFFFFFFFFFFFFFFFFFFFFFFFFFFFFFFFFFFFFFFFFFFFFFFFFFFFFFFFFFFFFFFFFFFFFFFFFFFFFFFFFFFFFFFFFFFFFFFFFFFFFFFF
FFFFFFFF   FFFFFFFFFFFFFFFFFFFFFFFFFFFFFFFFFFFFFFFFFFFFFFFFFFFFFFFFFFFFFFFFFFFFFFFFFFFFFFFFFFFFF
FFFFFFFF   NUMBER OF PAGES   8   FFFFFFFFFFFFFFFFFFFFFFFFFFFFFFFFFFFFFFFFFFFFFFFFFFFFFFFFFFFFFFFFFFFFFFFFFFFFFFFFFFFFF
FFFFFFFF   FFFFFFFFFFFFFFFFFFFFFFFFFFFFFFFFFFFFFFFFFFFFFFFFFFFFFFFFFFFFFFFFFFFFFFFFFFFFFFFFFFFFF
FFFFFFFFFFFFFFFFFFFFFFFFFFFFFFFFFFFFFFFFFFFFFFFFFFFFFFFFFFFFFFFFFFFFFFFFFFFFFFFFFFFFFFFFFFFFFFFFFFFFFFFFFFFFFFFFFFFFFFFFFFFFF

SECTION (5)

SELECTED GRAPHS OF POTENTIAL TO TIME FOR THE ANODISING PROCESS

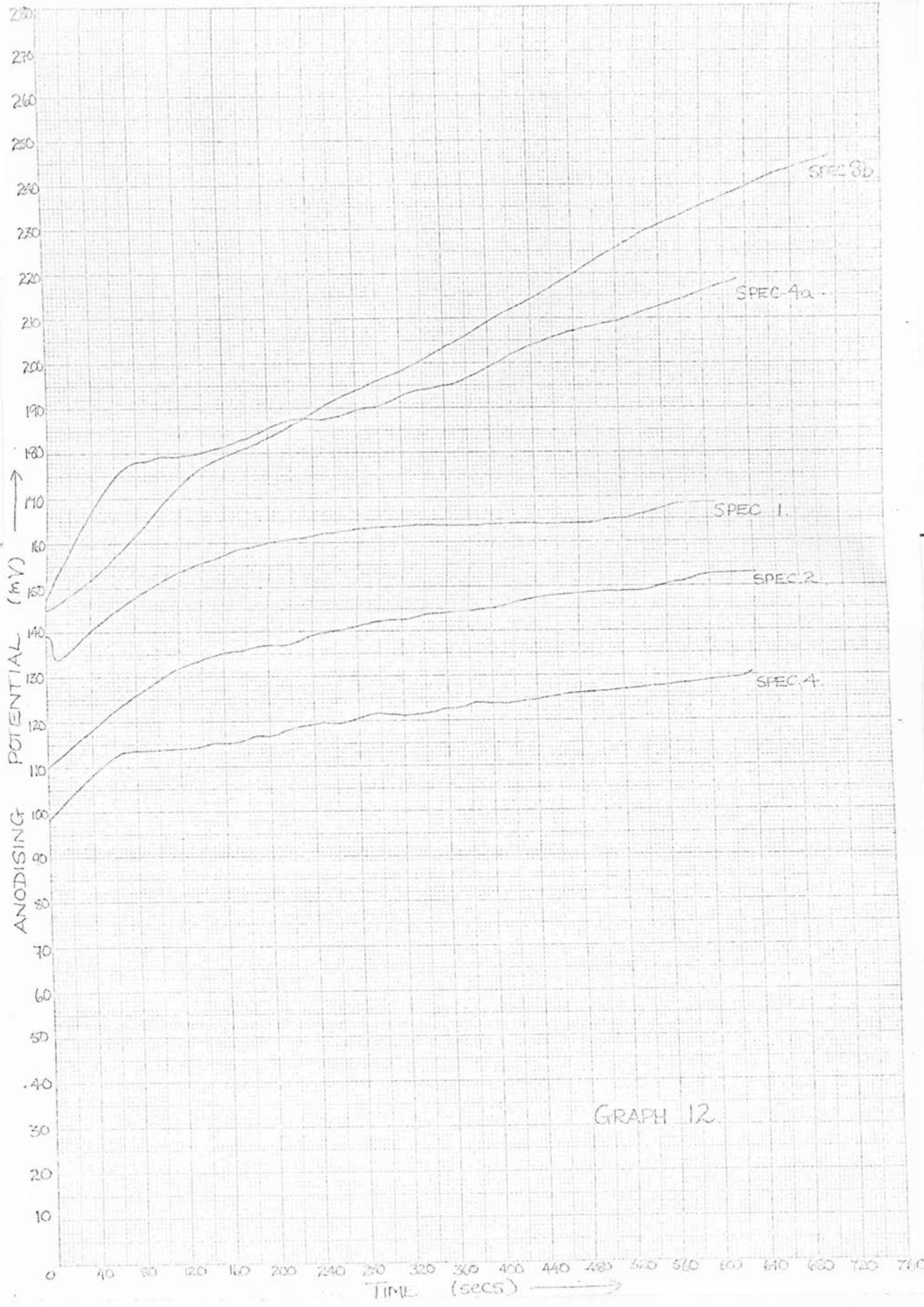
ANODISING POTENTIAL (mV)
TIME (secs)
SPEC 3b
SPEC 4a
SPEC 1
SPEC 2
SPEC 4
GRAPH 12.

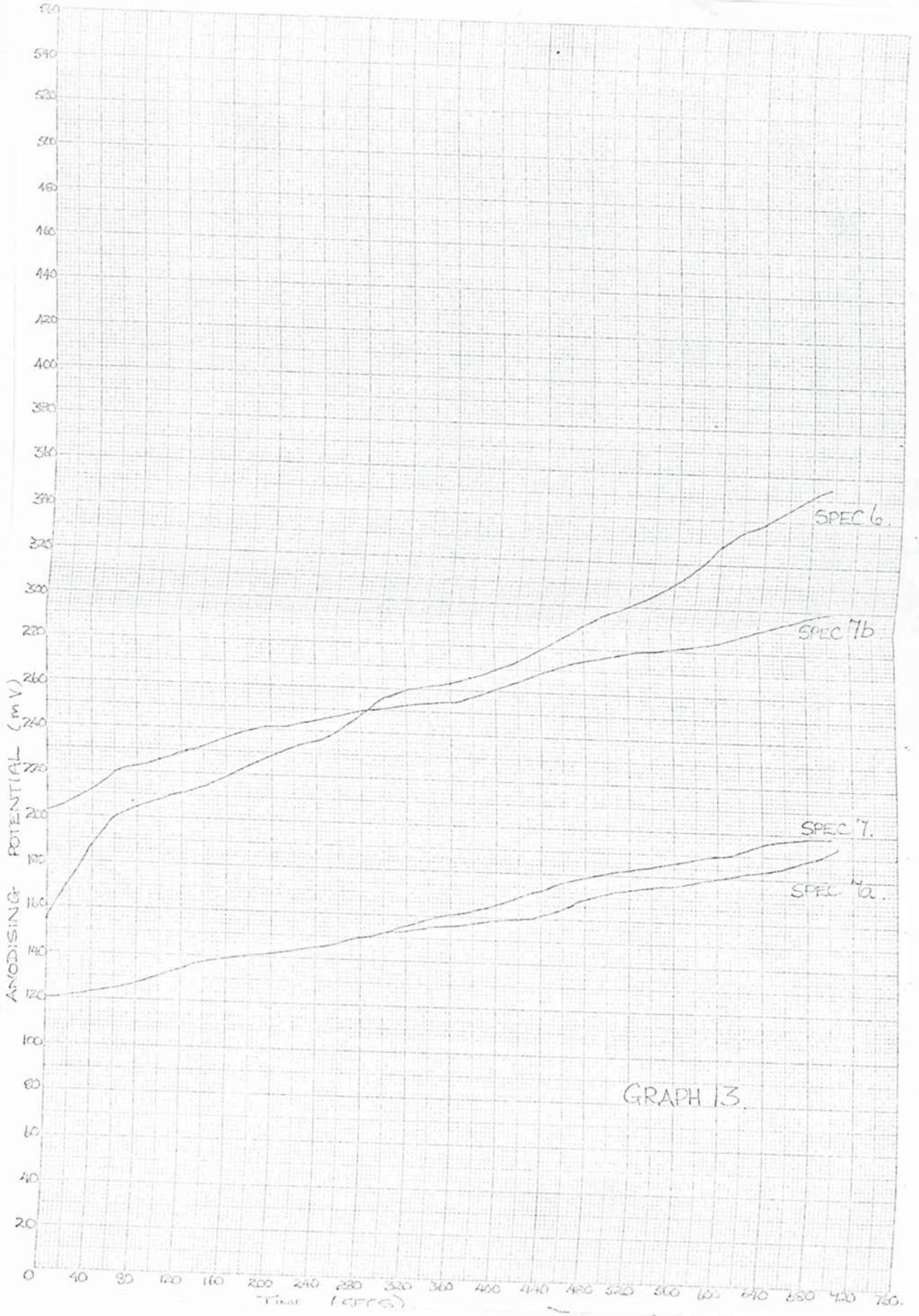
ANODISING POTENTIAL (mV)
TIME (SECS)
SPEC 6.
SPEC 7b.
SPEC 7.
SPEC 6.
GRAPH 13.

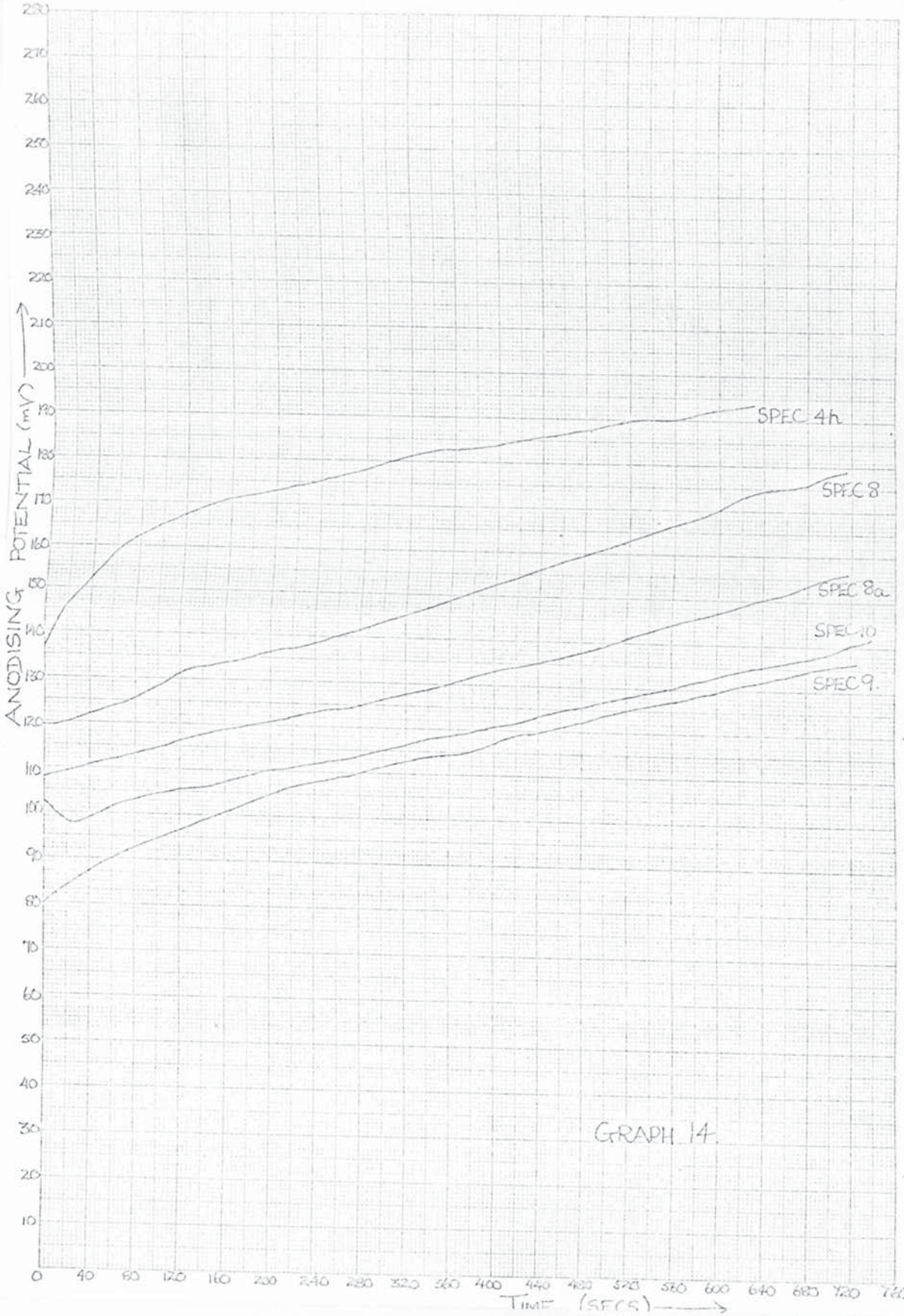
ANODISING POTENTIAL (mV) ——→
TIME (SECS) ——→
SPEC 4h
SPEC 8
SPEC 8a
SPEC 10
SPEC 9.
GRAPH 14.

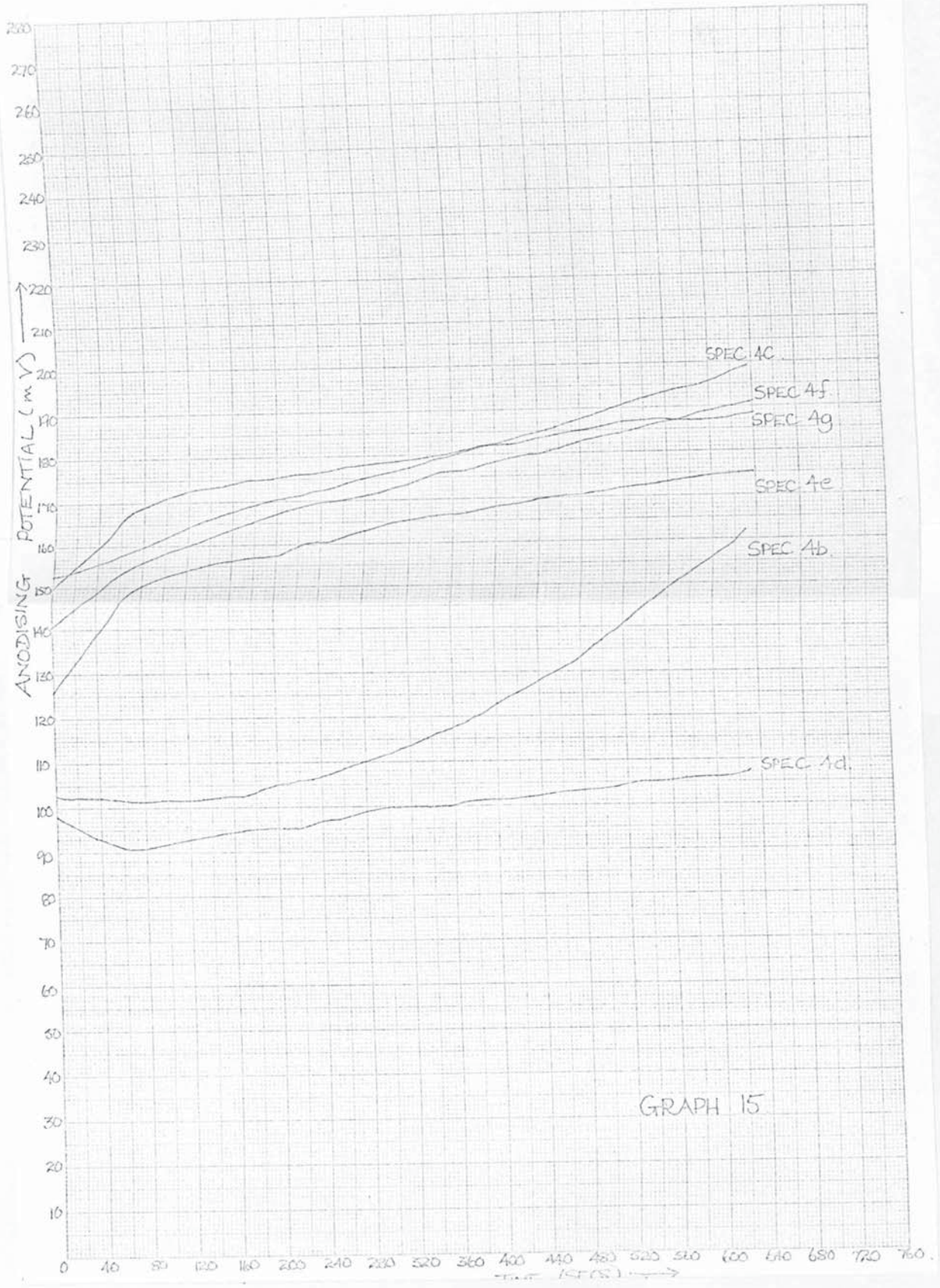
ANODISING POTENTIAL (mV)
SPEC 4c
SPEC 4f
SPEC 4g
SPEC 4e
SPEC 4b
SPEC 4d
GRAPH 15

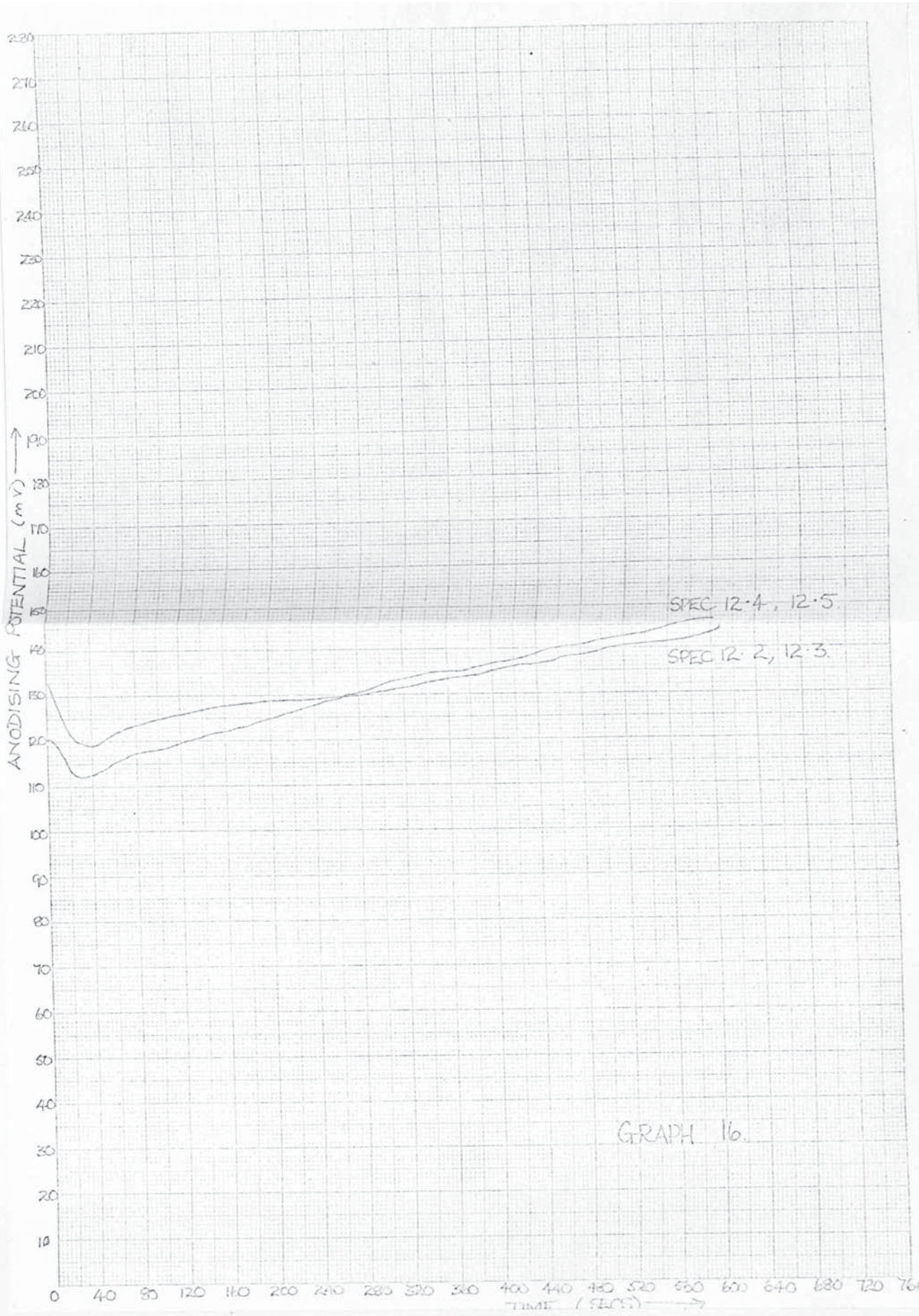
ANODISING POTENTIAL (mV) ——→
TIME (SECS) ——→
SPEC 12·4 , 12·5.
SPEC 12·2, 12·3.
GRAPH 16.

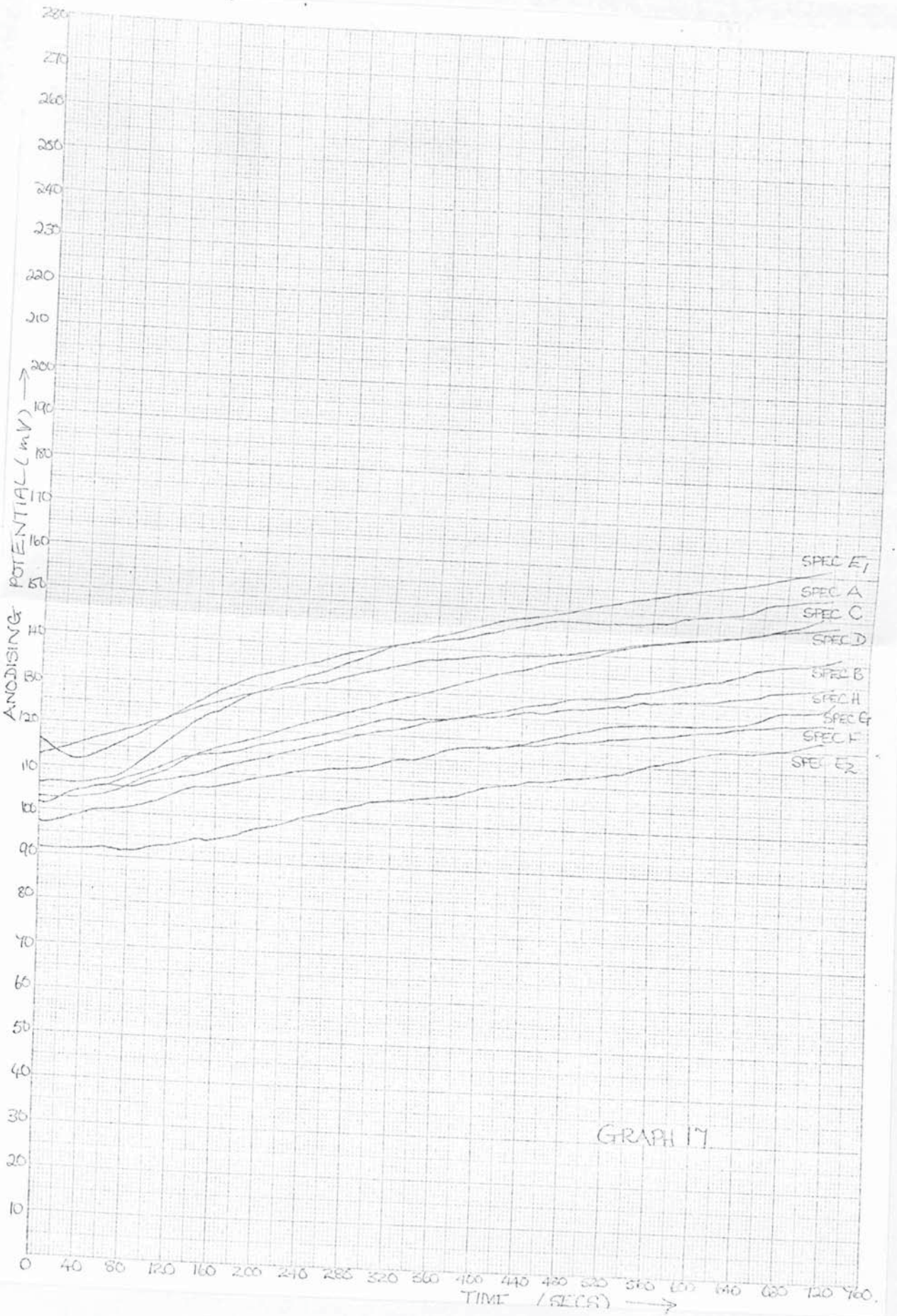
ANODISING POTENTIAL (in V) →
TIME (SECS) →
SPEC E1
SPEC A
SPEC C
SPEC D
SPEC B
SPEC H
SPEC G
SPEC F
SPEC E2
GRAPH 17

SECTION (6)

SELECTED GRAPHS OF POTENTIAL TO TIME FOR THE ELECTRODE AGING AND POTENTIAL STABILISATION PERIOD.

Graph Data Ref. SC/1

Log 2 Cycles x mm, ½ rad 1 cm

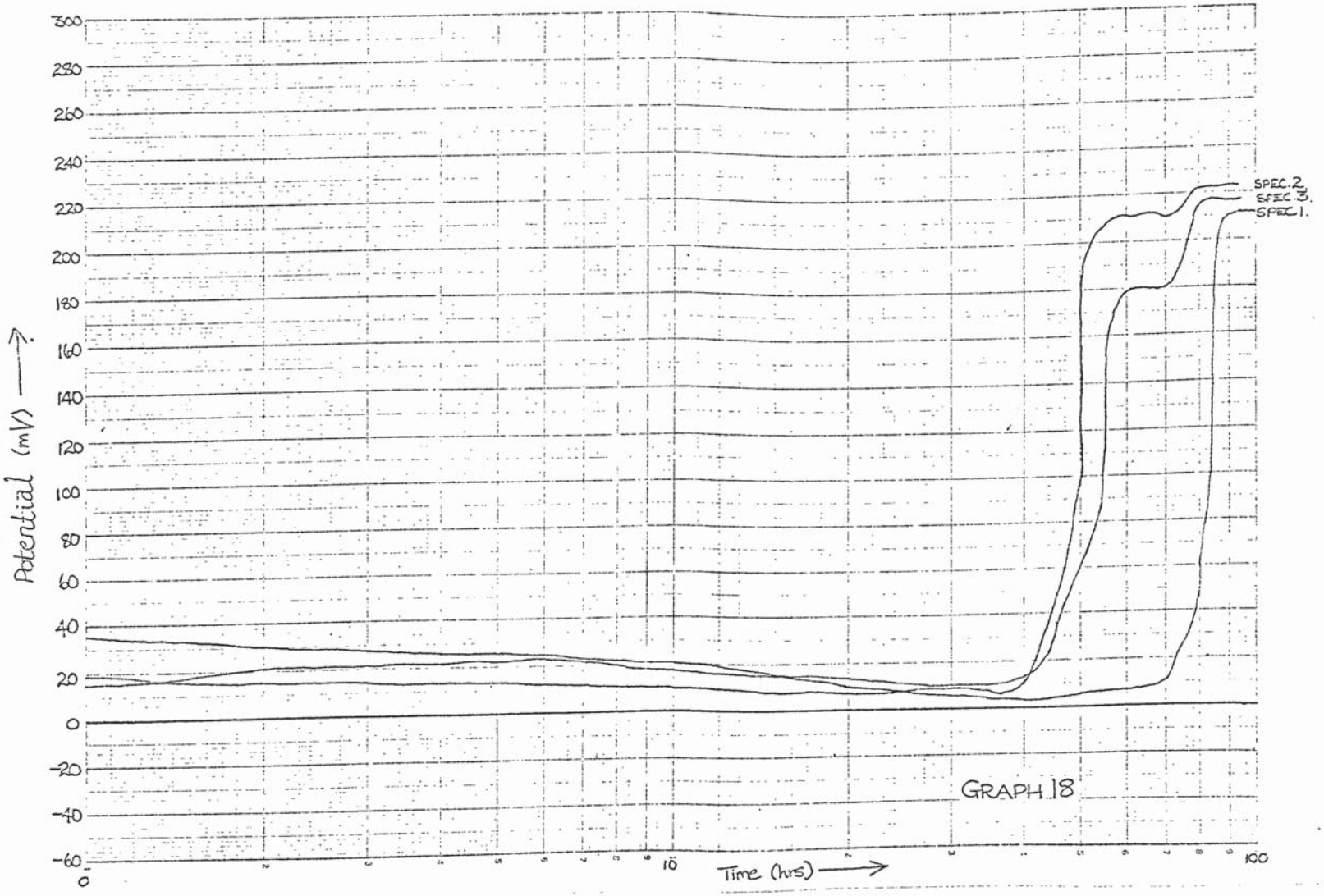

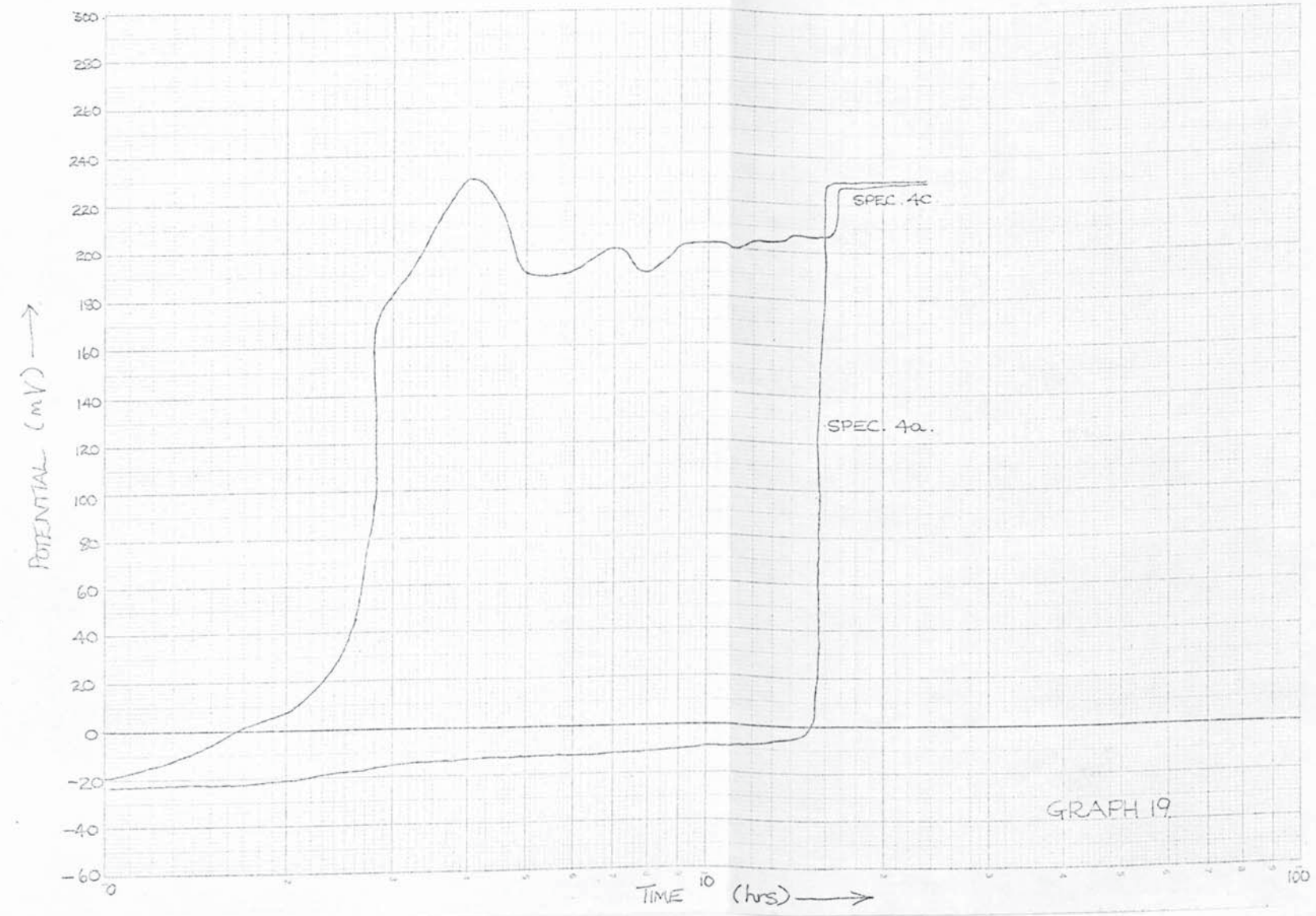
300
280
260
240
220
200
180
160
140
120
100
80
60
40
20
0
-20
-40
-60
POTENTIAL (mV) ⟶
0
10
100
TIME (hrs) ⟶
SPEC. 4c
SPEC. 4a.

GRAPH 19.

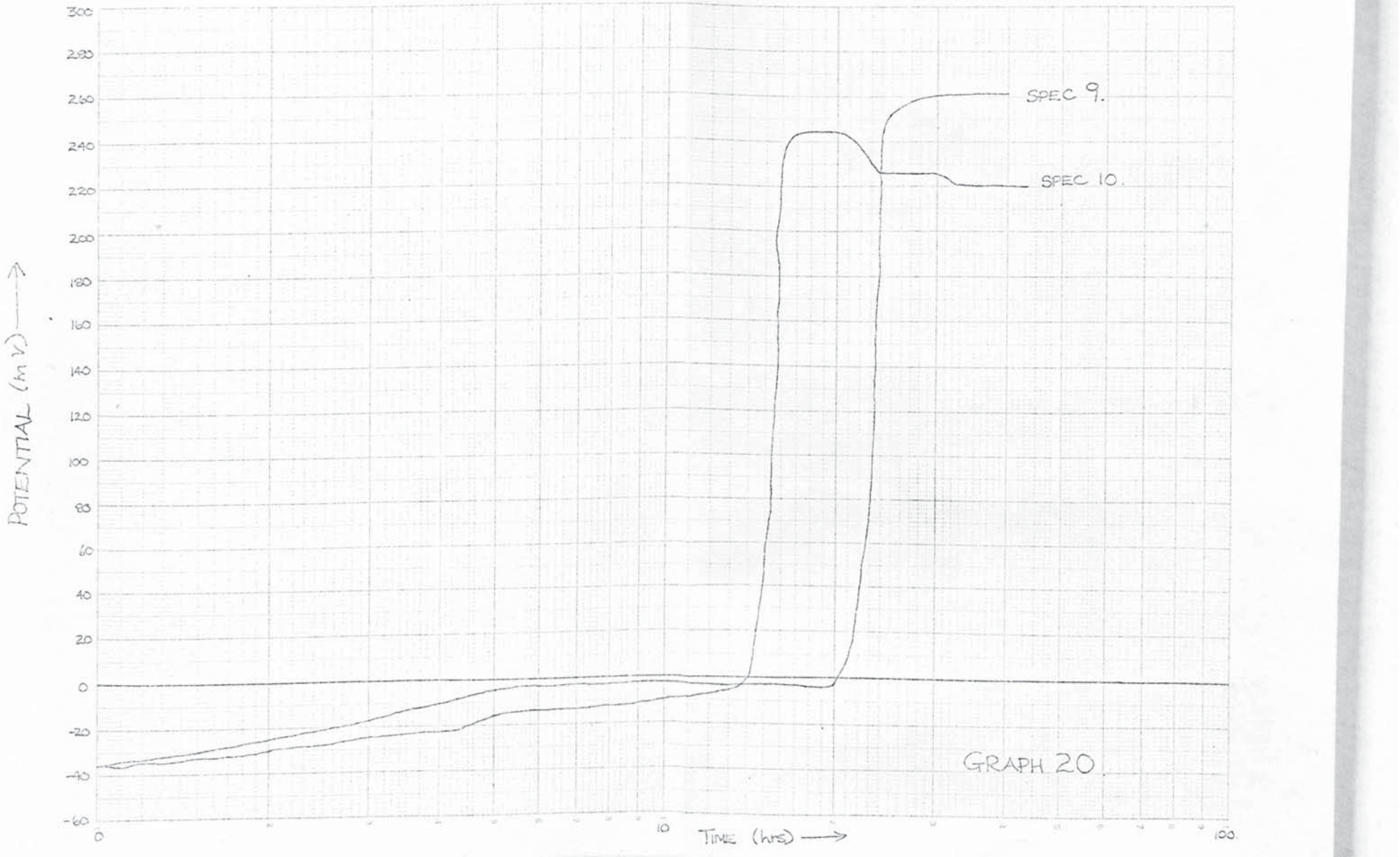
300
280
260
240
220
200
180
160
140
120
100
80
60
40
20
0
-20
-40
-60
POTENTIAL (mV) ——→
0
10
100
TIME (hrs) ——→
SPEC 9.
SPEC 10.
GRAPH 20.

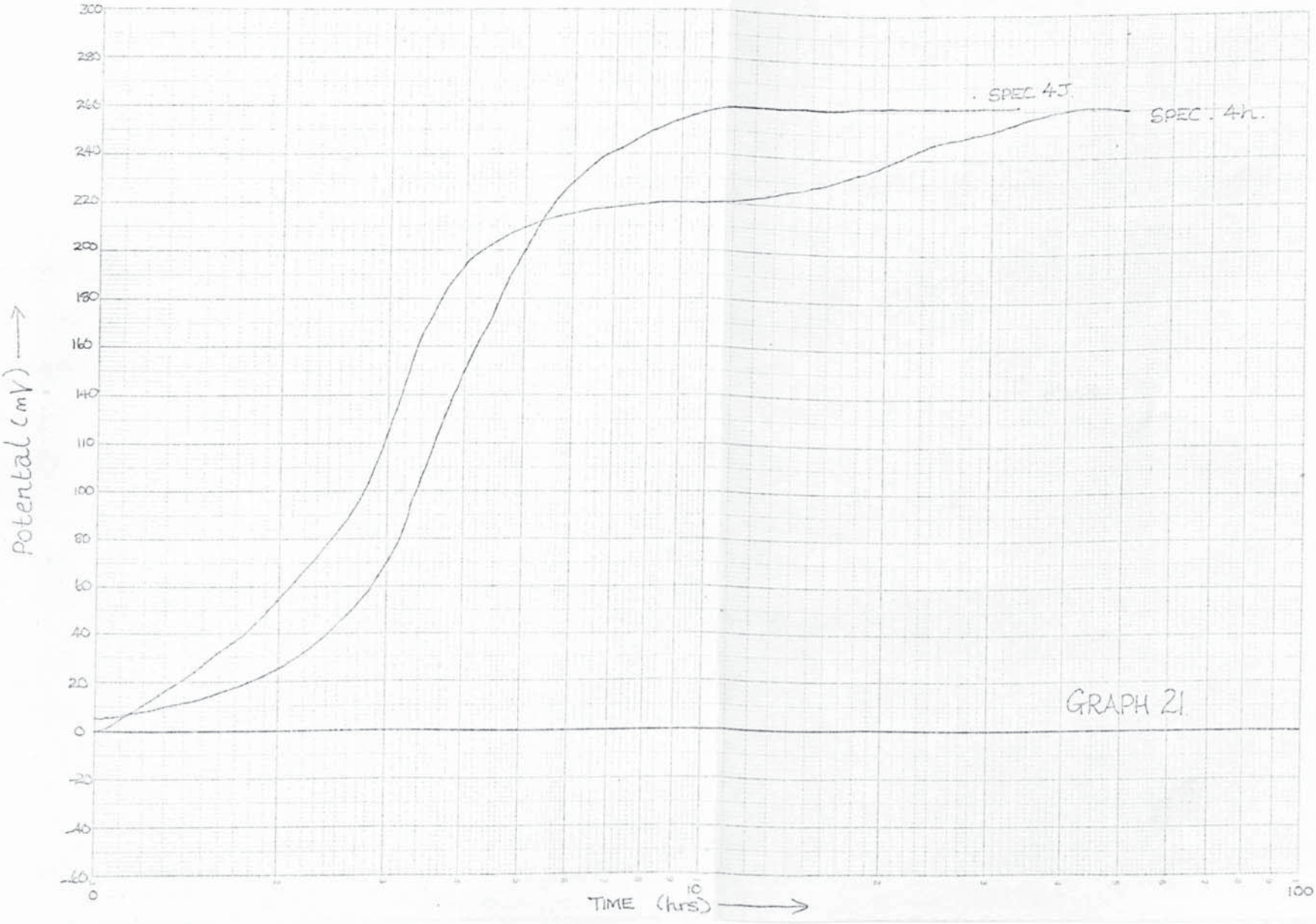
300
280
260
240
220
200
180
160
140
110
80
60
40
20
0
-20
-40
-60
0
10
100
Potential (mV) ⟶
TIME (hrs) ⟶
SPEC 4J.
SPEC. 4h.
GRAPH 21

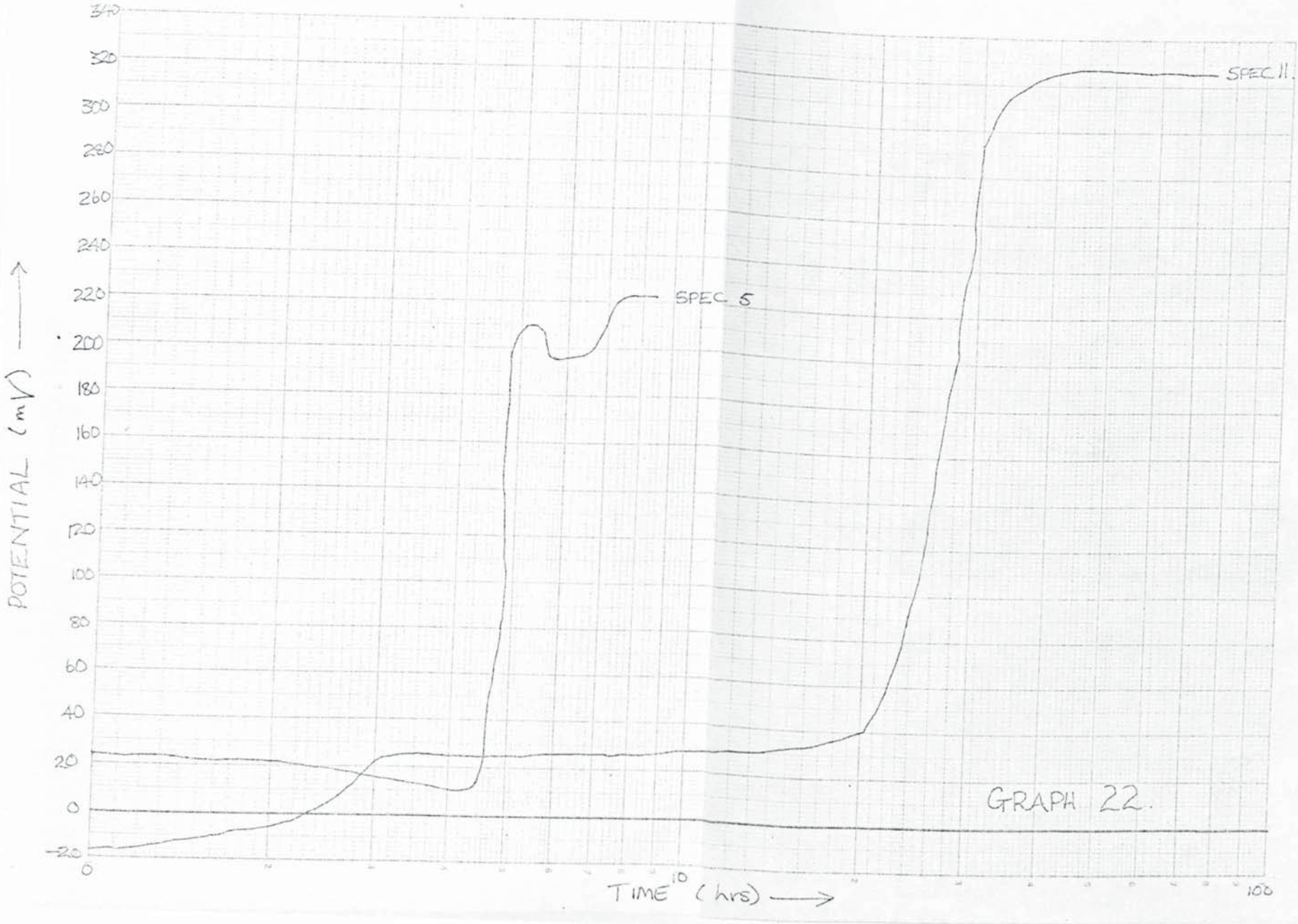
340
320
300
280
260
240
220
200
180
160
140
120
100
80
60
40
20
0
-20
POTENTIAL (mV) ⟶
SPEC 5
SPEC 11
0
10
100
TIME (hrs) ⟶

GRAPH 22.

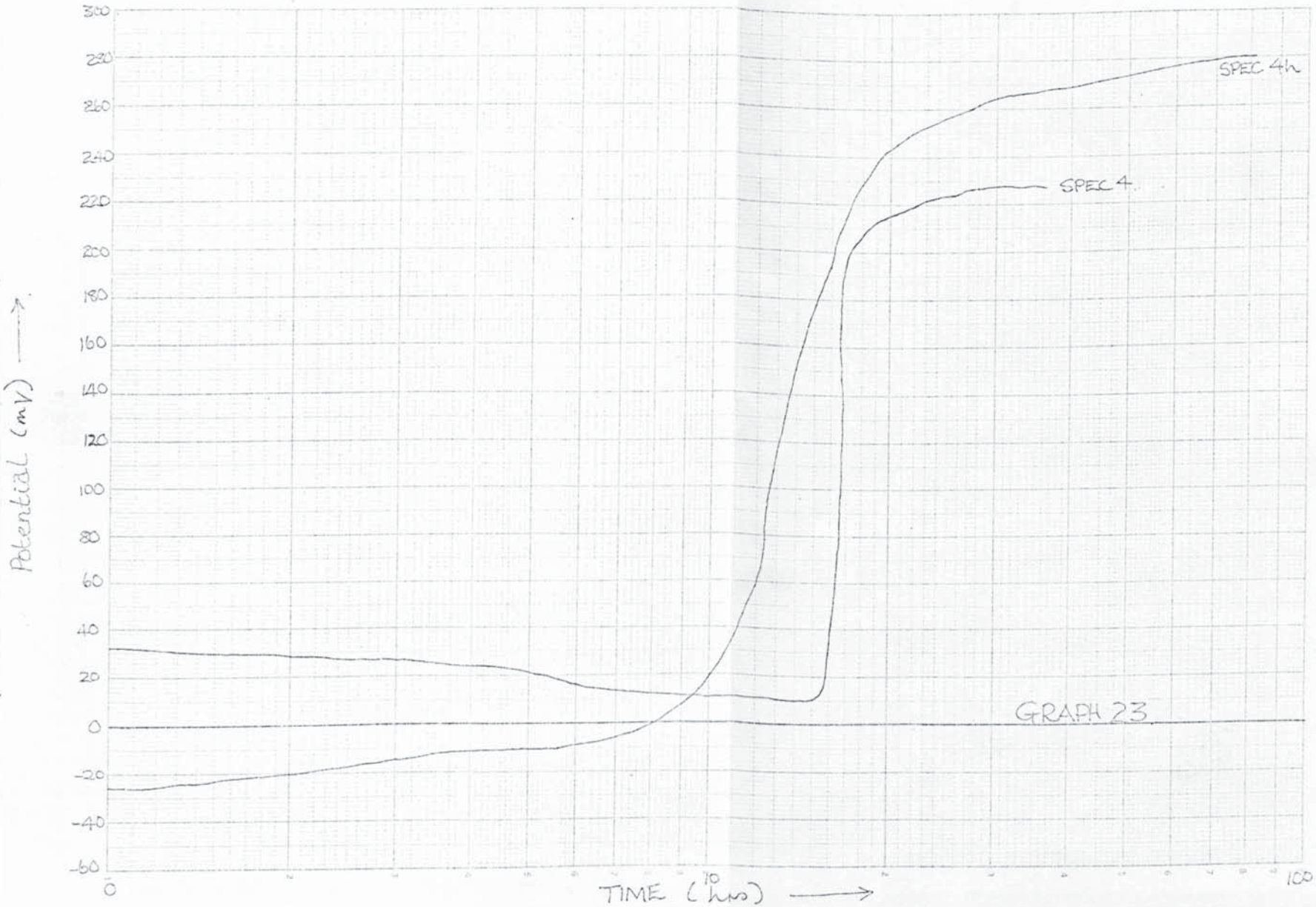
300
280
260
240
220
200
180
160
140
120
100
80
60
40
20
0
-20
-40
-60
Potential (mV) ——→
0
10
TIME (hrs) ——→
100
SPEC 4h
SPEC 4
GRAPH 23

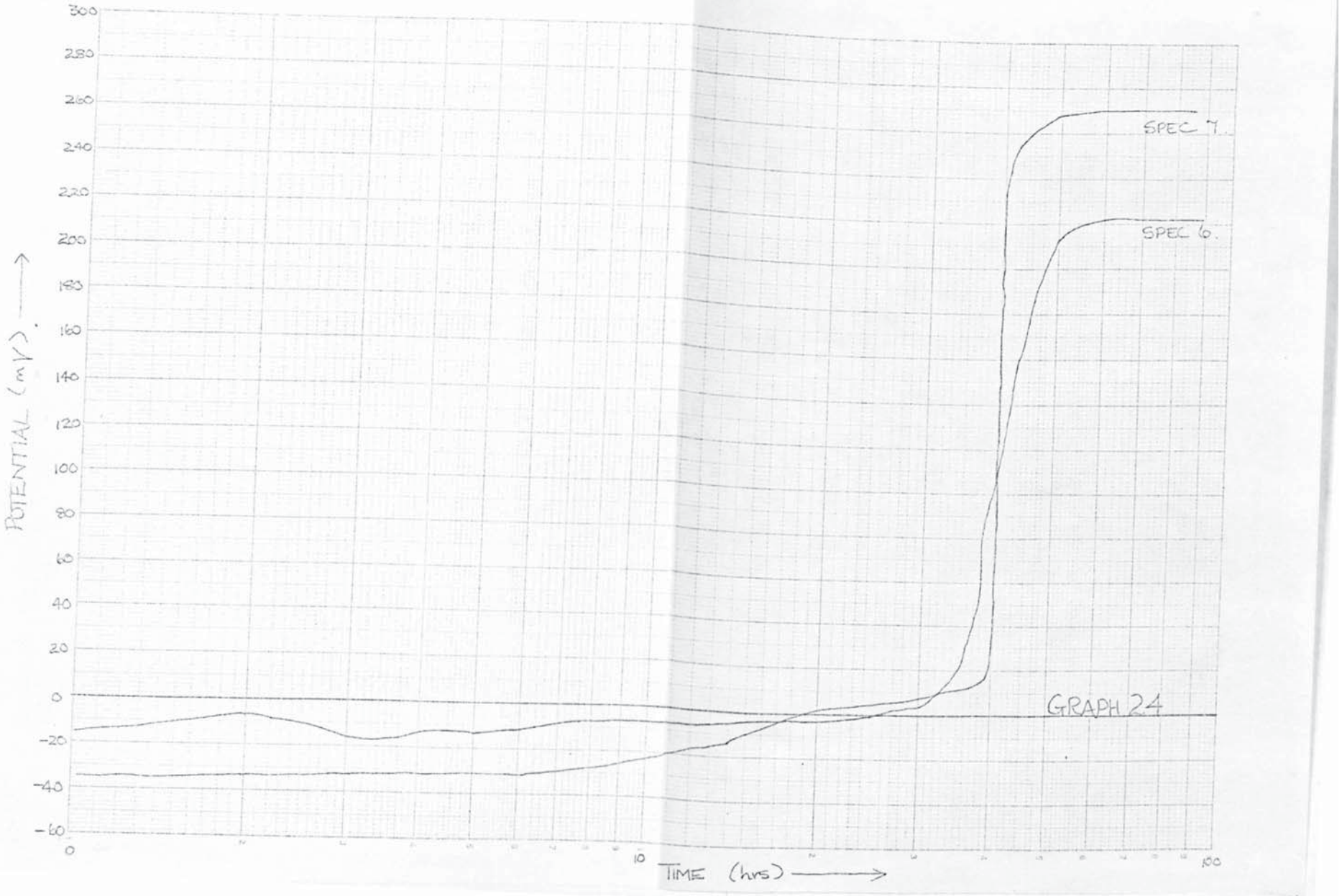
300
280
260
240
220
200
180
160
140
120
100
80
60
40
20
0
-20
-40
-60
POTENTIAL (mV) ⟶
0
10
100
TIME (hrs) ⟶
SPEC 7.
SPEC 6.
GRAPH 24

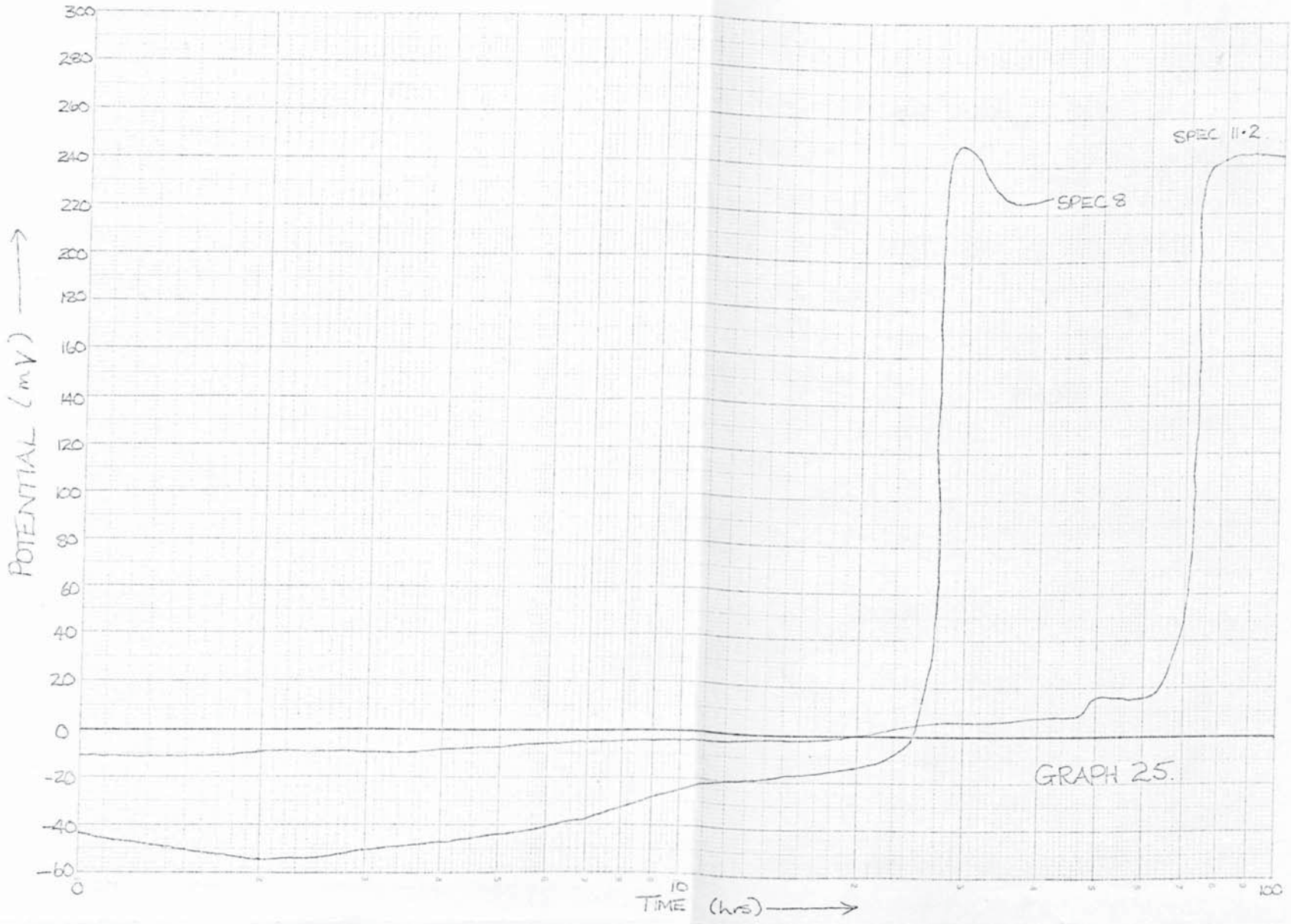
POTENTIAL (mV) ⟶
300
280
260
240
220
200
180
160
140
120
100
80
60
40
20
0
-20
-40
-60
0
10
100
TIME (hrs) ⟶
SPEC 8
SPEC 11·2
GRAPH 25.

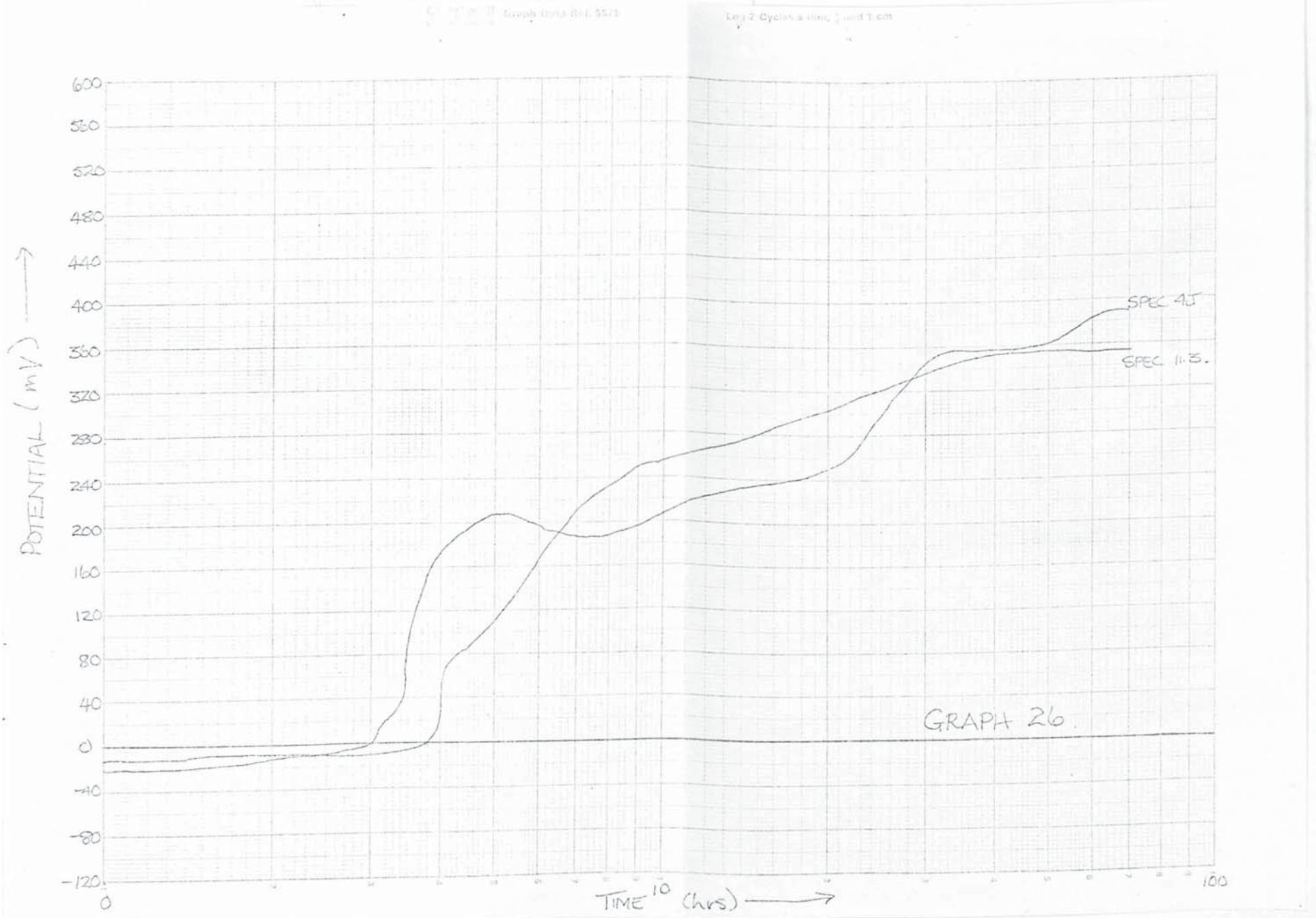
600
560
520
480
440
400
360
320
280
240
200
160
120
80
40
0
-40
-80
-120
POTENTIAL (mV) ⟶
0
10
100
TIME (hrs) ⟶
SPEC 4J
SPEC 11.5.
GRAPH 26.

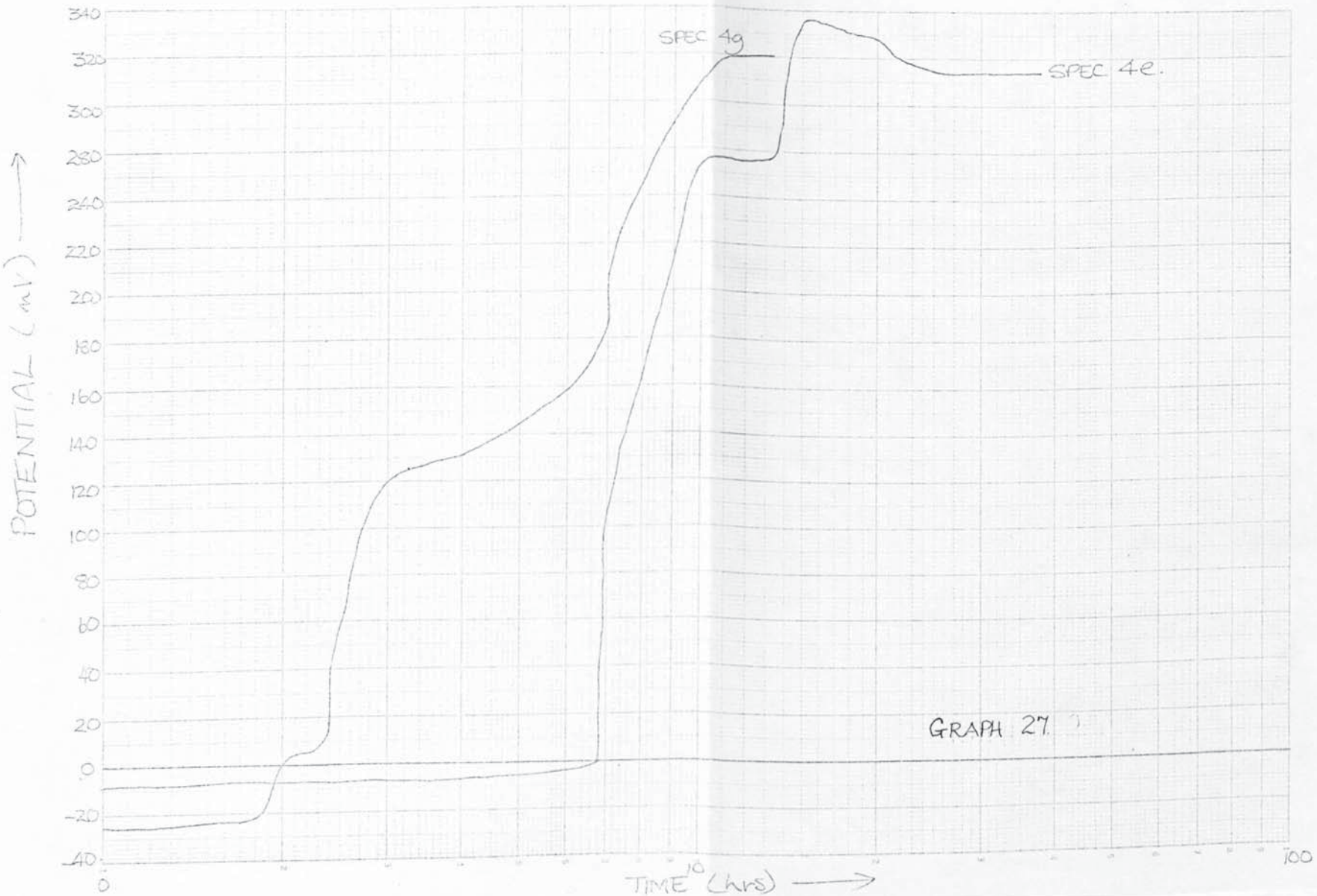
SPEC 4g
SPEC 4e.
GRAPH 27
POTENTIAL (mV) ⟶
340
320
300
280
240
220
200
180
160
140
120
100
80
60
40
20
0
-20
-40
0
10
100
TIME (hrs) ⟶

GRAPH 28.

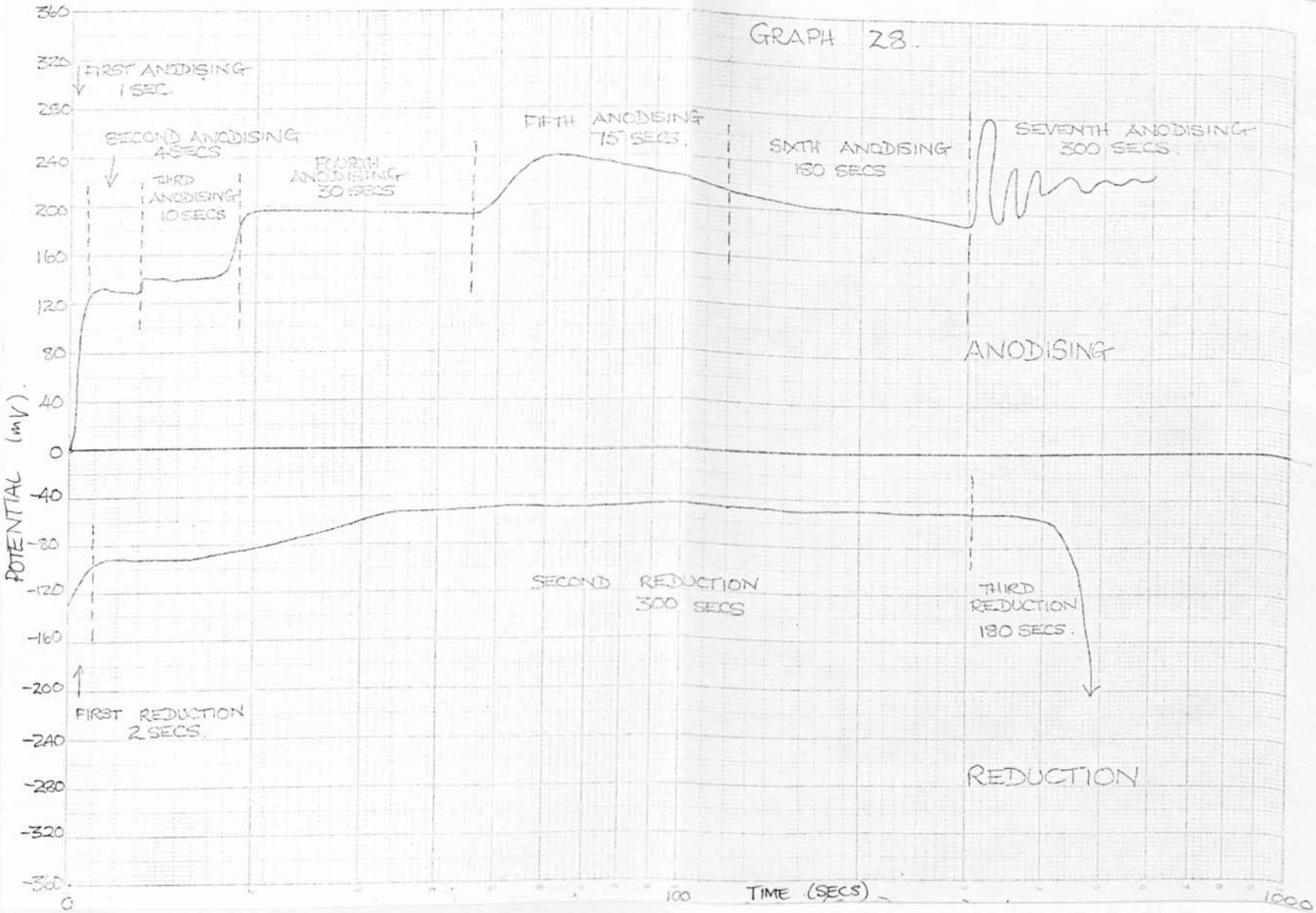
360
320
280
240
200
160
120
80
40
0
-40
-80
-120
-160
-200
-240
-280
-320
-360
POTENTIAL (mV).
FIRST ANODISING 1 SEC.
SECOND ANODISING 4 SECS.
THIRD ANODISING 10 SECS.
FOURTH ANODISING 30 SECS.
FIFTH ANODISING 75 SECS.
SIXTH ANODISING 180 SECS.
SEVENTH ANODISING 300 SECS.
ANODISING
FIRST REDUCTION 2 SECS.
SECOND REDUCTION 300 SECS.
THIRD REDUCTION 180 SECS.
REDUCTION
0
100
1000
TIME (SECS)

CHAPTER 5

DISCUSSION OF RESULTS

SECTIONS OF DISCUSSION

SECTION (I)

THE NUCLEATION AND GROWTH OF PARTICLES AND POROSITY IN THE INITIAL STAGES OF ANODISATION, AND THE STATE OF THE Ag SURFACE.

The anodic silver chloride film nucleates and grows to form a thin initial layer on the surface of the silver. This first layer is made up of small particles nucleating on the surface, and then growing together to form a coherent film.

Fleishmann (23) talks about discrete centres nucleating and growing over the surface until passivation, and Muller (43) also talks about film nucleation with the layer spreading to uniform thickness when growth in depth starts.

Examination of the silver surface by SEM, after anodising, revealed the nature of the nucleation and growth mechanism. It was found that the small nodules of silver chloride formed in association with irregularities on the silver surface, such as scratch or rolling lines or pits etc.

These nodules formed at the edges of the deformations on the surface, as can be seen in Pic 8 to 11, where the particles arranged along scratch lines and pits on the silver surface can be seen.

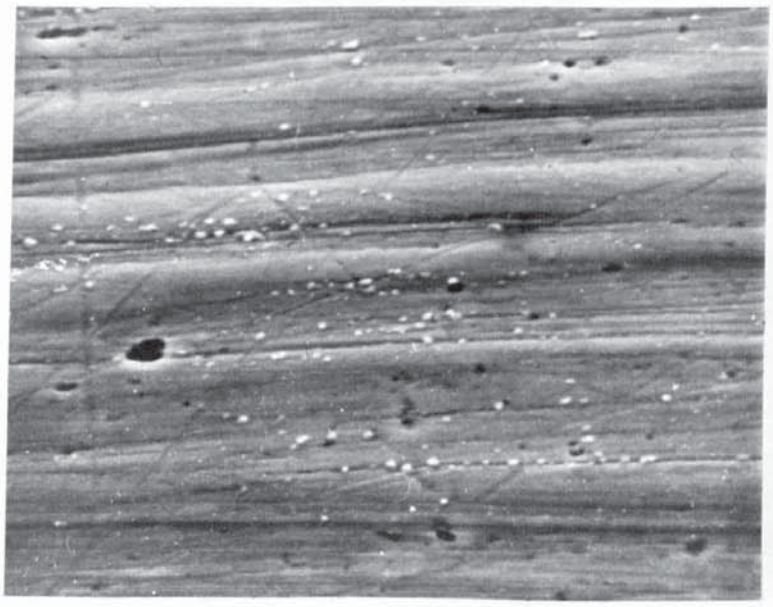

PIC 8 X 5K

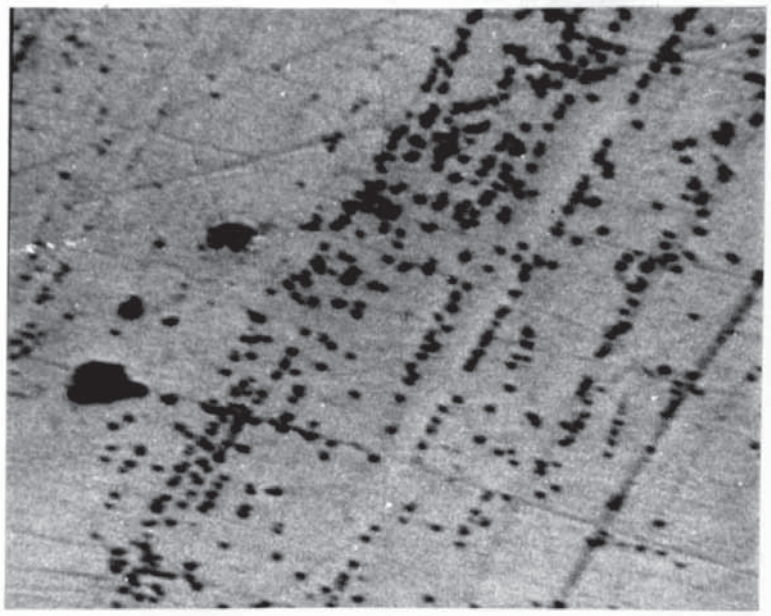

PIC 9 X 2K

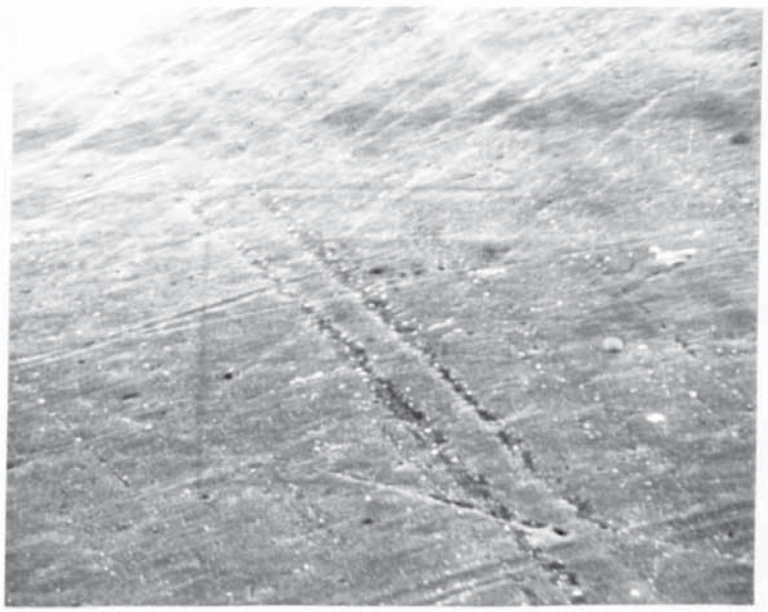

PIC 10 X 2K

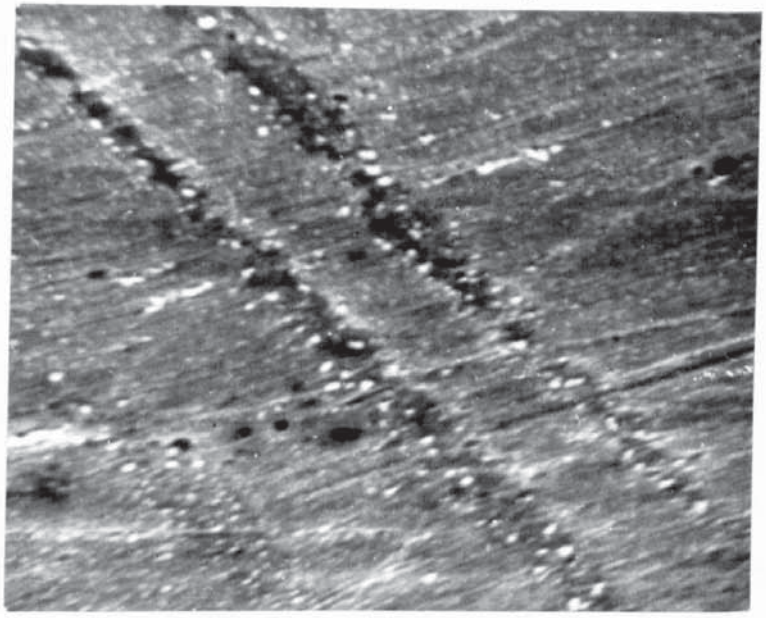

PIC 11 X 5K

In general two distinct particle types are seen in this layer, the MI and M5 type particles. The MI particles tend to be small and oval, with the particles long axis mainly at right angles to the direction of the scratch line that the particles are arranged along.

In Pic 12 we can see several MI particle examples.

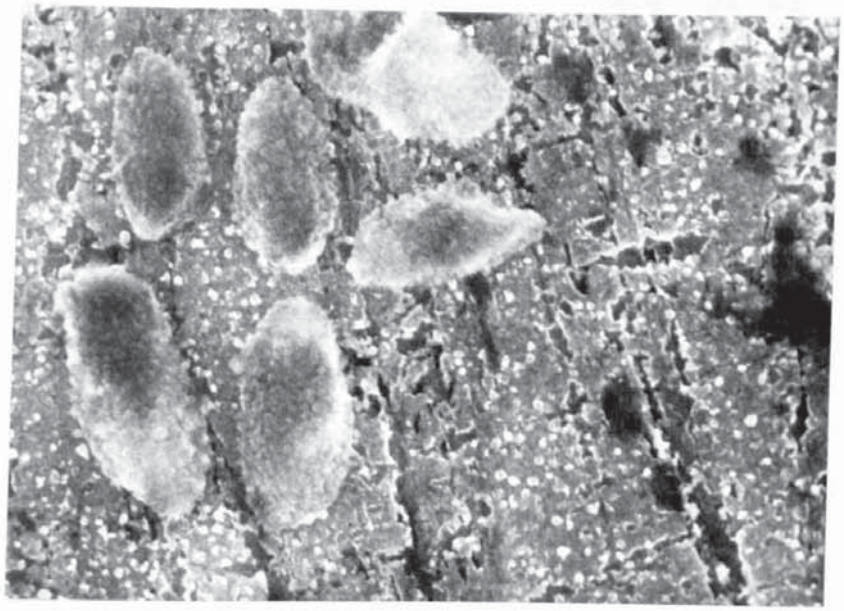

PIC 12 X 60K

This picture shows also the method of construction of these particles from much smaller nodules, the K type building blocks, and this will be discussed later. The main particle in the primary layer is the M5 particle. This particle is much larger than the MI particle and is roughly spherical. Examples of this can be seen in Pic 13 where the M5 particles are scattered on the silver surface, and also in Pic 14.

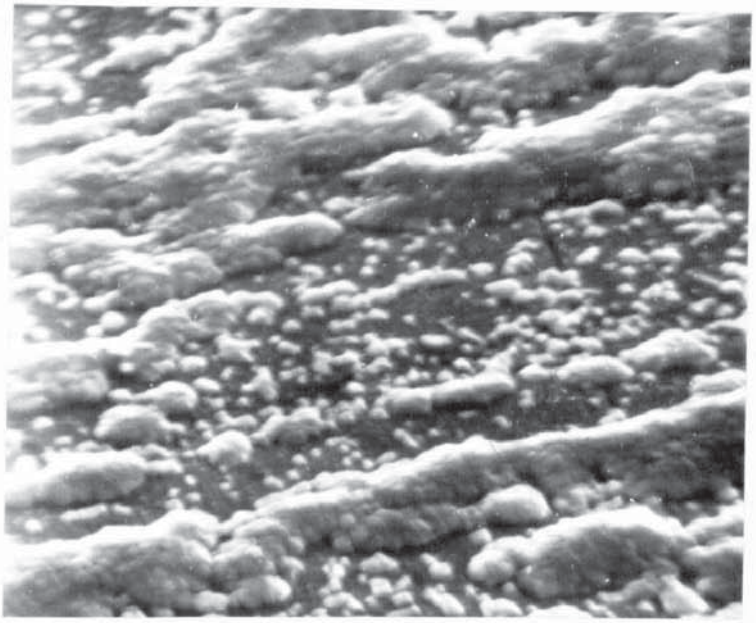

PIC 13 X 5K

PIC 14 X 20.2K

In this case the silver has been dissolved away after anodising, to leave the film free for analysis, and this picture is of the film base.

There seems to be a definite procedure followed in the nucleation and growth of the initial layer, with the MI particles nucleating at the edges of the irregularities on the silver surface. This is presumably due to the higher energy of dissolution at these points due to the presence of dislocations. The silver is easier to dissolve and transport from these sites, and deposition occurs at the closest point available on the silver surface, that is, the edge of the pit or scratch.

After a short period the rate of nuclei formation begins to diminish and the particles begin to pile up in certain areas corresponding to surface deformations, where the dissolution rate is high, forming growth bands as seen in Pic 15.

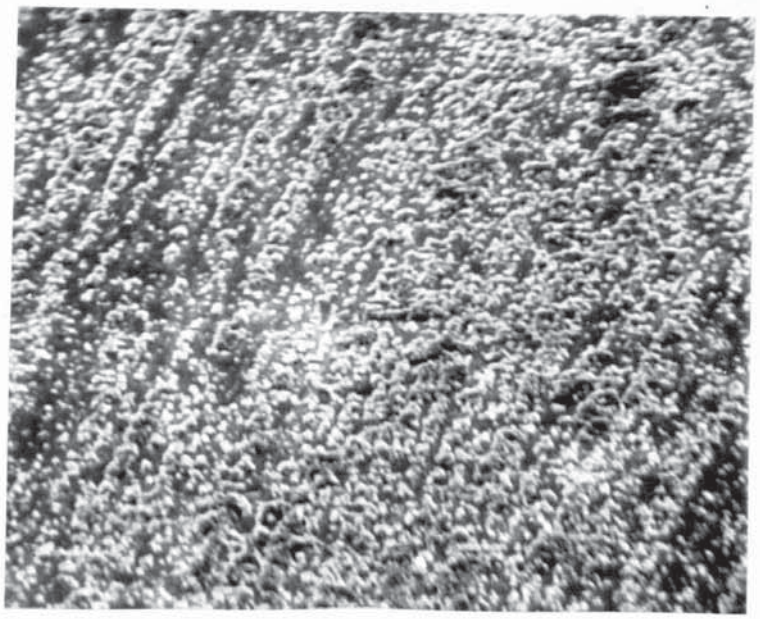

PIC 15 X 2K

These then begin to fill out as seen in Pic 16 and 17, until the surface is virtually covered, as seen in Pic 18, in a thin coherent porous film of silver chloride.

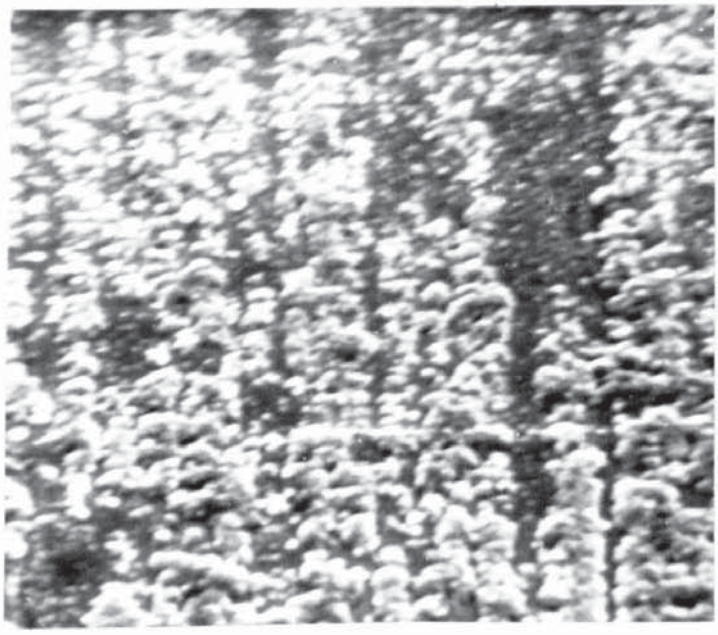

PIC 16 X5K

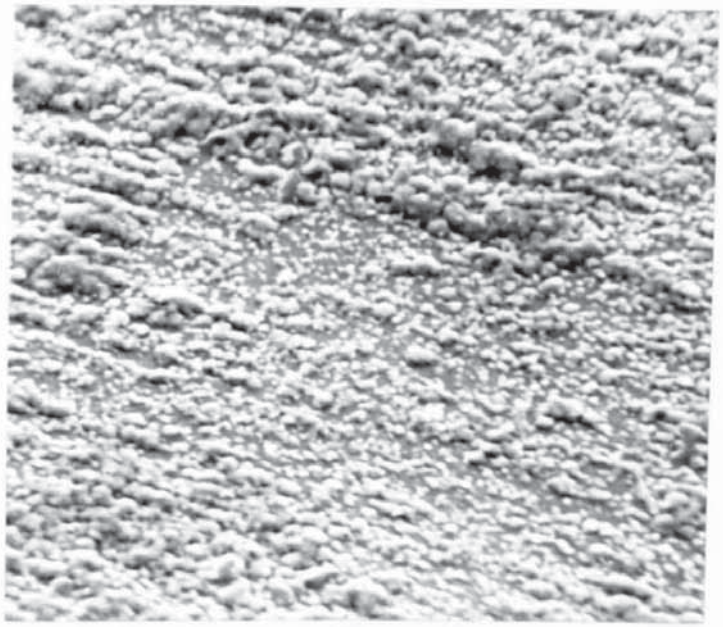

PIC 17 X 2K

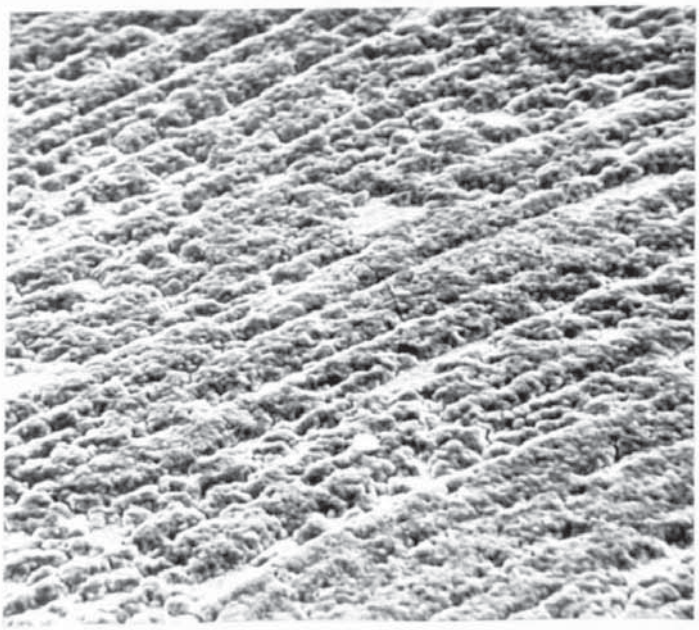

PIC 18 X 1K

It can be seen in Pics 19 and 20 that the layer is made up of growth bands of silver chloride with distinct troughs in between each band.

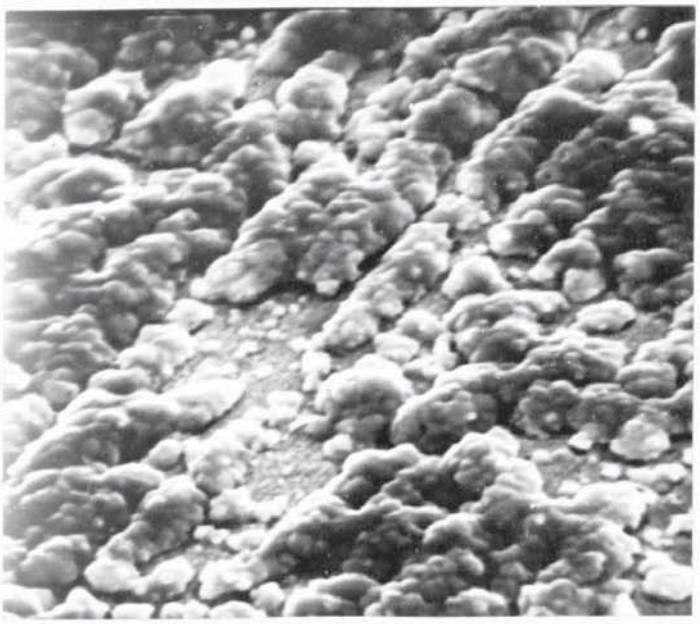

PIC 19 X 5K

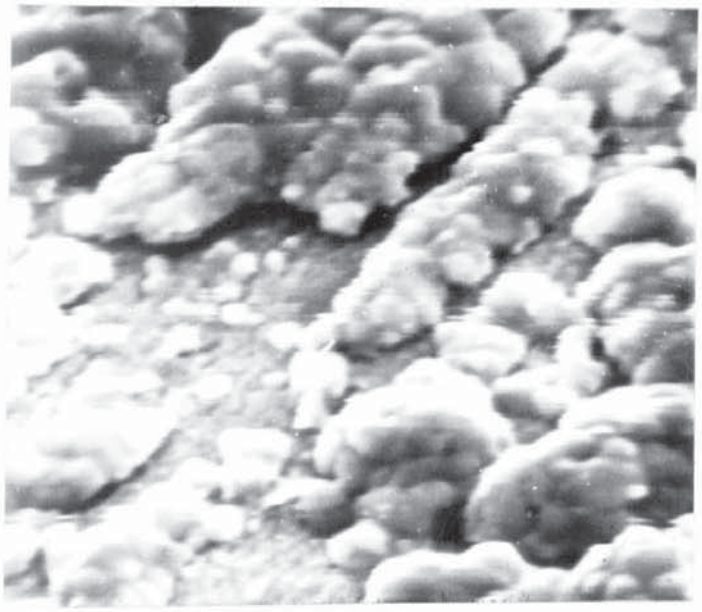

PIC 20 X 10K

The bands themselves are made up of small nodules of M5 type particles which can be seen lying singly on the surface. Under favourable conditions M1 oval particles can be seen in conjunction with the M5 particles. If anodising continues, then after the coherent initial porous layer has been laid down, further growth continues, not laterally as before, but vertically by the nucleation of a second layer on top of the first. This process will be discussed in the next section, and the nucleation and growth process for the first layer will now be looked at in more detail.

Katan et al (19) reports that at the beginning of nucleation, holes (presumably dislocation sites) appear in the silver, and the silver chloride deposits around the hole mouths. At this stage the number of nucleation centres is roughly the same whatever the anodising conditions.

From the results gained in this work, the main nucleation centres would seem to be the K type building block particles, as seen in Plc 12, which form very quickly after the start of anodising and cover the surface fairly evenly. If the chronopotentiometric graphs for the anodising process are examined, i.e. graphs 12, 14, 16, then a sharp drop, then recovery, in the potential is seen during the first few seconds of anodising. This is also reported by Lal et al (24, 25), and is suggested as being due to supersaturation at the surface at the initiation of the process. If this is so, then the level of silver chloride in solution rises to a point where nucleation can occur, assisted by swarm or embryo formation (20) in the solution.

Once the K type particles have deposited, then the level of silver chloride in solution drops drastically, and growth proceeds at the nearest point to the source of silver dissolution. This fits the report by Vermilyea (22) that nuclei formation occurs only for a short period after anodising starts, due to chloride ion depletion near the electrode; the driving force for continued nucleation therefore decreases and stops with nuclei of uniform size.

As again can be seen from Plc 12, the mode of growth is by the K type particles building up larger nodules of the MI type, as seen in Fig 7.

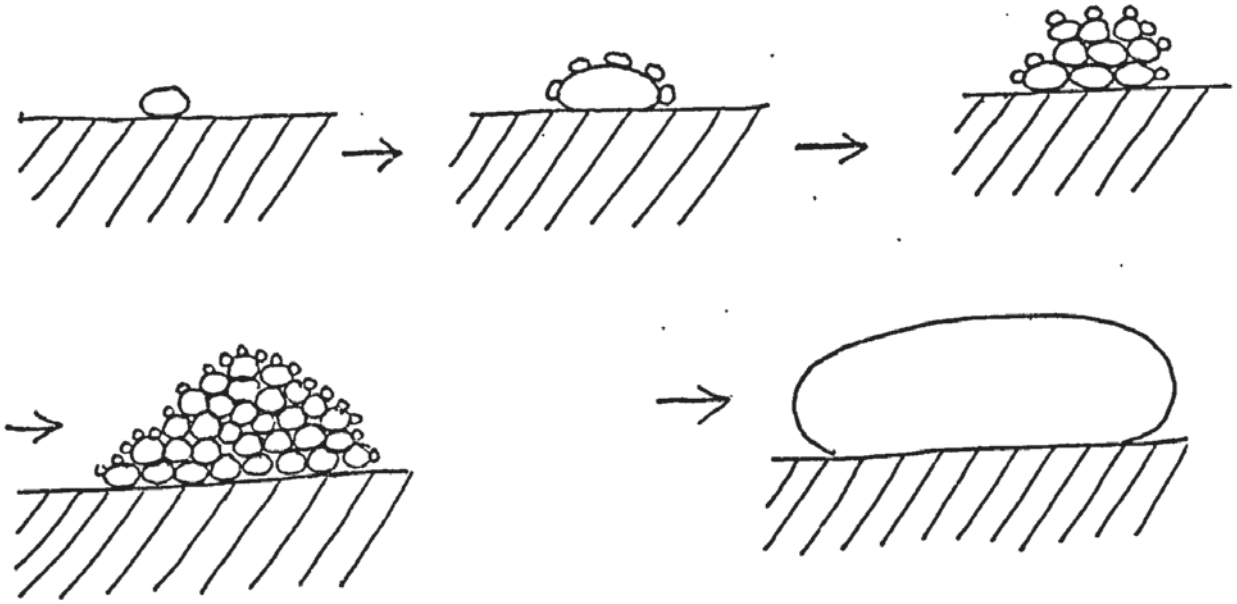

Fig 7

This is similar to the growth reported (14) of Cu Cl_2 on Cu. Here growth centres of various sizes are formed (like the M1 and M5 type particles perhaps), showing progressive nucleation, and the particles are also reported to have smaller individual nodular particles growing on their surfaces.

After a further period into anodising, the M5 particles appear. They are much larger than the M1 type, but are presumably a development of them and start to appear at the areas of highest silver chloride concentration. The spherical M5 particles would be formed by an increase in radius of the M1 particles by greater deposition of silver chloride from above the particle, i.e. from solution, as in Fig 8.

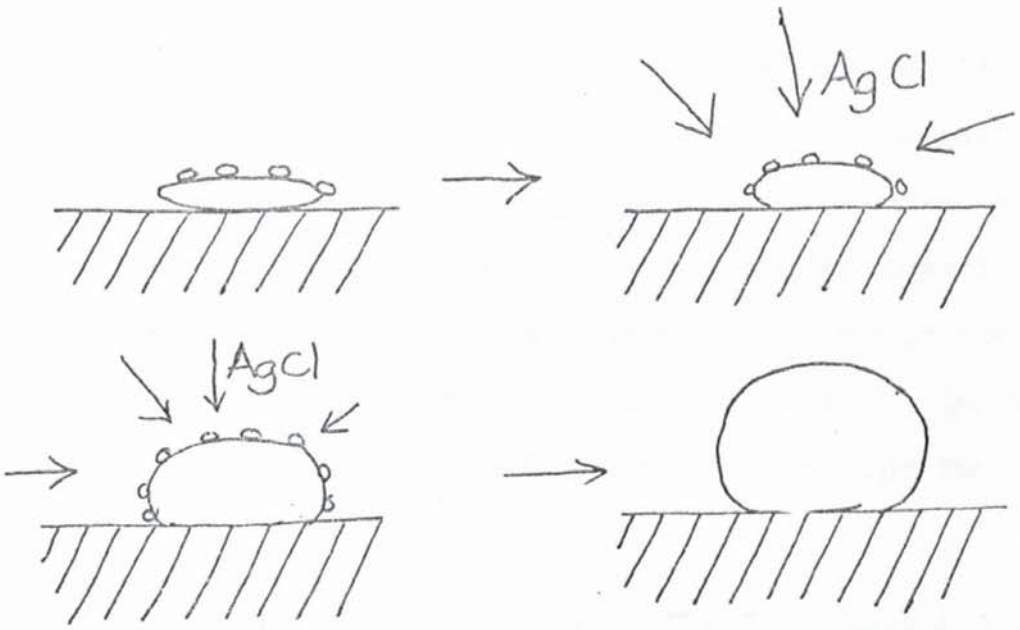

FIG 8

The spherical nature of silver chloride deposits, without crystal planes but with rounded smooth surface, is reported by Katan et al (19). An example of the nodular nature of the M5 particles, and its close relationship to the MI and K type nodules can be seen in Pic 21.

PIC 21 X 3001

To explain this type of formation, a particular type of dissolution, transport and deposition mechanism must be presumed. The porous nature of the whole film does not point to a solid phase transport mechanism of silver ions from the silver to the film surface, and the outward growth of the chloride film, with layer upon layer resting on top of one another progressively does not point to inward movement of chloride ions to form material at the metal/oxide interface, as happens in the anodisation of aluminium.

It would seem likely therefore that a solution transfer mechanism of complex ions is the most important transport process. Vijh (16) proposes a mechanism of metal chloride ion complex formation as below.

$M + n\,Cl \rightarrow M(Cl)_n + ne$	General reaction and deposition
$M(Cl)_n \rightarrow M^{n+} + n\,Cl^-$	Dissolution
$M^{n+} + m\,Cl^- \rightarrow (Mn\,Clm)^{(m-n)e}$	Complex formation and transport
$(Mn\,Clm)^{(m-n)e} \rightleftarrows M^{n+} + mCl^-$	Dissociation.

Dissociation in this case provides free chloride ions to participate in the metal/chloride complex formation cycle. With this mechanism Vijh states that it is the mode of transport which dictates the structure of the eventual film. Indeed this must be so, in no other way but by a similar transport mechanism to the above could the film porous structure be gained.

Work carried out by Giles (31) on the anodisation of silver and the reduction of the silver chloride films formed, supports the theory of solution phase diffusion of $AgCl_{(n+1)}^{-n}$ ion complexes, where n = 0, 1, 2, 3, and growth then is from supersaturated solution.

An experiment was carried out by the author to verify these theories and those of Katan to be mentioned later.

In this a fine nylon thread was attached to the bare silver surface before anodising, and then examined in situ when anodising was complete. If solution transport was the correct mode then fine particles of silver chloride should be found to have deposited on the nylon thread, and this, as seen in Pic 22, was seen to be the case.

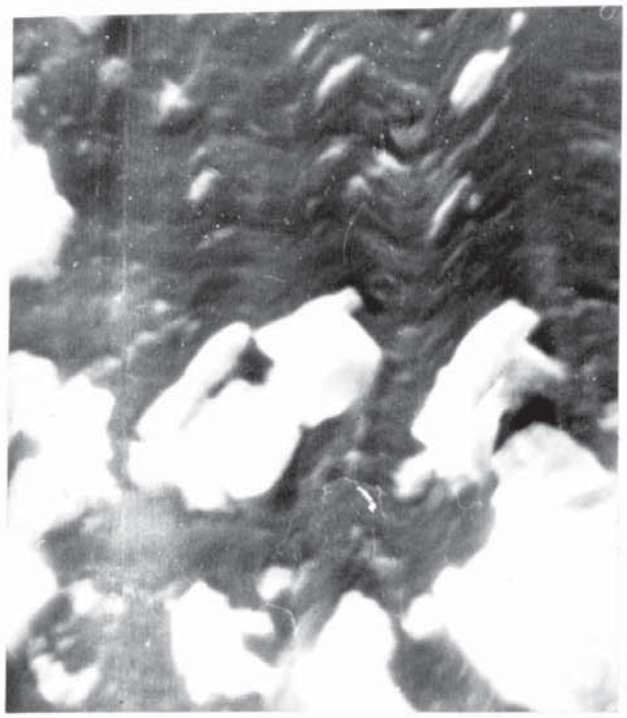

PIC 22 X 11K

It can also be seen, as in Pic 23, that the silver chloride has grown up the side of the thread and that when the thread is detached, as in Pic 24, that the silver surface beneath, where the thread touched, is devoid of particles except for a fine scattering of primary nuclei.

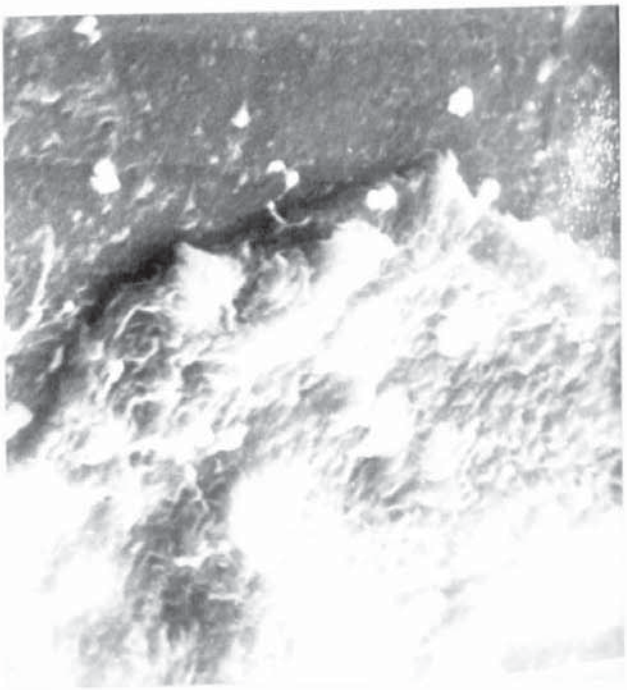

PIC 23 X 5.5K

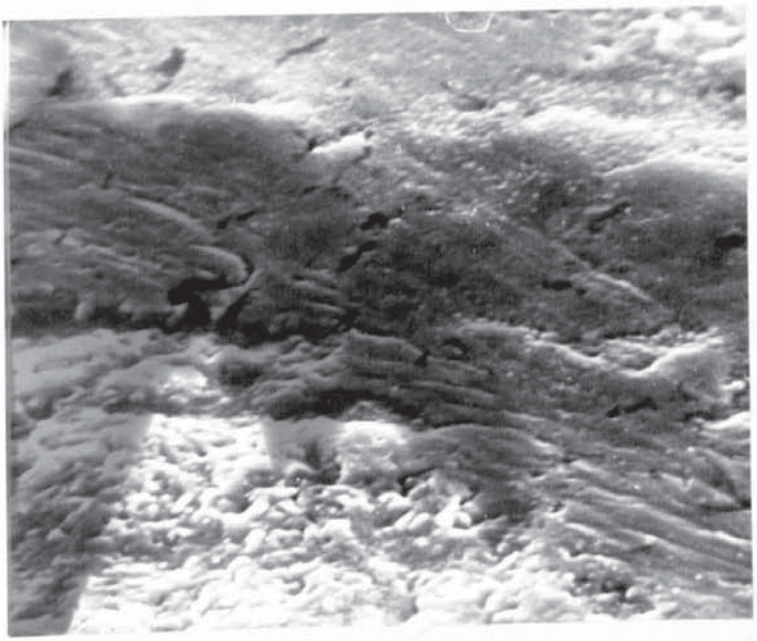

PIC 24 X 5.3K

Katan's work (20) on the formation of silver chloride provided the mechanism

$Ag \rightarrow Ag^{+} + e^{-}$	Dissolution
$Ag^{+} + (n+1)\ Cl^{-} \rightarrow Ag\ Cl_{(n+1)}^{-n}$	Complex formation
$Ag\ Cl_{(n+1)}^{-n}{}_{(a)} \rightarrow Ag\ Cl_{(n+1)}^{-n}{}_{(b)}$	Solution transport
$Ag\ Cl_{(n+1)}^{-n} \rightarrow Ag\ Cl + n\ Cl^{-}$	Deposition

where evidence for the solution phase transport was suggested as being the overhang(h) of the bulbed mounds of silver chloride, as seen in Fig 9.

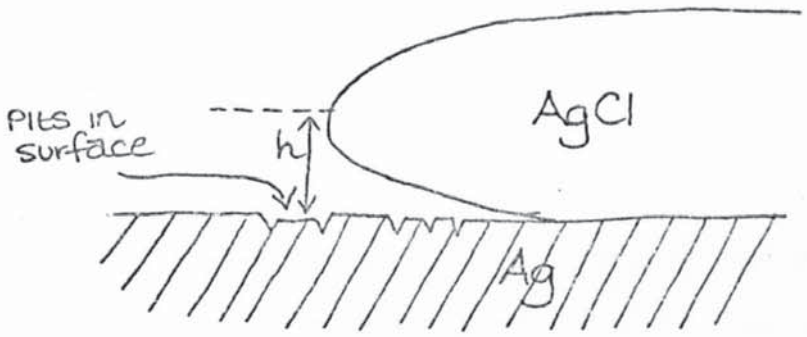

FIG 9

These bulbed mounds grow to a nearly constant thickness with the growing edges of the particles nearest the dissolution sites, i.e. the pits found beneath the overhang. This suggests that $Ag\ Cl_{(n+1)}^{-n}$ anions arrive from bulk solution, so bulk solution diffusion is probably the main transport process. This theory fits in with other results gained in this work, for example an examination of Pic 20 shows a definite overhang at the growing edges of the growth mounds on the surface, and this is also present in Pic 25.

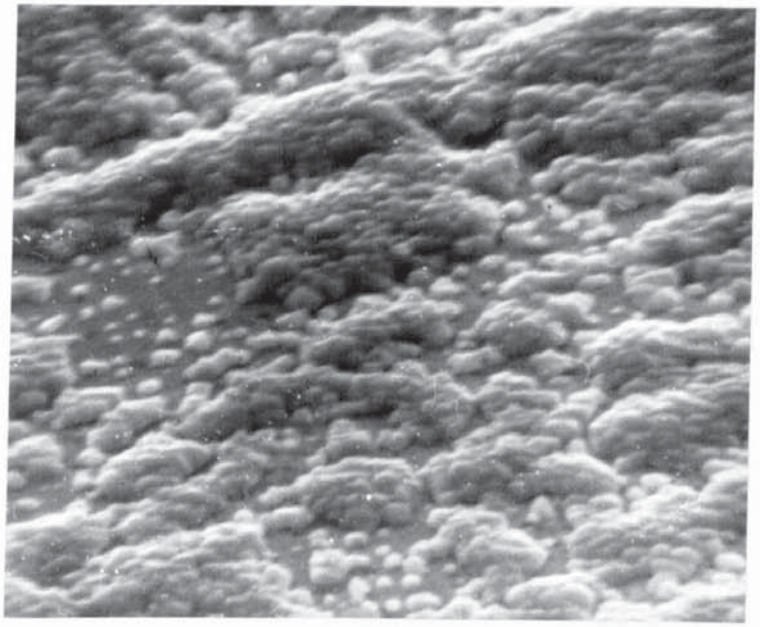

PIC 25 X 5K

Past work does not explain though the growth morphology seen in this work, with reference to the aforementioned growth bands and troughs. A theory has therefore been produced to explain this phenomena.

As mentioned before, and as quoted by Evans (2) in reference to oxidation on metals, the corrosion or dissolution process starts at the abrasion lines and continues parallel to the rolling lines, these being areas of internal stress. The particles of silver chloride nucleate and grow along the lines of abrasion and rolling, utilising material provided by the dissolution mechanism mentioned beforehand for transport, and the areas of high dissolution potential for the actual material dissolution.

Areas that would provide the material would be holes, dislocation pits (where it is accepted that dissolution rates are higher) and the bases of the abrasion lines which would themselves contain, from their production, many dislocation sites, pits or slip planes, as seen in Pic 26.

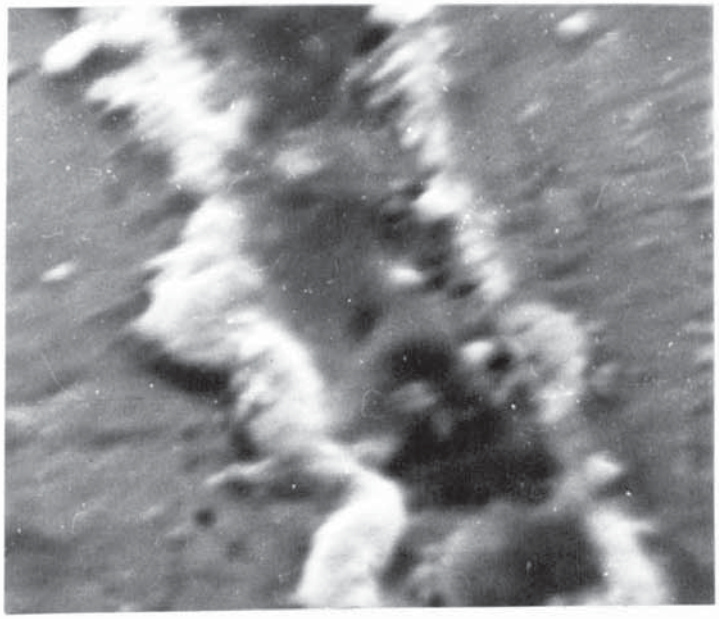

PIC 26 X 11.5K

These nuclei (originally of the K type) would grow into particles of the M1 and M5 types, and eventually grow into the growth moulds seen in Pic 13. At this stage it is necessary to bring into the picture the formation of porosity in the first layer.

Young (1) suggests that pores start where local rates of dissolution are high, and at these sites higher temperatures exist which further increases the rate of dissolution and produces a thicker film due to the pores, which themselves stand a good chance of being blocked.

Pores (2) can also be nucleated where three grains meet or on lines of disordered atoms such as slip planes. From the work undertaken there appears to be a definite mechanism whereby the pores, on this specimen type and surface structure, are formed.

On the silver surface are abrasion or rolling lines as seen in Fig 10.

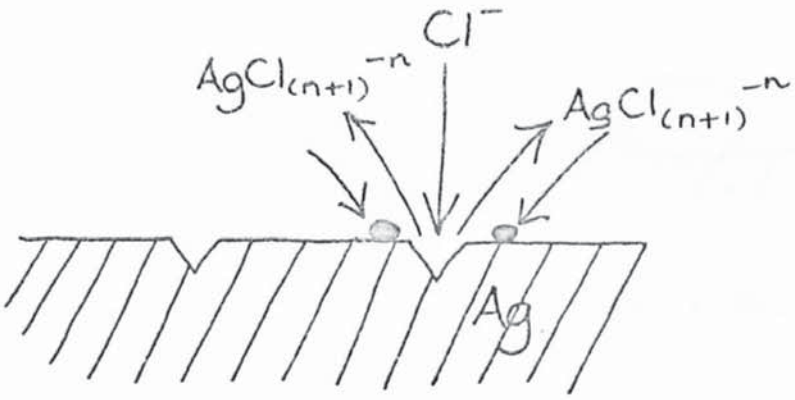

FIG 10

When the anodising is started, there is a build up to supersaturation of $Ag\ Cl_{(n+1)}^{-n}$ ions above the surface, and eventually this deposits as the nuclei, as explained before. There follows a growth of M1 and M5 particles, the most favourable sites for which are the nearest to the sites of silver removal, i.e. the abrasion line sides.

There now follows the process as in Fig 11, where the nodules begin to build up at the edges, and eventually grow over them, giving the growth band overlaying the abrasion/rolling line, the troughs between the bands, and the lines of pores down the growth band centres.

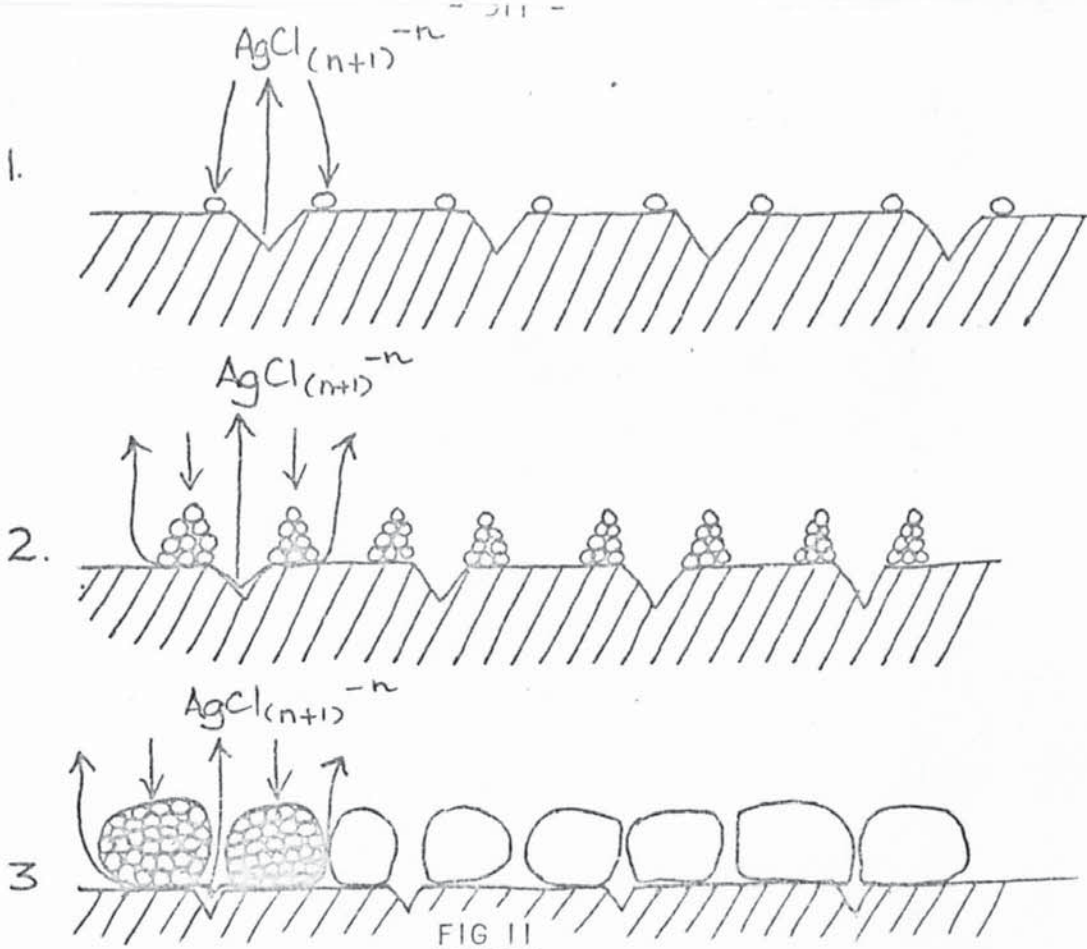

FIG 11

Fig 11 shows the start of the process as can be seen in Pics 27 and 28.

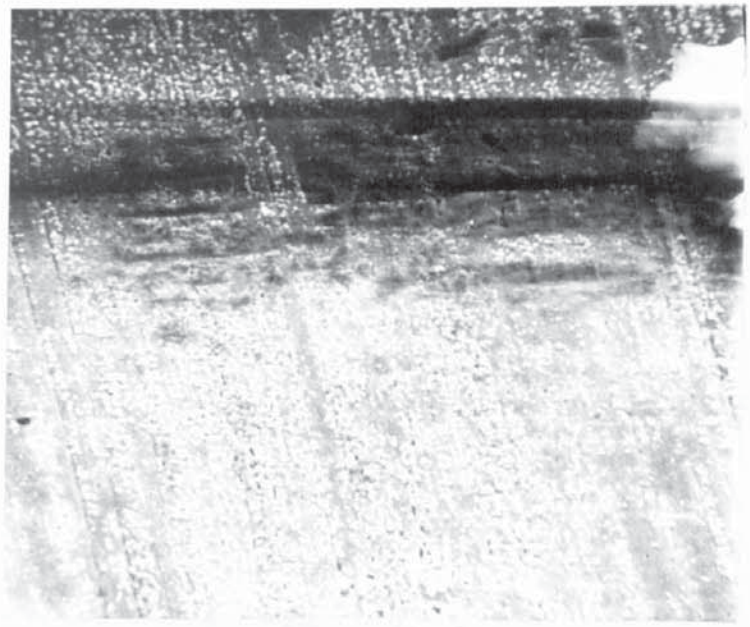

PIC 27 X 2K

PIC 28 X 10K

Pic 19 and 20 show this overlaying of the abrasion lines by the growth bands.

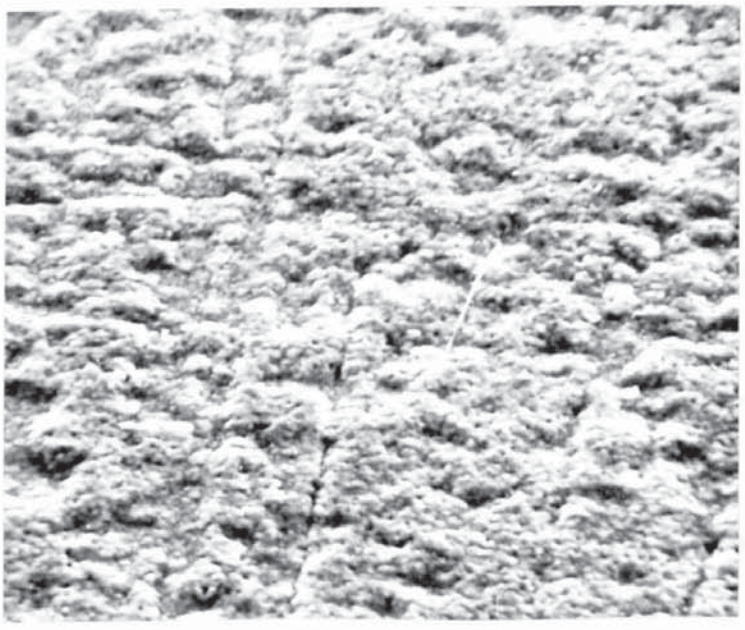

PIC 29 X 2K

Pic 29 shows the final stage of this first layer growth with the remnants of the troughs and the lines of pores parallel to the troughs. This can especially be seen on the underside of a film stripped from the silver, i.e. Pics 30 and 31, where the pores can clearly be seen following the troughs, and down the growth bands.

PIC 30 X 500

Internal tensile stress can also make the metal anodic towards unstressed metal, and following the lead of Evans (1) concerning the anodic film on rolled Ni, a theory can be proposed for the lines of pores seen radiating at each side of major trough lines, as can be seen in close examination of Pic 32 and Pic 33 and as can be seen schematically in Fig 12.

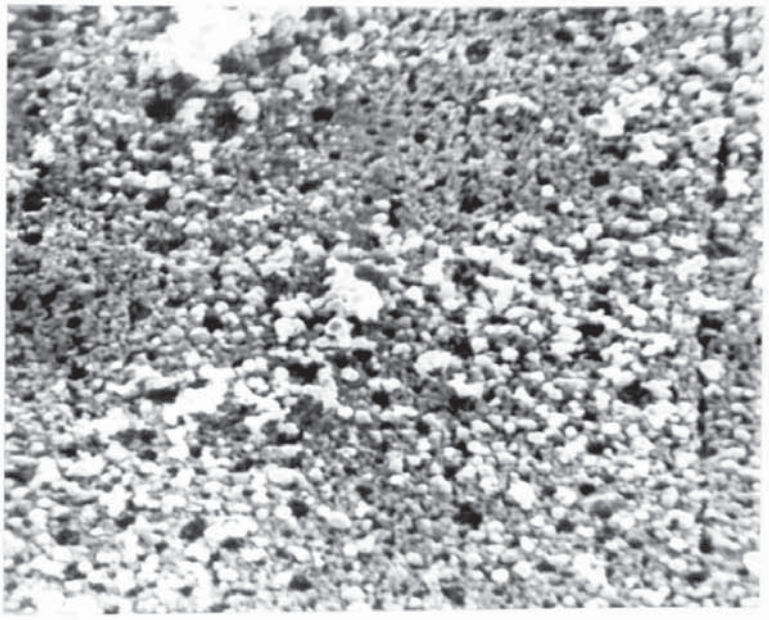

PIC 31 X 5K

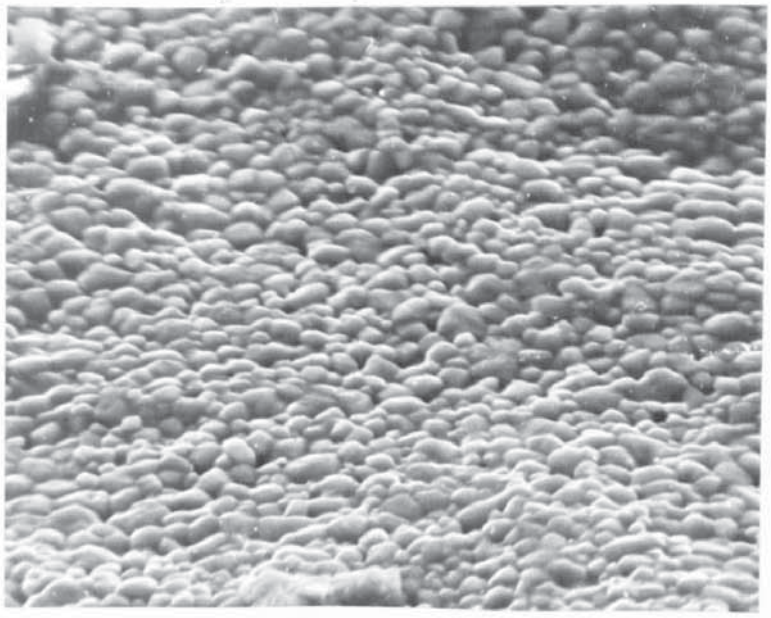

PIC 32 X 2.4K

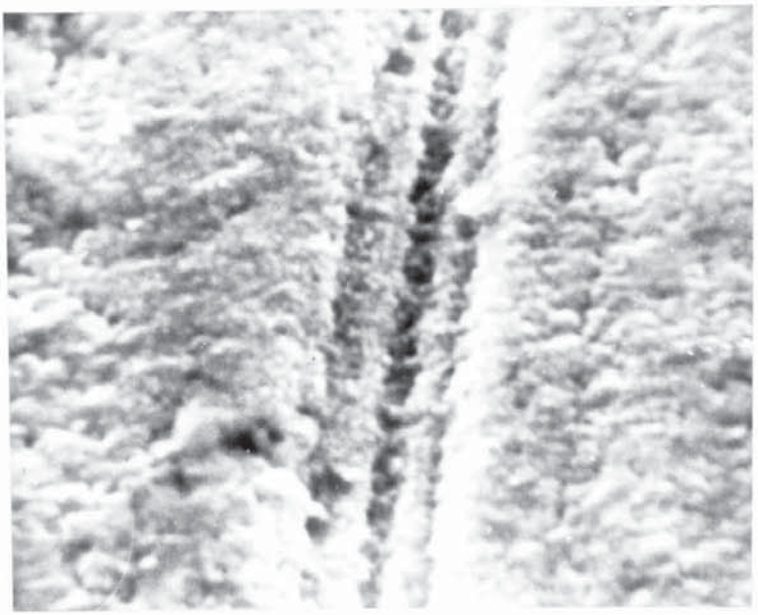

PIC 33 X 10.7K

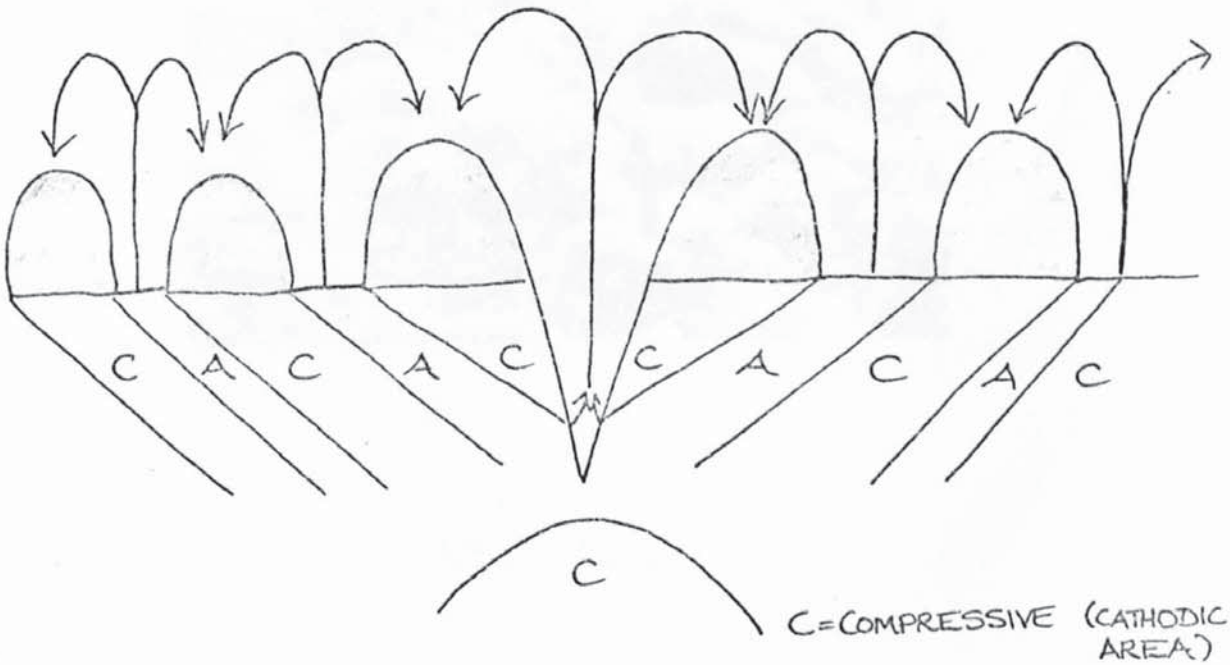

C=COMPRESSIVE (CATHODIC AREA)

A =TENSIONAL (ANODIC AREA).

FIG 12

The silver dissolves at the anodic tensional areas, such as the base of the abrasion line and at each side of the line, and deposits as chloride on the compressive cathodic areas (relatively cathodic that is, to the rest of the specimen surface). As the tensional/compressive forces weaken away from the main abrasion line, the pores would also be expected to weaken in presence, and this, as is seen in Pic 24 is as happens.

The bulbed moulds overgrowth of abrasion lines explains the pores central to these accumulations of material, but not the occurrence of pores central to actual particles, i.e. as seen in Pic 34.

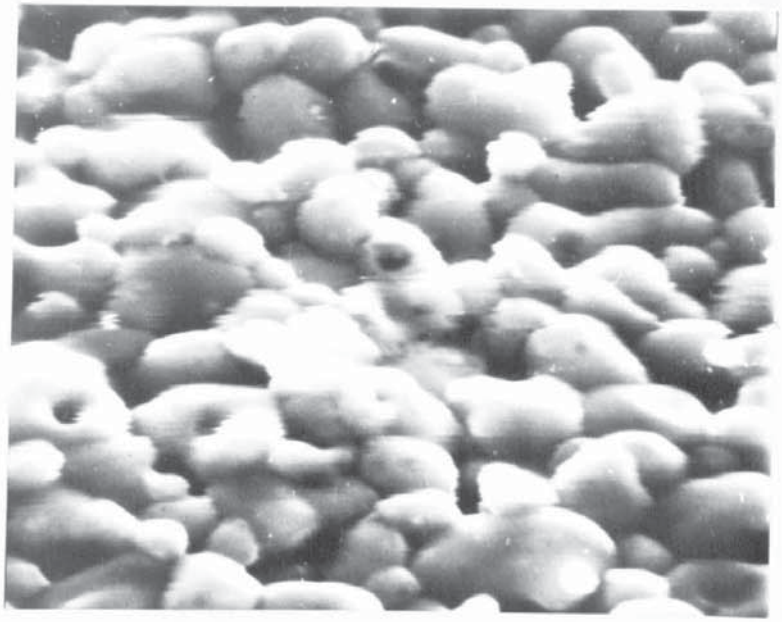

PIC 34 X 10K

These Q2 or Q5 type particles are common to all types of particles in all layers, and will be discussed later.

As a check of the validity of the growth procedure on the as received silver, a specimen of silver was prepared with an electrode deposited layer of bright silver. This can be seen in Pic 35 with an extremely fine structure and particles in the region of 1.2×10^{-8}m radius.

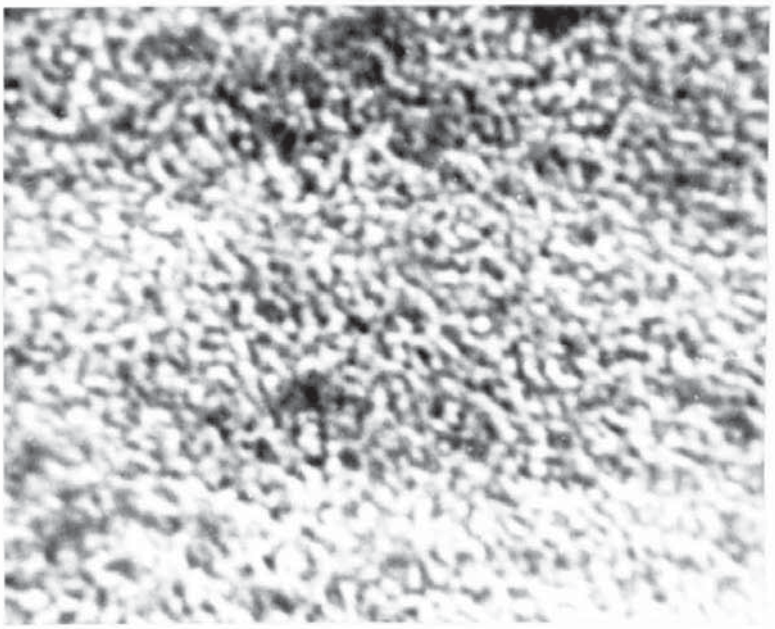

PIC 35 X 10.2K

This picture is showing the underside of the silver chloride film next to the silver, with the silver removed. Compared to Pics 30 and 31 with normal silver surfaces, it can be seen that the particle size is much smaller with the deposited surface, and that there is no orientation along irregularities like the previous observations.

The size of the particles indicates that the M1 and M5 particles have not formed, and an even distribution of silver chloride primary nuclei has been deposited, all growing after nucleation at an even growth rate.

This is due to the lack of surface irregularities on the bright smooth silver surface. It can also be seen that the mode of growth of the first layer does not seem to effect second layer growth morphology unduly, i.e. as seen in Pic 36.

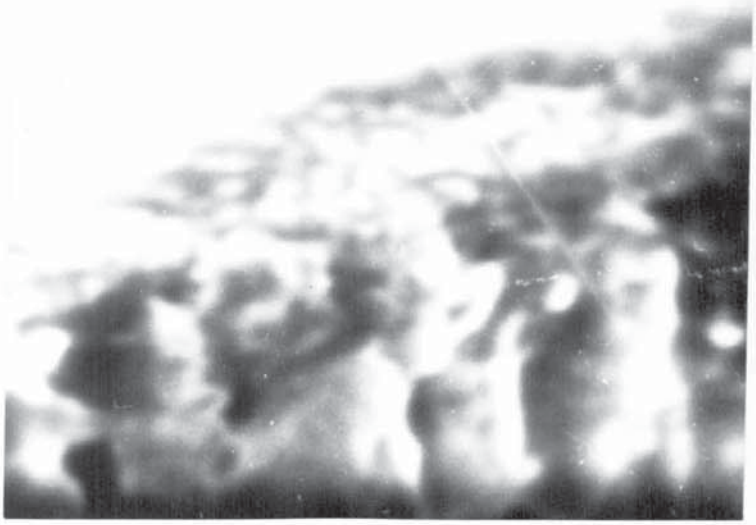

PIC 36 X 21.3K

The first layer can be seen on top (the picture is reversed) of the columnar structure of the second layer. The structure of the second layer does not seem different to normal second layer growth.

Gu and Benion (18) predict this effect on polished silver, where "a large number of nucleation centres exists and a porous film is produced which thickens with a slow decrease in porosity". The silver surface under the film is in a deeply etched condition after anodising, and the film has a tendency to detach when thick. This could be due to it having etched away its own foundations.

If Pics 37, 38 and 39 are examined then the etching of the silver surface along certain planes, producing a step like structure, can be seen.

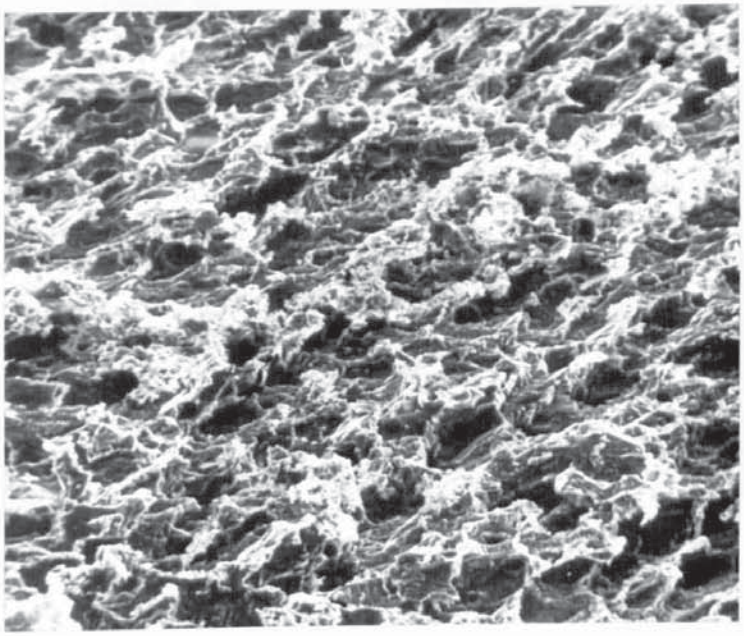

PIC 37 X 1.2K

PIC 38 X 500

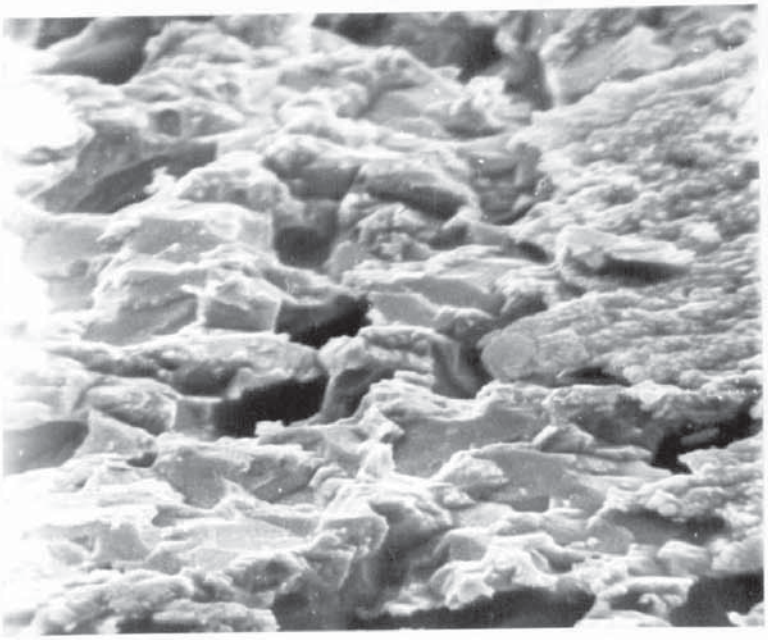

PIC 39 X 2.7K

The main dissolution occurs at certain points or planes on the surface, leaving peaks as seen in Pic 37 on the surface. These can be seen in greater detail in Pic 40 where the peaks can be seen to be coated in silver chloride (verified by KEVEX analysis on the SEM).

These peaks presumably aid contact between the film and the basal silver.

A large difference can be seen between the bare silver surface before anodising, as seen in Pic 41, and the anodised surface with the film removed as can be seen in Pic 42.

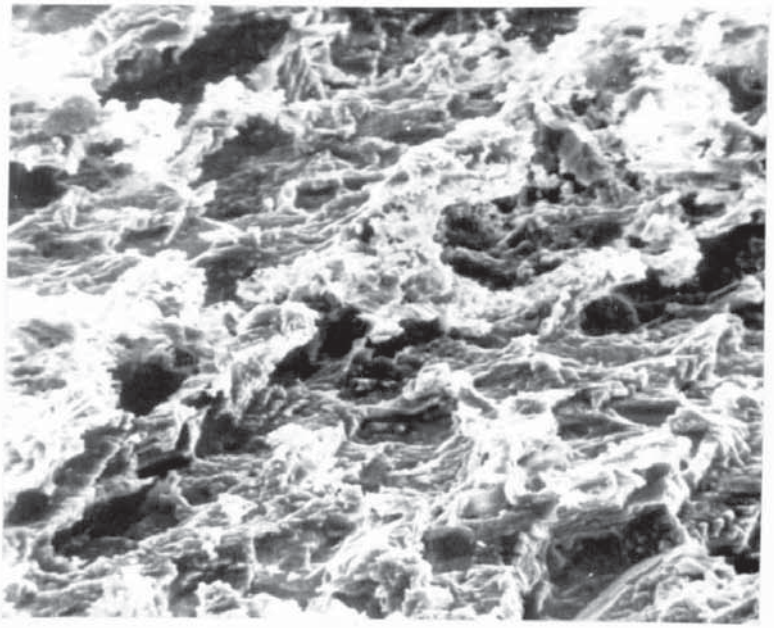

PIC 40 X 2.4K

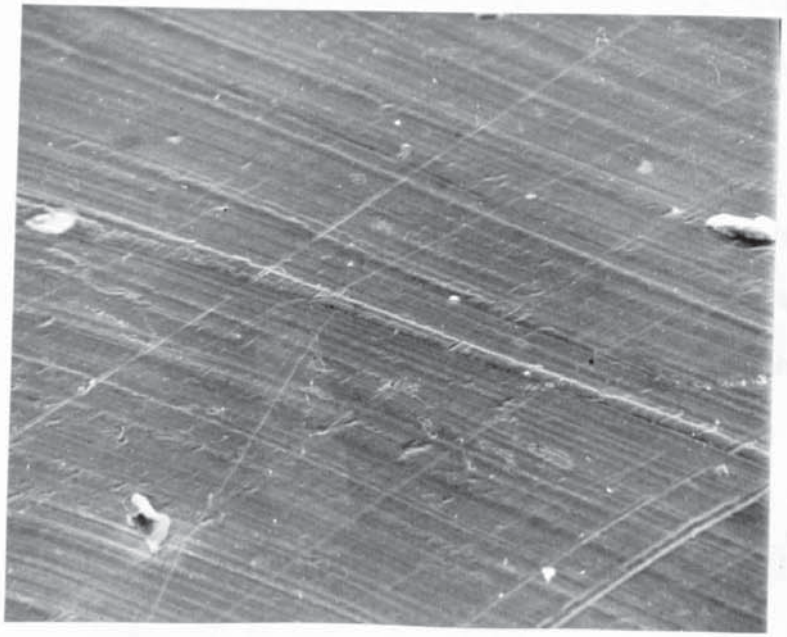

PIC 41 X 550

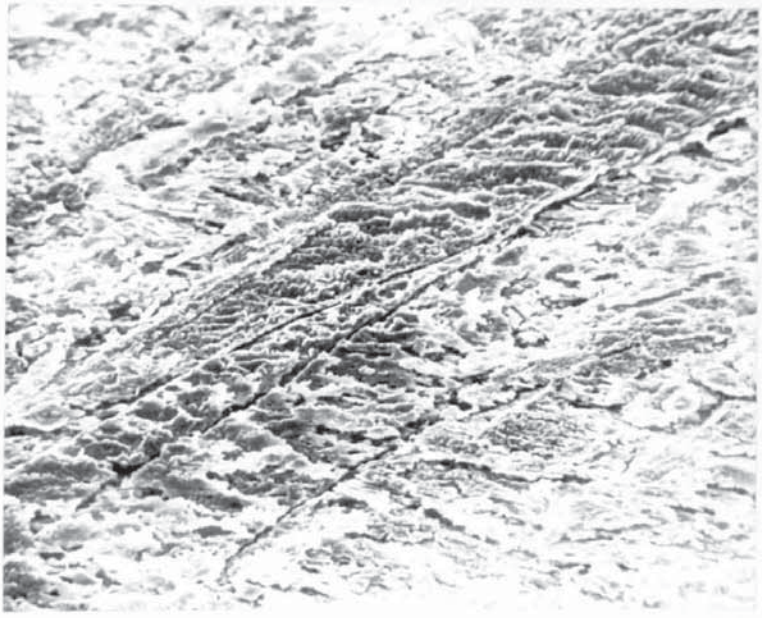

PIC 42 X 1.22K

In Pic 42 the abrasion lines can be seen to have been much deeply etched away, and where the film has detached when very thick, the fracture surface between the silver and silver chloride, as seen in Pic 43, can be seen to be even more greatly etched away.

Presumably this is then proof that the removal of silver from the base and its transfer through the pores, to deposit as silver chloride, eventually weakens the base contact, and so the film detaches. Apart from proving that main growth of silver chloride is at the Ag Cl/ solution interface, and not the Ag/Ag Cl interface, it can also be shown that new Ag Cl is deposited at the Ag/Ag Cl interface as Pic 44 seems to show on the film base, or as seen in Pic 45.

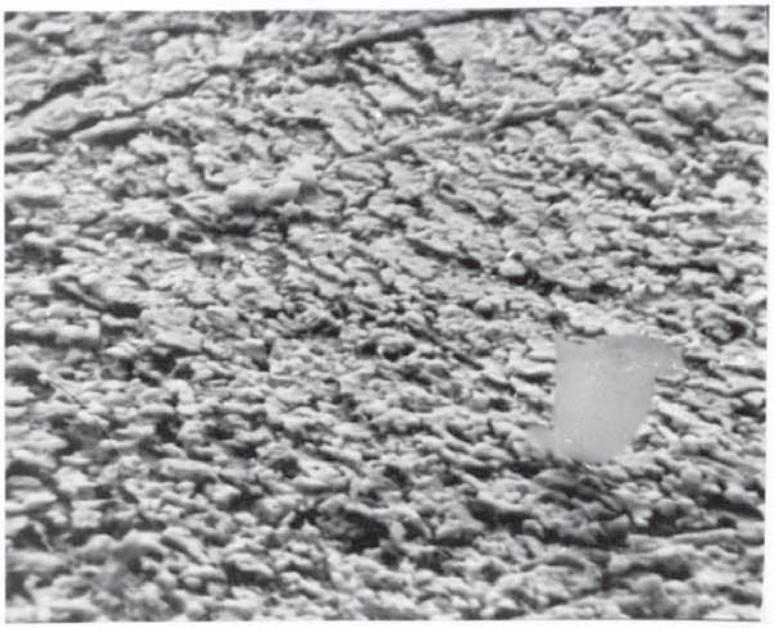

PIC 43 X 2.35K

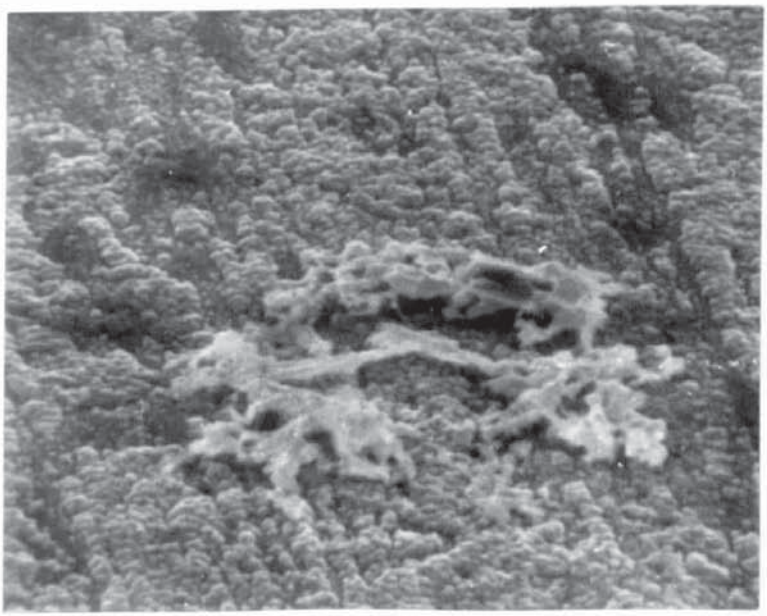

PIC 44 X 4.5K

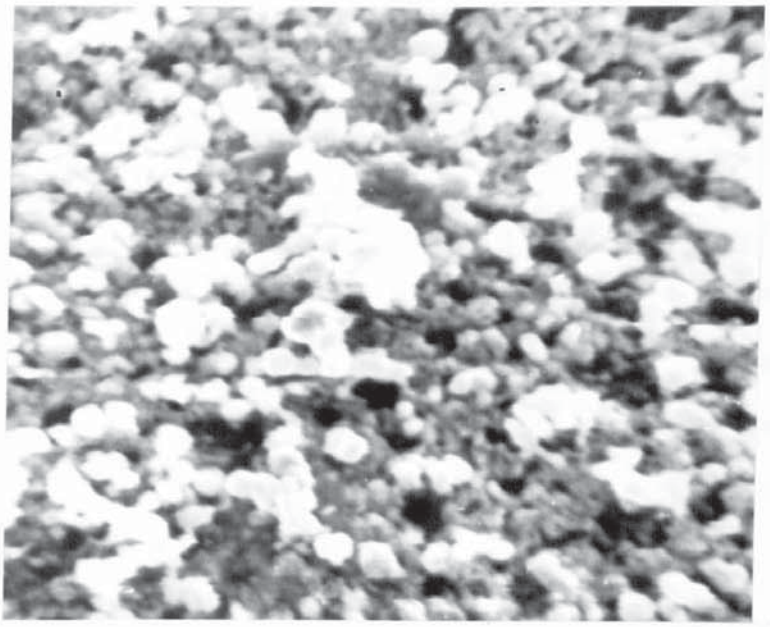

PIC 45 X 5K

In the computer aided regression analysis of the results of film parameter observations, relations are found that point to certain connections between the parameters or morphologies of particles or pores, film/layer thicknesses or other properties of the silver chloride film.

In this text, these relations will be referred to as CDR's (Computer Derived Relations). In the first layer HI layer thickness is effected by the dimensions of the MI particle, from CDR $\downarrow$ rMI(I) $\Rightarrow \uparrow$ HI.

This fits with the joint CDR argument

$\uparrow$HI $\Leftarrow \uparrow$ r/v M5(I)

$\uparrow$HI $\Leftarrow \downarrow$ r/v MI(I)

$\uparrow$ r/v M5(I) $\Leftrightarrow \downarrow$ r/v MI(I)

where it is seen that the larger one particle type in the first layer is, the smaller is the other.

Now if the M5 particle is the larger in the first layer, as it is, then of the two particle types it will have the greatest effect on the HI layer thickness, the MI particles therefore being smaller, by the aforementioned CDR arguments.

From $\uparrow$temp $\Rightarrow \uparrow$r/v M5(I), rise in temperature of anodising causes a rise in the dimensions of the large rounded M5 particles in layer I. Presumably the greater the thermal energy available, the greater the ionic mobility, so the larger the distance the ion can travel. If the temperature is low, and the mobility of the species is inhibited, then it follows that large numbers of nucleation sites near to the dissolution sites will be utilised during primary growth, by necessity.

At higher thermal energy levels, the ion can travel to more favourable nucleation and deposition sites further away from the dissolution sites, these progressively building up to produce particles of larger radius and volume. Also a rise in the anodising current results in the dissolution of more material, so the particles would tend to be larger as more material is available, the CDR $\uparrow C \Rightarrow \uparrow$ rMI is therefore valid.

M5 particles could therefore be looked on as extensions of MI particles, being of greater dimensions that the MI's and presumably formed from them, the MI's having a greater nucleation number. Also the smaller the MI's, of which there are many more than the M5's, the more material is therefore available for M5 growth.

In the first layer, porosity does not always refer to actual pore presence, but it can refer to distance between scattered particles on the silver surface in the initial stages of film growth.

This makes the CDR $\downarrow$r/v Q3 $\Rightarrow\uparrow$r/vM5 quite relevant, where the larger the particles the smaller the available gap between it and the next particle.

Normally the pores between particles increase in dimensions as the particles increase in size, but only if the particles are touching. Before this occurs the CDR above is correct. This also accounts therefore for the CDR's

$\downarrow$r Q6(1) $\Rightarrow\uparrow$vM5(1)

$\downarrow$r/v Q3(1) $\Rightarrow\uparrow$r/v M1(1)

$\downarrow$r/v M5(1) $\Rightarrow\uparrow$vM1(1)

for the reasons aforementioned. So when the volume of the M5 and M1 particles in the first layer decrease, then the radius of the Q3 pores in the layer increases, this being obvious in the case of none touching particles.

With the M5 particles, the nodules are spherical so the radius and volume of the particles run hand in hand. As the M1 particles are oval though, a change in volume is affected by change in particle length. As in M1 particles half the length equals the particle radius, then this also affects the radius, but not the depth h of the particle. So $\downarrow$r $\Rightarrow\downarrow$vol and $\downarrow$r $\not\Rightarrow\updownarrow$ h for M1 particles whereas h would decrease with decrease in r in M5 particles.

Now as the volume of the Q3 pores is a function of h, the pore length usually being the same as h in the first layer, so if as in the CDR $\uparrow$vM5(1) $\Rightarrow\uparrow$vQ3(1) the volume of the M5 particle increases, then the h factor increases so Q3 must also increase in volume therefore, especially as the packing gap between the particles increases.

The CDR $\downarrow$ vMI(1) $\Rightarrow \uparrow$ vQ3(1) is also valid as decrease in the particle volume simply lessens the radius, not the h factor, so v Q3 remains the same or increases. This is probably due to the total and individual volume of all the MI's being small compared to the relatively fewer M5's, and therefore less overall particles (and so $\uparrow$ r Q3(1)) and effect. The CDR's $\downarrow$ v M5(1) $\Rightarrow \uparrow$ rQ3(1) and $\downarrow$ vMI(1) $\Rightarrow \uparrow$ rQ3(1) can be explained by the previous arguments.

The CDR $\downarrow$ rQ6(1) $\Rightarrow \uparrow$ vQ3(1) is probably a relation indicating that the greater the volume of the Q3 pores, the less need there is for the large extended Q6 pore system. This is formed probably by redissolution after the initiation of the film second layer formation to allow further ion mobility. This by-passes the restricted Q3 pore system, but if this is adequate, no Q6 formation is initiated during primary layer growth.

SECTION (2)

THE GROWTH OF THE SECOND LAYER IN THE SILVER CHLORIDE FILM AND THE PARTICLE AND PORE MORPHOLOGIES.

The growth of the film second layer occurs after the completion of primary layer growth. The primary layer growth of about 1×10^{-6} to 2×10^{-6}m occurs, for instance, up to 2 minutes to 10 minutes at 5 ma cm^{-2}, then there is a burst of growth and morphological change. This is due to the nucleation and growth of the second layer which has thickness of up to 1×10^{-5}m.

An example of this change can be seen in Pic 46 and Pic 47, both specimens being anodised under the same conditions, but the specimen in Pic 47 has been anodised a further 8 minutes, anodising times being 2 minutes and 10 minutes respectively.

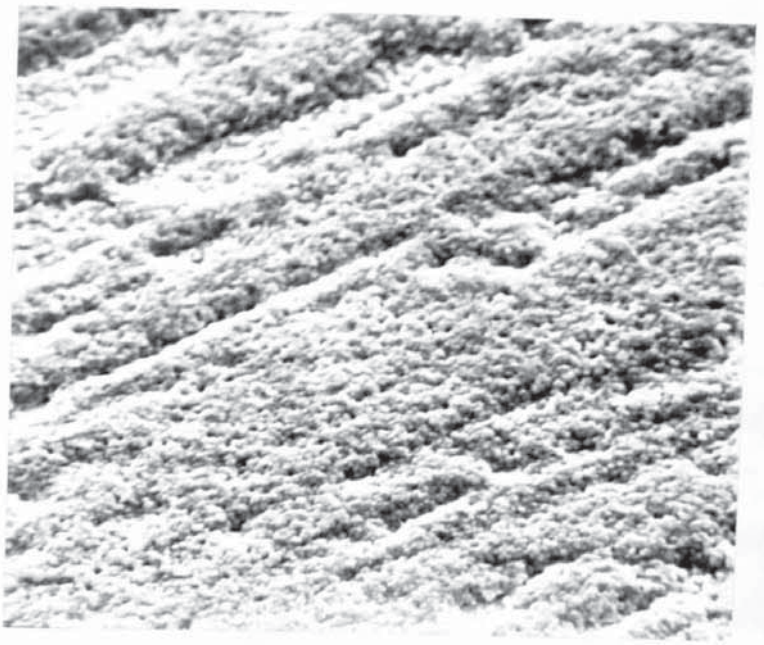

PIC 46 X 2K

The thicknesses of these layers are 2×10^{-6}m and 6.5×10^{-6}m respectively and the main difference in thickness is due to the second layer nucleation and growth. This difference can be seen very clearly in Pic 48 and 49, where the porous second layer can be seen overlying the thin primary layer.

PIC 47 X 2K (SIDE ON)

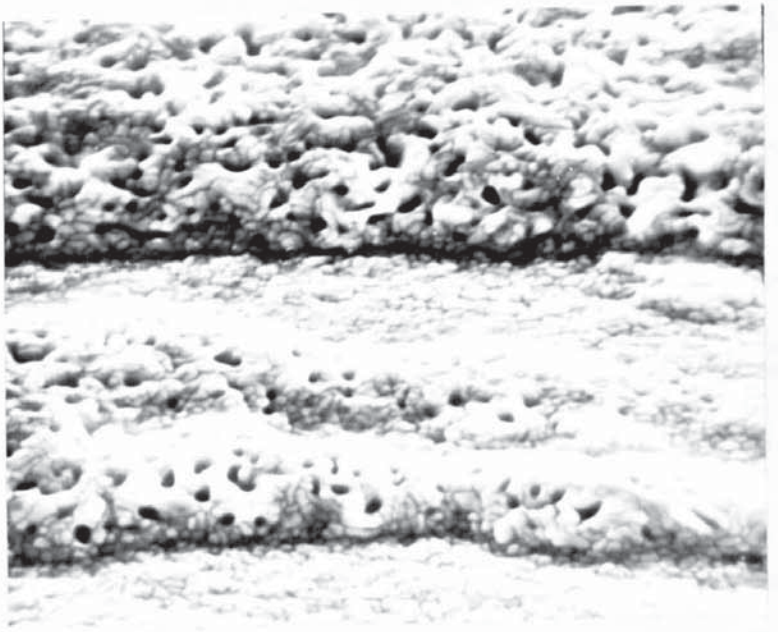

PIC 48 X 5.3K

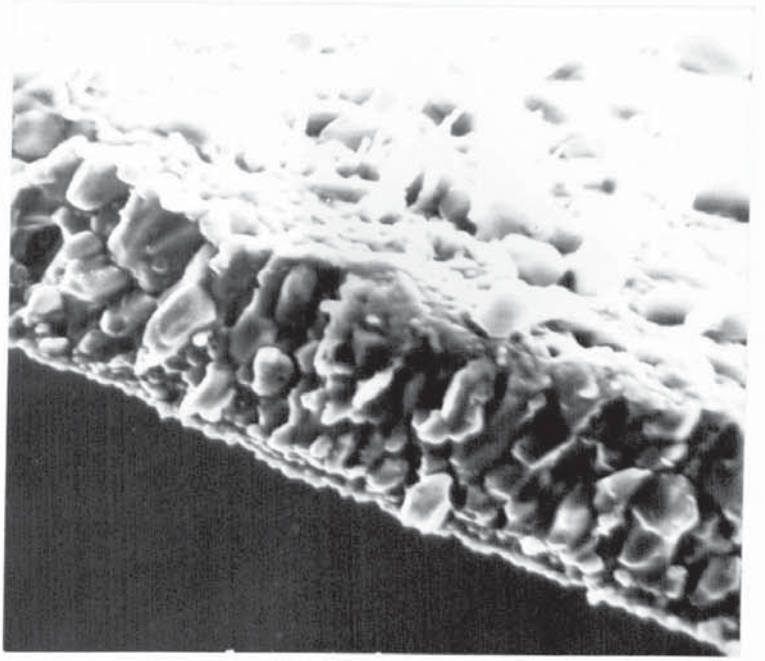

PIC 49 X 2K

In both these pictures the main constituent of the second layer is the MII type particle overlying M5 particles. The MII, related to the MI9 and M2a type film particles, forms a columnar layer with very large particles containing, and are bounded by, pores. We therefore have a two layer film with the layers being consequently thicker (in their final states) and each porous and made up of individual interlinked particles.

One explanation of the increase in thickness could be that as the silver dissolves beneath the first layer, then the surface area of the basal silver increases, as has been seen in Plcs 42 and 43. More silver can therefore dissolve over a much larger region than before, as dissolution would now not be restricted to the bases of irregularities on the surface.

The increased silver ion concentration, percolating up the pores, could now nucleate as a second layer of larger particles growing to greater film thickness, depending on the current density and anodising time. The porosity of the primary layer would be insufficient to allow the extremely large amounts of $Ag\ Cl_{(n+1)}^{-1}$ ions, or other species, to percolate, so larger pores are nucleated in the primary layer by methods of film redissolution to be discussed later. These pores are designated the Q6 type.

An excellent example of the Q6 pores, and also of the presence of the second layer growing on top of the first, is seen in Pic 50.

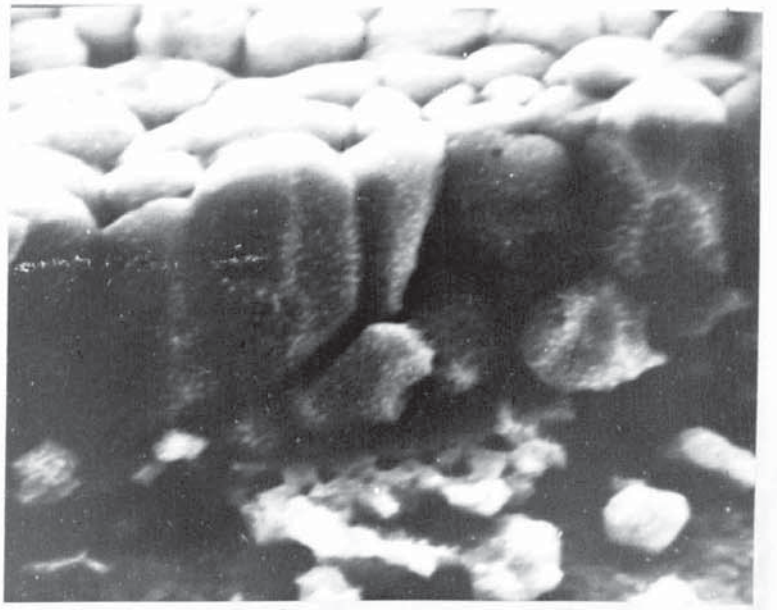

PIC 50 X 6.5K

This shows the columnar form of the second layer, and the M19 or M2a type particles making up this layer. Further views of this film structure can be seen in Pics 51 and 52.

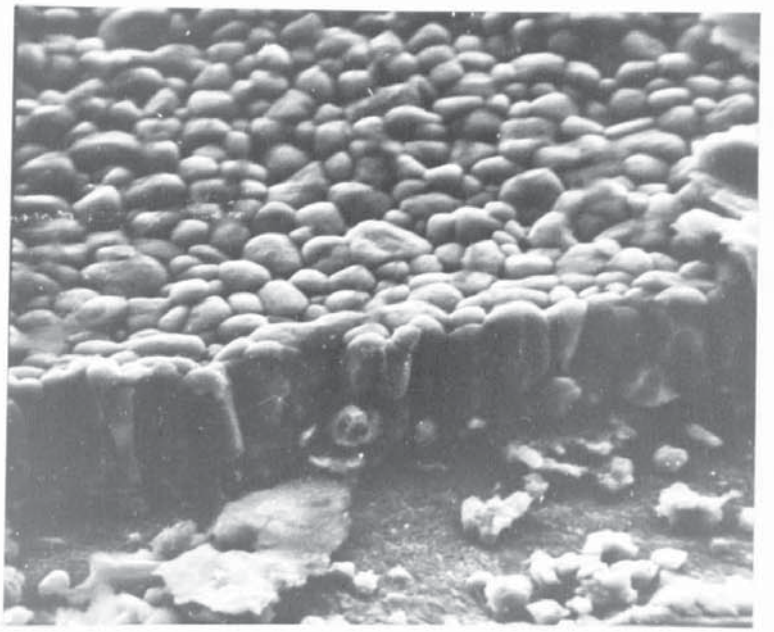

PIC 51 X 2.6K

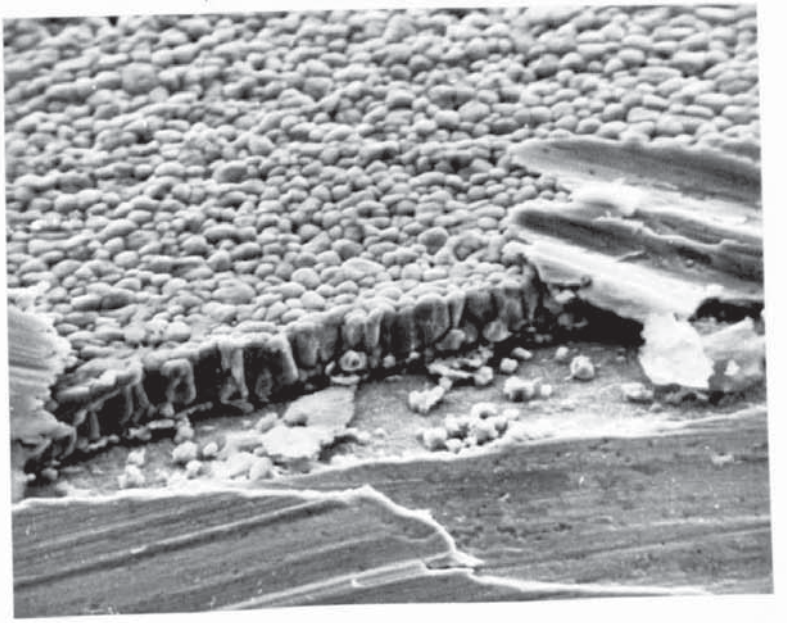

PIC 52 X 1.3K

This film is seen in the side view with the whole depth of film open. The pores in the underlying primary layer can be seen, especially in Pic 50, and in this the very large Q6 pores can clearly be seen.

The film can be removed from the basal silver by careful manipulation, or dissolution of the silver. If this is done, the Q6 pores originating at the silver/silver chloride interface, and formed at nucleation of the second layer, can be seen. Examples of these can be seen in Pics 53, 54 and 55, where they can be seen to follow the lines of existing original Q3 pores in the primary layer.

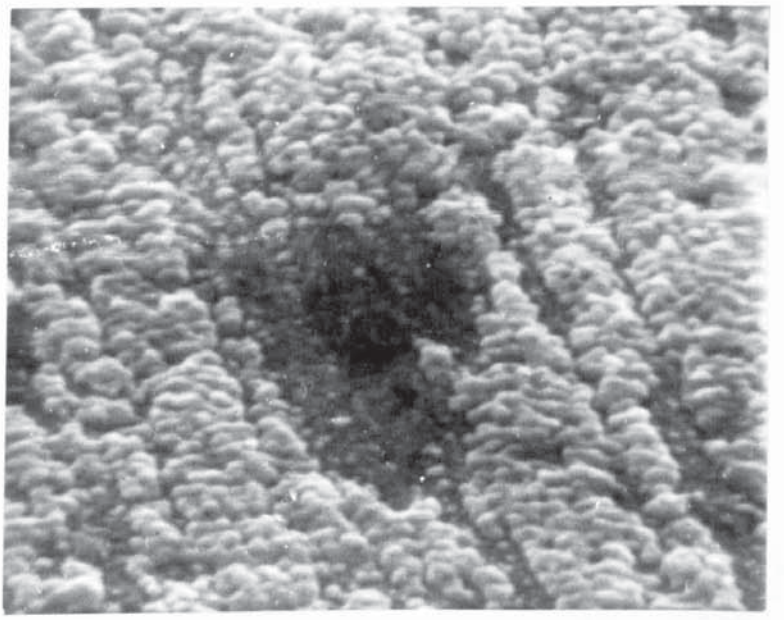

PIC 53 X 11K

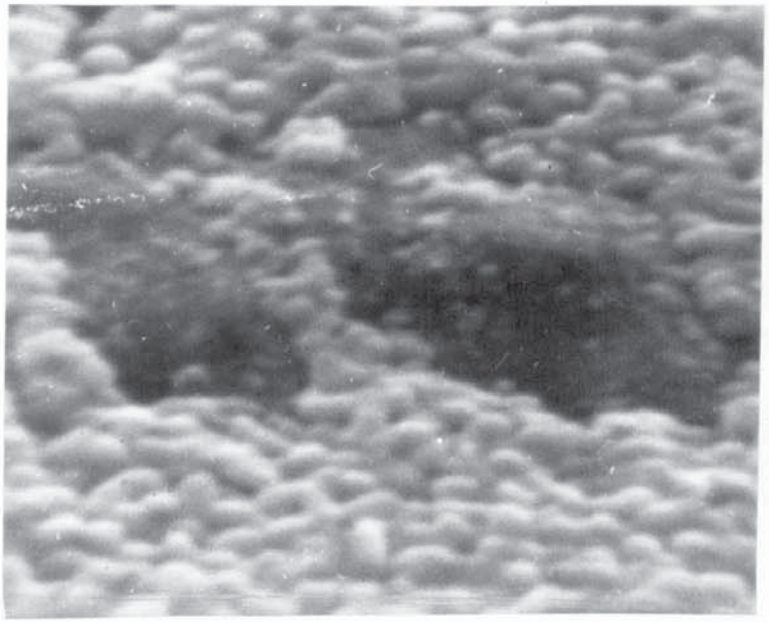

PIC 54 X 19K

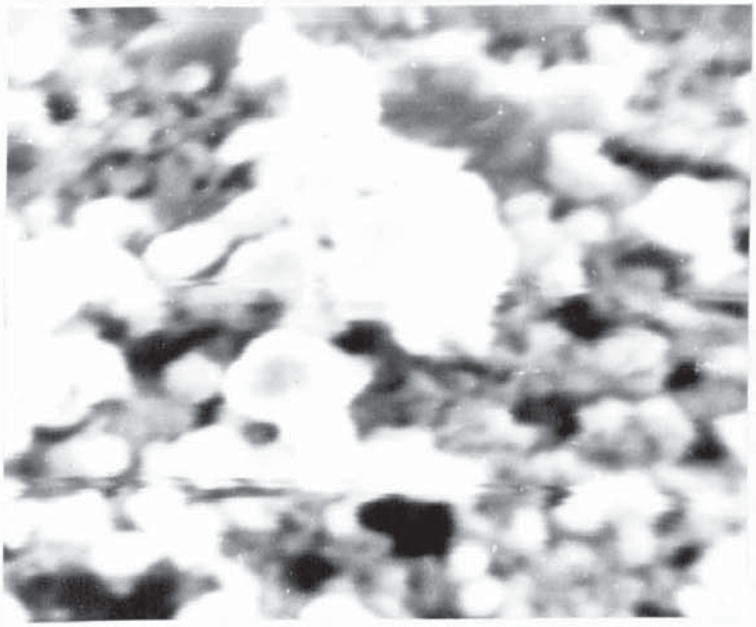

PIC 55 X 2K

This leads to the conclusion that Q6 pores are formed by redissolution of silver chloride, and pore widening to allow for increased ionic transport. Large Q6 pores can also be seen in the primary layer, under the secondary layer, in Pics 56 and 57. The top of the second layer in these pictures can be seen clearly in Pic 58, showing its nodular nature. Another view of the Q6 pores in the film base can be seen in Pic 59, where the basal silver has been dissolved away.

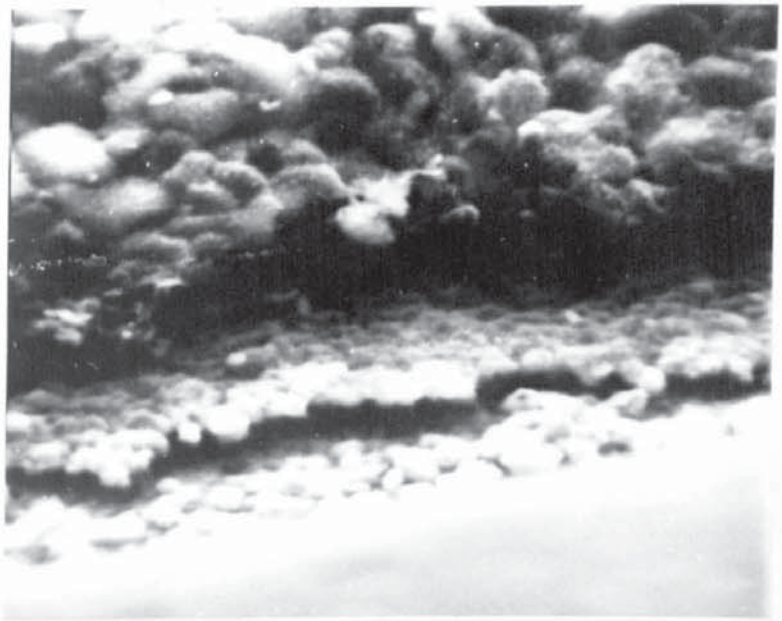

PIC 56 X 6K

It is interesting at this point to note that the second layer is not affected by the state of the silver surface to the same extent as is the primary. This can be seen in the side view of the film grown on a bright electrode deposit of silver, Pic 60.

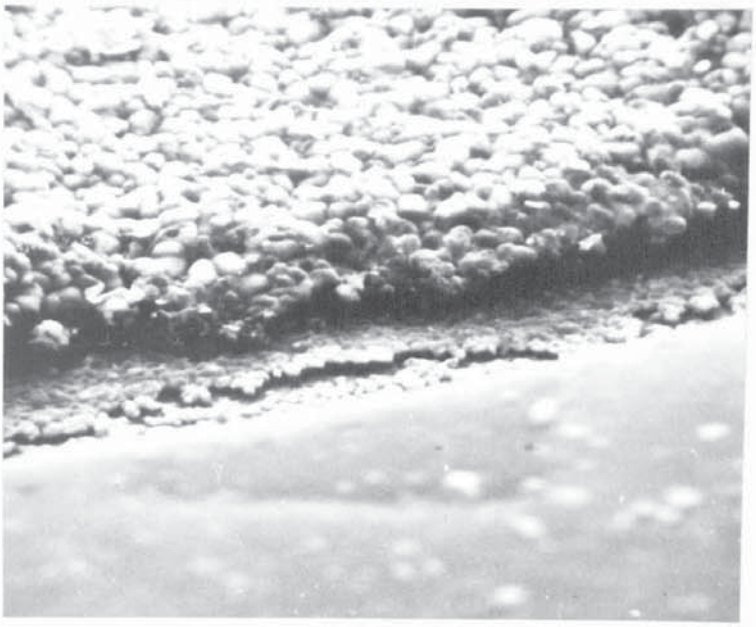

PIC 57 X 2.4K

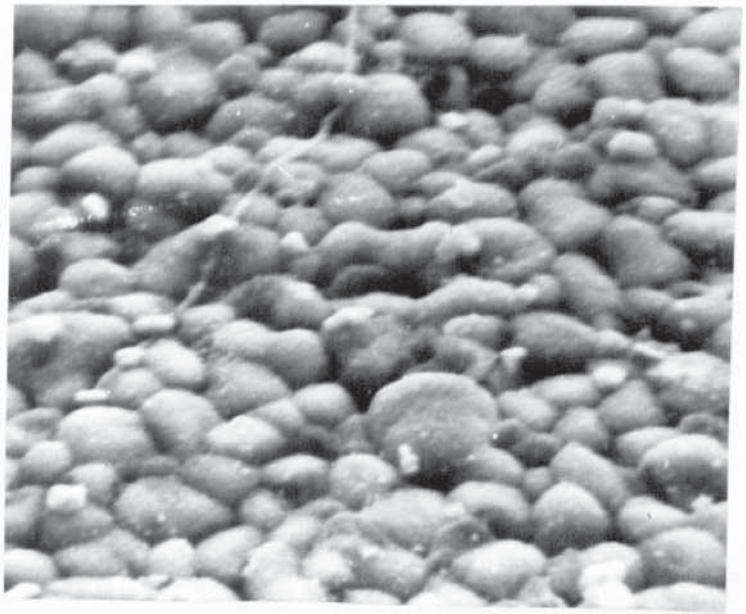

PIC 58 X 4.8K

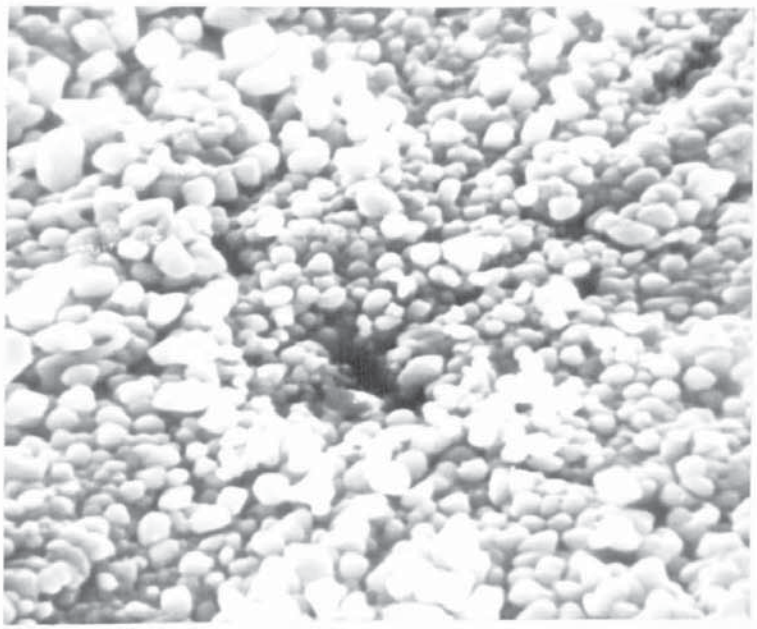

PIC 59 X 5.05K

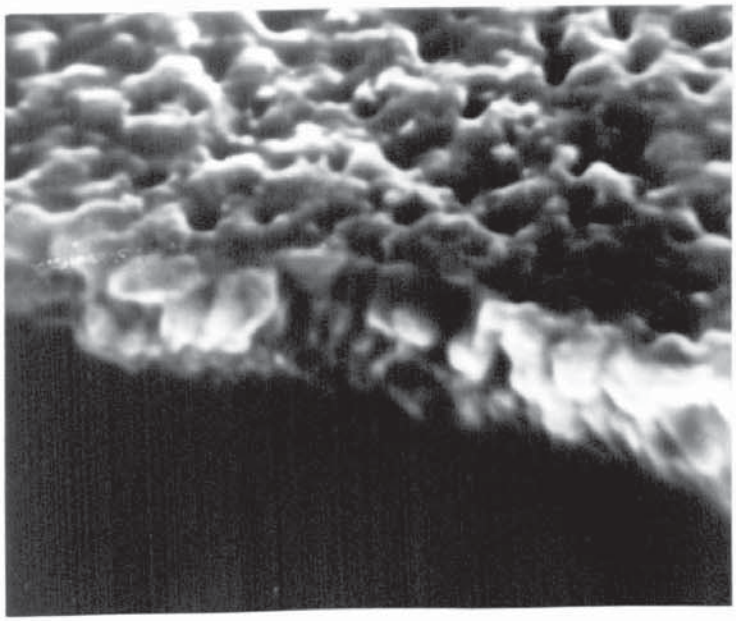

PIC 60 X 9.4K

The primary layer of this film is as Pic 35 and the secondary layer can be seen overlying this in Pic 36. In Pic 61 it can be seen that the basic structure is little different than the second layer of the specimen in Pic 58, except that the structure is much finer and the pores seem larger in proportion. This seems to indicate that the finer the structure of the primary layer, the finer that of the second layer. In the following CDR analysis of the second layer, this will be shown to be the case.

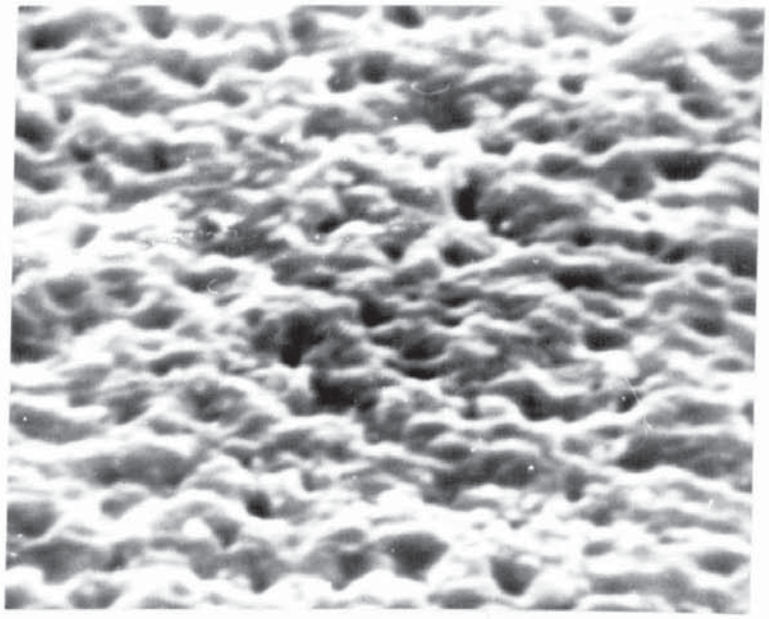

PIC 61 X 9.4K

The Q6 pores, as proposed before, are formed when the second layer nucleates. The film is porous with different layers nucleating on top of each other. The Q6 pores are nucleated or formed by a process of redissolution during pore blockage and clearing, presumably to facilitate material flow.

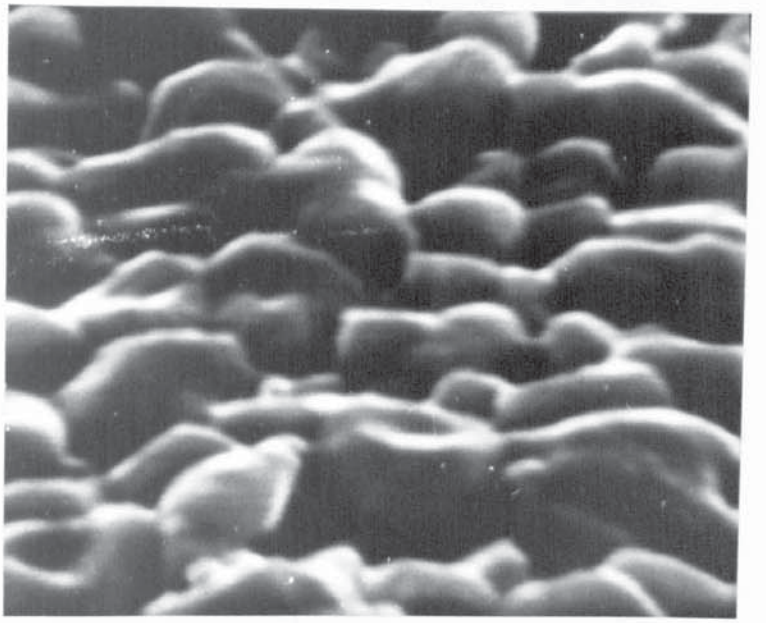

PIC 62 X 10K

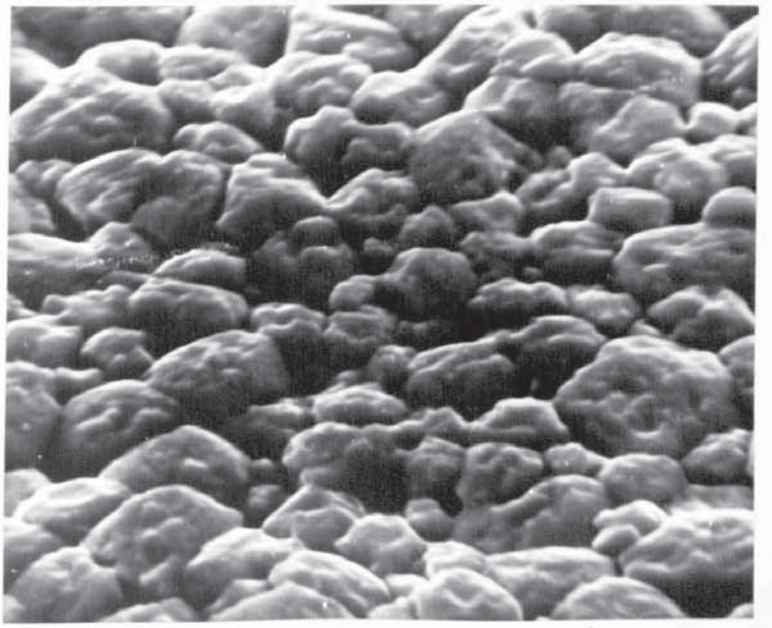

PIC 63 X 6.2K

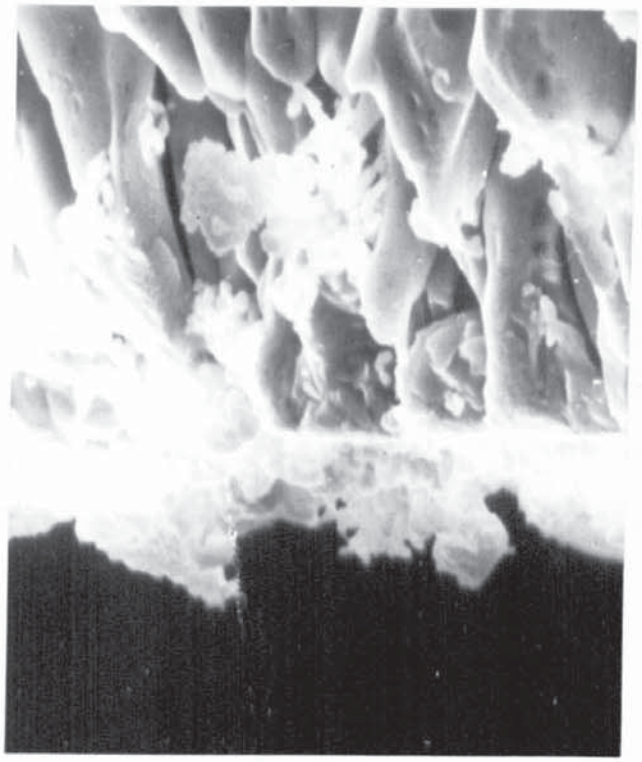

PIC 64 X 5K

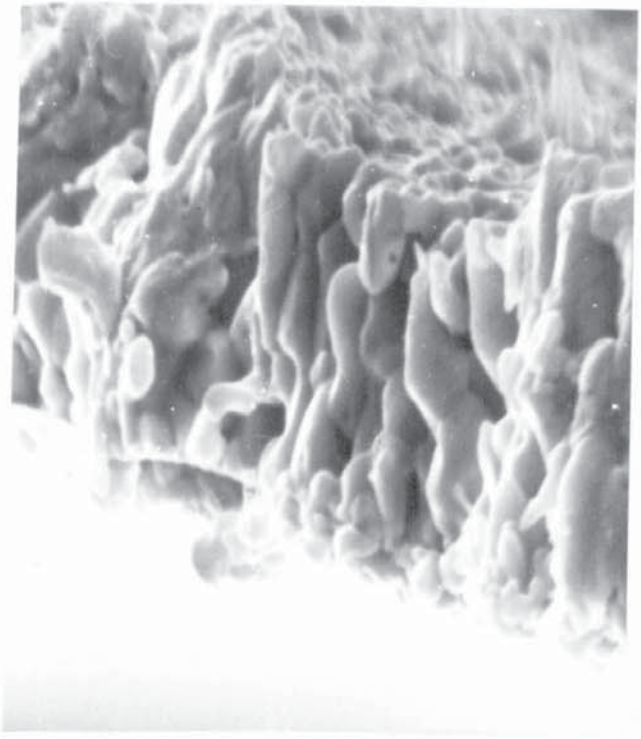

PIC 65 X 6.2K

This is probably aided by a dissolution process, at the Ag/Ag Cl interface, to free chloride ions to take part in further growth when the pores are blocked and chloride ion penetration from solution is restricted. There is therefore a very high silver ion concentration at the Ag/Ag Cl interface, and when the Q6 pores are formed, this concentration release produces a surge of growth at the Ag Cl/solution surface. This nucleates a further layer via the needle particle formations found on the Ag Cl surface. These formations will be discussed later, and the mechanisms of pore blockage will now be reviewed.

It is proposed that at certain thicknesses of layer, or tortuosity of pores (factor h), the $Ag\,Cl_{(n+1)}^{-n}$ ions deposit back Ag Cl onto the walls of the pores they are being transported within. This is probably due to the stability of the ions, and the concentration of Ag^+ and Cl^- ions at that point. This would then limit the transfer of Ag Cl to the outer growth areas, and chloride ions to the inner surfaces for the production of $Ag\,Cl_{(n+1)}^{-n}$ ions.

When pore blocking of this type occurs, redissolution of Ag Cl occurs on the surface forming pores of types Q2 and Q5, as seen in Pic 62, as rounded indentations on the top surfaces of the nodules.

A more extreme case of this can be seen in Pic 63 with the top surfaces quite deeply etched.

The pitting and irregularity that this produces within the layer, on the pore and the particle walls, can be seen in Pics 64, 65 and 81

In these the remains of the primary layer M5 particles can be seen overlain by the secondary layer of columnar particles, each of which is pitted, porous and with angular faces. The transverse porosity through the particles is unlikely to be produced during growth, but is likely to be produced during the process of redissolution of existing Ag Cl on the pore walls.

The silver chloride ionic species formed during redissolution of existing silver chloride, say at the growing surface, would deposit under high current density conditions at the surface, at certain nuclei, forming the MI5a and MI4 type needle growths at the pore mouths, which are presumed to be the nuclei for the next layer.

It is reported that the chloride film resistance increases, and becomes independent of concentration, when the film is a few microns thick. Presumably pore blocking can occur therefore which is independent of chloride ion concentration, due to complex formation with silver chloride forming silver complexes and free chloride ions, so silver is transported within the pores by a process of redissolution and complex formation.

The resistance is also larger (29) the slower the film is grown, or the lower the current density. This can be confirmed by the schematic plots of percentage porosity in the film, against film thickness and time of anodising for different values of current density, seen in graphs 29 and 30.

If the porosity of the film decreases with increase in thickness or anodising time, then two explanations can be put forward. The first is that the pores in any one layer decrease in number as the thickness increases due to blocking of these pores. Evans (2) shows three types of pore blocking:

(a) Log curve, time/thickness = mutual pore stifling.

(b) Asymptotic, time/thickness = self stifling pores.

(c) Sigmoid then parabolic, time/thickness = discrete nuclei over surface, then when thick enough, curve becomes parabolic.

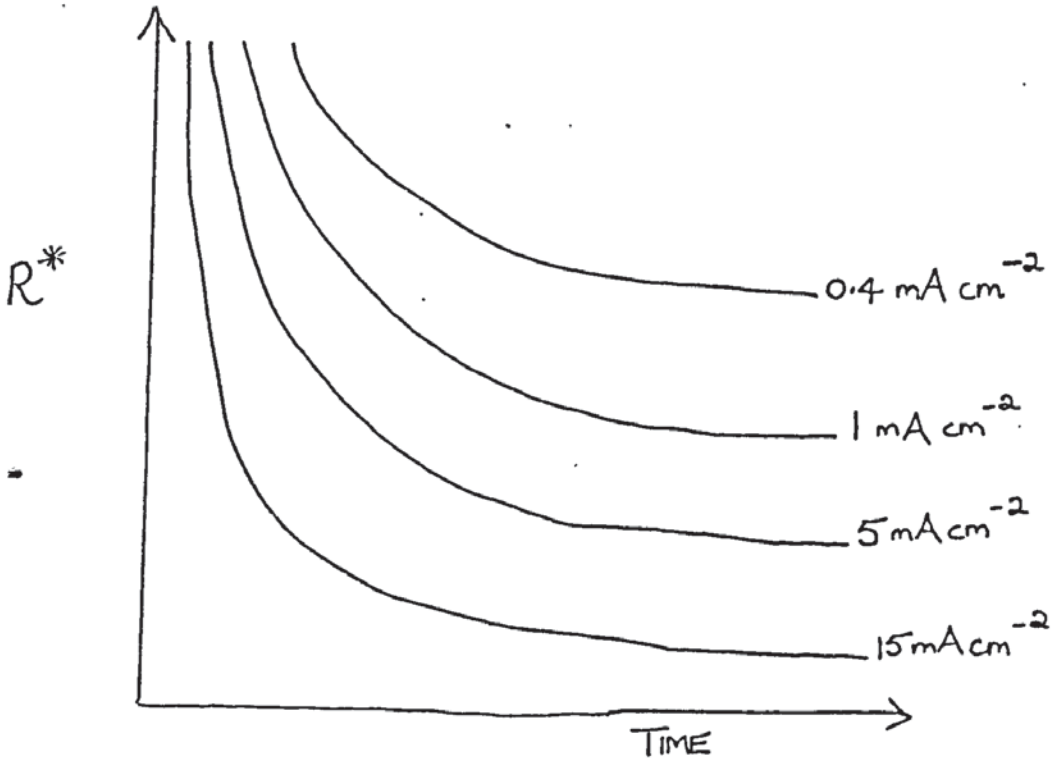

GRAPH 29

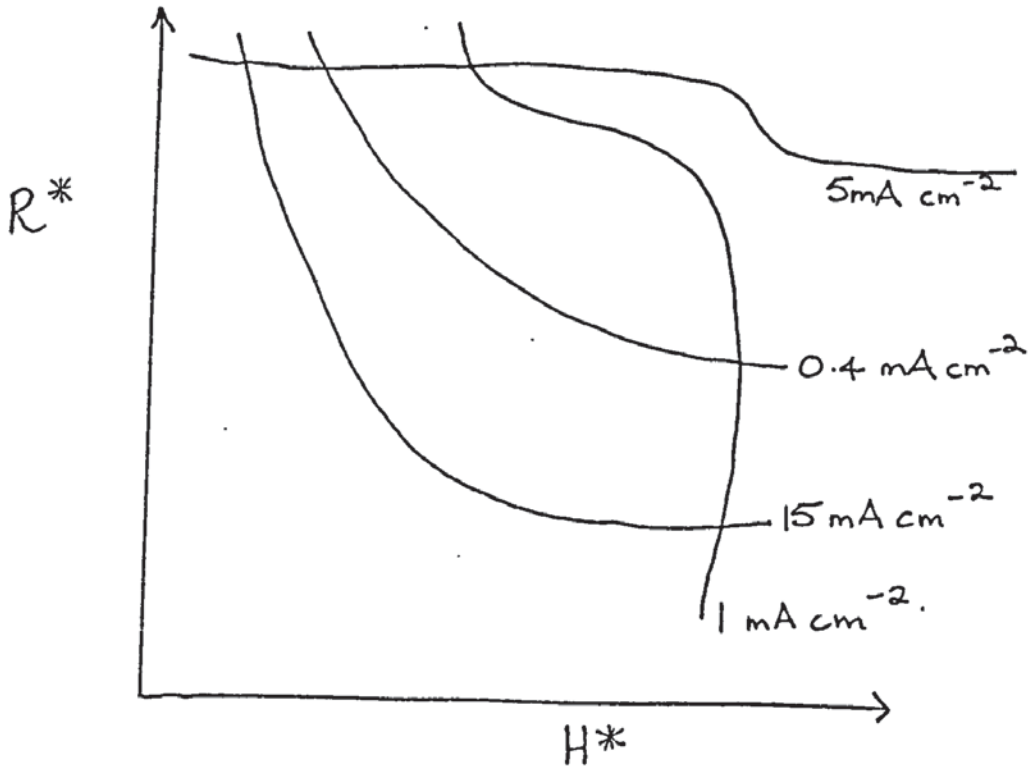

GRAPH 30

From schematic graph 31 and evidence discussed later, it can be seen that the pore blocking is of the self and mutual type.

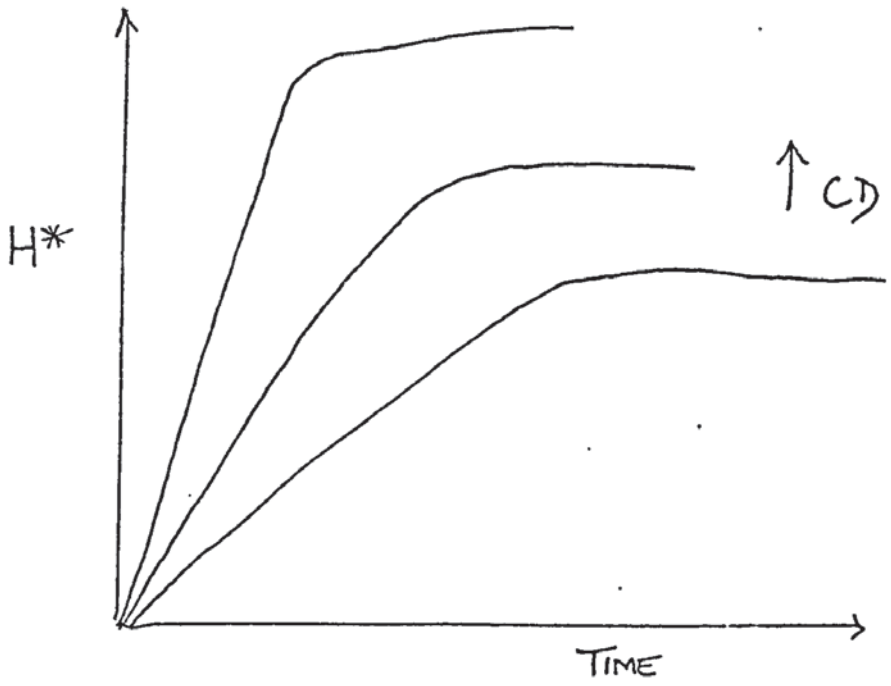

GRAPH 31

The second explanation is that subsequent layers have fewer pores in each due to the reduction in porosity of the subsequent layers. Therefore the next layer to form, which will not have more pores to start with than the last layer had when growth of that layer finished, will therefore have fewer pores. The pores will be of larger dimensions though, the Q6 pores being nucleated after pore blocking. The procedure would therefore be

1. Pores and particles of layer nucleated.
2. Both grow together to critical thickness.
3. Pores begin to block, layer continues to thicken but slower.
4. Growth stops completely with virtually all pores blocked, either by self or mutual blocking.

5. The very small amount of silver chloride penetrating the film, and that formed by redissolution of silver chloride, forms needle nuclei round the pore mouths.
6. Flow of ions resumed by nucleation of Q6 pores, by unblocking of some Q3 pores.
7. New layer of particles formed.

In Schematic Graph 32, it can be seen that at constant current density, the radii of the pores in the second layer increases in accordance with the increase in layer thickness.

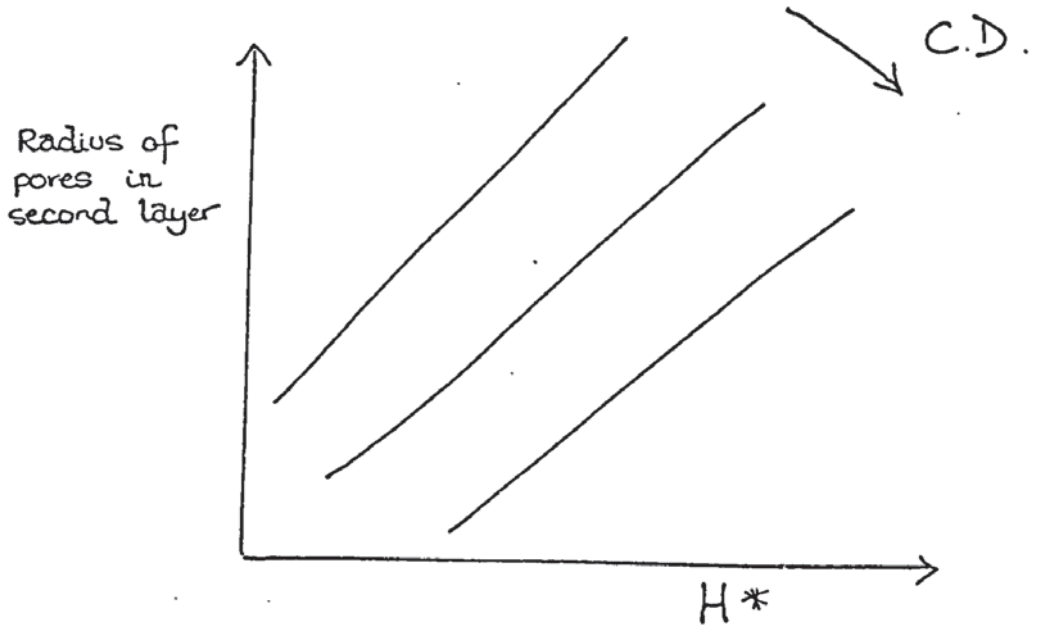

GRAPH 32

As can be seen with Graph 30, the percentage porosity of the layers decreases with increase in thickness. These two points combined point to a mechanism where the thicker the film the fewer, but larger the pores.

This is though a trend in progressive growth of different specimens, and in any one individual layer, in one film, the individual pores must decrease in radius as the layer thickens, eventually causing pore blocking as shown in Fig 13.

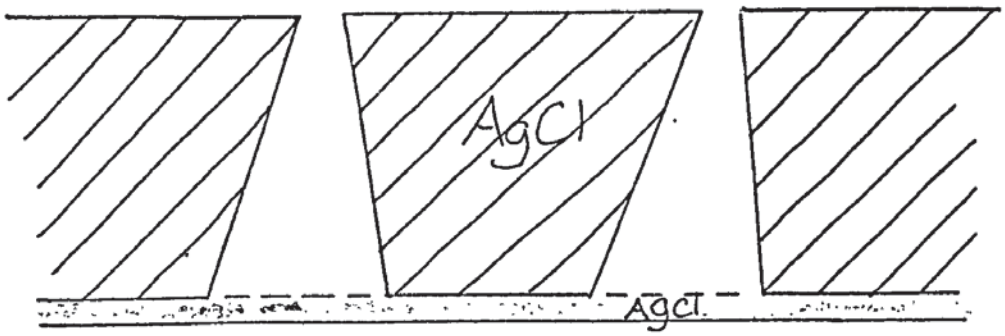

FIG 13

There is a pointer to this being the correct mode of growth, in that Briggs and Thirsk (26) report cylindrical or inverted truncated cones of silver being formed when layers of silver chloride are reduced.

It is proposed that pore blockage is not as prevalent as it should be in theory, and occurs later than would be expected (ending with a thicker layer) due to increased temperatures within the pores increasing dissolution of silver and also of silver chloride in the pore walls, keeping the pores open especially if there is a large current flow in the pore, where the redissolution could be field enhanced.

It could also be that the pore blockage may be as a result of an inbalance in an equilibrium between the absorption of chloride ions, which travel down the pore causing oxidation at the pore bases, and the formation of $Ag\ Cl_{(n+1)}^{-n}$ ions which travel up the pore.

From the polarity of the complexes, there is no ~~anxiety~~ DRIVING FORCE. of the complex to travel to the Ag Cl/solution interface, except by process of convection up the pores, aided by the increase in temperature of the solution at the pore base.

If the layer becomes thick, such that the stability time end point of the complexes is reached before the complex has traversed the whole pore length, then deposition will occur on the walls. The larger the pores, the greater the velocity of flow within them, so the more chance there is of these staying open, viz the reopened Q6 pores.

If the mode of growth was, as some authors suggest, solely by growth of the silver chloride at the Ag/Ag Cl interface, then this could not explain the formation of layers within the film. The film must though grow at this Ag/Ag Cl interface to some extent, or it would detach very quickly. Particles have been shown earlier that are formed at this interface to keep the film in contact with the surface.

It is also proposed that these particles are formed primarily during the period of pore blockage, the mechanism for this will be shown later. In the layer there is a proposed redistribution of silver chloride when depletion of chloride ions occurs, which is in the form of complexes of the type $Ag\ Cl_n^{-(n-1)}$ ions. These diffuse down the blocked pores, depositing as Ag Cl at such sites as the Ag/Ag Cl interface, so producing particles bridging the gap between the basal layer and the dissolving silver layer, and unblocking the pores.

The mechanism is as follows.

Dissolution

$$Ag\ Cl + (n-1)\ Cl^- \longrightarrow Ag\ Cl_n^{-(n-1)}$$

Transport

$$Ag\ Cl_n^{-(n-1)} \longrightarrow Ag\ Cl_n^{-(n-1)}$$

Deposition

$$AgCl_n^{-(n-1)} \longrightarrow AgCl\downarrow + (n-1)\,Cl^-$$

Some complexes deposit silver chloride at the pore mouths, producing the needle M15a and M14 growths. Before describing the purpose of the needle particles in the film, a mention must be made of the nucleation of the second layer from the primary.

It would appear that the second layer is nucleated when the primary has attained a limiting thickness which depends upon the anodising conditions. The reason for this change is probably not one of pore blockage, but that of complex ion stability.

It is presumed that at the thickness attained, the limit has been achieved at which chloride ions can easily penetrate the film and form $AgCl_{(n+1)}^{-n}$ ions at the silver surface. (It is presumed these complexes are formed, in later growth, at different zones higher up in the film and silver ions are formed originally).

Silver ions are therefore formed instead and conversion to $AgCl_{(n+1)}^{-n}$ ions formed at the Ag Cl/solution interface. At this point the morphology changes and the second layer is nucleated.

A check of this proposition was attempted in one series of experiments. In this series the specimen was anodised at intervals, and examined in between them. For instance the bare specimen before anodising is seen in Plc 66, and after 1 second anodising the same area is seen again in Plc 67, with a scattering of silver chloride nuclei and M5 and M1 particles.

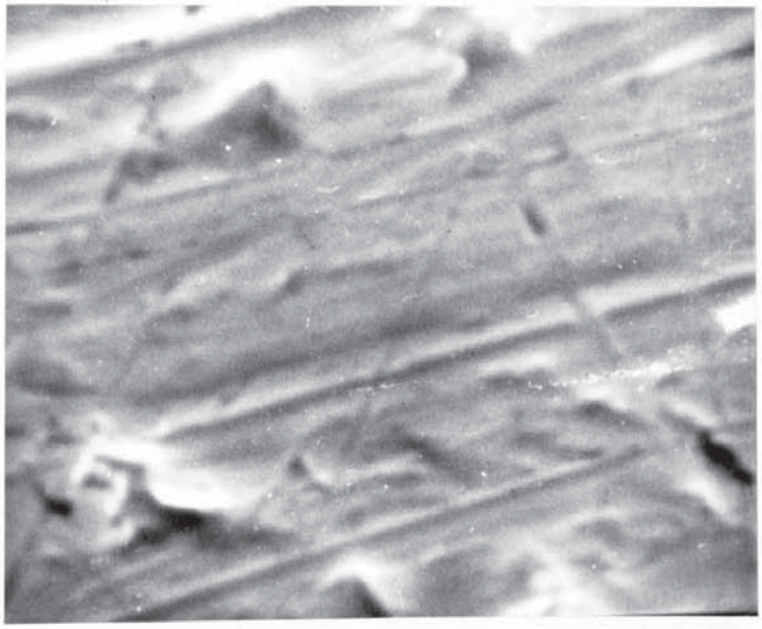

PIC 66 X 10.45K

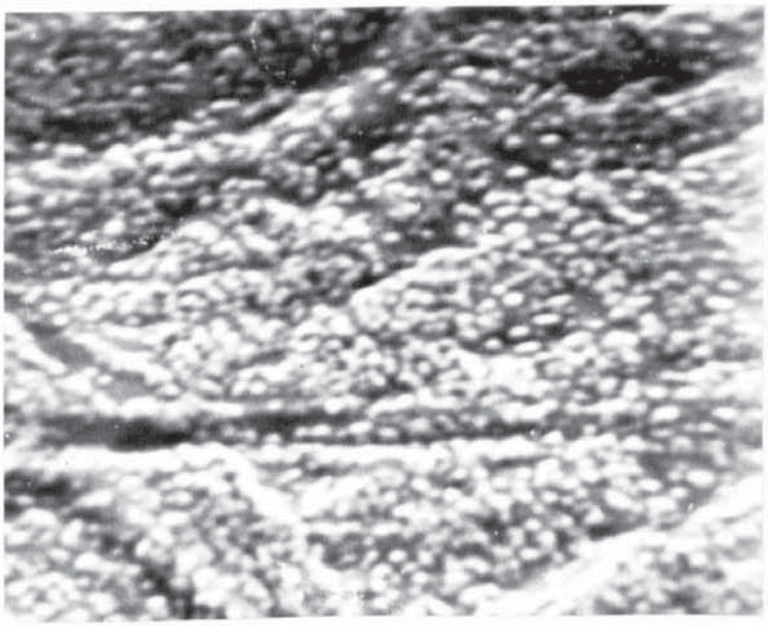

PIC 67 X 10.5K

After 5 seconds anodising the layer has grown more coherent, as in Pic 68, and after 15 seconds the primary layer is almost complete, as in Pic 69.

PIC 68 X 10.6K

After a further 30 seconds, at 45 seconds anodising, particles begin to appear on the surface. These can be seen in Pic 70, and in Pic 71, where they are seen coalescing. They are also seen in Pic 72, where the basis of the second layer can be seen forming.

This can be again seen in another specimen, where a more coherent layer of particles making up the basis of the second layer can be seen overlaying the primary layer, in Pic 73.

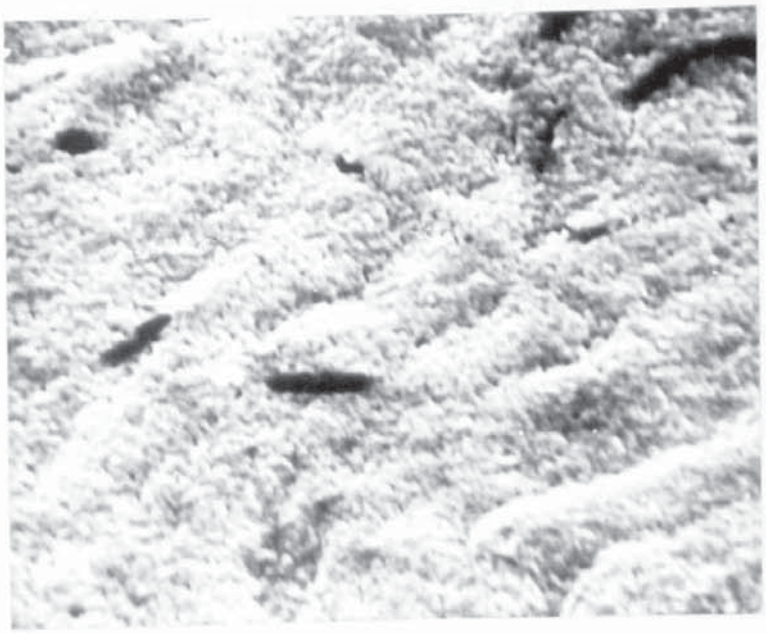

PIC 69 X 5.625K

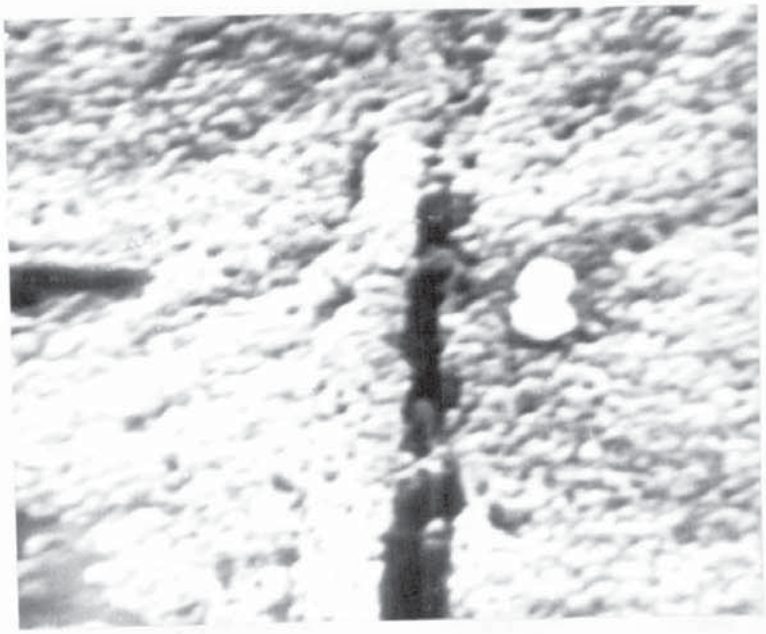

PIC 70 X 11.75K

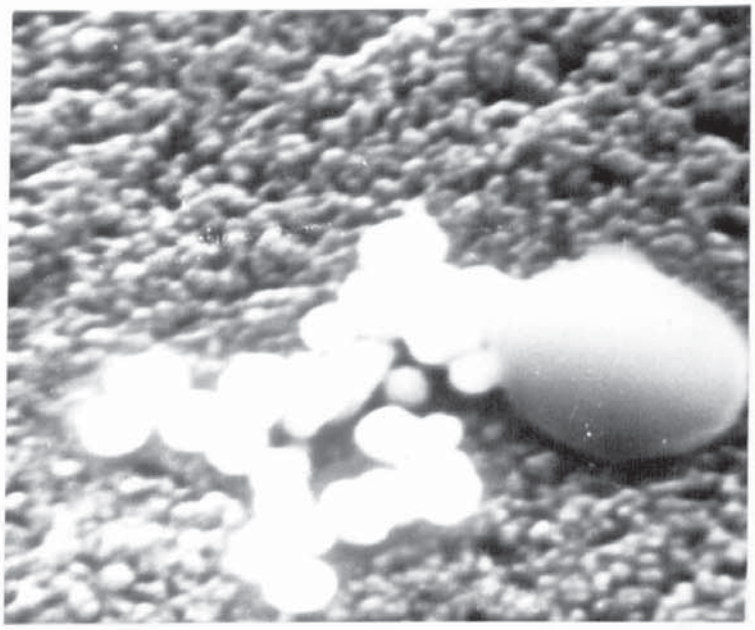

PIC 71 X 11.5K

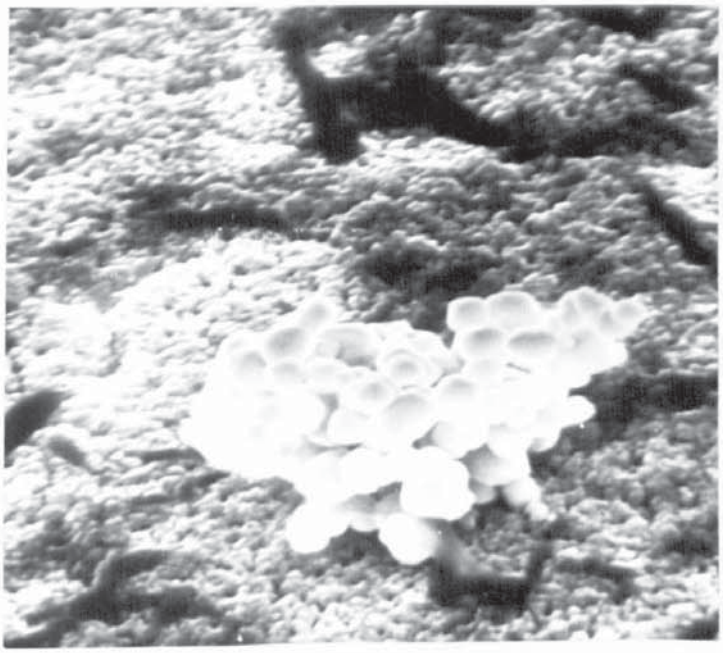

PIC 72 X 5.4K

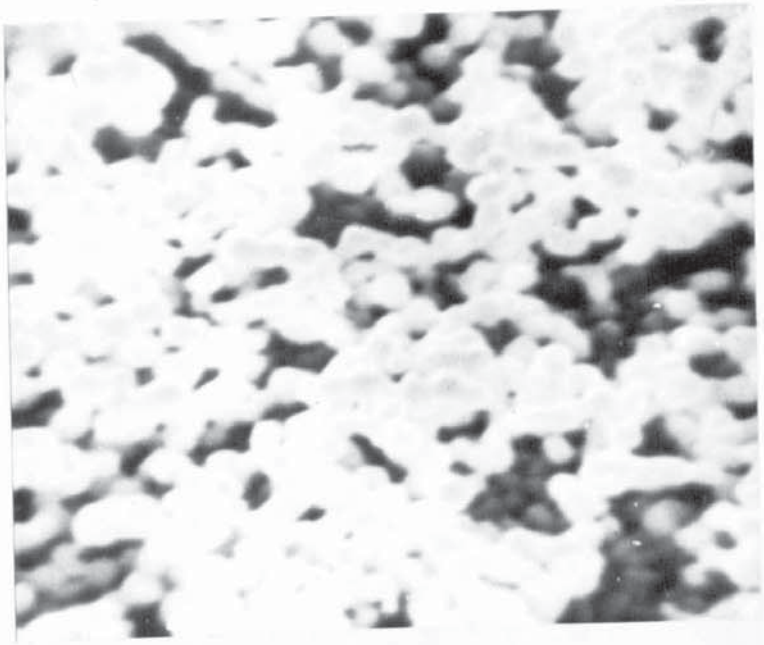

PIC 73 X 10.5K

PIC 74 X 22.8K

When these layers are detached from the basal silver, the primary layer can be seen with the second layer below, as in Pic 74, and the reverse of this can be seen in Pic 75 with the second layer overlaying the primary layer. In this picture a second layer type particle, of the M2a type, can be seen lying on the surface. It is stressed that these are only nuclei of the second layer particles and not of the end particle dimensions. Some of these particles will grow to attain the large columnar dimensions found normally in the M19 or M2a type layer.

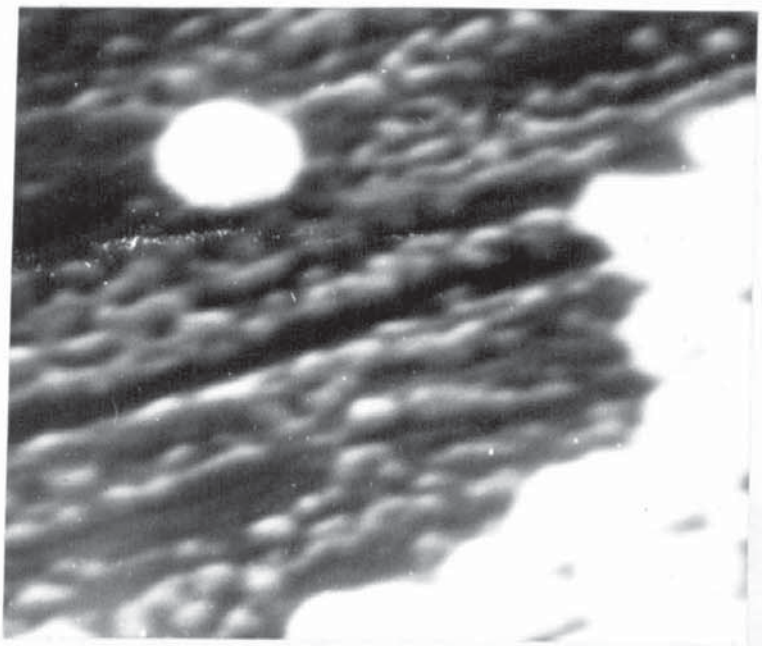

PIC 75 X 22.8K

This evidence indicates that selected M1 or M5 particles in the primary layer act as nuclei for the second layer growth. Probably M5 or M1 particles next to or near to pores, or irregularities, in the primary layer are the best candidates for this growth.

These particles grow preferentially to general growth and layer thickening when lateral layer growth becomes impossible, these particles then grow by the process shown in Fig 2, the same process as for the growth of MI or M5 particles in the primary layer from the K type nuclei.

The appearance of the MI4 or MI5a type needle particles heralds a different type of growth, and although it precedes the nucleation and growth of the third layer, it is a phenomena of the second layer. These needle particles are seen as outgrowths from the oxide film, originating from pores and at right angles to the film surface. This was also seen by Pfefferkorn (5).

The needles can be seen in Pic 76 where they are scattered round the pore mouths in the top of the second layer. A closer examination of these can be seen in Pic 77 where their orientation and structure can be seen more clearly.

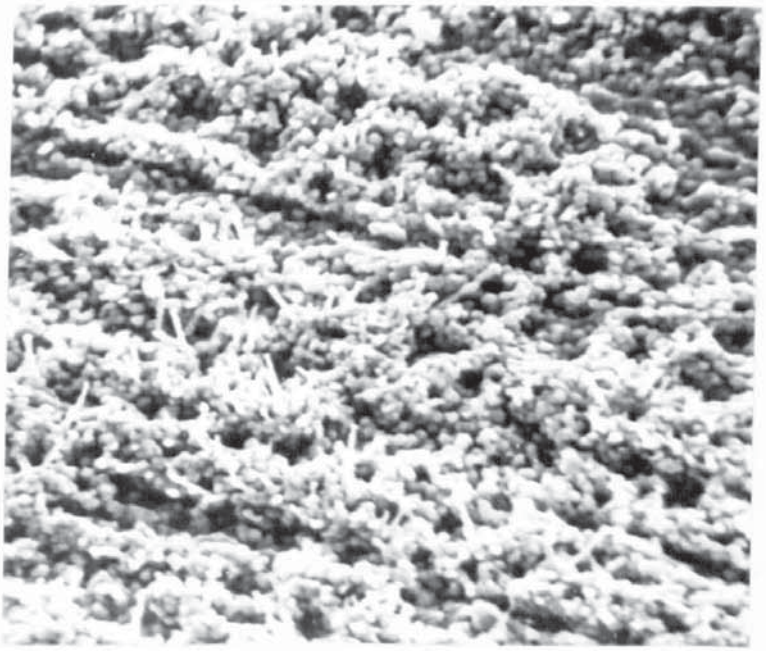

PIC 76 X 2K

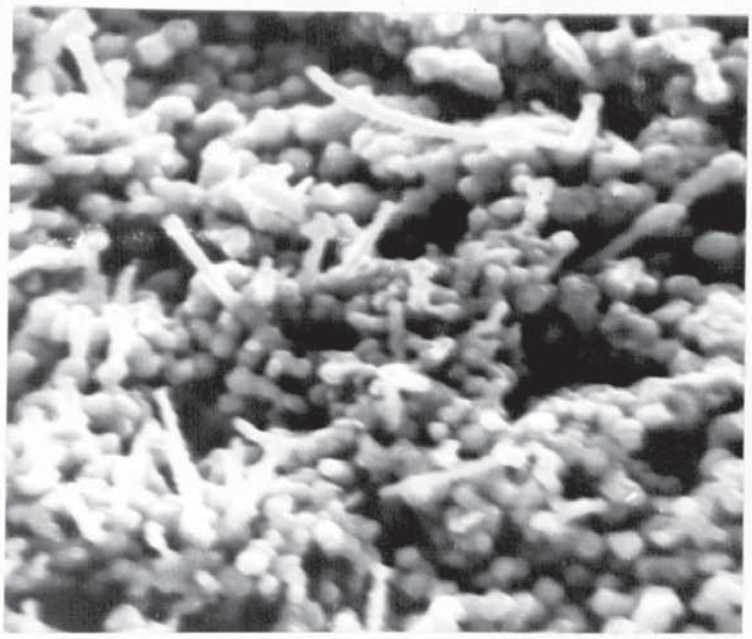

PIC 77 X 5K

From a picture taken on the Joel scanning transmission electron microscope, Pic 78, it can be seen that the needles are in fact of a dendritic nature, with nodules or branches growing out at right angles to the main stem. This can also be seen in Pic 79 where the needles have extended outwards and grown fins at each side.

It should be noticed in this picture that the base of the needles are made up of joined nodules of very much the same size as the layer they grow out of. This seems to suggest that the particles are formed from the nucleation of one nodule on top of another, until the needle type particle is formed by the stringing of these together. An advanced state of dendritic growth in these Ag Cl particles can be seen in a special case in Pic 80.

PIC 78 X 200K

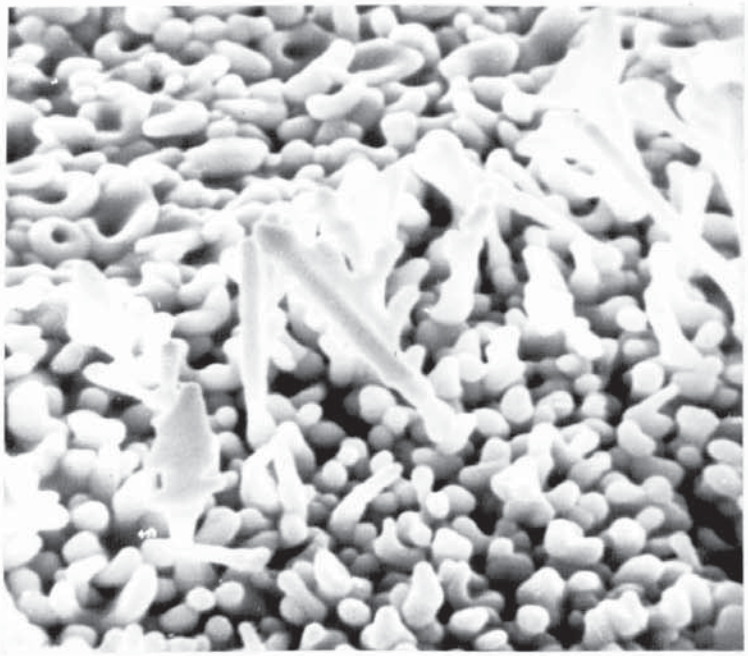

PIC 79 X 5.375K

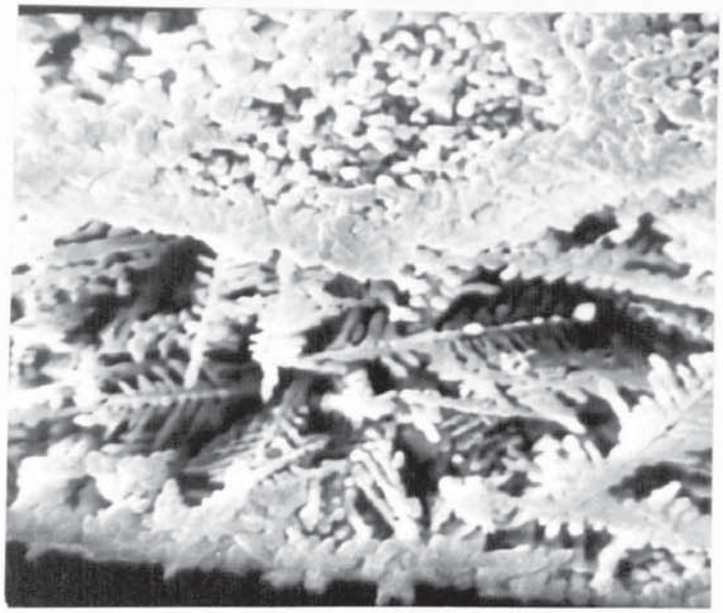

PIC 80 X 4.6K

In this case the film has grown up against the nylon thread, used in the experiment as described before, and a pocket of high silver chloride solution concentration was formed under the threads overhang. Needles nucleated here then grew to proportions not usually seen in normal growth.

In Pic 81 the normal association of primary layer, secondary layer and overlying needles can be seen clearly.

In normal growth the needles begin to spread out, as seen in Pic 82, and cover the surface more coherently. They then thicken and grow into large nodular and faceted particles, in much the same way as dendrites in molten metal form and grow into grains within the solidified structure. The large M9 type particles that the needles grow into can be seen in Pic 83.

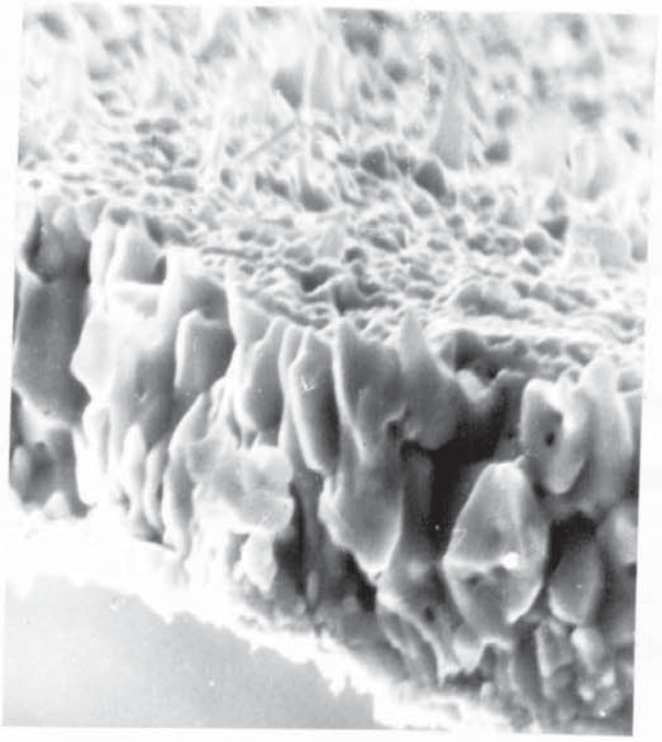

PIC 81 X 5.8K

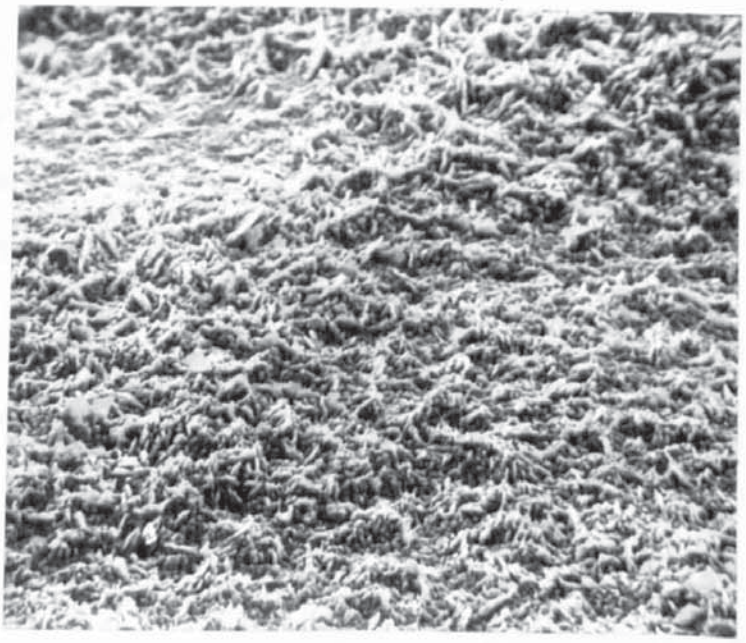

PIC 82 X 1K

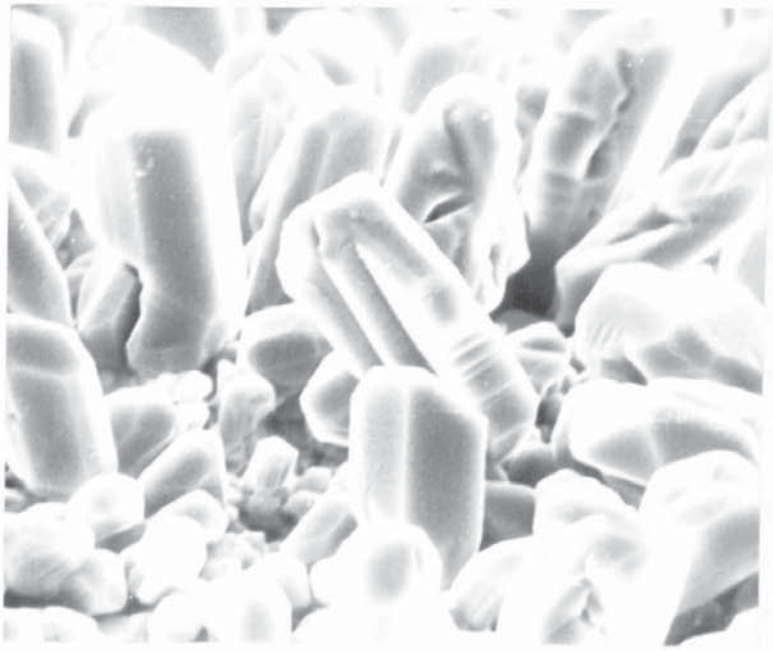

PIC 83 X 5.9K

Only some of the needles make this transformation, and the rest are left between the second and third layers. This can be seen in Pic 84 and 85, where the third layer has been carefully detached from the second layer, leaving a view of the base of the third layer with the remaining needle particles wedged below.

Another mode of growth, where the needles form a thick nodular layer, is described in the next section.

If we look for a moment at the growth of oxide films on other metals, similarities can be seen in the growth processes on silver. Young (1) reports that on zinc, crystalline platelets of ZnO can be seen. Also on lead, needles of micron size can be seen in lead sulphate films with large tetragonal or orthorhombic crystals on the surface. These sound very much like the large M9 particles to which the needles change in morphology.

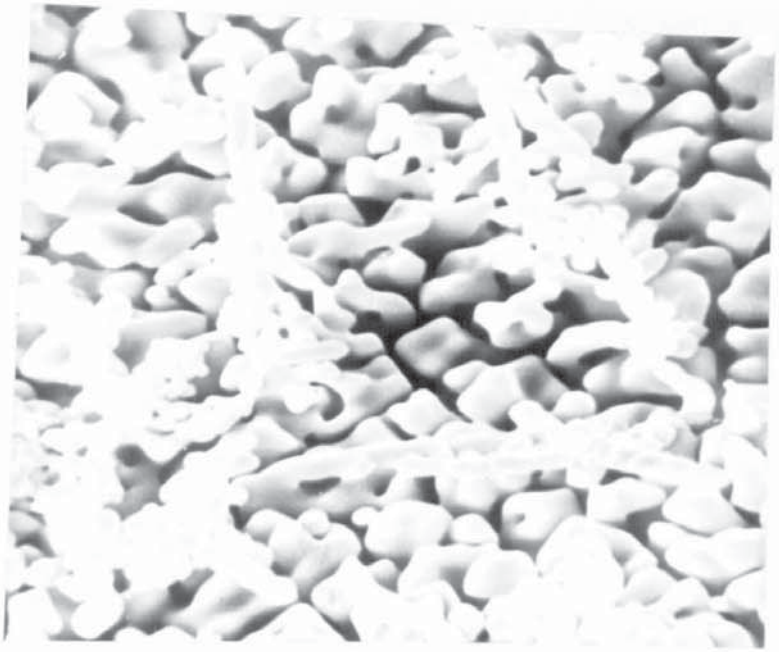

PIC 84 X 5.2K

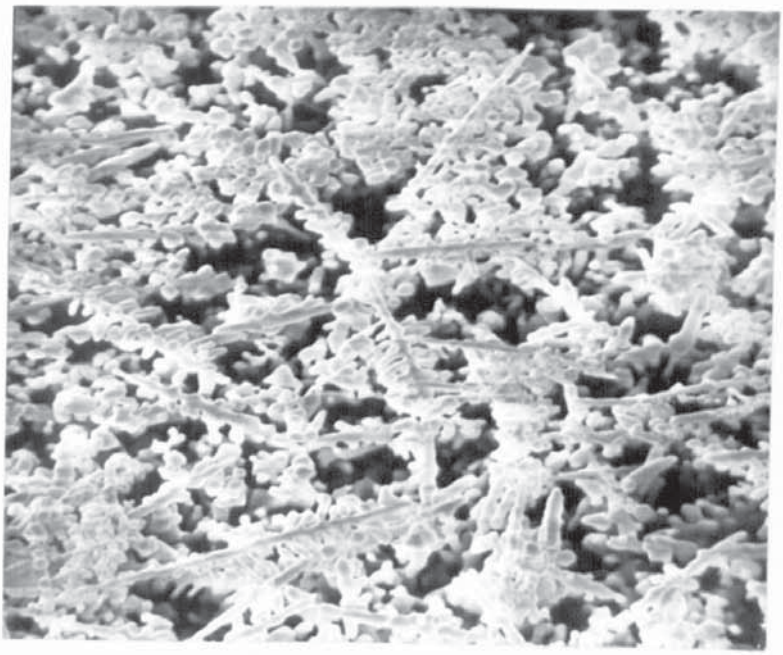

PIC 85 X 2.1K

These could also be crystalline solids formed on the film surface when it is held at constant temperature and potential after anodising. These are reported to be a form of recrystallisation or mechanical replacement, de nova, of the old film. Crystalline nodules of this type are seen in the Ag Cl and will be discussed later.

It is interesting that rise in temperature during the anodising (3, 4) of zinc and copper, caused a decline in growth, probably due to self and compressively mutual pore blocking. This indicates that the blocking mechanism proposed for Ag Cl is probably correct.

The growth of magnetite on iron (13) has special significance in that a primary layer is formed of nodules with pores left between them when they impinge, much like the Ag Cl primary layer. Another layer of larger nodules is then nucleated on top of these, growing by ions diffusing through the lower pores from dissolution sites at the pore bases.

In this film the growth follows the log law and there is a tendency for mutual pore blocking, much as in the growth of Ag Cl. It is interesting that the oxide also grows at the metal/oxide interface to keep in contact with the metal, as is found to be the case with Ag Cl also.

The most interesting report though is that of the growth (17) of Fe_3O_4. This starts, like Ag Cl, with very small nuclei which grow into a coherent film. Thin whiskers about 10^{-9}m long then appear, comprised of Fe_2O_3, and develop into plates. This also occurs (22) on halide films of lead and mercury, and from the evidence presented within, also in silver chloride films.

That the needles eventually develop into plates can be seen in the pictures taken of the three layers consecutively lying on top of each other. The plate like nature of the final particle morphology can be clearly seen in Pic 86, in which the primary layer can be seen at the top of the picture, the film having been removed from the silver base, with the second layer below the primary and the third layer at the bottom.

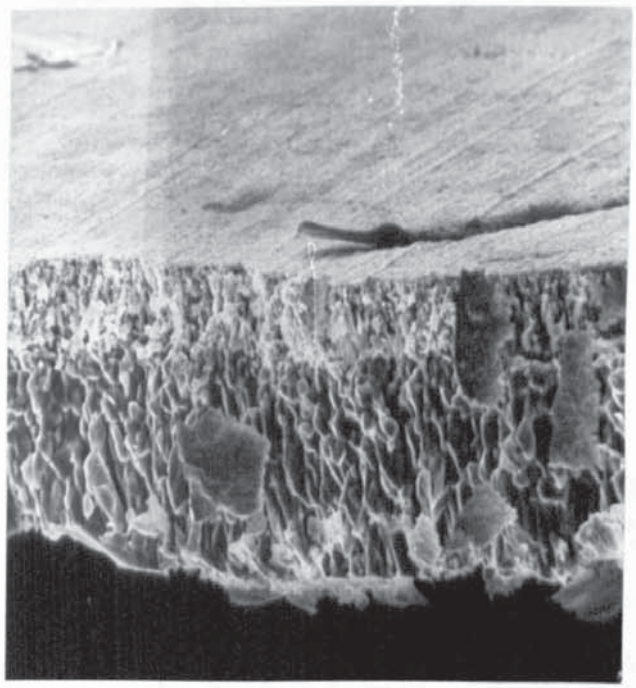

PIC 86 X 1.2K

This can be seen in more detail in Pic 87 where the primary layer can be seen to lie in rows of growth bands, with the second layer below. The cut off between the layers is seen to be very sharp indeed, and on the shelf at the base of the third layer, remains can vaguely be seen of MI5a needles.

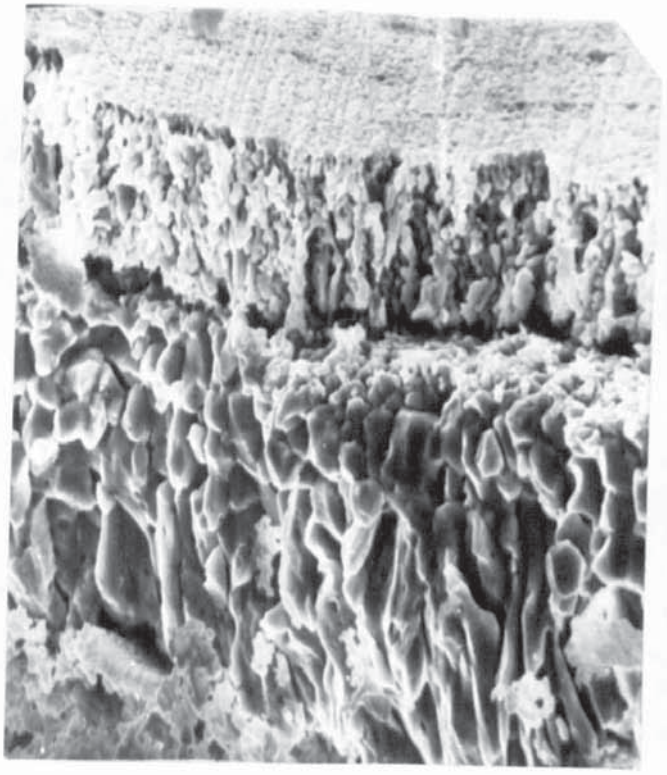

PIC 87 X 2K

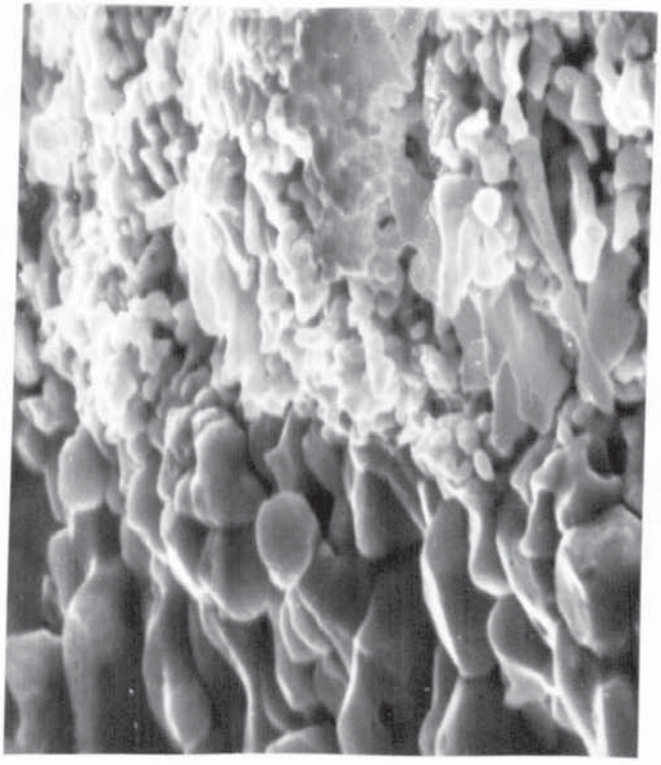

PIC 88 X 5K

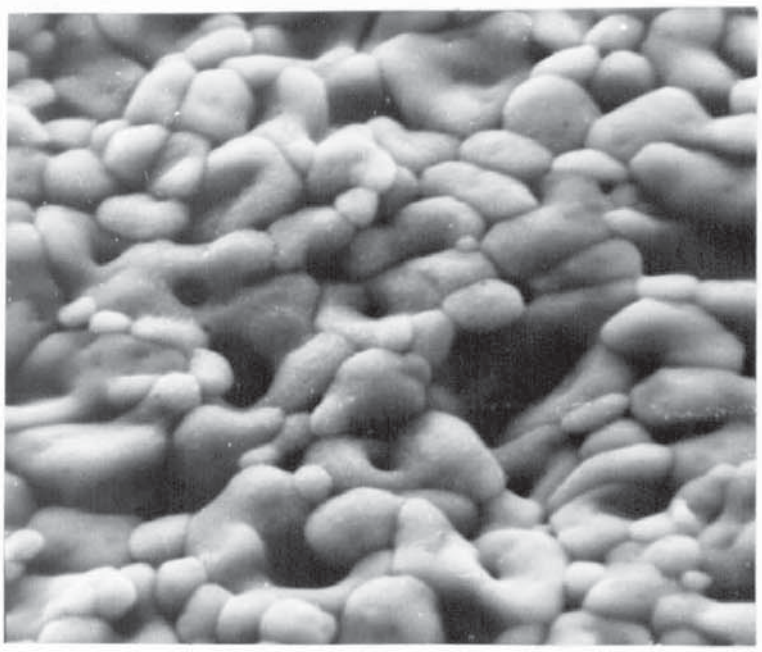

PIC 89 X 5.7K

This interface between the second and third layers can be seen in Pic 88, where the size differential between the particles in each layer can clearly be seen. In Pic 89 the interlocking nature of the particles in the second and third layers can be seen in this top view of the second layer particles and pores.

If the silver chloride film is reduced after anodising, then a granular film of silver particles is produced, much like the original silver chloride film. This porous granular structure, also reported on reduction by Schwab (27), can be seen in Pic 90, after a reduction period of 8 minutes.

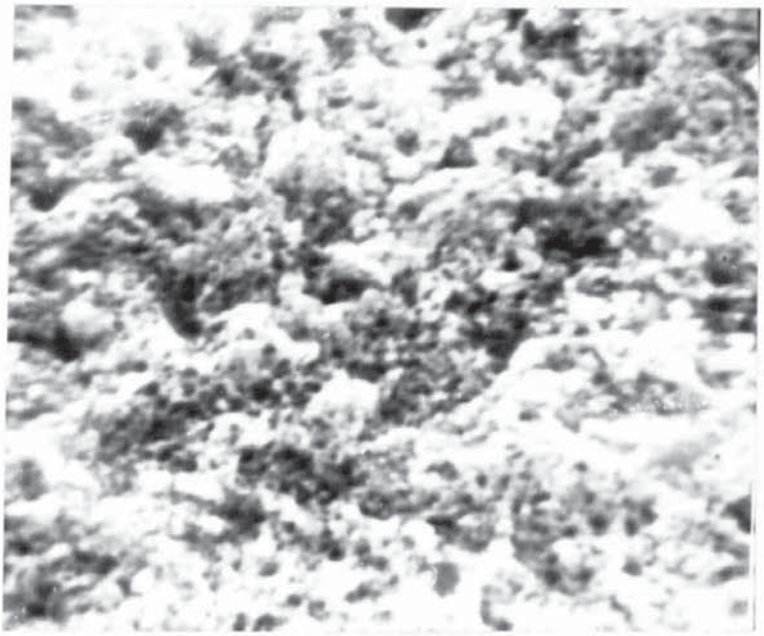

PIC 90 X 10.5K

When this film was anodised, the chronopotentiometric curves were recorded and shown in Graph 28. Up to a period of 300 seconds the Graph shows normal behaviour, but after this the curve shows oscillations, violent at first when the anodising is started, levelling out slowly to a steady value.

This seems to be an exact reproduction of the periodicity seen in the experiments of Lal, Thirsk and Wynne-Jones (25). They suggest that it could be caused by stress relief in the film by breakdown of the uniform structure, thus lessening the restriction on the diffusion of ions, or by a change in the concentration at the face of the electrode, changing the rate and morphology of deposition.

It is suggested in the light of the results gained in this work that both of these explanations are true to some extent. They find that the range of thickness within which oscillations occur is between about 2×10^{-6} to 5×10^{-6}m, which coincides quite well with the end of first layer growth and the beginning of second layer growth.

Also in the experiment carried out, the occurrence of periodic behaviour coincided with the appearance of needles on the surface, and therefore the nucleation of the third layer. Lal et al (25)also found that after the film attained a thickness of about 2×10^{-5}m, the periodic behaviour stops. This thickness fits in quite well to the growth of the third layer.

It is presumed therefore that the oscillations start to occur during the period of pore blockage and unblocking which occurs during needle growth, and is the start of the third layer nucleation stage. It is therefore a period of breakdown in the uniform film structure and of stress relief of the compressive forces, caused by pore blockage, producing mutual pore blocking. This also changes the concentration after pore unblocking at the Ag Cl/solution interface. This changes, as described before, the growth morphology and growth rate with the third layer growing very quickly to a much greater thickness than the previous layers.

Both theories put forward by Lal et al would seem therefore to be correct, and indicate that the pore blocking theory is correct.

As mentioned previously, crystalline solids can appear on the film when held at constant temperature or potential, probably due to a recrystallisation or mechanical replacement, de nova, of the anodic film. It is suggested that, depending upon the silver chloride concentration in solution, that complexes of the type Ag Cl/M_a Cl_b can form, and Ag Cl can be lost to the solution from the film.

A complex like $Ag\ Cl_2^{-1}$, a reasonably stable form, could therefore be produced and material lost or redistributed.

Light and U.V. light (I) can effect Ag Cl, as will be discussed later, causing transient complexes and changes in potential. It was for this reason that experiments in this work were undertaken in a dark-room, illuminated only by red safety light. This was used as it does not unduly affect sensitive photographic silver salts. It is reported that light can also cause Ag Cl films to exfoliate.

It would therefore appear that much material transport and redistribution takes place on rest, and as it is noticed that film detachment takes place always at the interface of one layer with another, then presumably this material redistribution is more prevalent in these regions, causing embrittlement of the film. The changes that are caused within the film when left at rest, at constant temperature, in solution (in this case KCl) can be seen in the following pictures.

In these experiments the anodised specimens were cut in half, half examined and half soaked in solution then examined. As can be seen the films have redistributed completely.

Pic 91 shows the specimen after anodising, with a coherent porous layer, but Pic 92 shows the film to have completely changed. It is now comprised of blocky crystalline nodules which follow, as seen in Pic 93, the original abrasion lines, or lines of growth bands of the primary layer. A complete redistribution has therefore taken place.

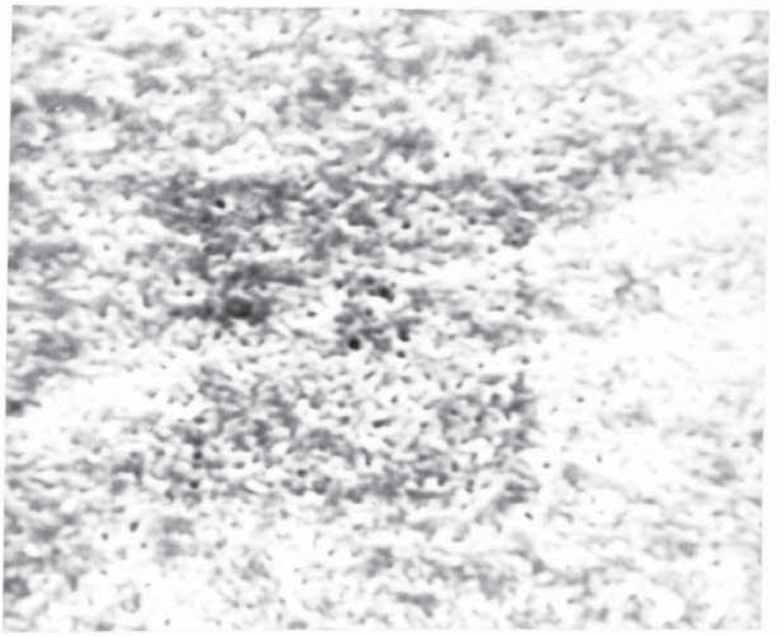

PIC 91 X 2K

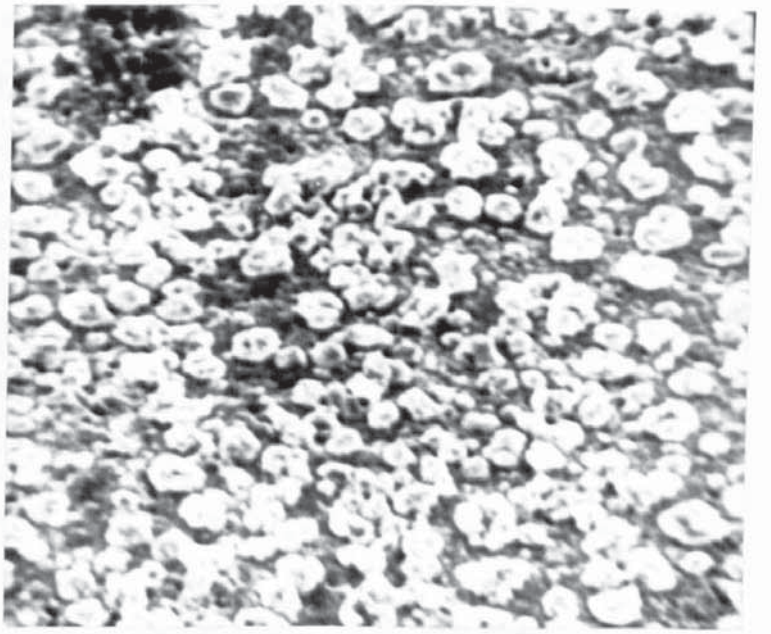

PIC 92 X 2.02K

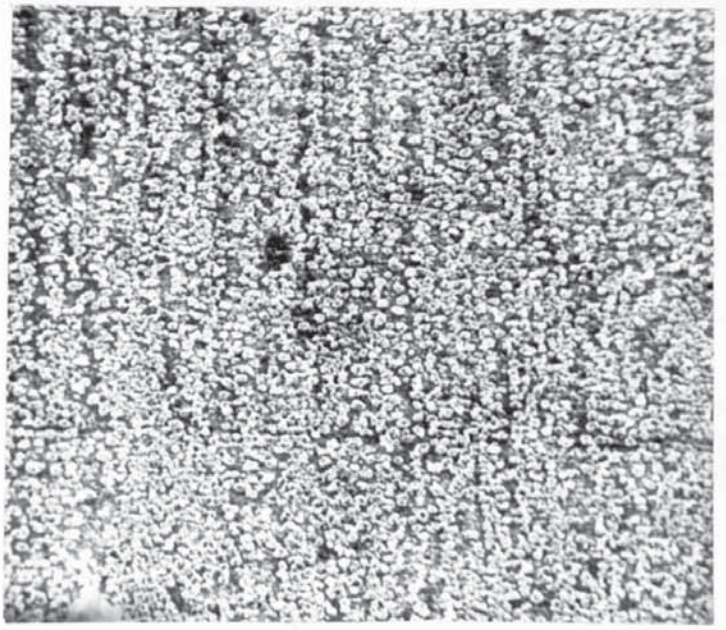

PIC 93 X 510

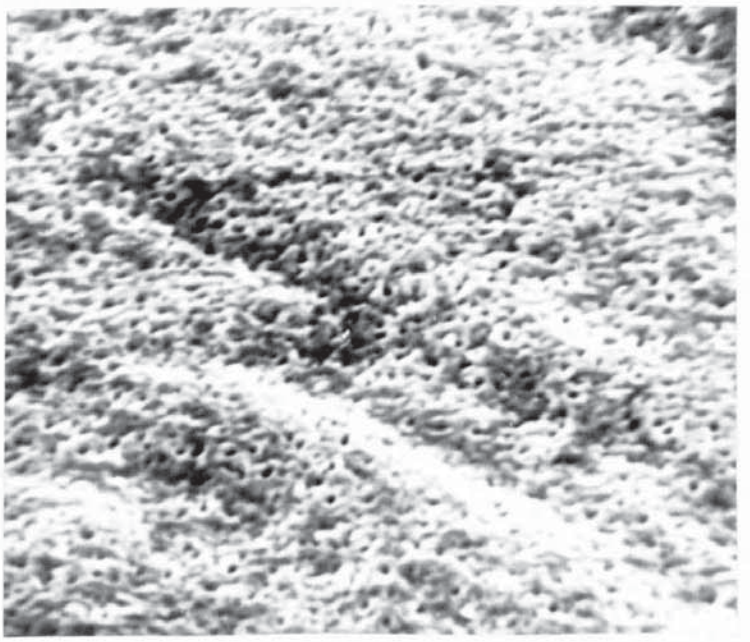

PIC 94 X 1.957K

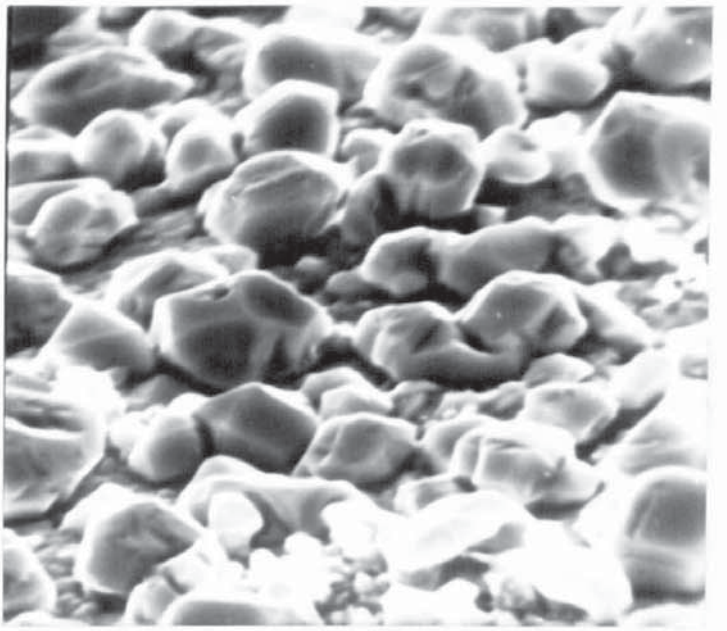

PIC 95 X 7.5K

This can again be seen in comparing a different specimen in Pics 94 and 95, where in the latter, the crystalline facets of the blocks can be seen.

It is presumed that this rearrangement takes place in the film during the period, on the potential to time curves for aging, up to the point when the potential becomes positive with respect to the calomel electrode. The length of time that the electrode takes to become positive depends on the film thickness, the thicker the film, the longer the time. If the process of film rearrangement takes place during this negative period, then the more material in the film, the longer it will take, so it does not seem as if rearrangement takes place then.

If the film has three layers then redistribution takes place, then the third and final layer may be the only one to suffer change of morphology.

This effect can be seen in Plc 96 and in Plc 97 where the third layer can be seen to have renucleated as faceted crystalline particles on top of the virtually unaffected second layer.

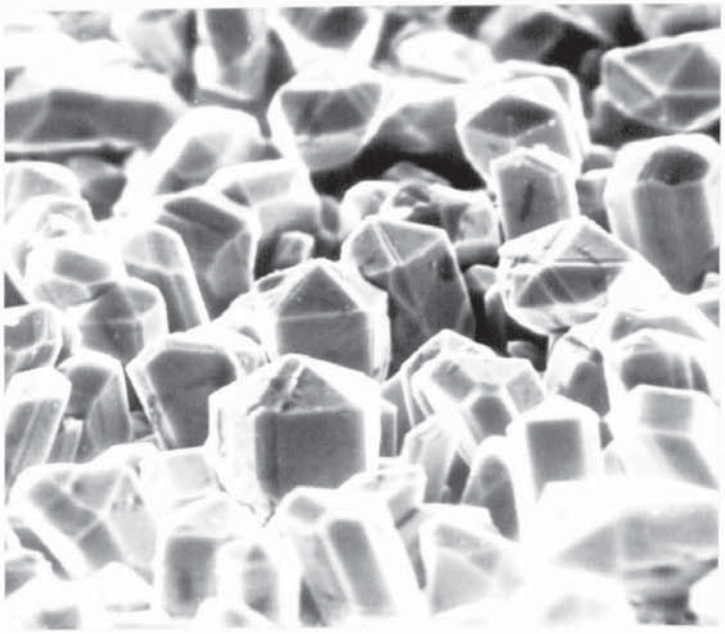

PIC 96 X 2.9K

It is interesting to note that when two specimens are anodised under the same conditions, except that one is at a temperature of 46.5°C and the other is at 25°C, then the thickness of the specimen anodised at the lower temperature is much greater. The thicknesses are 7.2×10^{-6}m compared to 6.45×10^{-6}m, although the dimensions of the basic particles in the films are identical, with M2a in each at 8×10^{-7}m radius.

PIC 97 X 3.8K

If the base silver is annealed before anodising, a different film is produced, as seen in Pic 98.

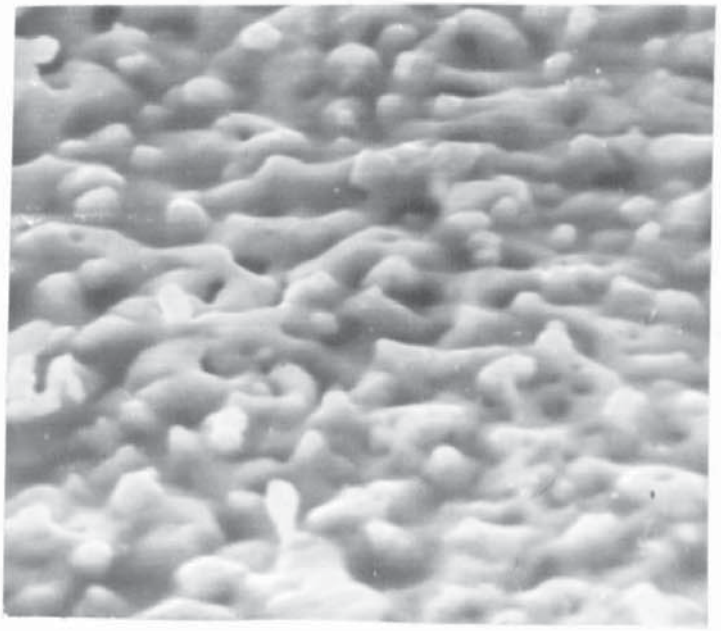

PIC 98 X 6.9K

Here the film is more coherent but still nodular and porous. The particle size, pore size and thickness, are much greater than for a specimen anodised similarly, but without the prior annealing.

It would seem therefore that the stress relief reduces the number of nucleation sites on the silver surface, but in doing so increases the particle size, and therefore the porosity between the particles. This increased voidage would increase the film thickness.

It is also interesting to note that if the anodised film is coated in an ionically passagable hydroplastic film directly after anodising, then rearrangement of the film material is at a minimum. The period of time after the electrode is negative, w.r.t. the calomel reference electrode in the cell, is reduced greatly compared to an uncoated electrode, and the aging time to arrive at the equilibrium potential is much less, only 2 hours compared to 15 hours.

The eventual equilibrium potential is very high compared to normal (370 mV compared to 227 mV) but is very stable over long time periods. The plastic can also be coloured to protect the electrode from light and U.V.

If the base silver is coated in plastic then the coated specimen anodised, a film of silver chloride is formed within the plastic shield. This has no real aging time to speak of, that is it is not negative w.r.t. the calomel electrode directly after anodising, but is immediately at about 180 mV, the equilibrium potential being 277 mV. It takes in the region of 40 hours to attain this value of 277 mV though, and remains very stable over long periods.

One interesting experiment carried out shows how the anodising conditions can unexpectedly change the film morphology. Two specimens were anodised, one for a very long period of 18 hours but at a very low current density of 0.04 ma cm^{-2}. The other was anodised at a higher current density of 1 ma cm^{-2} but a low set potential of 10 volts. The difference in morphologies can be seen in the next few pictures.

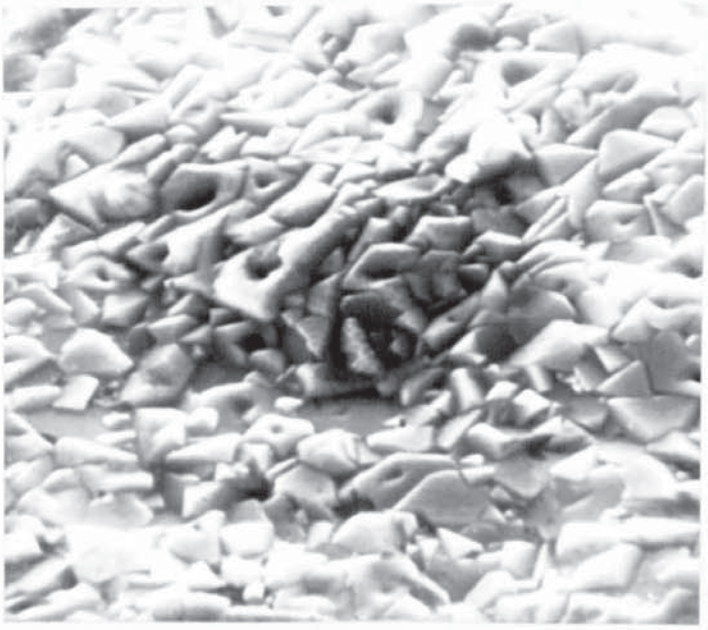

PIC 99 X 5.5K

In Pic 99 it can be seen that the particles, instead of being rounded and nodular, are pyramidal with flat faces and pores running down the apex of the structure, as can also be seen in Pic 100. In this case the slow anodising has obviously left time for the film to assume a semi crystalline state while growing, whereas the specimen anodised at higher current density but lower potential, assumes a film morphology comprised of very fine nodular particles, as seen in Pic 101, the side view of the film, and in Pic 102, the top view of the film.

PIC 100 X 19.8K

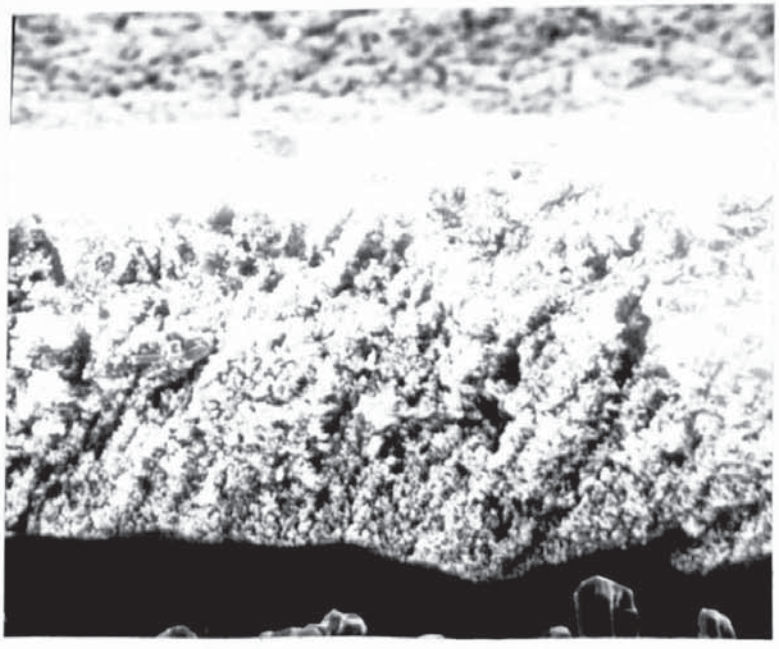

PIC 101 X 1.16K

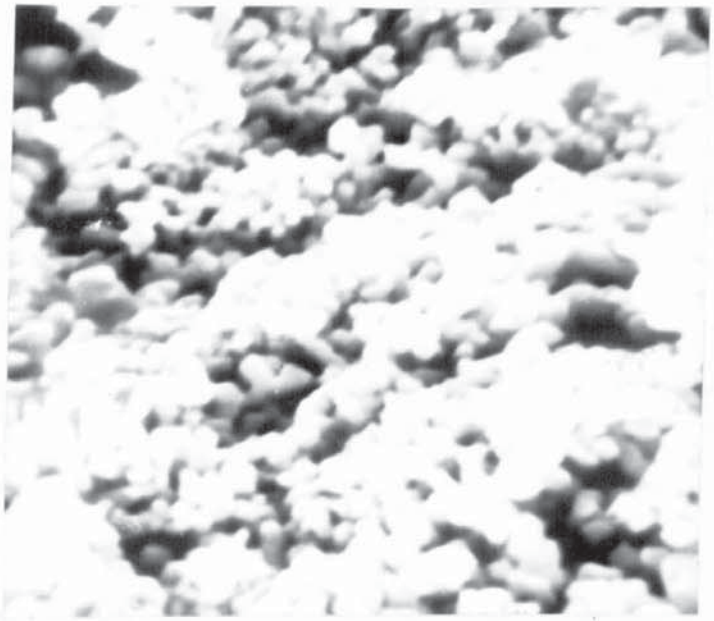

PIC 102 X 11.2K

The Computer Derived Relations for the second layer growth show that the thicker the primary layer, the thicker the second layer will be also. If the conditions for growth are such that the primary layer forms a thick coherent porous layer quickly, then dissolution energy is quite high, and the second layer will also be thick, so $\uparrow H2 \Leftarrow \uparrow H1$.

If M5(1) dimensions are large also, then the second layer will also tend to be thicker, i.e. $\uparrow$ r/v M5(1) $\Rightarrow \uparrow H2$.

This is presumably as the Q3(1) pores will be larger in the primary layer if M5(1) radius is greater, as the Q3(1) pores denote M5 packing. This will affect second layer porosity and particle size. If the pores are larger then the particles are probably larger also (the M2a(2) or M19(2) particles) and so the layer thickness will probably be larger also, as shown by the CDR $\uparrow$r Q3(2) $\Rightarrow \uparrow H2$.

There is a relation between the dimensions of the MI9 and M2a particles and the Q3 pore dimensions in the second layer, $\uparrow$ r/v MI9/2a(2) $\Rightarrow \uparrow$ r/v Q3(2), this being obvious as the Q3 pores are the interstetese between the MI9 or M2a particles. The larger the particles, the larger therefore the packing gaps between them.

With the Q6 pores though, these exist as holes or tunnels through the film sometimes with radii several times that of the individual particles or pores in the film. Usually though these pores comprise of a group of particles missing, so the larger the particles the larger the Q6 pores, so $\uparrow$ r/v MI9/2a(2) $\Rightarrow \uparrow$ r/v Q6(2).

As the hole penetrates through the first layer also, it will probably penetrate at the same diameter, so the same relation holds and the CDR is $\uparrow$ rMI9/2a(2) $\Rightarrow \uparrow$ rQ6(1). Where the radius of the oval MI particle in the primary layer is low, or the volume of the round M5(1) particle is high, then the volume of the MI9/2a(2) increases.

We see here the divergence in effect of the two particle types in the first layer, and the dependence of the second layer particles on the M5(1) dimensions. Not only does one increase in size as the other reduces, but their effect on second layer particles is contrary.

This would explain the CDR between the first layer particles and the second layer pores

$\uparrow$ rQ3(2) $\Rightarrow \downarrow$ vMI(1) $\Rightarrow \uparrow$ rMI9/2a(2)

$\uparrow$ rQ3(2) $\Rightarrow \uparrow$ r/vM5(1) $\Rightarrow \uparrow$ vMI9/2a(2)

in terms of the joining relation with the MI9/2a(2) particle dimensions, and suggests that the M5(1)'s are the nuclei for the MI9/2a(2) particles.

This increase in second layer particle dimensions produces an increase in needle length, ↑r/vMI9/2a(2) => ↑lMI5a(2), where the needles grow at the pore mouths.

If the particles are larger, then so are the pores and their number decreases. The sites available for needle growth therefore reduced, but if the material available for growth is the same then the fewer needles nucleated will grow therefore to larger dimensions. Where ↓C => ↑rMI9/2a(2), the lower the current, the larger the particle dimension. We know that ↑C => ↑rMI(1) where the higher current probably produces an overpotential favourable to a high rate of material dissolution. Low current will produce an MI particle of small dimensions, but presumably a conversely large M5.

From the CDR ↑vM5(1) => ↑vMI9/2a(2), a large M5 would produce a large MI9/2a, and this leads again to the supposition that the M5(1) particle is the nuclei for the MI9/2a(2) particles. The CDR ↓YR => ↑vMI9/2a(2) can be explained as a function of the CDR ↑H3 => ↓r/vMI9/2a(2). Here the larger the MI9/2a(2) the thinner the third layer, which is the thickest layer and contains most of the pore volume in the film.

The larger therefore the MI9/2a, the thinner the third layer which contains most of the pores and so the lower the value of YR, the total pore volume. Physically this could mean that anodising conditions are below those suitable for third layer nucleation and growth, and favour a coherent thick second layer. It could also mean, as the CDR ↑H3 => ↓H2/HI shows, that the thicker the second layer the thinner the third layer, so we have a thin or undeveloped third layer over a thicker second layer with particles of large dimension.

This shows that unless conditions favour the explosive exponential growth of the third layer, the stable growth phase always is the thick second layer. When limiting thickness occurs, needle MI4 or MI5a particles are formed and the third layer nucleates.

The MI4 and MI5a growth morphologies are virtually identical, except MI4 has a tendency for branched or dendritic type growth, and as such is probably an extension or later form of the MI5a. Both favour the same conditions, as the CDR ↑IMI4(2) <=> ↑IMI5a(2) shows, and both increase their dimensions with those of MI9/2a.

↑IMI5a(2) => ↑r/vMI9/2a(2)

↑vMI4(2) => ↑rMI9/2a(2)

This is presumably due to the smaller number of the Q3 or Q6 pores as explained before, and as the two CDR's below show.

↑I/vMI5a(2) => ↑r/vQ3(2)

↑I/vMI5a(2) => ↑rQ6(2)

In the CDR ↑IMI4(2) => ↓r/vMI(1) and ↑IMI4(2) => ↑r/vM5(1) we can again see that the effect of primary layer particle effect transposition.

We know that small MI(1) dimensions give large M5(1) dimensions, which leads to large MI9/2a(2) and likewise increases the MI5a(2) or MI4(2) dimensions. This also blends in relations

↑IMI5a(2) <= ↑rQ3(1)

↑IMI4(2) <= ↑vQ3(1)

↑IMI4(2) <= ↑rQ6(1)

as, presuming that the particles are touching, if the M5(1) particles are greater in size, then the apparent pore dimensions will increase.

Increase in M5(1) dimensions will then cause increase in MI5a(20 or MI4(2) for the reason stated before.

The longer the anodising time T, where the CDR gives $\uparrow T \Rightarrow \uparrow 1/v$ MI4(2), then the greater the time for needles to attain their maximum dimensions. Also $\uparrow H3 \Leftarrow \uparrow 1/vMI5a(2)$ which reflects on the CDR $\uparrow YR \Rightarrow \uparrow IMI4(2)$ and could mean that the greater the MI4 dimensions, the thicker the third layer and so the greater the porosity, as the needles are the third layer nuclei.

It could also mean though that the physical measurements of the film may have in some cases included the needle length, and so calculation of layer parameters including porosity could show as being artificially higher than they should be. This would influence porosity by including the "fresh air" between needles on the surface, as pore volume.

If the first layer has small particles and is thin, then the interstitial pore volume will be small, so the relation below can be valid.
$\uparrow vQ3(2) \Leftarrow \downarrow HI \angle \downarrow vQ3(1)$

Also the Q6 pore dimensions will vary with those of the Q3 pores, as the Q3 pore sites are probably the starting point for the larger Q6 pore growth, and also the Q3 pore dimensions are related, as are the Q6 dimensions, to the layer particle radii so the CDR's below should be valid.
$\uparrow vQ3(2) \Rightarrow \uparrow rQ6(2)$
$\uparrow vQ3(2) \Rightarrow \uparrow vQ3/6(2)$
If $\uparrow C \Rightarrow \uparrow vQ3(2)$ but $\downarrow CD \Rightarrow \uparrow vQ3(2)$ this must mean that, if a large current and a low current density produce the same effect, that the surface area of the specimen must be high. The large pore volume provides the answer, insofar that large pore volume will increase the surface area of the anodic film.

By increase in anodising time the volume of the pores increases as the CDR $\uparrow vQ3(2) \Leftarrow \uparrow T$ shows, and this would seem obvious as the longer the anodising, the thicker the film.

The relation $\downarrow Vol \Rightarrow \uparrow vQ3(2)$ indicates again that $\uparrow H3 \Rightarrow \downarrow H2$, so if the film volume is low the likelihood is that H2 is quite thick, with there only being the primary and secondary layers. If then H2 is thick, the likelihood is that considering pore geometry, then the pores will be of greater volume. This also again indicates that the greater the thickness and volume of the film the less the porosity or number of layers.

Concerning the Q2 pores or indentations on the particle surfaces, the CDR's show

$\uparrow vQ3(1) \Rightarrow \uparrow rQ2(2)$

$\uparrow vQ3/6(2) \Rightarrow \uparrow rQ2(2)$

$\uparrow vQ3/6(2) \Rightarrow \uparrow vQ2(2)$

$\uparrow rQ6(2) \Rightarrow \uparrow vQ2(2)$

that large Q3 or Q6 pore dimensions give large Q2 pores in the second layer. The Q2 pores are of two types as the CDR below shows.

$\uparrow rQ2(2) \Rightarrow \downarrow vQ2(2)$

$\uparrow vQ2(2) \Rightarrow \downarrow rQ2(2)$

This is not as contradictory as it seems but indicates the presence of pores of large volume but small radius, and small volume but a large radius. Large Q2 pores could be indicative of high dissolution rate and secondary dissolution from the particles themselves by the mechanism described before, the material being deposited perhaps as the MI5a or MI4 needles.

The relations

$\uparrow vQ6(2) \Rightarrow \uparrow rMI9/2a(2)$

$\uparrow vQ6(2) \Leftarrow \uparrow rQ3(1)$

$\uparrow vQ6(2) \Leftarrow \uparrow vQ3(2)$

$\uparrow vQ6(2) \Leftarrow \uparrow rQ3(2)$

$\uparrow vQ6(2) \Rightarrow \uparrow r/vQ2(2)$

seem to indicate that large pore dimensions in the film give a large Q6 pore volume, for reasons given before. Also

$\uparrow rQ6(2) \Rightarrow \downarrow vQ3(2)$

$\uparrow rQ6(2) \Rightarrow \downarrow vQ6(2)$

seems to show that the larger the Q6 radius the smaller the volume of the pore and vice versa. This may indicate that Q6 pores of small radius penetrate further into the film.

As a further point it is noted that the growth of the M2a or MI9 and other second layer particles is presumed to take place by a similar mechanism to that of the M5 particles in the primary layer. That is, they are presumed to grow by nucleation and growth of small particles on the surface, as shown in Fig 8. The presence of the small nodules on the surface of the particles can be seen Pics 103 and 104.

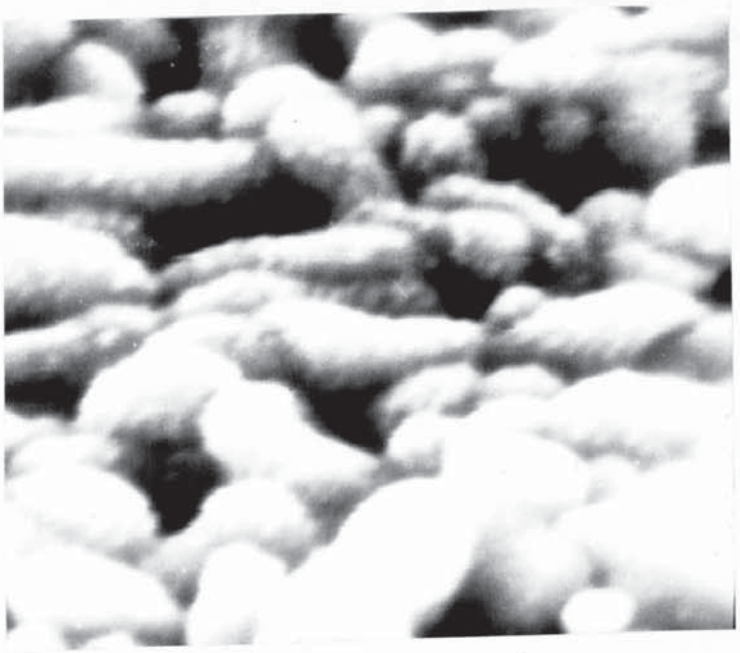

PIC 103 X 22,5K

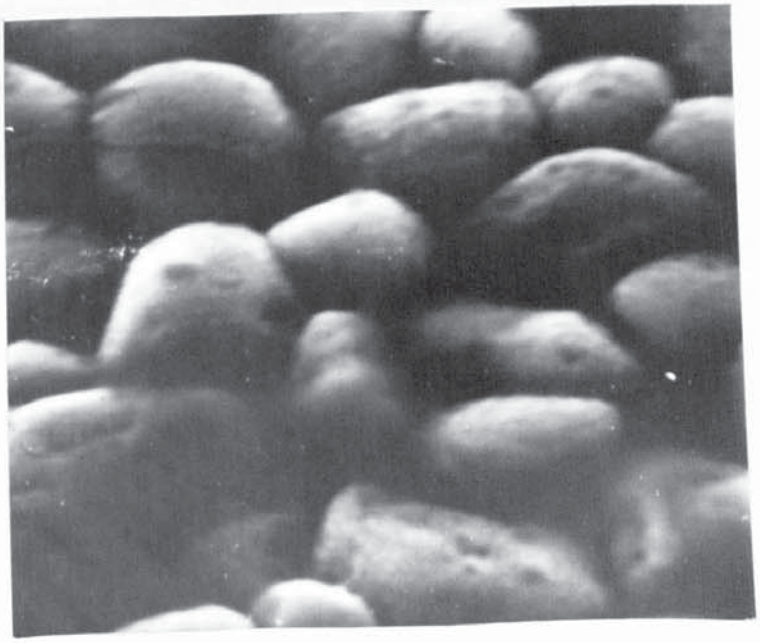

PIC 104 X 12,4K

SECTION (3)

THE NUCLEATION AND GROWTH OF PARTICLES AND POROSITY IN THE THIRD LAYER

The nucleation of the third layer, as described in the last section, is a process of growth from needle particles nucleated on top of the second layer. In most of the cases where the third layer formed, the anodising conditions were such that the current density was high, over 10 ma cm^{-2}, and/or the temperature of anodising was high, over $40^{o}C$.

Indira and Doss (7) report also that below 10 ma cm^{-2} the potential quickly gains a steady value, but above this current density it keeps on rising steeper, presumably where a different growth mechanism takes over. Vermilyea (22) also reports that a coarse fluffy layer of very fine dendritic type particles is precipitated at the pore edges, at very high current densities. This fits in well with the observed practice of third layer growth.

The very coarse platelet form seen in Pic 86, 87, 88, occurs only after long anodising under high current density conditions.

The primary third layer growth can take two forms, the thickening needle form to produce crystalline nodules, as seen in Pic 83, or the "cactus" type particle which occurs in two forms as M8 or M8b. This form of cactus growth appears as a layer of interlinked small nodules (the M8 particle), all joined together and forming a very porous but thick layer, as seen in Fig 14.

Young (1) found that the film had two growth modes, above about 18 ma cm^{-2} uniform growth proceeds, then a white layer (like Vermilyea's) formed. Below about 18 ma cm^{-2} no white layer formed. It is presumed the white layer is of M8b cactus particles.

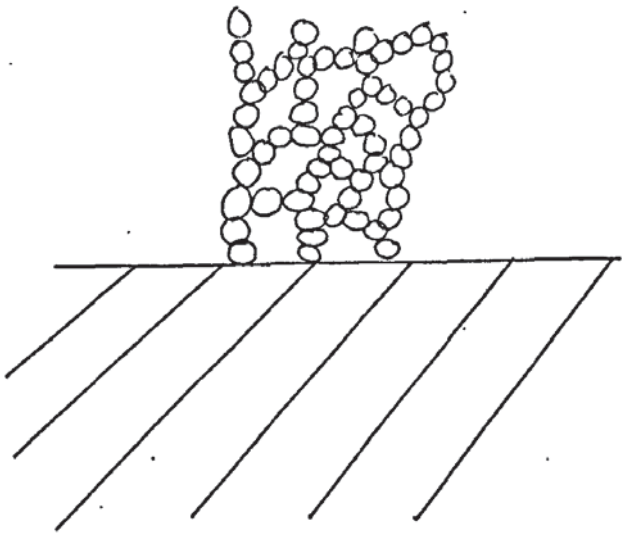

FIG 14

The effect of current density on the film is quite marked, for instance it is reported that Gerisher found that below 3 ma cm^{-2} only patchy coverage occurred, but if the current density was raised then the film covered over the surface by the patches growing together.

The cacti grow from the needles on the second layer, the growths being an extension of needles which are themselves made up of nodules especially at their bases. The two forms of growth from the needles can be seen in Figs 15 and 16.

The reason why the needles should immediately change in some cases to the M9 particles, and in other cases first convert to the cactus particles, is unclear. The third layer eventually forms the coarse plate like layer seen in Pics 86, 87, 88, after long anodising time, but the process of conversion of cactus particles has not been found by this work.

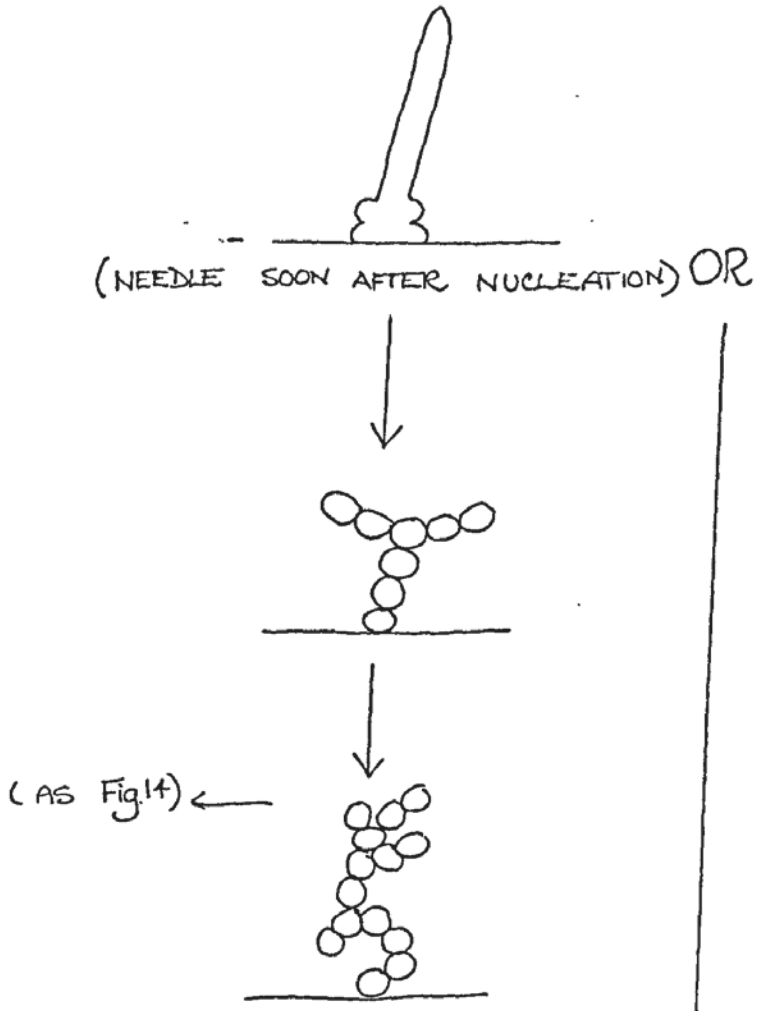
(NEEDLE SOON AFTER NUCLEATION) OR
(AS Fig.14)

FIG 15

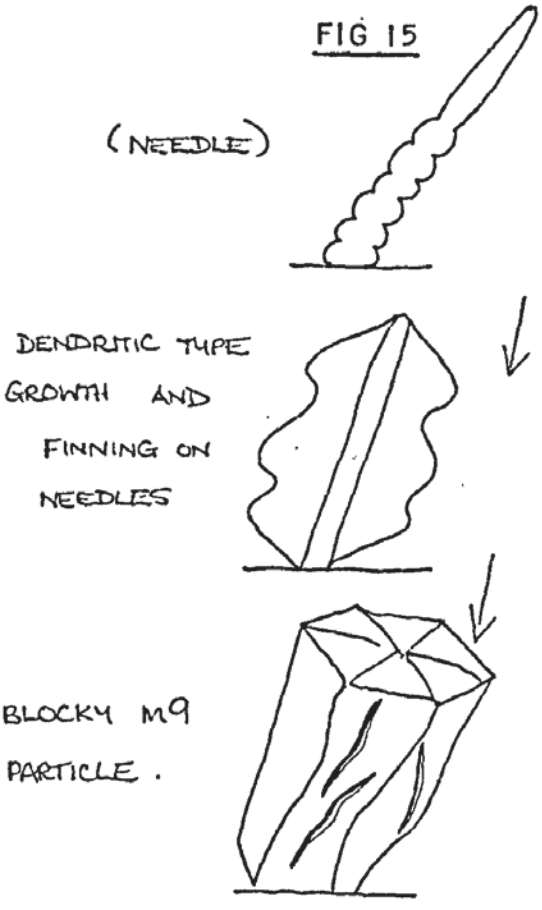
(NEEDLE)
DENDRITIC TYPE GROWTH AND FINNING ON NEEDLES
BLOCKY M9 PARTICLE.

FIG 16

One pointer is that the blocky third layer is itself sub-divided insofar as the base of the third layer is made up of very much finer nodules than towards the top of the layer. This could be due to silver chloride depositing at these areas and causing poor blockage.

The film eventually stops growing and exfoliates from the silver, usually at the interface of one layer with another. This could be due (7) to compressive stresses developed in the film at high current density which loosen the film, or by complex ions causing embrittlement at the interfaces.

The start of the cactus growth can be seen in Pic 105 and 106, and the way in which the cacti build up to form a layer can be seen in Pics 107 and 108.

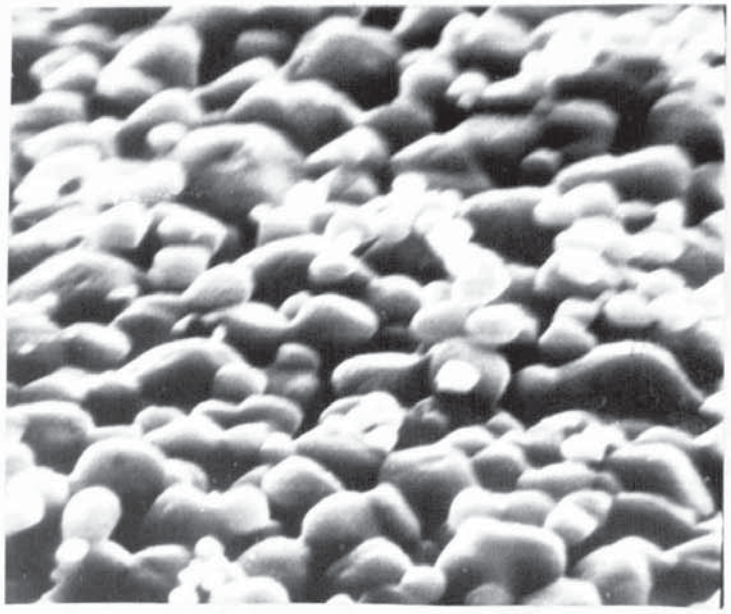

PIC 105 X 6.4K

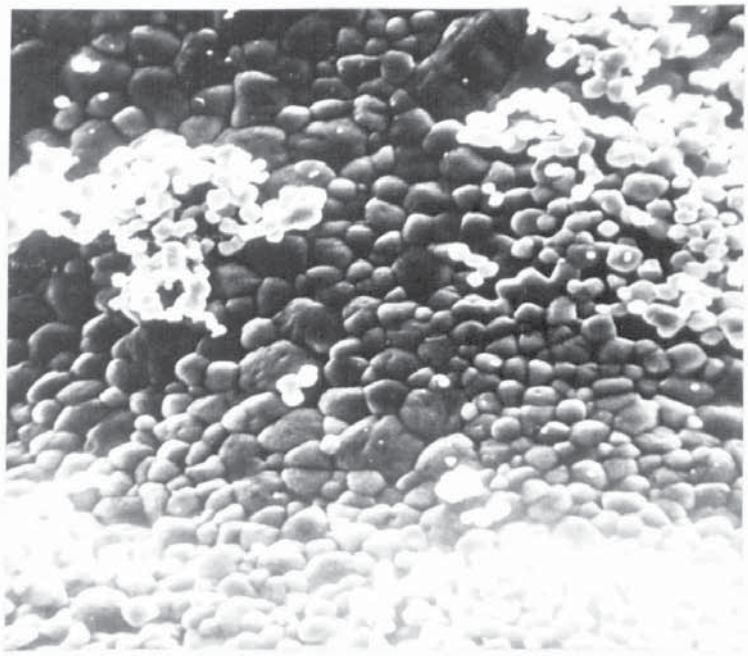

PIC 106 X 2.1K

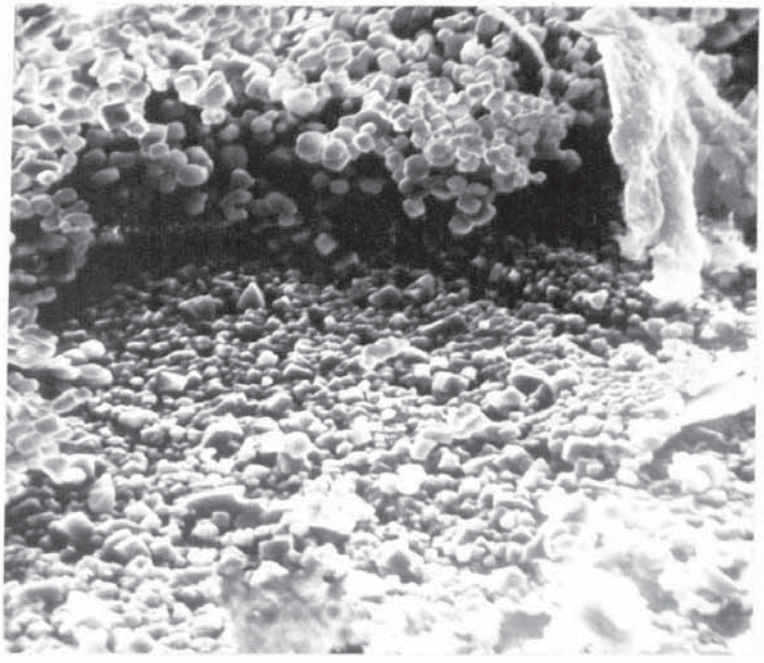

PIC 107 X 2.2K

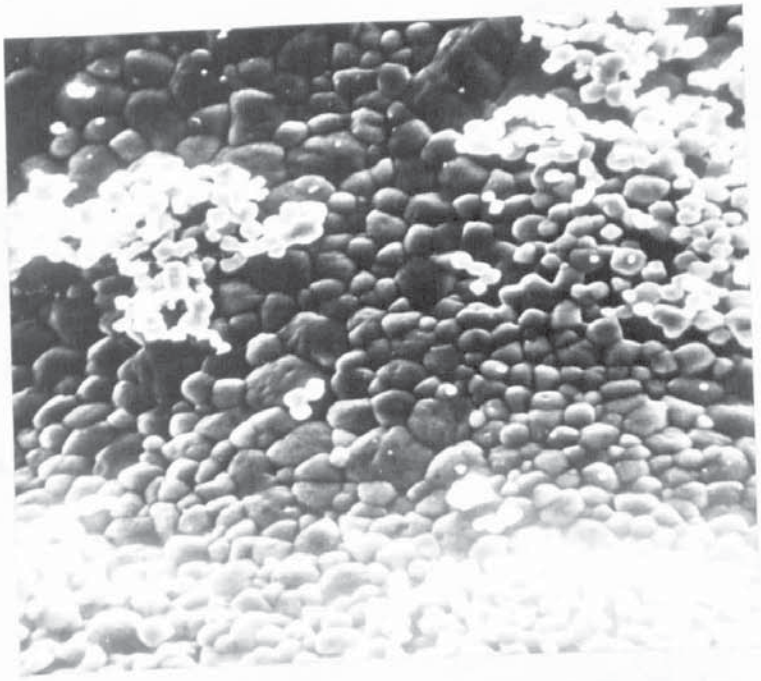

PIC 106 X 2.1K

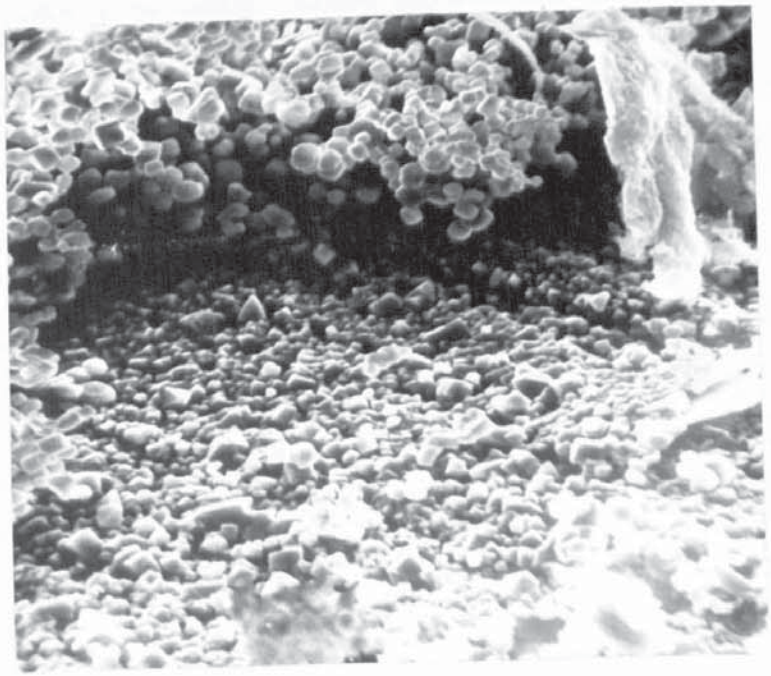

PIC 107 X 2.2K

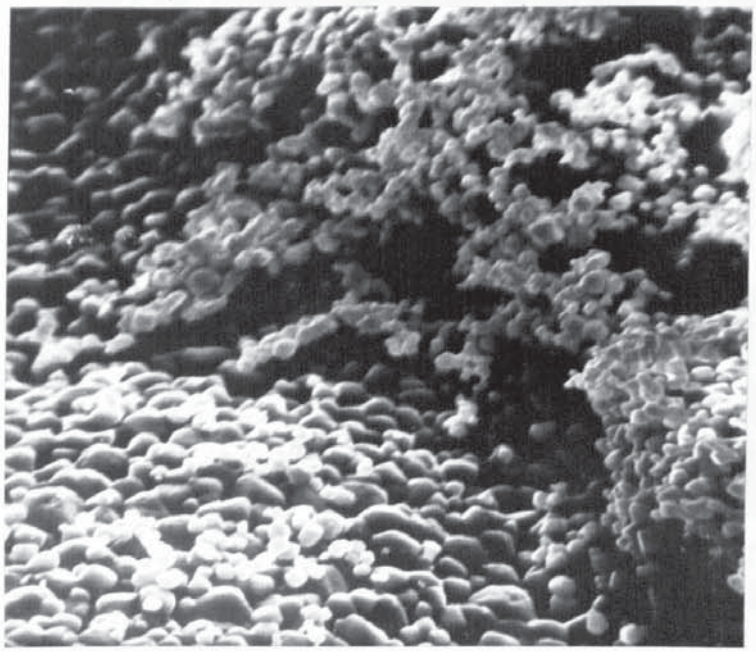

PIC 108 X 2.5K

The connection between the initiation of layer growth, as seen in Pics 105 and 106, and the fully formed layer can be seen in Pics 109 and 110, where the needle nuclei are beginning to grow up into a coherent cactus layer, which can be seen in Pic 111, and in a patchy state covering the surface of the second layer in Pic 112.

Examination of the CDR's for the third layer show that the shorter the anodising time the thicker the layer, $\uparrow H3 \Leftarrow \downarrow T$. This can be true if the energy available, or the current density, is high. Dissolution will then take place at a higher rate, providing large quantities of material for third layer deposition.

The first two layers will form quickly and will be relatively thin as seen in the CDR $\downarrow H1 \Rightarrow \uparrow H3 \Leftarrow \downarrow H2$, followed by the nucleation of the thick third layer on top.

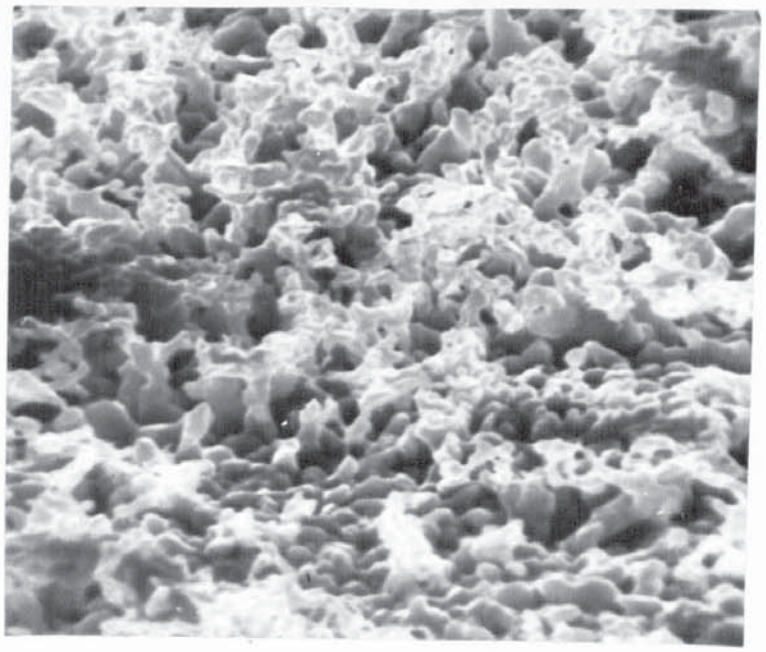

PIC 109 X 5.59K

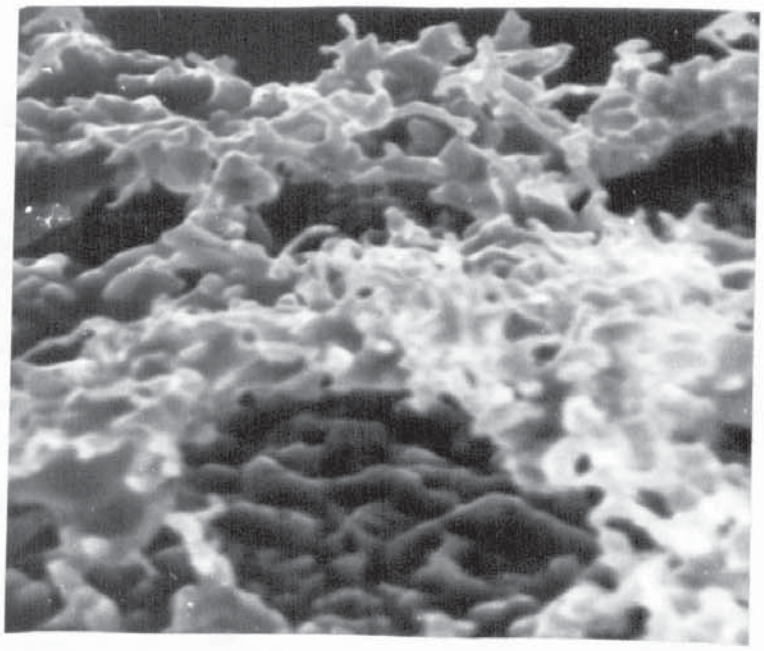

PIC 110 X 6.9K

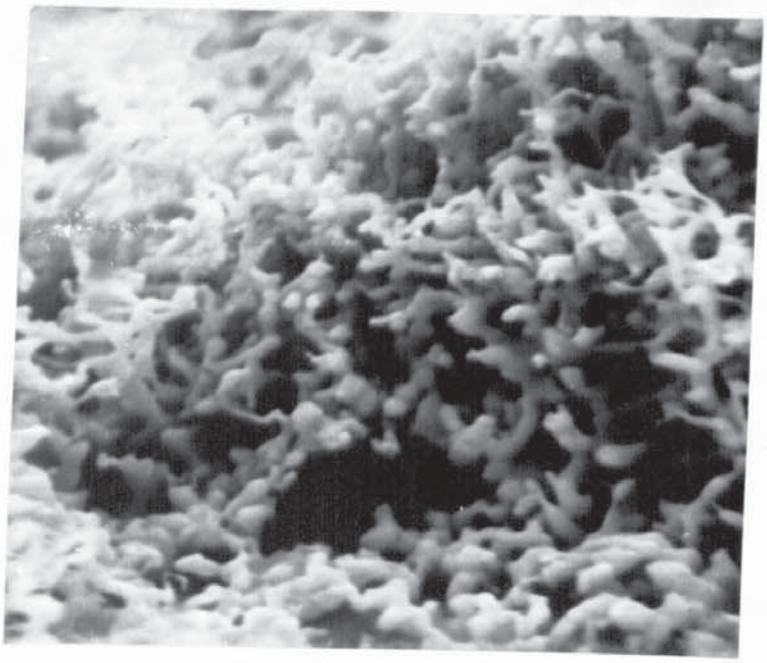

PIC 111 X 6.2K

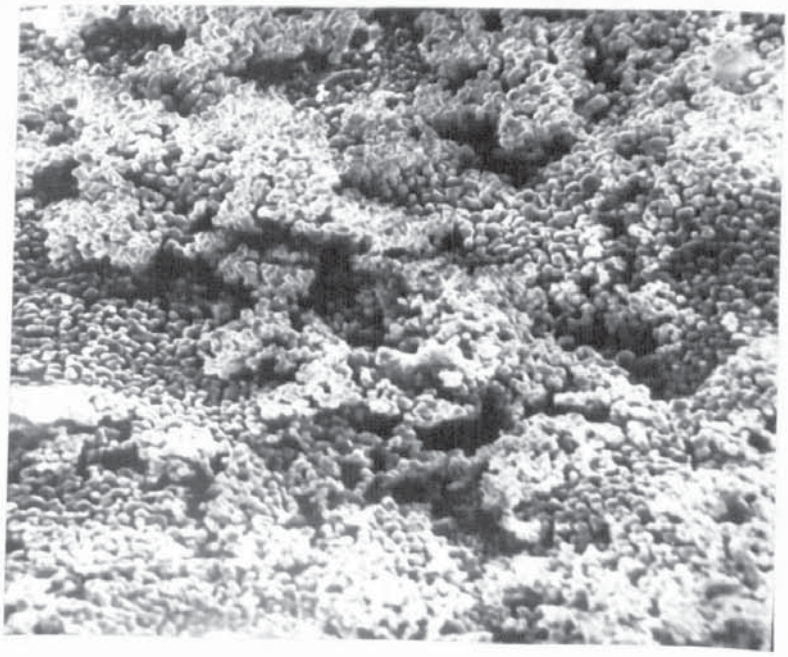

PIC 112 X 1.2K

If the length of the MI5a (3), found in conjunction with the cactus layers, is taken into the calculation of third layer thickness, then the CDR$\uparrow$H3 $\Leftarrow$ $\uparrow$lMI5a(3) can be accepted.

Also if the MI5a(2) acts as a nucleant for the third layer, then the relation $\uparrow$H3 $\Leftarrow$ $\uparrow$ l/vMI5a(2) also holds. If the relation $\downarrow$HI $\Rightarrow$ $\uparrow$H3 is also true then this would cover the relation $\downarrow$rM5(1) $\Rightarrow$ $\uparrow$ H3, as the M5 particle diameter is virtually the same as the first layer thickness, or is a direct ratio of this, as the primary layer can be considered as a virtual monolayer.

If the form $\downarrow$H2 $\Rightarrow$ $\uparrow$H3 also holds, then this would cover the relation $\downarrow$r/vMI9/2a(2) $\Rightarrow$ $\uparrow$ H3 as the larger the second layer particles, the thicker the second layer and vice versa.

If the MI9/2a particle is small, then the Q3(2) packing pore will consequently be small, so the relation $\downarrow$rQ3(2) $\Rightarrow$ $\uparrow$H3 will be true. From the relations $\uparrow$H3 $\Leftarrow$ $\downarrow$vM8b(3) and $\uparrow$H3 $\Leftarrow$ $\downarrow$rQ3(3) it would seem that the average size of the particles in the third layer is smaller in a thick film, but the packing is normal instead of in the relation where H3 is thin, producing large needle particles, and small M8b particles with large packing pores in between them. In this case the particles are scattered, with large numbers of M8b(3) nuclei produced on the surface by the high current density and short anodising time conditions, so the particles and pores between them are smaller.

The dimensions of the M8(3) cacti seem to increase with $\downarrow$HI and $\downarrow$T. Following the relation $\uparrow$HI $\Rightarrow$ $\uparrow$H2 $\Rightarrow$ $\downarrow$H3, and considering the anodising time element, it becomes likely that M8 particles are larger where the growth conditions are of high current density, which is indicated by the third layers ability to form in a short anodising period.

The Q3 pores also increase in dimensions $\uparrow r_{M8(3)} \Rightarrow \uparrow r/v_{Q3(3)}$, which is not surprising as these are packing pores, so the larger the particles the larger the pores.

The CDR's $\uparrow v_{Q6(3)} \leftarrow \uparrow r_{M8(3)}$ and $\uparrow r_{Q6(1)} \leftarrow \uparrow v_{M8(3)}$ can be explained as showing that a more direct access to the silver base gives a greater ion flow through the film, but only at certain sites near to which the M8 size will be expected to be greater. Also the Q6 pores will be formed from missing M8 particles, so the larger the M8 the larger the Q6. If this is so, then if the Q6 extended directly to the silver surface, then Q6(1) = Q6(3), so Q6(1) are related to M8(3).

MI5a and MI4 also occur at the sites, the Q6 pore mouths, and the CDR's $\uparrow r_{M8(3)} \leftarrow \uparrow l_{MI5a(2)}$ and $\uparrow r_{M8(3)} \leftarrow \uparrow l_{MI4(2)}$ can be explained by the MI5a(2) or MI4(2) being the nuclei for the M8 cacti.

With the M8b particles the CDR's below occur.

$\uparrow r/v_{M8b(3)} \leftarrow \downarrow H2$

$\uparrow v_{M8b(3)} \leftarrow \downarrow HI$

$\uparrow r/v_{M8b(3)} \leftarrow \uparrow C$

$\uparrow r/v_{M8b(3)} \leftarrow \downarrow r/v_{MI9/2a(2)}$

These all seem to indicate that the M8b's, like the M8's, increase in dimension with high current, and therefore higher current density, causing a fast growth of the primary and secondary layers to a thin limiting thickness, and the early nucleation of the final third layer.

The relation $\uparrow T \Rightarrow \uparrow r_{M8b(3)}$ seems to indicate that, contrary to that shown with M8(3), the extended form of M8b needs a longer time to form, as the thick M8b layers would seem to show, M8b being an extension of the M8 particle.

The relation $\downarrow$H3 $\leftarrow$ $\uparrow$vM8b(3) does seem to show though that the presence of the extended form of cactus, the M8b, is indicative of a thinner third layer than formed with platelets. This points again to the theory that cacti are the initial form of third layer growth which are followed by platelet growth forms.

This brings in the relations

$\uparrow$ rM8b(3) $\leftarrow$ $\uparrow$r/vQ3(3)

$\uparrow$rM8b(3) $\leftarrow$ $\downarrow$rQ3(1)

$\uparrow$rM8b(3) $\leftarrow$ $\downarrow$vQ3(2)

$\uparrow$rM8b(3) $\leftarrow$ $\downarrow$rQ6(1)

$\uparrow$rM8b(3) $\leftarrow$ $\downarrow$vQ6(3)

$\uparrow$vM8b(3) $\leftarrow$ $\uparrow$r/vQ3(3)

$\uparrow$vM8b(3) $\leftarrow$ $\downarrow$vQ3(2)

$\uparrow$vM8b(3) $\leftarrow$ $\downarrow$rQ6(1)

$\uparrow$vM8b(3) $\leftarrow$ $\downarrow$vQ6(3)

which show that the lower the Q3 porosity dimensions in the first two layers and the greater the Q3 porosity in the third layer, then the longer the M8b(3) particle dimensions.

The relations seem therefore to show that if porosity is low in the primary and secondary layers, then material transfer is also low, and insufficient material is transferred to form a thick third layer, or that anodising conditions are such that the nucleation of the third layer has only just occurred when anodising ceases. Under these circumstances the M8b(3) particles are formed by low nucleation and therefore the particles grow larger than if there were a large number of nucleation centres.

The Q6 pores are also of low dimensions so material flow is low as these are the main transport media. If the M8b particles are large, then the packing pores between them are also large, so the Q3 pores will be large but small Q6 pores will mean the M15a or M14 needles associated with them will be small.

So if these conditions hold true, then large M8b(3) particles will be associated with small Q3(2) pores and small Q6(1, 2, 3) pores, so the relations

$\downarrow$IMI4(2) $\Rightarrow\uparrow$vM8b(3)

$\downarrow$IMI5a(2) $\Rightarrow\uparrow$vM8b(3)

would seem to hold.

YR is the total pore volume, and the relation $\uparrow$YR $\Leftarrow\uparrow$vM8b(3) seems logical if the third layer thickness, even when it is relatively thin, is still thicker than the previous two layers, so if the M8b particles are large and the porosity therefore large, then as the third layer contributes most to film volume and porosity, then the film pore volume will be large.

The effect on Vf, the change in potential across the cell when anodising $\left(\frac{dV}{dT}\right)$ is as the relation $\uparrow$vM8b(3) $\Rightarrow\uparrow$VF shows. The potential across the cell, or the film resistance, increases as the M8b(3) particles rise in volume. This effect is probably illusionary insofar as the first two layers have limited porosity, so the resistance of these layers is increased by the nucleation and growth of the third layer, causing an increase in VF and in M8b particle dimensions.

The relation should probably therefore be written as

$\downarrow$r/vQ3(1)
$\downarrow$r/vQ3(2) $\Rightarrow\uparrow\!\!\not\!\!\downarrow$/$\uparrow$V = $\uparrow$VF = $\uparrow$r/vM8b(3)

In the relation $\uparrow$H2 $\Rightarrow\uparrow$IMI5a(3), the thicker the second layer the longer the MI5a(3) needles. From the CDR $\downarrow$HI $\Rightarrow\downarrow$H2 $\Rightarrow\uparrow$H3 we see that the thicker the second layer the thinner the third, so we have the possibility of the second layer being thick and the third relatively thin, as when the third layer has just been nucleated.

The growth morphology must therefore be such that restriction in material flow, from the silver base, by the coherent first and second layers causes a high energy distribution round the pore mouths, favouring nucleation of needles which use most of the material emerging from pores. If this is so then the dimensions of the other particles in the layer would be smaller, as the CDR $\uparrow$IMI5a(3) $\Rightarrow\downarrow$vM8b(3) seems to show.

Particles would be widely scattered, and the packing pores between them larger, as the CDR $\uparrow$rQ3(3) $\Leftrightarrow\uparrow$1/vMI5a(3) also shows, and the pores in the second layer would be smaller, causing a restirction giving $\downarrow$vQ3(2) $\Rightarrow\uparrow$IMI5a(3).

The relation $\downarrow$r/vM5(1) $\Rightarrow\uparrow$IMI5a(3) must fit into this as $\downarrow$r/vM5(1) $\Rightarrow\downarrow$r/vQ3(2), so the smaller the M5(1) particles the smaller the Q3(2) pores, and therefore the larger the MI5a(3) needles.

This also means that large Q6 pore direct communication between the silver base and the surface must be restricted, giving $\downarrow$vQ6(3) $\Rightarrow\uparrow$IMI5a(3). With the relation $\uparrow$T $\Rightarrow\uparrow$ IMI5a(3), it seems fairly obvious that once the critical time T has elapsed, T being the time to nucleation of the third layer, then any further time increments will, while the needles are growing, add to their length. Also the slower the anodising, if the current conditions are right, the thicker and more coherent are the first and second layers.

If therefore the anodising time is long, and the anodising conditions low as in the CDR's

$\downarrow$ C $\Rightarrow\uparrow$vQ3(3)

$\uparrow$H2 $\Rightarrow\uparrow$vQ3(3)

then the first and second layers will grow to be thick and coherent.

The energy conditions are not available for fast nucleation and growth of the third layer, this only occurring when limiting thickness of the second layer and limiting reduction in material transport has been effected by pore blockage. The CDR's $\uparrow$IMI5a(3) $\Rightarrow\uparrow$r/vQ2(3) and $\uparrow$vM8b(3) $\Rightarrow\downarrow$r/vQ2(3) must refer to the redissolution of the silver chloride with the restriction in flow of the new material.

If the energy requirements are met, the silver chloride will redissolve and transport to new sites, presumably at a needle particle. This would account for the indentations on the M8b(3) and MI9/2a(2) particles, the increase in dimensions of the Q2's with needle length, and their reduction in size as the dimensions of the M8b particles grow, presumably at the expense of growth morphology like the MI5a needles.

With the relations $\uparrow$r/vQ3(3) $\Rightarrow\uparrow$r/vQ2(3) and $\uparrow$rQ3(3) $\Rightarrow\uparrow$r/vQ5(3) it can be seen that the larger the Q3 dimensions, the larger also the indentations on the particles which would probably be M8b(3). Now from the relations $\uparrow$vQ3(3) $\Leftarrow\downarrow$rQ3(2) and $\downarrow$vQ3(2) $\Rightarrow\uparrow$IMI5a(3) and $\uparrow$IMI5a(3) $\Rightarrow\downarrow$vM8b(3) it can be seen that $\uparrow$vQ3(3) $\Leftrightarrow\downarrow$vM8b(3), which agrees with the relation $\uparrow$vM8b(3) $\Rightarrow\downarrow$r/vQ2(3). Small M8b particles, presumably caused by the restriction in material flow by small Q3(2) pores, as seen in $\downarrow$vQ3(2) $\Rightarrow\uparrow$vQ3(3), probably therefore causes material redistribution and redeposition, causing pits on the silver chloride particle surfaces.

SECTION (4)

FACTORS EFFECTING THE FILM THICKNESS, VOLUME, WEIGHT AND NUMBER OF FILM LAYERS.

Df is the solid film thickness if no pores are present and is calculated using Faradays Laws. It is equivalent to the measured film thickness and represents the amount of solid material present in the film. From the CDR models the film volume and thickness have the relations

↑ Vol => ↑rQ5(3)

↑ Vol => ↑vQ6(3)

↑H* => ↑vQ6(3)

↑H3 => ↑rQ5(3)

which seem to indicate that increase in the pore dimensions leads to increase in the film volume, thickness and third layer thickness.

If this then leads, as it must, to an increase in Df, then the relation between Df and film volume or thickness, with all its implications on porosity, cannot be linear but must be as in Graph 32.

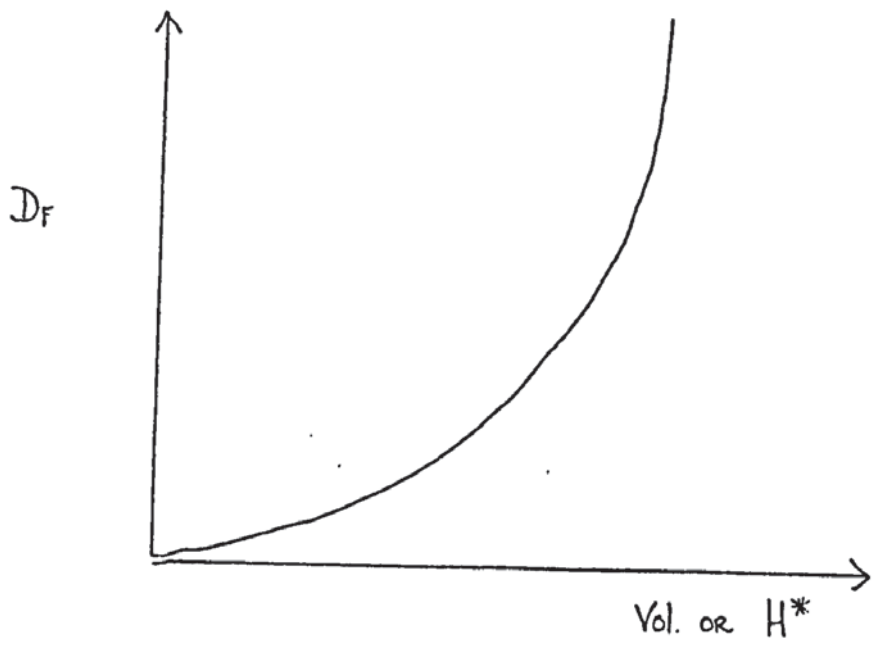

GRAPH 32

With film thickness H*, the greater the film weight and volume the greater the film thickness, especially as when the pore volume increases, then so does the film thickness, as the solid volume Of plus the pore volume is equivalent to the film thickness. Also the thicker any of the layers, the thicker the final film thickness but the thicker the film, the less the number of layers. This would seem contradictory and must mean that relatively speaking, a two layer film is proportionally thicker than a three layer film.

Again the divergence of effect of the M5(I) and MI(I) particles can be seen in the effect on film thickness in the CDR's $\uparrow$rM5(I) $\Rightarrow\uparrow$H* and $\downarrow$rMI(I) $\Rightarrow\uparrow$H*. The CDR's $\uparrow$vM8b(3) $\Rightarrow\uparrow$H* and $\uparrow$vQ6(3) $\Rightarrow\uparrow$H* show as expected that a rise in extended cactus M8b(3) particle dimensions, which would give rise to a thicker third layer, naturally gives rise also to a thicker film. If the volume of the main ion transport medium, the Q6 pores, increases then so does the film thickness as expected.

The increase in the number of layers in the film depends upon the primary layer being relatively thin, and the second and third layers (from the CDR's) being comparatively thick. This can be explained by reference to the current density conditions, high current density producing a large number of layers, a thin primary layer and thick second and third layers. Also the smaller the percentage porosity, but the greater the volume of pores in the film, the larger the number of layers.

If the volume of pores is greater then material flow will be enhanced, so allowing a thicker film with more layers. Percentage porosity is though a function of the number of pores in the film surface, so if the volume increases giving increase in the number of layers, then the number of pores must decrease but individual pore dimensions increase.

This is also indicated by the increase in the dimensions of the Q3(1) pores, the Q3(2) pores and Q2(3) give increase in the number of layers, which follows from the CDR's concerning percentage porosity and total pore volume.

If the radius of the Q3(1) pores increases with decrease of the M1(1) and M5(1) radii, then this would indicate many small scattered particles on the silver base surface, with large gaps between them. Coupling this with the CDR's $\downarrow$HI $\Rightarrow\uparrow$Z and $\uparrow$C $\Rightarrow\uparrow$Z then high current gives a large overpotential for nucleation, so a large number of nuclei are formed giving a large number of small scattered particles over the surface, eventually leading to a thin coherent film of small particles.

As the particles are small, the Q3(1) packing pores radii are small and restriction in material flow occurs. This leads as shown before to renucleation of a new layer with large particle dimensions and formation of reordered Q3(1) pores in the form of Q6 pores. This primary coherent layer of small particles would be thin, and in terms of the number of layers formed in the anodising time available, it would lead to more layers being nucleated.

The increase in dimensions of the M19/2a(2) particles leads to more layers, presumably as the Q3(2) pore dimensions between the particles are larger as the CDR $\uparrow$ r/vQ3(2) $\Rightarrow\uparrow$Z shows, with the effects this has on material flow. It also indicates that the formation of plate like growths of M9 particles in the third layer could be synonymous with large particle dimensions in the second layer, and cactus particle growth in the third layer may follow nucleation from a second layer comprising smaller particles and more pores, although available information seems surprisingly to show the opposite.

The greater the film and second layer thicknesses, the greater the weight of the film, which would seem correct especially when coupled with the CDR $\uparrow vQ3(2) \Rightarrow \uparrow Wt$ which indicates that the thicker the film. the greater the weight as the greater the porosity the larger the film volume and the more material can therefore pass for the growth of that and subsequent layers.

Any increase in particle dimensions should increase the weight, as the CDR $\uparrow rM8(3) \Rightarrow \uparrow Wt$ indicates. The CDR $\downarrow r/vQ3(1) \Rightarrow \uparrow Wt$ indicates that a thin first layer produces eventually a greater film weight, which is accounted for in the relation $\downarrow H1 \Rightarrow \uparrow H3$. A thin first layer therefore results in a thicker third layer, the layer of greatest dimensions and therefore weight.

The CDR $\downarrow vQ6(3) \Rightarrow \uparrow Wt$ must indicate that in the last layer, minimum porosity leads to a denser layer. As this is the last layer, and no further material need be transported across the film and no new larger Q6 pores need be nucleated in the third layer for a new further layer construction, then a large pore volume will not then indicate greater film weight, so the less the porosity the better as this will produce a denser more coherent film.

It is fairly obvious that as the thickness of the film and second layer increases, then so will the film volume. Also if the pore volume increases, then so will the film volume, but from the CDR $\downarrow Df \Leftarrow \uparrow YR$, then as the film volume increases the solid volume decreases proportionally. This must indicate a non linear change in porosity with film volume and therefore film thickness, as seen in Graph 33.

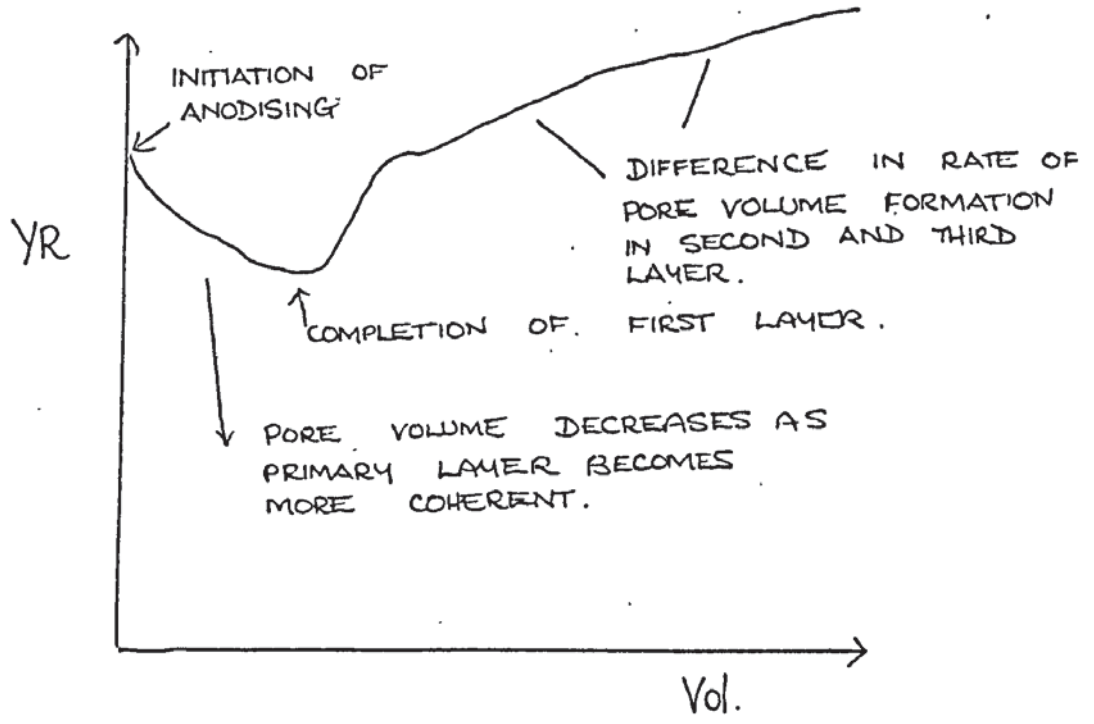

GRAPH 33

This is presumably due to differences in porosity in the different layers, and as seen in Graph 32, the thinner the film, i.e. the less Df, then the greater the relative porosity. As, from the CDR $\downarrow$ R* $\Rightarrow \uparrow$ Vol, then this must mean that individual pore volume increases with film volume, as do the Q6 pores, and by the fact that Q3 pores are larger in each progressive layer, but the relative increase in the rate of total pore volume formation decreases with increase in thickness.

No explanation can be given for the apparent CDR paradox $\downarrow$ H3 $\Rightarrow \uparrow$ Vol as the third layer contributes the most to the film volume. The only rational is that prevalence of the two layer film, and scarcity of three layer films grown has weighted the statistical analysis onto the side of two layer films, thus indicating the volume of these films is greater when no third layer is present.

If the third layer is thin or virtually non existent, then the volume is much less, backed up by the CDR $\downarrow$ rQ3(2) $\Rightarrow\uparrow$ H3, so pores of less volume in the second layer cause a thicker third layer, and as $\uparrow$ H3 $\Rightarrow$ $\uparrow$ Vol then also a greater film volume.

Also there is the CDR $\uparrow$ R* $\Rightarrow\downarrow$ vQ3(2), so the number of pores will probably increase in the second layer with corresponding decrease in individual pore volume, probably not linearly but as in Graphs 34, 35 and 36.

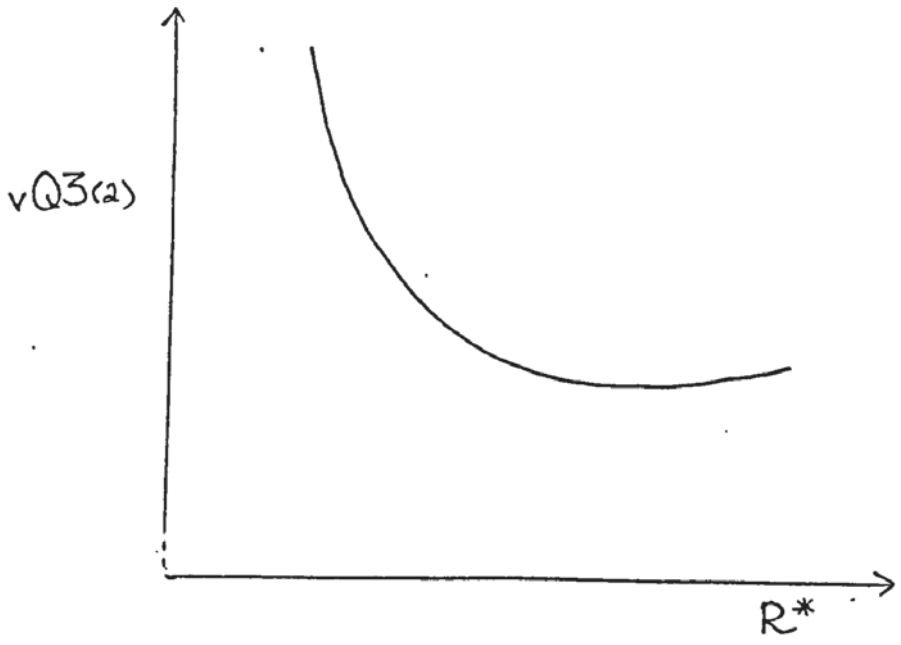

GRAPH 34

As would be expected though, increase in dimensions of the pores in the third layer would increase the pore volume, from the CDR's below.

$\uparrow$ rQ2(3) $\Rightarrow\uparrow$ Vol

$\uparrow$ rQ5(3) $\Rightarrow\uparrow$ Vol

$\uparrow$ vQ6(3) $\Rightarrow\uparrow$ Vol

The models for the third layer seem to indicate that a more rounded particle grows where the film volume is of greatest value, and the particles are large. Where the film is thin, large angular type M8 particles grow.

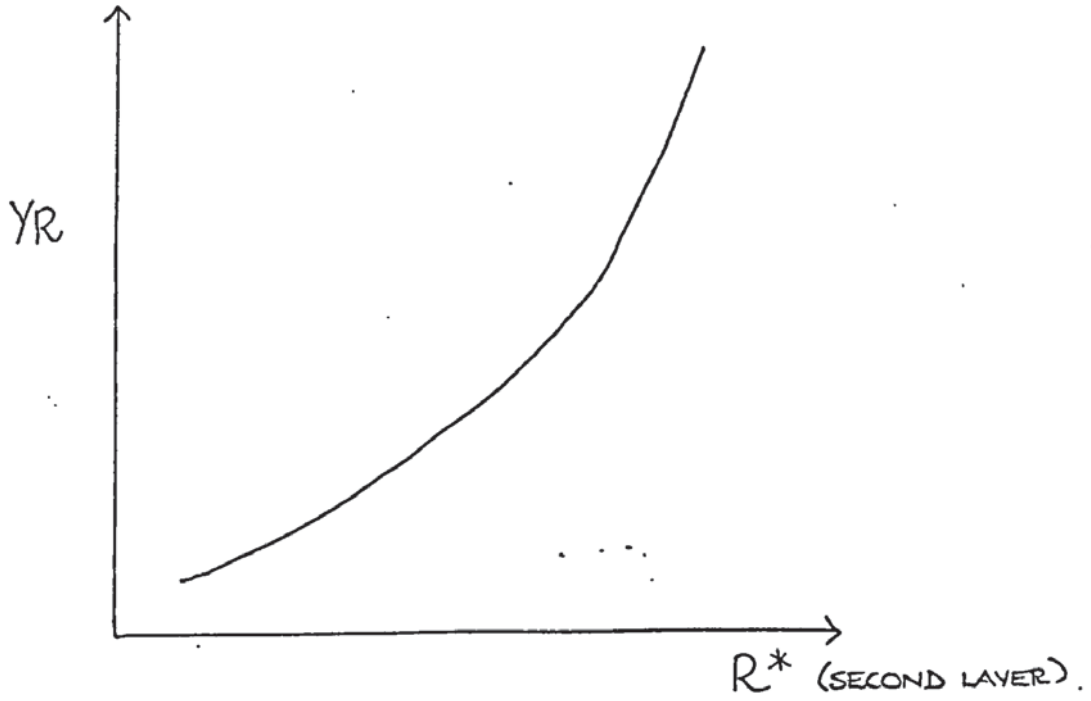

GRAPH 35

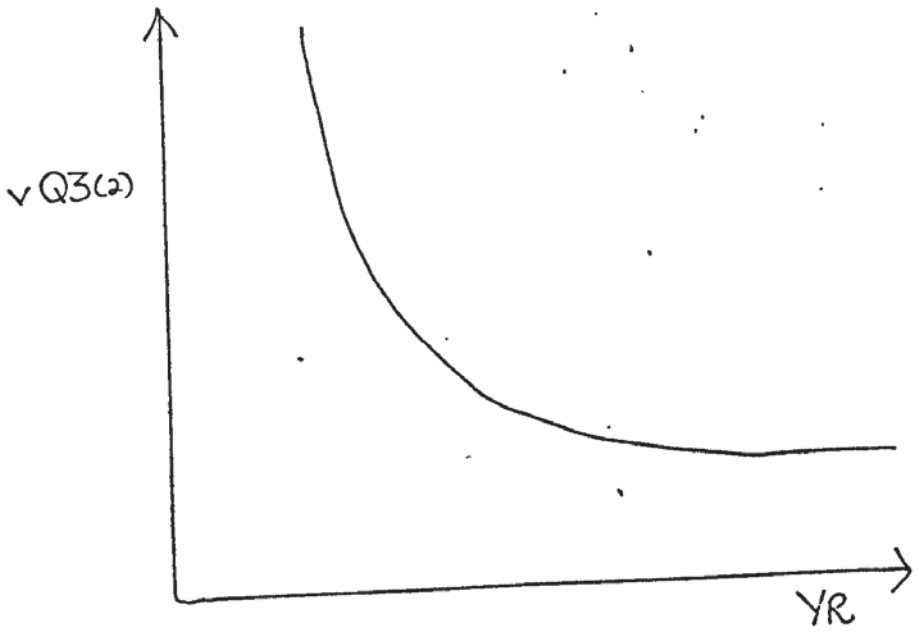

GRAPH 36

That is, if two films are grown, one of which will eventually have a third layer but the other will not, due to anodising conditions, if both films are examined after only two layers have grown then the film which will stay with only two layers will be thicker than that film on which a third layer will eventually grow.

This can be shown by the CDR's

$\uparrow H1 \Rightarrow \uparrow H2$

$\downarrow H2 \Rightarrow \uparrow H3.$

So $\downarrow H1 \Rightarrow \uparrow H3$ and $\downarrow H2 \Rightarrow \uparrow H3$. So the thinner the first two layers the thicker the third and the converse should be true such that if the third layer does not exist, the first two layers reach maximum values of thickness and volume, and then detachment occurs with a new film beginning to grow.

If the third layer is much thicker than the first two, then the lack of thickness of these will be taken up in the greater thickness of the third layer such that the CDR's

$\uparrow H1 \Rightarrow \uparrow H^*$

$\uparrow H2 \Rightarrow \uparrow H^*$

$\uparrow H3 \Rightarrow \uparrow H^*$

$\uparrow H^* \Rightarrow \uparrow Vol$

still hold true. If then the particles and pores in a layer increase in dimensions, then that layer thickness should also increase, so if $\uparrow rM1(1) \Rightarrow \uparrow Vol$ and $\uparrow rQ6(1) \Rightarrow \uparrow Vol$ is true, then so will be the CDR's $\uparrow rM1(1) \Rightarrow \uparrow H1$ and $\uparrow rQ6(1) \Rightarrow \uparrow H1$. Also true would be $\uparrow IM15(2) \Rightarrow \uparrow H2 \Rightarrow \uparrow Vol$ and $\uparrow IM14(2) \Rightarrow \uparrow H2 \Rightarrow \uparrow Vol$, but the CDR $\downarrow vQ3(2) \Rightarrow \uparrow Vol$ does not seem to follow this trend.

If considered in converse though, $\uparrow vQ3(2) \Rightarrow \downarrow Vol$, this indicates that the larger the pores the thinner the third layer is likely to be.

SECTION (5)

FACTORS EFFECTING THE TOTAL FILM PORE VOLUME AND THE PERCENTAGE POROSITY.

In the models the principal components show fairly obvious relationships with the primary function, the total pore volume in the film. As the film and third layer thickness increases, then so does the total pore volume in the film, this being fairly obvious. As the second layer thickness decreases though then the total pore volume increases, presumably as a thin second layer is associated with a thick third layer.

This can be seen in the case where three layers are present, so explaining the variation in the number of layers where $\uparrow Z \Rightarrow \uparrow YR$. It can be seen from the CDR $\uparrow H3 \Rightarrow \downarrow H2$ that a thinner second layer results in a thicker third layer. In the case where only two layers are present, this must indicate that porosity decreases with increase in thickness, and that the film becomes more coherent as the growth proceeds.

The CDR $\uparrow YR \Rightarrow \uparrow R^*$ is then fairly obvious and should be a direct relationship as is $\uparrow Vol \Rightarrow \uparrow YR$, as film volume is a direct function of film thickness. The CDR $\uparrow YR \Rightarrow \downarrow Df$ shows that the less material in the film, the greater the proportion of film volume comprised of pores. This does not compromise the relation $\uparrow H^* \Rightarrow \uparrow YR$ as this simply means that a thicker film has more total pore volume than a thinner one.

The CDR $\downarrow rQ6(3) \Rightarrow \uparrow YR$ corresponds to the relation $\uparrow R^* \Rightarrow \uparrow YR$, so any rise in total pore volume will affect the size of the pores in the third layer, causing a rise in the number of pores and a drop in their individual volume, as in Graphs 37 and 38.

This argument also covers the relation $\downarrow rQ3(2) \Rightarrow \uparrow YR$ which can also be compared to the relation $\downarrow H2 \Rightarrow \uparrow YR$, that is, decrease in pore dimensions here leads to decrease in second layer thickness, leading to increase in third layer thickness and eventually greater total pore volume.

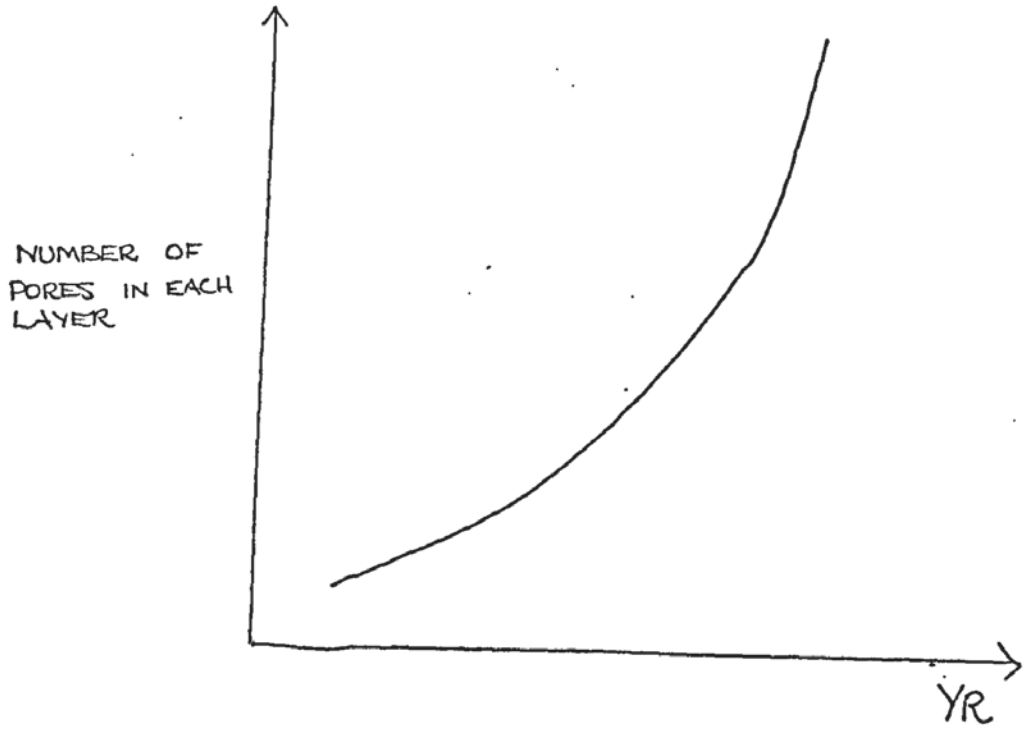

GRAPH 37

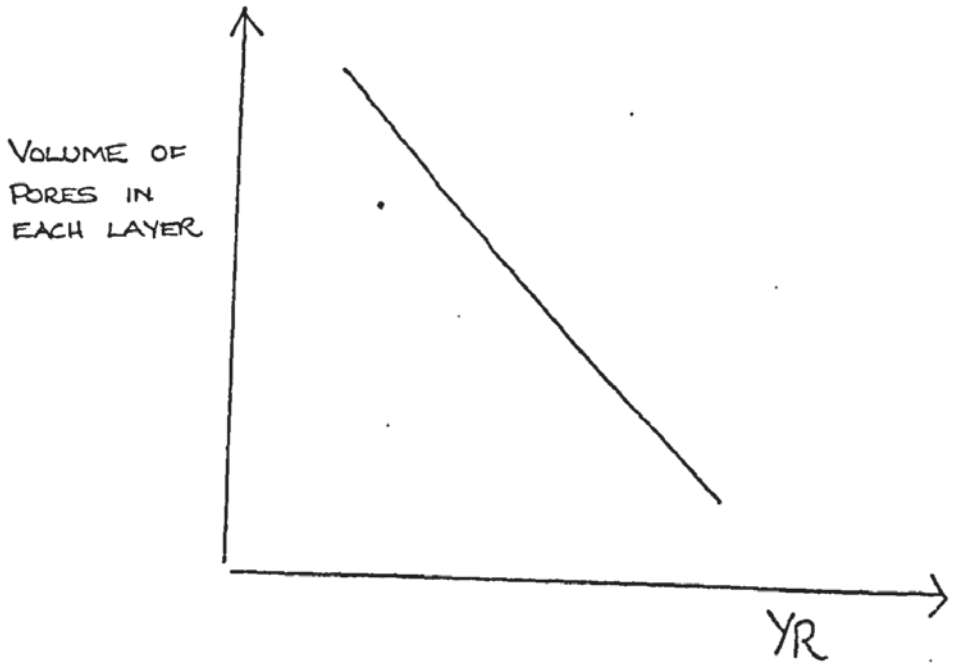

GRAPH 38

In $\uparrow$ rMI(1) $\Rightarrow\uparrow$ YR

$\downarrow$ rMI(1) $\Rightarrow\uparrow$ HI

$\uparrow$ HI $\Rightarrow\uparrow$ H2

It can be seen that $\downarrow$ rMI(1) $\Rightarrow\uparrow$ H2 or $\uparrow$ rMI(1) $\Rightarrow\downarrow$ H2 $\Rightarrow\uparrow$ H3 $\Rightarrow\uparrow$ YR, so the smaller the radii of the MI particles in the first layer, the greater the total pore volume will eventually be probably due to the divergence in effect between MI and M5 particles where for the M5 particles $\downarrow$ rM5(1) $\Rightarrow\uparrow$ YR, but as $\downarrow$ rM5(1) $\Rightarrow\uparrow$ H3, then these relations can be proved as the third layer contains most of the pores.

In the second layer the relation $\downarrow$ vMI9(2) $\Rightarrow\uparrow$ YR is easily explained. Reduction in the volume of these particles easily reduces the layer volume and therefore thickness. Following again the relation $\downarrow$ H2 $\Rightarrow\uparrow$ YR, the reduction in particle volume should give increased pore volume in a three layer film. In a two layer film the reduction in particle volume means more Q3 type pores, as more particles per unit area, and even though the individual volume of these is less the total pore volume is increased in respect to the film volume.

The relation $\uparrow$ lMI4(2) $\Rightarrow\uparrow$ YR can be explained by the fact that the needle lengths are taken into consideration when calculating layer thickness. As they are scattered particles, voidage between them is high and gives an artificial increase to the porosity value, so the CDR is an artificial relation.

It is fairly obvious that as the total pore volume increases then the percentage porosity in the film will also increase, indicating that the pore radii actually increases. The model indicates though that the film volume decreases, i.e. $\uparrow$ R* $\Rightarrow\downarrow$ Vol, with increase in percentage porosity, which indicates that in general thin films have greater relative pore volume than thicker films, as R* is an indication of pore density, although the opposite can be true in the third layer.

Pores in progressive layers tend to be larger, especially as the main pores are between particles, and particle size grows as the number of layers increases. This is also indicated by the CDR $\downarrow Z \Rightarrow \uparrow R^*$, so the less layers or the thinner the film the greater the pore density.

The percentage porosity increases as the anodising temperature decreases. This could be due to the number of layers decreasing as anodising temperature decreases also, where the relative volume and number of pores in the initial layers is higher than in subsequent ones. An increase in primary layer particle volume, $\uparrow vM5(1) \Rightarrow \uparrow R^*$, could mean the larger the M5(1) particles the less there are of them in the layer. The CDR $\uparrow vQ3(2) \Rightarrow \uparrow R^*$ is fairly obvious, as any increase in the particle volume will lead to increase in radius, so if the radii of the pores increases, relative to the radii of the particles, then the value of the percentage porosity will rise.

The relation $\downarrow IM15a(2) \Rightarrow \uparrow R^*$ is not surprising as these needles invariably grow at the edges of pores, if there are few pores or few sites for growth, then only a small number of needles can utilise the available material, and so these will grow to a greater extent as the CDR $\downarrow R^* \Rightarrow \uparrow IM15a(2)$ shows. Rise in the dimensions of Q3(3) seems likely to increase percentage porosity as the CDR $\uparrow R^* \Leftarrow \uparrow r/vQ3(3)$ shows, rise in radius of the M8b(3) particles would also cause increased radii of the Q3(3), so this seems correct.

SECTION (6)

FACTORS EFFECTING THE ELECTRODE AGING TIME, THE ELECTRODE EQUILIBRIUM POTENTIAL AND THE CHRONOPOTENTIOMETRIC CONSTANT

The equilibrium potential arrived at by the electrode is greater the shorter the time, the aging time, taken to arrive at this potential. The CDR's $\downarrow$rM5(1) $\Rightarrow\uparrow$VS and $\uparrow$rM19/2a(2) $\Rightarrow\uparrow$VS indicate that large porosity in the second layer facilitates solution concentration equilibrium. When considering the rate of change of potential during anodising, we find that from the CDR $\uparrow$rM8b(3) $\Rightarrow\uparrow$VF, that the rate of potential change increases as the dimensions of the third layer particles increase. This not only indicates high current density conditions, but also increase in porosity giving easier solution and material flow, as the larger the particles the larger the pores between them.

The effect of light on the electrode is marked. When the electrode is illuminated there is a reduction in potential, as has been reported by Carmody (41) and Moody (9), and for these reasons anodising was carried out under controlled light conditions.

Electrodes need aging time to adjust to normal potential. Examination of Graphs 18 to 27 show the way in which the potential changes with time after anodising. In most, the steady rise from negative potential during the first few hours is followed by an extremely rapid transition to positive potential, levelling off suddenly to a value near to the equilibrium potential. The equilibrium potential is then slowly attained.

Aging could be (38) due to concentration polarisation within the pores, causing chloride ion depletion which needs to be equalised. The temperature effects this time, as the CDR $\downarrow$t $\Rightarrow\uparrow$A shows, such that the lower the cell temperature the longer the aging time.

One would expect this from kinetics, but if it is presumed that aging time be a function of the porosity in the film, such that open pores exist, and solution concentration can be equalised between bulk solution and the internal pore matrix, then it can also be presumed that as percentage porosity increases as the temperature decreases, then the pore volume varies likewise such that pores penetrating deep into the film produce a lower aging time by enhancing solution transfer. Short pores take longer to produce solution equilibrium.

If layer thickness increases then this exchange will be prolonged, so the rise in the second layer thickness producing a rise in aging time is expected. If the anodising time is also extended, a thicker film is produced, so the aging time increases.

The equilibrium potential eventually arrived at at stabilisation is lower the longer the aging time. This may be due to the rearrangement that occurs in the film after anodising. Also the smaller the porosity the larger the film resistance, so the greater the available energy for material redistribution.

If the porosity is large then the amount of solution to come to equilibrium is also large, but larger pores facilitate transfer, so the shorter the aging time. A small volume of porosity will therefore lead to a low equilibrium potential and high aging time.

This explains the effect of the CDR's $\downarrow$vQ3(1) $\Rightarrow\uparrow$A and $\downarrow$vQ3(2) $\Rightarrow\uparrow$A. Also $\uparrow$rM5(1) $\Rightarrow\uparrow$A and $\downarrow$vM5(1) $\Rightarrow\downarrow$A, indicating that the smaller the particles the less the aging time. If the particles are small in the first layer, the pore space between them is very large as the particles are scattered, so the volume of the pores is high, giving $\uparrow$vQ3(1) $\Rightarrow\downarrow$A which explains the CDR $\uparrow$vM2a/19(2) $\Rightarrow\uparrow$A from previous explanations.

We know that small M5(1) particles result in a thin primary layer, which itself results in a thick third layer. A thick third layer results in a thick film which has a long aging time.

With reference to the change in the film structure, the potential varies to negative after anodising and only changes back to positive after some time. The longer the negative phase of the potential change the lower the eventual equilibrium potential. This indicates that if the negative potential occurs during change in film structure after anodising, then this change involves an unblocking of pores, dissolution of film material or cracking of the film by stress relief, or some other mechanism like renucleation such that film resistance is reduced.

This would allow for the part model $\uparrow A \Rightarrow \downarrow VS$. The relation $\uparrow vQ6(3) \Rightarrow \uparrow A$ could be interpreted as meaning that, $\uparrow vQ6(3) \Rightarrow \uparrow YR$ is also true, and as it is the solution in the pores that needs to come to equilibrium, then if the total pore volume is small, and as the third layer contains most of the pores, then the aging time will also be short if the Q6(3) pores have low dimensions.

CHAPTER 6

CONCLUSIONS

In the anodic film the silver chloride first nucleates at the edges of irregularities on the silver surface, at the start of anodising, in the form of very small K type nodular nuclei. These coalesce to form the MI and M5 type particles in areas of high material dissolution.

These particles agglomerate to form the bulbed mounds found following in bands along the rolling or scratch lines on the silver surface. The bands of silver chloride, made up mainly of M5 particles, eventually grow over the troughs left between them and form a coherent porous silver chloride layer.

Two main pore types appear in the layers, the Q3 packing pores produced by the gaps left between particles, and the Q6 pores. These Q6 pores are very large and are proposed to be the main arteries for material transport, formed by the enlargement of existing Q3 pores.

The MI and M5 particles are repeatedly seen to be opposite in their effect on the film parameters, though the MI particles are proposed as a nuclei for the larger M5 particles. An example of this is that analysis of film dimensions show that increase in the size of the M5 particles in the first layer positively effects the primary layer thickness, but the opposite is true for the MI particles.

The outward growth of the film, and the porosity of it, points to the movement of silver ions from the silver surface to the Ag Cl/solution interface as the main transport process. Initial material transport is by complex ion formation, of the $Ag\,Cl_{(n+1)}^{-n}$ type, and one of the main reasons why the Ag Cl is laid down in parallel growth bands is due to stresses in the metal. These produce local anodic and cathodic areas on which the complexes deposit silver chloride, and from which material is removed, producing parallel bands of fine pores.

Transport of material up pores, after the initial nucleation and deposition of silver chloride from solution as a thin layer of scattered particles has been achieved, is by a process of convection. The anode pulls chloride ions down the pores, forming complexes at the pore bases. These are transferred up the pore to the surface by convection mostly caused by heating at the pore base from the dissolution process, and by field enhanced diffusion.

Silver at the pore bases is etched preferentially along certain planes, causing the surface to assume a step like structure. Structures can be seen on the silver chloride base, below the primary layer, which are presumed to be chloride deposited during film growth, especially during pore blockage, enabling the film to remain in contact with the silver base.

After the primary layer forms a coherent film, a second porous layer of much greater thickness is nucleated on top, and is made up of MI1, MI9 or M2a columnar particles. In the layer are again Q3 and Q6 pores, the Q6 pores forming channels for the passage of large amounts of material.

Primary layer growth is very much affected by the state of the silver surface, but the second layer is not. The second layer is affected though by the state of the primary layer, insofar as the finer the primary layer particles, the finer the ones in the second layer. The second layer is therefore affected to some extent by the silver surface state, but at a very much reduced level.

The nuclei of the second layer are the M5 particles, or more accurately, the K type nuclei on the M5 particle surface. Nodules on selected M5 particles in areas of high ion concentration, such as around pores, grow to form the large MI9 or M2a nodules in the second layer.

The second layer itself is nucleated when the thickness of the primary layer is such that the chloride ions find it difficult to reach the silver surface and form complex ions. The second layer is then nucleated due to the different growth processes called for when the main transport of ions is by silver ions and not $AgCl_{(n+1)}^{-n}$ ions. The silver ions diffuse up the pores by convection, forming Ag Cl or Ag Cl complexes within the pores, or as it enters solution.

When the layer is thick, deposition onto the pore walls occurs causing blocking. Some silver chloride then redissolves in the form of the complex ion $AgCl_n^{-(n-1)}$ which transports and redeposits as silver chloride at areas of low chloride ion concentration, such as pore bases and the Ag Cl/Ag interface.

Deposition also occurs at the pore mouths as these are the main points of entry of negatively charged ions to the anodic silver surface. The concentration of the complex ions at the pore mouths will therefore be higher and the opportunity for deposition greater. Deposition at the pore mouths causes the formation of the needle MI4 and MI5a particles which are the nuclei for the third layer. These are associated with pore blockage in the second layer and are produced in the same way as the nculei for the second layer, except they grow into long needle lengths by the growth of one nodule on another in one direction only.

The periodic behaviour of the potential when anodising, associated with the growth of the second layer, seems to support the pore blockage theory.

The third layer grows primarily in two modes, the large crystalline platelet form where the needles thicken by first growing fins or arms, much like dendrites, and then grow into large platelets, and the second mode of growth being the "cactus" type growth.

In this mode the needle nuclei continue to grow in nodular form, producing a thick continuous film composed of large jointed nodules with large pores associated with them.

Whatever the primary mode of the third layer growth, the layer eventually forms the characteristic particular plate like structure.

It would seem that the structure of the second layer, and its parameters, governs the mode of primary third layer growth, but the actual connection is unclear. Porosity seems to decrease relatively as the film thickens, that is, it actually increases but the rate of increase in total pore volume decreases as the film gets thicker. The first and second layers are relatively more porous therefore than the third layer, although the third layer due to its greater thickness contains the majority of the pore volume in the film.

Increased pore dimensions in any layer results in increase in the number of layers in the film. This is presumably due to enhanced material transport, but decrease in the second layer pore dimensions will cause a thicker third layer to form. This contradiction states that large pores in the second layer will cause a thin third layer, presumably made up of cactus particles, though theory would have it that large platelets should form. The mechanism of third layer growth in the initial stages is therefore not completely clear.

The first and second layers of a two layer film will grow quicker though than those in a three layer film. High anodising temperatures usually result in thick or three layer films. The pore volume of these films is presumably high, whereas lower temperatures increases the number of pores present and reduces the number of film layers.

Also the shorter the electrode aging time the higher the ultimate equilibrium potential.

The indications are that the equilibrium potential and aging time are governed by the rate of solution concentration equalisation across the film, this itself being restricted by the pore dimensions and aided by silver chloride redissolution and film rearrangement. As temperature affects ion mobility, it is not surprising that the lower the cell temperature, or the anodising temperature, the longer the aging time. Reduction in pore dimensions also results in a longer aging time as does increased film thickness or anodising time, as would be expected.

The aging process would therefore seem to be one of solution equalisation of chloride ions in the pores. As the solution chloride concentration front moves deeper into the pore from the solution and travels towards the basal silver, then the potential becomes more positive. Eventually the change in potential becomes almost exponential when the front has almost reached to the base.

The CDR relations were used, in this work, to conveniently assess the bulk affects of the various anodising parameters on the film. In this context the use of this regression technique has been quite successful, but in many ways clumsy. Its use resulted in a very large quantity of results being gained, but not always used to their full effect, or to provide useful comparisons.

If this work were to be repeated, very many changes would, in the light of experiences gained in the completion of this research, be made in its planning and execution. For a start the number of variables in the anodising experiments would be reduced, varying the concentration of solution, the time and the current density only, perhaps with changes in anodising temperature with these limited to $-75^{o}C$, $-25^{o}C$, $0^{o}C$, $25^{o}C$, $75^{o}C$.

Changes in variables would be made one at a time producing a simple bracketing technique rather than varying several at the same time, and using the regression technique here utilised. Also the attempt to find the "mythical" film of minimum percentage porosity would be abandoned.

A simple technique was originally used in this work to find this film, the regression equation for which, and therefore the anodising condition recipe for which, can be found in Section 4 of Chaper 4 which deals with this "optimum film regression equation" for minimum film porosity. Instead of this search, the aging time and electrode stability over a long period, especially in demanding environments, would be measured and the parameters found to give an electrode film to stand up to severe conditions.

This would seem the much more sensible and useful line of research, especially for medical use, than that here undertaken. Unfortunately this, like many things, can only be seen with hindsight.

The CDR analysis and breakdown of how the variables affect the film parameters, and how change in these parameters affect other parameters, is seen in Section 3 of Chapter 4. This breakdown is useful in showing the effect of one variable or parameter upon another even though, as has been stated, the use of the CDR analysis has its limitations, especially when trying to tie the information gained from picture analysis to that in the CDR's.

If the work were to be attempted anew, the two modes of investigation, the SEM pictoral and the CDR analysis would not be so obviously segregated.

Probably if one film were to be chosen to provide an "ideal" electrode in the light of this research, with low aging time, steady equilibrium potential, a simple two layer film and relatively low porosity, then specimen index No. 5 in the results section would be chosen, with anodising conditions of:

Current Density	=	1.5ma/cm^2
Potential	=	55 Volts
Temperature	=	30^{o}C
Time	=	690 Seconds
Concentration	=	0.1 Normal hydrochloric acid.

From the deductions and evidence given in this work, we see that the anodic chloride film on silver has a very complex structure with varied films forming depending upon the anodising conditions.

This work will be of value when applied in the field of anodic films, especially in corrosion monitoring and neurology. In the latter field the silver chloride reference electrode is used extensively in brain wave analysis. The use of a modified single or two layer film, or the plastic shielded electrode, may be of much use in eliminating spurious peak "artifacts" during brain monitoring which can lead to incorrect diagnosis.